

# High efficacy Extremely Low Frequency (ELF) Pulsed Electromagnetic Field (PEMF) device for wound healing promotion

A thesis submitted in fulfillment of the requirements for the degree of  
Doctor of Philosophy by

**Istiaque Ahmed**  
MEng, BSc

**Electrical and Computer Engineering**  
**College of Science, Engineering and Health, RMIT University**

**October 2013**

## Statement

The work presented within this thesis holds no material or information that has been accepted for the award in any university for any degree. To the best of my knowledge and belief, this thesis does not contain any material written by another person except for the places denoted by specific references. The content of this thesis is the product of research work carried out at RMIT University, since the starting of this research program.

-----

Istiaque Ahmed

15/10/2013

## Dedicated to my Mother

*-Have I told you lately that I love you?*

*-For all the times I have wavered your hopes;*

*I hope this achievement  
erase them all...*

## Acknowledgements

This work acknowledges important inputs given by the following persons or organizations during the entire course of this PhD research project:

I would like to acknowledge the opportunity given to me by my primary supervisor, Dr. Elena Pirogova, in order to undertake this PhD. She undoubtedly had the most profound influence behind the achievements resulting for this PhD research project. On that note, I would like to thank her for showing patient support, constant encouragement, and assistance throughout the entire research. Most importantly, I am thankful to her for easing me into this program and for trusting my capabilities during the research tenure.

I deeply acknowledge Dr. Taghrid Istivan, my second supervisor, for her engagement in many constructive discussions and also for providing adequate training prior to commencing work in the Microbiology Lab at RMIT University, Bundoora Campus. I would like to thank Dr. Vuk Vojisavljevic, my consultant during this PhD, for his vital inputs during different phases of my research.

I appreciate the research facilities offered by RMIT Engineering and Microbiology Labs. In particular, I would like to thank Mr. El Taher Elshaqmani (School of Applied Science, RMIT University, Bundoora campus) for his invaluable friendship and patience in providing me with hands on training pertaining to handling of live organisms and techniques required as a part of live cell counts. I highly appreciate the technical assistance of Mr. David Welch (School of Electrical and Computer Engineering, RMIT University, City campus) for his help in machining precise shaped acrylic structures and countless constructive discussion regarding the structure of the lab-built ELF PEMF exposure system. I also acknowledge the help and

support of all my friends and colleagues during my time at RMIT University.

I would like to extend a special note of thanks to my beloved wife, Shila, for her tremendous patience and support during the entire stretch of this PhD program. I would also like to thank my little daughter, Inaaya, for not complaining about missed family times and for being a true blessing in my life. Finally, for moral support I extend many thanks to my beloved mother, brother and sister.

*This study was supported by Australia Postgraduate Award (APA).*

## Abstract

Over the past decade, applications of pulsed electromagnetic fields (PEMFs) have proven to be an effective non-invasive method in treating several medical conditions, such as soft tissue injuries, skin ulcers, non-uniform bone fractures and degenerative nerves. A number of investigations have successfully demonstrated that low frequency (LF) PEMF enables the induction of significant current in tissues and allows for an enhanced biological effect and thus, can facilitate wound healing. However, researchers have used PEMF stimulators to promote healing, with the results varying significantly and there are inconsistencies between the deployed PEMF parameters. Additionally, little data to date have been documented on the possible impact of PEMF on the specific agents that influence the process of damaged and infected tissue repair.

This research project successfully presents and discusses the design and construction of an extremely low frequency (ELF) PEMF device built on the basis of a Two-Axis (2-Axis) Helmholtz coil system (HCS) that is capable of producing a uniform time varying magnetic field in the frequency range of 2-500Hz and magnetic induction (magnetic flux density) of 0.5mT - 2.5mT. A custom software program was written in order to systematically analyze the induced magnetic field distribution and its region of uniformity within 10%, 1% and 0.1% of the center field, prior to commencing experimentation with the selected biological model systems. The applications of the developed ELF PEMF exposure device have been investigated in terms of the experimental evaluation of ELF PEMF irradiation on protein, i.e. Collagenase enzyme, and gram-positive and gram-negative bacterial cultures of *Staphylococcus aureus* (*S. aureus*) and *Escherichia coli* (*E. coli*) respectively.

Through this study it was experimentally proved that it is possible to optimize ELF PEMF parameters (frequency,  $f$ , and magnetic flux density,  $B$ ) of the applied irradiation which can modulate (increase or decrease) the biological activity of the studied Collagenase enzyme.

Important findings from the conducted experiments showed that the biological activity of Collagenase enzyme is increased by **7-15%** and **4-15%** upon irradiation at **3Hz** and **8Hz** for the magnetic flux densities of **0.5-2.5mT**.

The effects of the applied ELF PEMF exposure system on growth and proliferation of bacterial culture of *S. aureus* and *E. coli* have also been experimentally evaluated. All bacterial cultures exposed to ELF PEMF showed a decrease in their growth rate when compared to control samples. For *S. aureus*, a specific viability pattern “quadrature polynomial” was observed upon ELF PEMF irradiation. The occurrence of the frequency and magnetic flux density “windows” was observed at the higher end of the studied frequencies range and all magnetic flux densities except 1.5mT. Maximum relative decrease of **68.56%** was observed at the frequency **300Hz** and magnetic flux density **1.5mT**.

For *E. coli*, the overall observation is that *E. coli* bacteria were generally more responsive to the applied irradiation treatment, where the exponential relationship between the colony-forming unit (CFU) values (bacterial growth) and applied exposures was observed. *The results obtained clearly demonstrate that the effects of irradiation on bacterial growth are frequency and magnetic flux density dependent.* In general, the decrease in bacterial cell viability was achieved at all studied range of frequencies (2-500Hz) and every magnetic flux density (0.5mT, 1mT, 1.5mT, 1.5mT, 2mT and 2.5mT). Minimum and maximum changes in bacterial cells growth for the exposed samples were recorded at **3Hz** and **0.5mT**, and **500Hz** and **2.5mT**, respectively. The maximum effect observed at the **500Hz** and **2.5mT** corresponds to the relative decrease of **77.26 %** in bacterial growth.

The outcomes of this research project provides evidence based support to the hypothesis that optimal ELF PEMF parameters can induce therapeutic effects in proteins and cells and thereby, ELF PEMF therapies have a great potential for possible treatment of wounds and overall wound healing promotion.

## List of Figures

Figure 2.1: The electromagnetic (EM) spectrum.....	38
Figure 2.2: Suggested mechanisms of action of ELF PEMF at molecular and cellular levels. .....	41
Figure 2.3: Block diagram of a typical PEMF exposure system: Three main modules of PEMF system, typical PEMF waveform, output terminal of the PEMF device and simulation of the corresponding magnetic field profile produced by the output coils.....	51
Figure 2.4: A typical output module of a PEMF device in form of a pair of Helmholtz coil. .	53
Figure 2.5: Different waveforms used on a trial basis.....	56
Figure 2.6: Commonly used coil references for ELF PEMF device (a) Helmholtz coils (b) Ruben’s coil and (c) Fransleau-Braunbeck coil.....	58
Figure 2.7: Field polarity illustration for AC EMF and PEMF.....	62
Figure 2.8: Potable PEMF device: (a) PE200 Coils and (b) Somapulse. ....	66
Figure 2.9: In vivo PEMF systems: (a) PEMF therapy for the foot; (b) PEMF therapy for the shoulder; (c) PEMF therapy for the whole body; and (d) A modern portable, disposable pulsed electromagnetic field device is incorporated into a dressing for the postoperative treatment of an incisional wound. ....	67
Figure 2.10: <i>In vitro</i> PEMF systems (a) PEMF system for exposure of large number of cell culture plates (b) Tetracoil prototype for producing highly uniform magnetic field and (c) One-axis Helmholtz coil system with a sample holder at the center. ....	68
Figure 2.11: Response to tissue injury. ....	73
Figure 2.12: Hemostasis phase- First stage of wound healing. ....	74
Figure 2.13: Inflammatory phase- First stage of wound healing.....	75
Figure 2.14: Proliferation- Second stage of wound healing.....	75
Figure 2.15: (a) Primary and (b) tertiary structure of collagen. ....	77
Figure 2.16: (a) A proposed view on how Collagenase might have multiple beneficial effects	



on wound healing and on wound bed preparation (b) Collagen degradation into smaller fragments upon reaction with Collagenase. ....	79
Figure 2.17: Gram positive and Gram negative bacteria.....	83
Figure 2.18: Block diagram depicting the relationships between bacteria and wound. ....	84
Figure 2.19: (a) Process of Phagocytosis (b) Bacteria binding to receptors.....	85
Figure 2.21: Methicillin-Resistant <i>Staphylococcus aureus</i> (MRSA) soft tissue infections. ....	88
Figure 2.22: A typical tissue infection (diabetic foot ulcer) caused by <i>E. coli</i> . ....	89
Figure 3.1: Coordinate systems for (a) 2-Axis (four coils) Helmholtz coil system, (b) Pair 1 (top and bottom coil) (c) Pair 2 (side coils) and (d) New coordinate system for Pair 2 after transformation of coordinate.....	95
Figure 3.2: Flow chart of the custom built program for the Two-Axis Helmholtz coil system. ....	99
Figure 3.3: Geometrical orientation of biological sample containment (not to scale): (a) Standard cuvette used for experiments with collagenase enzyme solution and (b) 2.5ml centrifuge tube used for experiments with bacterial culture of <i>S. aureus</i> and <i>E. coli</i> .....	100
Figure 3.4: Simulation results of B-field distribution corresponding to 10%, 1% and 0.1% of the centre field in the $xy$ plane for various $z$ values of -0.5cm, 0cm and 0.5cm, respectively. ....	102
Figure 3.5: (a) B-field produced by Pair 1 coils (b) B-field produced by Pair 2 coils and (c) Superimposed B-field resulting from Pair 1 and Pair 2 coils.....	104
Figure 3.6: Simulation results of B-field distribution corresponding to 1% of the centre field in the $xy$ plane for various $z$ values of (a) -0.5cm, (b) 0.0cm and (c) 0.5cm for One-Axis Helmholtz coil system. ....	105
Figure 3.7: Simulation results of B-field distribution corresponding to 0.1% of the centre field in the $xy$ plane for $z = 0.7$ cm in case of (a) Two-Axis Helmholtz coil system and (b) One-axis Helmholtz coil system. ....	106

Figure 3.8: Simulation results of B-field distribution corresponding to 0.1% of the centre field in the $xy$ plane for $z = 0.0\text{cm}$ in case of a Two-Axis Helmholtz coil system (Pair 1: radius=7cm, Pair 2: radius=9cm).....	106
Figure 3.9: CST EM STUDIO used in (a) modelling the initial structure of ELF PEMF chamber and (b) Simulation results showing 2D representation of the magnetic field within and around the ELF PEMF chamber.....	106
Figure 3.10: Evolution of ELF PEMF chamber (a) Initial design and (b) Exposure chamber with novel cuvette holder design in place.....	110
Figure 3.11: (a) Modified ELF PEMF chamber and (b) Close up view- coil stand (c) Viewing for coil connection to binding posts. ....	111
Figure 3.12: Sham exposure chamber structure (a) without sample holder (b) with cuvette holder and (c) with 2.5mL centrifuge tube holder. ....	113
Figure 3.13: Conventional cuvette holders.....	115
Figure 3.14: Design 1 of the cuvette holder. ....	116
Figure 3.15: Design 2: Novel cuvette holder.....	117
Figure 3.16: Schematic of the custom built water regulatory system used as part of the ELF PEMF system (bottom). Practical setup (top right), with the upper lid taken off for aiding visualization. Arrows showing the water pipe connection between the cuvette (top left) and the schematic and practical water regulatory system setup.....	118
Figure 3.17: Water circulating through the cuvette holder demonstrated in five stages from S1 through S5. ....	120
Figure 3.18: Switching circuit used in the ELF PEMF experiments.....	122
Figure 3.19: (a) Block diagram for pre-testing setup for (b) Set-up to check for any current loss in the coil.....	123
Figure 3.20: Circuit setup for ELF PEMF experiments. ....	124
Figure 3.21: Oscilloscope trace of a 10Hz pulse signal set by the signal generator and a 10Hz	

pulse signal used to drive the coil pairs.....	125
Figure 3.22: (a) Determining the local (coil network) coordinate system inside the ELF PEMF chamber (b) Grid mat used in the ELF PEMF chamber for determining x and y axis and the placement of Pair 2 coils (c) Assembly of the Laser module.....	128
Figure 3.23: Demonstration of magnetic flux density measurement with EFA 200 Analyser along (a) z axis (axial axis of Pair 1 coils) and (b) x axis (axial axis of Pair 2 coils).....	129
Figure 3.24: EFA 200 Analyser displaying a magnetic flux density value of 1.0mT at 250Hz. ....	131
Figure 3.25: Comparison of theoretical and experimental results.....	132
Figure 3.26: (a) Experimental setup for temperature control within the ELF PEMF coil network caused due to Joule heating (b) A two-socket digital temperature controller thermostat.....	138
Figure 3.27: Angle between two Helmholtz pair: a) 0° and b) 90°.....	139
Figure 3.28: Measurement conducted at 250Hz for 0.5-2.5mT over the period of 90 minutes (duration of exposure with experiments relating to bacterial culture), shows excellent field stability during the entire duration of experiment.....	140
Figure 4.1: Typical setup of a Spectrometer with the light source and USB connections. A demonstration of a cuvette with experimental solution showing the absorption site and the location of cuvette placement for measuring absorption coefficients is also shown..	146
Figure 4.2: Spectrometer USB2000 along with component markings used for measuring optical density. ....	146
Figure 4.3(a): Relative changes in the collagenase enzyme activity (%) induced by the ELF PEMF at the frequency range of 2-500Hz magnetic flux densities 0.5mT and 1.0mT. .	152
Figure 4.3(b): Relative changes in the collagenase enzyme activity (%) induced by the ELF PEMF at the frequency range of 2-500Hz and magnetic flux densities 1.5mT and 2.0mT.	

.....	153
Figure 4.3(c): Relative changes in the collagenase enzyme activity (%) induced by the ELF PEMF at the frequency range of 2-500Hz and magnetic flux density 2.5mT.....	153
Figure 4.4(a), 4.4(b) and 4.4(c): Bar charts with the standard errors (standard deviation) of the relative change in the Collagenase enzyme activity (%) versus frequencies: 3Hz (Figure 4.4(a)), 8Hz (Figure 4.4(b)), 300Hz (Figure 4.4(c)) and magnetic flux densities 0.5-2.5mT. The percentage represents relative change to the non-exposed samples. ....	156
Figure 4.5(a), 4.5(b) and 4.5(c): The activity of the Collagenase enzyme was measured after PEMF exposures at frequencies of 2-500Hz and magnetic flux densities of 0.5-1.0mt (Figure 4.5(a)), 1.5-2.0mT (Figure 4.5(b)) and 2.5mT (Figure 4.5(c)). The ordinate represents the rate of change of the buffered solution of Collagen Type 1. The rate of change represents the rate of change of the buffered solution of Collagen Type I concentration per unit of time, or activity of Collagenase enzyme. Horizontal bold line represents an average ( $\bar{x}$ ) for the non-exposed samples. Horizontal dash lines are values distant for one standard deviation(s) up and below for average value. ....	158
Figure 5.1: Schematic of cross-section of bacterial cell walls: A) Gram-positive bacteria and B) Gram-negative bacteria. ....	160
Figure 5.2: Bacterial growth curve. ....	161
Figure 5.3: Using the Eppendorf BioPhotometer Spectrophotometer UV/VIS for OD measurements.....	162
Figure 5.4: Working methodology of a Photometer for measurement of the OD of a culture. A) For a clear sterile medium contained in the cuvette, the intensity of the light that reaches the photoelectric cell is taken as the reference intensity and adjusted to zero OD. B) With bacterial cells in the cuvette, a significant portion of light is scattered and no longer reaches the photoelectric cell. The weaker electric signal is converted to an OD value. ....	163

Figure 5.5: Growth curve: Typical control and ELF PEMF exposed bacterial culture of a) *S. aureus* and b) *E. coli* monitored via OD reading..... 165

Figure 5.6: Block diagram of the experimental procedure for investigating the effect of ELF PEMF exposures on bacteria *Staphylococcus aureus* and *Escherichia coli*..... 166

Figure 5.7: Typical fresh bacterial culture in Colombia agar medium: A) *S. aureus* B) *E. coli*.  
..... 167

Figure 5.8: A) Colombia broth B) Bacterial colonies suspended in Colombia broth..... 167

Figure 5.9: Top view of the ELF PEMF chamber used during exposure of the bacterial culture..... 168

Figure 5.10: A) Spread-plating, B) Colombia agar plates kept inside the incubator C) After incubation- isolated colonies of bacteria are clearly visible and the value of CFU can easily be determined (in this particular case, CFU, n= 24)..... 169

Figure 5.11: Changes in CFU value of *S. aureus* after ELF PEMF exposure: (n- number of bacteria in 100µl of suspension). ◊-control sample, ◻-ELF PEMF exposed sample at 0.5mT. .... 173

Figure 5.12: Changes in CFU value of *S. aureus* after ELF PEMF exposure: (n- number of bacteria in 100µl of suspension). ◊-control sample, ◻-ELF PEMF exposed sample at 1.0mT. .... 173

Figure 5.13: Changes in CFU value of *S. aureus* after ELF PEMF exposure: (n- number of bacteria in 100µl of suspension). ◊-control sample, ◻-ELF PEMF exposed sample at 1.5mT. .... 174

Figure 5.14: Changes in the CFU value of *S. aureus* after ELF PEMF exposure : (n- number of bacteria in 100µl of suspension). ◊-control sample, ◻-ELF PEMF exposed sample at 2.0mT. .... 174

Figure 5.15: Changes in the CFU value of *S. aureus* after ELF PEMF exposure: (n- number of bacteria in 100µl of suspension). ◊-control sample, ◻-ELF PEMF exposed sample at

2.5mT.....	175
Figure 5.16: Relative change (%) in the number of bacteria count for <i>S. aureus</i> after ELF PEMF exposure at 0.5mT and 1.0mT.....	175
Figure 5.17: Relative change (%) in the number of bacteria count for <i>S. aureus</i> after ELF PEMF exposure at 1.5mT, 2.0mT and 2.5mT.....	176
Figure 5.18: Viability pattern “quadrature polynomial” of bacterial culture of <i>S. aureus</i> exposed to ELF PEMF.....	178
Figure 5.19: Relative minimum and maximum change (%) in CFU value: CFU values corresponds to individual frequencies after <i>S. aureus</i> exposure to ELF PEMF from 0.5-2.5mT.....	179
Figure 5.20: Sorted results of Colombia agar plates after incubation showing the formation of <i>S. aureus</i> colony-forming units (CFU). CFU values, <i>n</i> , for each plate are specified.....	180
Figure 5.21: Changes in the CFU value of <i>E. coli</i> after ELF PEMF exposure: ( <i>n</i> - number of bacteria in 100µl of suspension). ◊-control sample, ◻-ELF PEMF exposed sample at 0.5mT.....	183
Figure 5.22: Changes in CFU value of <i>E. coli</i> after ELF PEMF exposure: ( <i>n</i> - number of bacteria in 100µl of suspension). ◊-control sample, ◻-ELF PEMF exposed sample at 1.0mT.....	183
Figure 5.23: Changes in the CFU value of <i>E. coli</i> after ELF PEMF exposure: ( <i>n</i> - number of bacteria in 100µl of suspension). ◊-control sample, ◻-ELF PEMF exposed sample at 1.5mT.....	184
Figure 5.24: Changes in the CFU value of <i>E. coli</i> after ELF PEMF exposure: ( <i>n</i> - number of bacteria in 100µl of suspension). ◊-control sample, ◻-ELF PEMF exposed sample at 2.0mT.....	184
Figure 5.25: Changes in the CFU value of <i>E. coli</i> after ELF PEMF exposure: ( <i>n</i> - number of bacteria in 100µl of suspension). ◊-control sample, ◻-ELF PEMF exposed sample at	

2.5mT. ....	185
Figure 5.26: Exponential trend of CFU corresponding to exposure of ELF PEMF to <i>E. coli</i> . .....	186
Figure 5.27: Relative change (%) in the number of bacteria count of <i>E. coli</i> after ELF PEMF` exposure at 0.5mT and 1.0mT.....	188
Figure 5.28: Ralative change (%) in the number of bacteria count of <i>E. coli</i> after ELF PEMF exposure at 1.5mT, 2.0mT and 2.5mT. ....	188
Figure 5.29: Ralative minimum and maximum change (%) in CFU value: CFU values corresponds to individual frequencies after <i>E. coli</i> exposure to ELF PEMF from 0.5- 2.5mT. ....	189
Figure 5.30: Sorted results of Colombia agar plates after incubation showing the formation of <i>E. coli</i> colony-forming units (CFU). CFU values, n, for each plate are specified.....	190
Figure A.1: Magnetic field $d\vec{B}$ , at point P due to a current-carrying elements $I d\vec{l}$ . ....	221
Figure A.2: Circular current carrying loop with x as the axial axis.....	222

## List of Tables

Table 2.1: Advantage of existing ELF PEMF system.....	50
Table 4.1: Components of the spectrometer USB 2000.....	147
Table 4.2: Experimental parameters of ELF PEMF exposure to Collagenase enzyme solution. .....	151
Table 4.3: Activity of the enzyme and standard deviation upon exposure to ELF PEMF.....	155
Table 5.1: Experimental parameters of ELF PEMF exposure to bacterial culture of <i>S. aureus</i> and <i>E. coli</i> .....	171
Table 5.2: Minimum CFU number and Maximum percentage change for ELF PEMF exposure of bacterium <i>S. aureus</i> .....	177
Table 5.3: Minimum CFU value and Maximum percentage change for ELF PEMF exposure of bacterium <i>E. coli</i> .....	187



## List of Acronyms and Abbreviations

ATCC	American Type Culture Collection
AWG	American Wire Gauge
ATP	Adenosine Triphosphate
1-Axis HCS	One-Axis Helmholtz coil system
2-Axis HCS	Two-Axis Helmholtz coil system
B&S	Brown and Sharpe
CFU	Colony- forming unit
DF	Diluting Factor
EC	Enzyme Commission
<i>E. coli</i>	<i>Escherichia coli</i>
EGF	Epidermal growth factor
ELF	Extremely low frequency
EM	Electromagnetic
EMF	Electromagnetic field
FDA	Food and Drug Administration
FGF	Fibroblast growth factor
ICR	Ion cyclotron resonance
IPR	Ion parametric resonance
IR	Infrared
MOSFET	Metal-oxide-semiconductor field-effect transistor
OD	Optical Density
PBA	Perfect Boundary Approximation
PCB	Printed Circuit Board
PDGF	Platelet-derived growth factor
PEMF	Pulsed Electromagnetic field
PMNs	Polymorphonuclear neutrophils

PVC	Polyvinyl Chloride
PRF	Pulsed radiofrequency field
SAR	Specific absorbance rate
<i>S. aureus</i>	<i>Staphylococcus aureus</i>
TGF- $\beta$	Transforming growth factor-beta
VLF	Very low frequency
WHO	World Health Organization

# Table of Contents

<b>STATEMENT</b> .....	2
<b>ACKNOWLEDGEMENTS</b> .....	4
<b>ABSTRACT</b> .....	6
<b>LIST OF FIGURES</b> .....	8
<b>LIST OF TABLES</b> .....	15
<b>LIST OF ACRONYMS AND ABBREVIATIONS</b> .....	17
<b>CHAPTER 1:</b> .....	25
<b>INTRODUCTION</b> .....	25
1.1 Introduction .....	26
1.2 Research Aims .....	30
1.3 General Objective .....	31
1.4 Specific Objective.....	31
1.5 Thesis Composition .....	33
<b>CHAPTER 2:</b> .....	36
<b>LITERATURE REVIEW AND BACKGROUND UNDERSTANDING</b> .....	36
2.1 Overview .....	37
2.2 Electromagnetic Field (EMF) Radiation .....	37
2.3 The Electromagnetic (EM) spectrum .....	38
2.4 Characteristics of EM Wave.....	39

2.4.1 Magnetic Field .....	39
2.4.2 Magnetic flux .....	39
2.5 EMF Biological Effects .....	40
2.6 ELF PEMF Mechanisms .....	40
2.7 Application of PEMFs in Wound Healing .....	42
2.8 Therapeutic ELF PEMF Systems .....	45
2.9 PEMF Device .....	50
2.10 Characteristics of PEMF Device .....	54
2.10.1 Frequency.....	55
2.10.2 Waveform .....	55
2.10.3 Coils and Coil System.....	56
2.10.4 Magnetic Field Uniformity .....	60
2.10.5 Field Polarity and Intensity .....	61
2.10.6 Temperature Concerns .....	63
2.10.7 Sham Exposure .....	63
2.10.8 Construction Material .....	63
2.10.9 Time Schedule .....	64
2.10.10 Power Constrain.....	64
2.11 Window Effect.....	65
2.12 Commercial PEMF Device: <i>In vivo</i> Application.....	66
2.13 <i>In vitro</i> PEMF System .....	68
2.14 Safety .....	70

2.15 Wound Healing.....	71
2.15.1 Types of Wound.....	71
2.15.2 Response to Tissue Injury.....	72
2.16 Process of Wound Healing .....	73
2.17 Collagen in Wound Healing .....	77
2.18 Collagenase in Wound Healing .....	78
2.19 Conventional Debridement Methods and Limitations .....	80
2.20 Bacterial Infection of Wounds.....	82
2.21 Mechanism of Bacterial Infection .....	85
2.22 Conventional Treatment Method and Limitations for Bacteria Infected Wound.....	86
2.23 <i>Staphylococcus aureus</i> in Wound Infection .....	88
2.24 <i>Escherichia coli</i> in Wound Infection.....	89
2.25 Summary.....	90
<b>CHAPTER 3: .....</b>	<b>92</b>
<b>ANALYTICAL APPROACH, DESIGN, MODELLING, AND INSTRUMENTATION</b>	
<b>OF ELF PEMF DEVICE.....</b>	<b>92</b>
3.1 Overview .....	93
3.2 Analytical Approach for Generating Uniform Magnetic Field Using a Two-Axis (Four	
Coils) Helmholtz Coil System.....	93
3.2.1 Custom Software Program.....	98
3.2.2 Geometric Orientation of Biological Sample in the ELF PEMF Exposure Chamber	100
3.2.3 Analytical Results .....	101

3.3 Design and Construction of ELF PEMF Exposure Chamber.....	108
3.3.1 Designing of Cuvette Holder for ELF PEMF Experiments .....	113
3.3.1.1 Current Limitations of Cuvette Holders .....	113
3.3.1.2 Custom Made Cuvette Holders.....	115
3.3.1.3 Integrated Custom Made Water Regulatory System .....	117
3.4 Equipment and Experiment Setup .....	121
3.5 Measurement of ELF PEMF .....	127
3.5.1 Experimental Setup for Magnetic Flux Density Measurement within the ELF PEMF Chamber.....	127
3.5.2 Actual Measurement of Magnetic Flux Density .....	130
3.6 Comparison of Theoretical and Experimental Results.....	132
3.7 Temperature Control and Power Constrains .....	133
3.8 Data Acquisition.....	138
3.9 Inductance and Stability of Magnetic Flux Density .....	138
3.10 Summary .....	140
<b>CHAPTER 4:</b> .....	142
<b>RESULTS: EFFECT OF ELF PEMF ON COLLAGENASE ENZYME KINETICS ..</b>	142
4.1 Overview .....	143
4.2 Collagenase Enzyme.....	143
4.3 Collagenase Enzyme Assay.....	143
4.4 Experimental Equipment .....	145

4.5 Measurement of Collagenase Enzyme Activity .....	148
4.5.1 Experimental Procedure.....	149
4.6 Results and Discussion .....	151
4.7 Summary.....	158
<b>CHAPTER 5:</b> .....	159
<b>RESULTS: EFFECT OF ELF PEMF ON SURVIVAL OF BACTERIA <i>Staphylococcus aureus</i> AND <i>Escherichia coli</i></b> .....	159
5.1 Overview .....	160
5.2 Characterization of Bacteria .....	160
5.2.1 Characteristics of Bacterial Growth Curve.....	161
5.3 Experimental Equipment .....	162
5.4 Experimental Materials.....	164
5.5 Experimental Procedure .....	164
5.5.1 Experimental Stages .....	166
5.6 Effects of ELF PEMF Interaction with Bacteria .....	170
5.7 Results and Discussion .....	171
5.7.1 Effect of ELF PEMF on Bacterial Culture of <i>S. aureus</i> .....	173
5.7.2 Effect of ELF PEMF on Bacterial Culture of <i>E. coli</i> .....	182
5.7.3 General Discussion .....	191
5.8 Summary.....	192

<b>CHAPTER 6:</b> .....	194
<b>CONCLUSIONS</b> .....	194
6.1 Conclusions .....	195
6.2 Suggestions for Further Research.....	197
6.3 Publications .....	199
<b>REFERENCES</b> .....	201
<b>Appendix A:</b> Biot-Savart Law to calculate magnetic field. ....	221
<b>Appendix B:</b> Power MOSFET IRF520N .....	225
<b>Appendix C:</b> Purchasing information for material used in this study .....	229
<b>Appendix D1:</b> Resistivity of Copper .....	230
<b>Appendix D2:</b> Cross-sectional Area and Allowable Current for Copper wire.....	230
<b>Appendix D3:</b> Density of Copper.....	232
<b>Appendix D4:</b> Specific heat capacity of Copper .....	234
<b>Appendix E:</b> Aseptic Techniques.....	235
<b>Appendix F:</b> Serial Dilution Technique and Viable Cell Count .....	236



## **CHAPTER 1:**

## **INTRODUCTION**

## 1.1 Introduction

Wound healing is a complex and dynamic process of restoring cellular structures and tissue layers [1]. Primary healing, delayed primary healing, healing by secondary intention and epithelization constitute the four main categories of wound healing [1]. Process for wound healing can be divided into three distinct phases: the inflammatory, proliferative, and remodeling phases [2]. However, certain systematic diseases such as injuries to the nervous system, metabolic changes and aging have negative impact on the healing process that can lead to chronic wound formation [3]. The electro-potential of healthy cells causes a steady flow of ions across the cell membrane. In an unhealthy or damaged cell, there is a sodium influx resulting in cytotoxic oedema. Injured tissues are categorized by higher healing potential as compared to an unbroken skin [4].

The actual mechanisms by which electromagnetic fields (EMFs) produce biological effects are under intense study. Evidence suggests that the cell membrane may be one of the primary locations where applied EMFs act. Electromagnetic forces at the membrane's outer surface could modify ligand-receptor interactions, which in turn would alter the state of large membrane molecules that play a role in controlling the cell's internal processes. The mechanism of action of EMF signals at the molecular and cellular level is now much better understood and strongly suggests ion/ligand binding in a regulatory cascade could be the signal transduction pathway [5, 6-9]. It is reported that cells respond to the rate of change in magnetic field and not to the peak field magnitude or total flux exposure [10].

There is ongoing interest in applications of pulsed electromagnetic field (PEMF) radiation as an alternative therapy for different medical conditions [11]. Studies have demonstrated that extremely low frequency (ELF) PEMF radiation facilitates the process of wound repair [12, 13]. ELF PEMF is a sub-class of EMF that displays frequencies at the lower end of the

electromagnetic spectrum from 6Hz up to 500Hz [11]. ELF PEMF radiation is non-ionizing radiation that uses electrical energy to direct a series of magnetic pulses through biological media, whereby each magnetic pulse induces a tiny electrical signal that stimulates cellular response. Significant number of peer-reviewed publications already showed that EMFs can result in physiologically beneficial *in vivo* [14, 15] and *in vitro* [16, 17] biological effects. Time varying EMFs consisting of rectangular or arbitrary waveforms (referred to as PEMFs), pulse modulated radiofrequency waveforms, particularly in the 15–40 MHz range (referred to as pulsed radiofrequency fields (PRF)), and low frequency sinusoidal waveforms (< 100 Hz) have been shown to enhance healing when used as adjunctive therapy [5].

Exposures in the vicinity of extremely low frequency part of the electromagnetic spectrum [18- 20] have been applied for various medical conditions, such as non-uniform bone fracture, skin ulcers, migraines and degenerative nerves [11]. Reduced healing time can produce significant cost savings and improve patient's care [21]. A pilot study on the effect of ELF pulsating magnetic field on soft tissue injuries was carried out by [22]. Several randomized clinical trials utilizing PEMF on joints and soft tissues have provided sufficient evidence on their effectiveness in accelerating healing of soft tissue injuries [23] as well as providing symptomatic relief in experimental subjects with arthritis [24, 25], osteoporosis [26], and bone [27] and joint conditions [28]. Accelerating the rate of healing [23] would reduce both the likelihood and effect of secondary complications. Up to date, research on wound healing is focused on the stimulation of cell growth, development of anti-infection treatment/agents and wound bed preparation. Wound bed preparation involves debridement and managing exudates. Wound debridement is the process of removing foreign materials or contaminated tissue from the wound bed until healthy tissue surfaces [29]. Multiple techniques for wound debridement are: surgical, conservative sharp, mechanical, high pressure fluid irrigation, ultrasonic mist, autolysis, enzymatic and larval therapy [30, 31].

Almost every biochemical reaction inside a living organism is controlled by enzymes. Enzymes are specific group of proteins with a catalytic role and are present in every organ and cell in the body. Specific and unique chains of amino acids constitute enzymes building blocks. Enzymes are neither consumed nor are their physical structure altered during any given reaction. The standard classification of enzyme is according to the Enzyme commission (EC) and constitutes of four digits separated by decimal points (e.g. EC 1.2.3.4), where the first digit refers to the classes of enzyme (Oxidoreductase, Transferases, Hydrolases, Lyases, Isomerases and Ligases), the second digit to a subclass, the third digit to sub-subclass and the fourth to individual enzymes serial number within its sub-subclass [32]. Official enzyme naming criteria are based on adding the suffix – ase to the name of the substrate. For example, the enzyme acting upon the substrate collagen is thus named collagenase (EC 3.4.24.3) [33]. Collagenase treatment provides at least two mechanisms to enhance cell migration: (i) collagenase itself and (ii) collagen degradation products [34].

There are many factors that can affect wound healing and cause improper or impaired tissue repair. One of these factors is wound infection by bacteria [35]. Infection of a wound may be defined as an invasion of organisms through tissues following a breakdown of local and systemic host defences [36]. Wound infection is the common and most troublesome problem within wound healing process [37]. Of particular interest are the infected wounds where bacteria or other microorganisms have colonized that cause either a delay in wound healing or a deterioration of the wound. Types of wounds include: burns, bullet/stab puncture wounds, pet/insect, snake bites, rust nails (tetanus), diabetes foot ulcer, bruising from an assault, amputation due to road side accidents or bombing. Bacteria seek to establish themselves in biological positions like an open wound to ensure their own survival and evolution [37]. Conventional treatment methods for wound infected with bacteria are drainage of puss collection, surgical removal of dead tissues and appropriate dosage of

antibiotics. However, drainage of puss collection is a problem for patients with blood disorder like leukemia and lymphoma. Surgical removal of dead tissues gives way to the entrance of bacteria from skin or environment to the surgical incision site [38]. Two common types of bacteria involved in infecting wounds are *Staphylococcus aureus* (*S. aureus*) and *Escherichia coli* (*E. coli*) [39, 40].

*S. aureus* is reported to be the almost-universal cause of furuncles, carbuncles, and skin abscesses, and worldwide is the most commonly identified agent responsible for skin and soft tissue infections which frequently begin as minor boils or abscesses and may progress to severe infections involving muscle or bone and may later spread to the lungs or heart valves [41]. *S. aureus* infections are common amongst people with frequent skin injury. 25% - 30% of health humans carry these bacteria in their skin or nose. It is the commonest bacteria to enter the surgical incision site. In addition, *S. aureus* is an important pathogen in the dairy farm industry as it causes mastitis in cows [42].

Wound infection caused by *E.coli* can easily be experienced by coming into contact with the feces, or stool, of humans or animals [43]. *E. coli* has been described as the second most common single pathogen involved in postoperative wound infections [36]. *E. coli* are the common cause of infection in surgical wound, especially those following operation in the abdomen where it is often mixed with other gut bacteria. It is the most common bacteria to enter the blood stream and causes a series of clinical events leading to a high temperature, circulatory collapse with low blood pressure and blood clotting. *E. coli* causes skin and soft tissue infection especially in people who have diabetes.

The use of ELF PEMF for selective control of cellular function [44 – 46] has added a new dimension to therapeutic intervention strategies. The characteristics of the EMF stimulation

therapy performed to date includes exposure levels [47, 48] and waveforms [49, 50], dose response pattern [51, 52], optimal exposure [53, 54] to static and varying magnetic fields [5, 55, 56], localization of stimulation and spatial orientation of the exposure system [57 – 59]. Major factors that can influence the response to magnetic-field exposure systems are in the likes of frequency and modulation, field uniformity, combination of coil system and their precise placement, field intensity and polarization, noise, vibration and temperature of conducting materials, voltage carrying wires and metal equipment, sham exposure, construction materials and the time schedule for the actual experiment [60].

In this research the effects of ELF PEMF exposures on specific agents that influence the process of damaged and infected tissue repair were studied and experimentally evaluated. These agents are: Collagenase enzyme, gram-positive bacteria *S. aureus* and gram-negative bacteria, *E. coli*. For the first time, the experimental evaluation of the effects of the entire range of ELF PEMF (2-500Hz) corresponding to magnetic flux density of 0.5-2.5mT is reported for the above mentioned agents.

## 1.2 Research Aims

Research aims for this project can best be presented in the following manner:

1. Experimental evaluation of the effects of the entire range of ELF PEMF exposure on specific agents that influence the process of damaged and infected tissue repair: Collagenase enzyme, gram-positive bacteria, *Staphylococcus aureus* and gram-negative bacteria, *Escherichia coli*.
2. Positive outcome of the research should determine the optimal ELF PEMF characteristics via its exposure efficacy upon inducing change in Collagenase

enzymatic activity, and decreasing the viability of selected bacterial culture of *S. aureus* and *E. coli*.

3. To demonstrate and provide evidence-based conclusions that ELF PEMF of optimal parameters can induce therapeutic effect on wound healing process.

### 1.3 General Objective

The general objective of this research is to investigate the effects of extremely low frequency (ELF) pulsed electromagnetic field (PEMF) on Collagenase enzyme activity and on the survival of the bacteria *Staphylococcus aureus* and *Escherichia coli*. This investigation consists of: a) experimental design and b) experimental evaluation.

### 1.4 Specific Objective

Numerous studies have shown that the application of PEMF to damaged cells can promote cell proliferation, increase the rate of healing, reduces swelling and bruising. However, future advances in wound healing needs to focus on affecting the agents that influence the processes of damaged tissue repair. Collagenase enzymes were shown to act more selectively on denatured collagen in devitalized tissues. The selectivity is beneficial as it keeps the vital tissue and growth factor crucial to wound healing intact. Collagenase can effectively digest collagen isoforms that are present in necrotic wound tissues. However, a very few studies have been undertaken to measure enzyme activities under influence of non-ionizing ELF PEMF radiation.

The significant increase of bacterial resistance to almost all currently available antibiotics has paved way to the development of *in vitro* exposure systems for studying the effects of magnetic fields on bacterial cultures. The outcome from these type of studies suggest that parameters like magnetic flux density, frequency and exposure duration of ELF

electromagnetic field (EMF) can negatively perturb functional parameters like cell growth and viability in bacteria. The object of importance for many experiments has been the gram-positive and the gram-negative bacterial culture of *Staphylococcus aureus* and *Escherichia coli*, respectively. However, almost all of these experiments pivots around environmental influences on human health and therefore deals with increasing exposure of man-made ELF fields generated from appliance with a frequency of 50Hz. Therefore, the focus has predominantly been on the effect of ELF EMF on bacteria adaptability corresponding to different time of exposure and magnetic flux density but at the single frequency of 50Hz.

Up to date researchers have used PEMF stimulators to promote healing, with the results varying significantly and there are discrepancies between the usages of PEMF parameters. Most of the laboratory-based exposure systems for studying ELF EMF effects on biological samples utilize electric coils to generate electromagnetic exposures. A larger volume of uniform field inside the coils setup can be obtained via well positioned pairs of coil in Helmholtz configuration. Previous results of ELF EMF on biological objects have been deemed controversial due to experiments not carried out in well-defined conditions. Extensive research still needs to be done to categorize the parameters required for optimal magnetic field conditions and average duration of effect at different laboratory settings in order to produce the best possible treatment. Couple of essentials required prior to evaluating the effect of magnetic field on a biological sample in order to increase the throughput of replicating results for statistical validation are: (i) calculation of the field's magnetic flux density at the center of the exposure system (location for the placement of biological sample) and (ii) visualization of the magnetic field and its region of uniformity in the vicinity of the biological sample. Realization of the above mentioned criterions prior to the actual hardware design and development of the exposure system is extremely important in terms of design flexibility and efficacy.



The above facts and reason entail that determining the optimal ELF PEMF exposure parameters that can modulate Collagenase enzymatic activity, and decrease the viability of selected bacterial culture of *S. aureus* and *E. coli* is vital in the development of efficient and non-invasive treatment of damaged and infected tissue and thus, wound healing promotion.

## 1.5 Thesis Composition

To document the details of this research, this thesis has been organized in the following fashion:

Chapter 1 presents an introduction to the research. This preamble includes research aims, and objectives. It also presents the motivating factors behind undertaking this study and briefly outlines the approach taken towards the aim of final outcome of this particular research.

Chapter 2 lays focus on the literature reviews and essential understanding of PEMF devices; its application, characterization and major limitations pertaining to experiments concerning ELF PEMF exposure on biological samples. Conducted literature survey also discuss the process of wound healing, conventional methods of treating wound and their limitations, bacterial infection of wound and their conventional treatment methods and limitations. Also, discussed are the integral agents that influence the process of damaged and infected tissue repair. These agents are Collagenase enzyme, *Staphylococcus aureus* and *Escherichia coli*.

Chapter 3 provides the design and development of the ELF PEMF system built on the basis of a Two-axis air core Helmholtz coil configuration capable of producing a uniform time varying magnetic field (magnetic flux density,  $B$ , 0.5–2.5mT over the frequency range,  $f$ , 2-500Hz). A brief theoretical analysis of the systems coil configuration has been documented.

Merit for using a Two-Axis Helmholtz coil system (2-Axis HCS) as opposed to the conventional One-axis (1-Axis) HCS is discussed by means of simulation results. Flow chart of the custom software program built to systematically evaluate the induced magnetic field distribution and its region of uniformity prior to commencing experimentation is provided along with simulation result which clearly illuminates region of field uniformity within 10%, 1% and 0.1% of the center field. Theoretical and experimental results are compared and steps taken for temperature control inside the ELF PEMF chamber have been discussed.

Chapter 4 reports an application of the lab built ELF PEMF system by studying the effect of varying parametric changes of ELF PEMF exposure on Collagenase enzyme that play a key role in wound healing. Concerned materials and methodology are presented. A comparative analysis of change in the enzymatic activity of the irradiated vs. non-irradiated Collagenase performed for selected frequencies and magnetic flux densities is provided. Results will reveal that Collagenase enzyme can be modulated at particular frequencies for ELF PEMF for magnetic flux densities between 0.5-2.5mT.

Chapter 5 reports two more applications of the lab built ELF PEMF system by showing the effect of ELF PEMF exposure in affecting the growth and proliferation of selected bacterial cultures of *Staphylococcus aureus* (*S. aureus* American Type Culture Collection (ATCC 25923)) and *Escherichia coli* (*E. coli* ATCC 25922) which plays vital role in infecting wound tissues. Concerned materials and methodology are presented. The viability of these bacterial cultures (number of live cells as colony-forming units (CFUs)) was measured before and after the exposures to quantify the effects of applied ELF PEMF on survival of the bacterium. Special trends emerging from experimental evaluation are discussed.

Chapter 6 presents a summary of the research contribution and also provides suggestions to

future works. This section is rounded up by a list of peer-reviewed publication yielding from this research project.

## **CHAPTER 2:**

# **LITERATURE REVIEW AND BACKGROUND UNDERSTANDING**

## 2.1 Overview

Biological effects of ELF EMFs are discussed in this chapter to present the current hypothesis on ELF PEMF mechanism and its impact on wound healing. ELF PEMF therapeutic systems are discussed in greater details in particular the advantages of using these systems for wound healing promotion. The design and constructed prototype of the PEMF system are presented along with their characterization. Special attention was given to the output module of the PEMF system (treatment coils system/exposure chamber) for reasons made apparent through this literature review. *In vivo* and *in vitro* PEMF systems are discussed along with their limitations and areas for improvement. Key concepts revolving around wound healing (types, process, treatment methods and limitations) for both normal and infected wounds are explained in considerable details.

## 2.2 Electromagnetic Field (EMF) Radiation

EMF can be termed as a field of force caused by electric charge in motion. EMF comprises of both electric and magnetic components and is associated with a definite amount of electromagnetic (EM) energy. Normally, electric and magnetic fields occur together and both fields weaken with increasing distance from the source. However, both these fields produce different effects on living organisms. Regardless of whether an appliance is switched on or off, electric fields will always be present. On the other hand, a magnetic field will disappear as soon as the appliance is turned off. Electric field between two points is created when there is difference in voltage between the two points. Higher potential difference correlates to stronger electric field. Magnetic field, on the other hand, is created due to current flow in a conductor. Higher current correlates to stronger magnetic field [61].

## 2.3 The Electromagnetic (EM) spectrum

The EM spectrum (Figure 2.1) is spectral band of various waves in terms of frequency or wavelength. EM wave interact with biological systems in terms of frequency and penetration depth of the wave in medium.

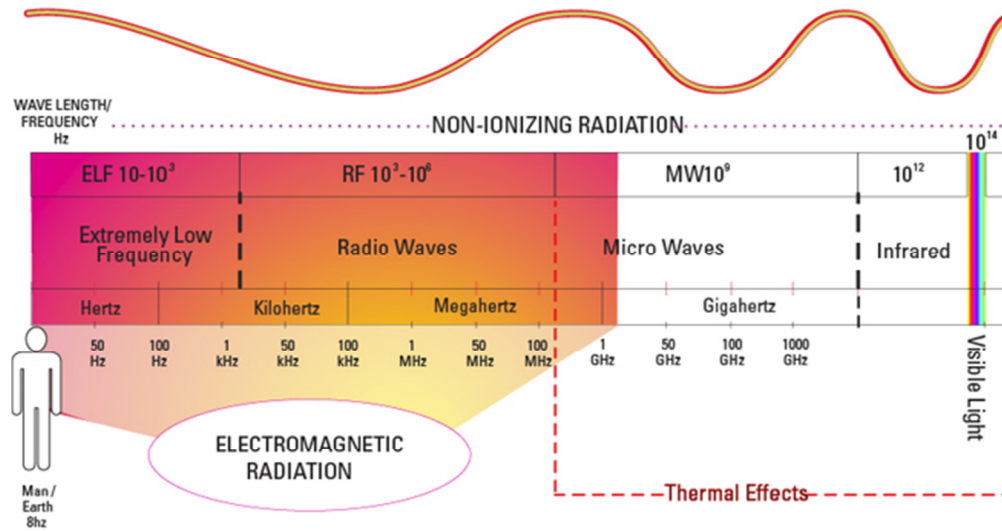


Figure 2.1: The electromagnetic (EM) spectrum [61].

Frequencies in a EM spectrum are categorized from extremely low frequencies (ELFs) such as the power line at 50 or 60 Hz, radio waves, microwaves, infrared (IR), visible light, ultra violet, X-rays to gamma rays based on increasing frequency of the wave. In electromagnetic spectrum, radiation from EM fields with high order of frequencies is classified as ionizing radiation. Low frequency EM fields whose quanta are insufficient to break molecular bonds are called non-ionizing radiation. Gamma rays, X-rays are examples of ionizing radiation whereas radiations from microwaves, radiofrequency fields and ELF are found at the relatively long wavelength and are classified as non-ionizing radiation. Non-ionizing radiation ranges from 0 to approximately  $3 \times 10^{11}$  Hz. Similarly, radiation above  $3 \times 10^{11}$  Hz is considered as ionizing radiation [62].

## 2.4 Characteristics of EM Wave

EM radiation produces energy that can be calculated as follows:  $E = h\nu$ , where  $E$  = energy,  $h$  = Planck's constant and equals  $6.626 \times 10^{-34} \text{ Js}$  and  $\nu$  = frequency, cycles per second or Hz. For example, radiation at 500Hz (upper limit of the ELF spectrum) would produce an energy equivalent to  $2.068e^{-12} \text{ eV}$ . EM wave consists of electrical  $\mathbf{E}$  and magnetic  $\mathbf{H}$  field components vibrating in phase and perpendicular to direction of propagation. The Maxwell's equation relates the electric and magnetic fields in different conditions.

### 2.4.1 Magnetic Field

Magnetic fields has two components namely Magnetic Force (F, or mmf), and the Magnetic Flux ( $\Phi$ ). Amperes law states that the total magnetic force, F, integrated along any closed path is equal to the total current enclosed by that path. SI unit of magnetic force is N. The unit of magnetic- field strength or magnetic-flux density is given in Gauss or Tesla (1T= 10,000G).

### 2.4.2 Magnetic flux

Magnetic flux ( $\Phi$ , in Webers) can be described vectorially, or in more physical terms, as lines. Flux lines always form closed loops. In any homogeneous region, flux lines are normal to the magnetic force equipotential surfaces. The spacing between flux lines indicates magnetic flux density (B, in Tesla). For any homogeneous region, magnetic flux density, B, is proportional to field intensity,  $\mathbf{H}$  (Amps/meter) and related by the following expression:  $B = \mu H$ , where  $\mu = \mu_0 \mu_r$ . The expression  $\mu_0 = 4\pi \times 10^{-7}$  is the permeability of free space or any nonmagnetic material and  $\mu_r$ , the permeability of a magnetic material relative to free space.

## 2.5 EMF Biological Effects

The well documented effect of EM fields is heating effect. The greater the absorption rate, the more likely that significant heat occurs [63]. Higher frequency and high intensity of EM field give rise to specific absorbance rate (SAR) effect. In this research, however, the effects of low intensity (0.5-2.5mT) and extremely low frequency (2-500Hz) pulsed electromagnetic fields were studied on the selected Collagenase enzyme and bacterial cultures. The mechanisms by which ELF fields affect a biological tissue are still not fully elucidated. However, a simple quantitative approach in understanding the mechanism of interaction of ELF electric fields and biological systems is presented in [64]. It has been shown that cells and tissues are affected by ELF magnetic field. However, not all ELF exposures lead to an alteration at cellular level. Some effects are only noted at discrete frequencies and amplitude of the magnetic field. Others depend on the strength, orientation and duration of the exposed field. The effects of ELF EMFs on biological media have been studied by many researchers using a variety of *in vitro* exposure systems [65-72]. ELF magnetic field therapy is considered as useful and beneficial treatment for different diseases, especially those involving skin and bones [12, 13, 73]. ELF PEMF stimulation has been investigated as a therapy for wound healing following results that PEMFs can promote healing by potentially increasing collagen synthesis, angiogenesis, and bacteriostatic [11].

## 2.6 ELF PEMF Mechanisms

A biological sample reacts to external stimulation through a complex series of specific and non-specific responses [74]. The specific response is determined by the physical nature of the stimulation, while the non-specific response depends upon the intrinsic features of organism system. Electrical signals form the basis of information transportation in the nervous system [75]. These electrical signals in the form of minute electric currents flow around and within the cells and are of critical importance for their normal functioning [75] and can accelerate



normal cellular function such as endocytosis [76]. PEMF perturb these currents and charges [77] and positively influence the process of cellular functioning. It has been suggested that PEMFs, by altering or augmenting pre-existing endogenous electrical fields, may trigger specific, measurable cellular responses such as DNA synthesis, transcription, and protein synthesis [78]. This adds further evidence to the fact that external non-invasive electric stimulation is a very powerful tool in augmentation of cells, tissue and organs. A well-established phenomenon in physics, ion cyclotron resonance (ICR) and ion parametric resonance (IPR) models were proposed, which state that ions resonate when exposed to certain combination of fluctuation (AC) and static (DC) magnetic fields [79]. A number of experimental observations also indicate an apparent interaction of weak ELF magnetic fields with neural tissues [80].

The fundamental physical properties of ELF PEMF and the mechanism through which these fields interact with a human body are at the microscopic level. Evidence suggests that cell membrane play an important role in transducing ELF signals [81]. From available literature the following logical events can be suggested: PEMF signal induces alternating electric signal to direct a series of magnetic pulses through injured tissues/cells where by each magnetic pulse induces a tiny electrical signal that initiates as a cascade of biochemical reactions which ultimately plays a role in the process of wound healing (Figure 2.2).

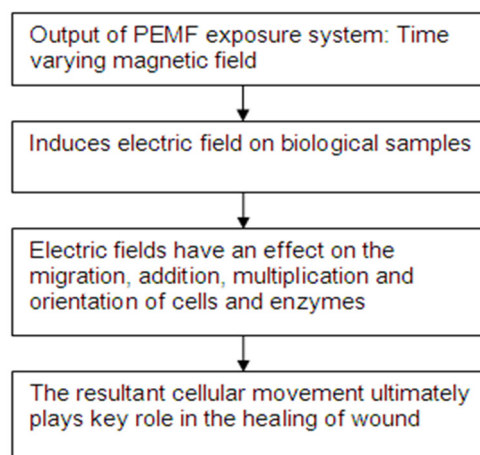


Figure 2.2: Suggested mechanisms of action of ELF PEMF at molecular and cellular levels.

## 2.7 Application of PEMFs in Wound Healing

Almost all diseases are the result of impaired cellular function. A healthy cell operates at a voltage between 70-110mV in order to produce ATP molecules (Adenosine Triphosphate), which are vital for a healthy body. A wounded cell, with voltage range between 40-50mV loses energy as there is not enough ATP available. Studies have shown that the application of PEMF radiation to damaged skin can accelerate re-establishment of normal potentials and thereby facilitate the process of wound healing [11, 13, 23].

EMF has been used over the past ten years to effectively treat various types of wounds and skin transplants [82]. Use of EMF therapy in rats resulted in rapid improvement of wounds incurred by burns. Most importantly, it was also observed that a decrease of microbial flora accelerated the healing process of wounds [83]. Most wound studies involve arterial or venous skin ulcers, diabetic ulcers, pressure ulcers, and surgical and burn wounds. Since cell involved in wound repair are electrically charged, some endogenous EMF signals may facilitate cellular migration to the wound area [84], thereby restoring normal electrostatic and metabolic conditions. The development of therapy that utilizes PEMF has resulted in a large number of clinical studies which supports the fact that PEMF help in blood circulation and stimulation of the immune and endocrine systems [85]. There is accumulating and substantial evidence that use of PEMF is beneficial in treatment of chronic pain associated with connective tissues injury and soft tissue injuries [86, 87].

PEMF devices have been accredited by the Food and Drug Administration (FDA) (USA) for the relief of acute and chronic pain and the reduction of edema and other wound symptoms of wounds from post-surgical procedures. PEMF therapy has also been accredited for the treatment of fractures and is now part of the standard armamentarium of the orthopedist [88]. A meta-analysis [89] conducted on clinical trials using PEMF on soft tissues, showed that

PEMF was effective in accelerating healing of skin wounds [90]. PEMF signals have demonstrated the acceleration in the production of growth factor at various stages of tissue repair [91]. Post-surgery application of PEMF can accelerate healing in two ways: (i) by reduction time in the inflammatory phase of healing and (ii) from acceleration of, e.g., collagen production in later phase of wound healing.

Wounds in diabetes patients frequently exhibit a decreased inflammatory response, fibroblast proliferation, and collagen deposition, ensuing in wounds that have reduced tensile strength [92]. It has been reported that PEMF stimulation decreases the doubling time of fibroblasts and endothelial cells, and induces differentiation of skin fibroblasts in culture [93]. It has also been shown that *in vitro* PEMF exposure favors the production of collagen by fibroblasts, and *in vivo* enhances the tensile strength of scar tissue in rats [94, 95]. The increased tensile strength of the scar tissue is a result of the increase in synthesis, alignment, and maturation of collagen [96]. The application of electromagnetic fields, configured to enhance  $\text{Ca}^{2+}$  binding in the growth factor cascades involved in tissue healing, achieved a marked increase of tensile strength at the repair site in this animal model [97]. Studies have also demonstrated that PEMF application increased Achilles' tendon repair in a rat model by approximately 70% [98]. PEMF with 20 Hz pulse at 4 mT was used by [3], for 30 min twice a day for 10 days, after surgery in treatment groups of rats. Results from the study showed that PEMF treatment decreases wound-healing time and increases the tensile strength of scar tissue.

Studies show that increased collagen synthesis, angiogenesis, and bacteriostatic are some mechanisms by which PEMFs may contribute to wound healing [93, 99]. Prevention of tissue necrosis in response to a standardized ischemic insult, suggest that noninvasive angiogenic stimulation by PEMFs may be beneficial in preventing necrosis, ulcer

formation, and amputation in diabetic patients. It is possible that in chronic wounds, delay of wound healing is a result of defects in the inflammatory and proliferative phases and that electrical stimulation results in restart of these phases. Reports suggest that electrical stimulation increase fibroblast functional capacity, collagen synthesis, and induction of wound re-epithelialization, and thereby accelerates the process of wound healing [100]. Therefore, it is probable that PEMF promote angiogenesis [101, 102] and as a result improve oxygen and nutrition supply to the wound. Alarming concern in wound healing is the impeding problem in the treatment of bacterial wound infection. This is largely due to the bacterial resistance to current antibiotics [103]. This have however, prompted researcher to conduct *in vitro* studies with the objective of studying the effects of time varying magnetic field on bacterial cultures [69, 104-111] but predominantly at a single frequency of man-made frequency, i.e. 50Hz [107].

Several randomized clinical trials using PEMF on soft tissues and joints showed that PEMF were effective in accelerating healing of skin wounds [112, 113] and soft tissue injury [114, 115]. Results of a double-blind study Stiller et al., 2006 [116], showed that pulsed EMF PEMF stimulation promotes cell activation and proliferation by an effect on cell membranes, particularly endothelial cells. Since skin wounds have unique electrical potentials and currents, stimulation of these electrical factors by a variety of EMFs can aid in the healing process by causing dedifferentiation (i.e., conversion to a more primitive form) of the nearby cells followed by accelerated cell proliferation [101]. Additionally, PEMF increases the rate of formation of keratinocytes cells in partially healed skin wounds [117].

PEMF have been shown to promote healing when used as adjunctive therapy for a variety of soft-tissue injuries [118]. It was also demonstrated that specific changes in the field configuration and exposure pattern of low-level electromagnetic radiation (EMR) can result in

highly specific biological responses [119, 120]. Conducted laboratory studies on animals and cell cultures have revealed that exposure to weak magnetic fields might affect several biological processes, like alteration enzyme levels and the rate of movement of various chemicals through living tissue [121]. A powerful means of understanding the unknown effects of proteins upon non-thermal ELF PEMF exposures is by studying the effect of irradiation on protein activity (molecular level of interaction). Proteins are the macromolecules found in a living cell and play a crucial role in almost every biological process. The effects of ELF PEMF exposure on proteins were analyzed within the framework of this research project [122, 123]. As an application to ELF PEMF device, the focus was on enzymes, which are a specific group of proteins crucial in accelerating metabolic reactions in living organisms. In other studies isolated aqueous enzyme solutions were also taken as models to determine if external radiation could influence the selected biological processes [124, 125].

## **2.8 Therapeutic ELF PEMF Systems**

Traditional methods for treating certain injuries to a body (e.g., humans, animals) involve setting and immobilization of the injured member to allow natural healing of the injury. Often, it is anticipated that natural healing will restore damaged structures to their original uninjured condition without substantial inconvenience to a patient. Traditional problems in injury treatments have been associated with the inability of the patient's body to heal correctly or rapidly resulting in the inability of the healed part to regain its full strength. These problems are especially acute in patients with suboptimal health and reduced healing capacity such as elderly, immune compromised and patients with diabetes or multiple disorders. Attempts to address these problems and to promote more rapid healing have led to the therapeutic usage of PEMF.

The benefit of pulsed electromagnetic field therapy has been shown to cover a wide array of conditions, with well documented trials carried out by hospitals, rheumatologists and physiotherapists. Pulsed electromagnetic therapy is considered a common standard of care and is a reimbursed treatment not only in the US, but also in the UK and the European Common Market. US Medicare and Medicaid also reimburse for bone growth stimulation as well as the treatment of chronic stage III and IV wounds. Currently, the technology is being evaluated by major pharmaceutical manufacturers for several new products. The New Technology Committee of the American Society of Aesthetic Plastic Surgeons has evaluated and approved the PEMF treatments for edema reduction, accelerated healing and post-operative surgical pain.

There are several electrical stimulation therapy devices, approved by the FDA, that are widely available to patients for use. Interest in the therapeutic use of electromagnetic fields has grown over the past two decades since PEMF therapy gained approval from FDA for the treatment of human patients with non-uniform fractures and congenital pseudoarthrosis [126]. PEMFs have as inherent advantage over DC systems in that the electromagnetic signal penetrates the dressing and tissue involved. PEMF interact with electrically conductive elements in tissue, resulting in induced currents. Use of PEMF has been incorporated into the treatment of tendinitis in both humans [127] and horses [128]. In addition, PEMF has been shown to enhance wound healing in dogs [129]. Relief from chronic pain has been a common finding associated with PEMF treatment in human patients [130]. Selective control of cell function by applying weak, time-varying magnetic fields has added a new and exciting dimension to biology and medicine [126].

There are two [131] different non-invasive methods for application of PEMF stimulation to biological system: (i) capacitive coupling and (ii) inductive coupling. Capacitive coupling

constitutes of placing opposing electrodes in direct contact with the skin surface surrounding the tissue of interest. On the other hand, inductive coupling does not involve direct contact with the skin surface. The advantages of therapeutic PEMF systems are manifold. Few of them are provided below:

- No direct contact of electrodes with the wounded area- this is extremely important since duration of treatment can give considerably rise to the rate of bacterial wound infection. Also, patients are not subjected to any pain during PEMF treatment.
- Non-invasive (no skin contact) form of advanced treatment where the time-varying magnetic field of the PEMF induces an electric field, which in turn produces a current in the body's conductive tissues [131]. PEMFs noninvasive nature is of utmost important for treatment purpose for those patients who have bleeding disorder.
- FDA approved the usage of PEMF for treatment [132].
- NASA scientists assayed all forms of electric and electro-magnetic devices alleged to restore tissues after injury and found PEMF up to 4 times better than any other device [133].

PEMF therapy induces a field effect, not a direct electric effect on the wound. PEMF are usually low frequency fields with very specific shapes and amplitudes and do not exhibit the complications of contacts of electrodes. In both *in vivo* and *in vitro* models, a wide variety of PEMF signals and configurations have been used, with magnetic field intensities ranging from a few  $\mu\text{T}$  to several mT. Additionally, they can be applied in the presence of a cast or wound dressing and therefore significantly reduce the risk of wound healing infection [134]. Several studies have assessed the efficacy of PEMF therapy in the healing of pressure ulcers [135], which is one of the most common complications in health care settings [136].

The invention by Haines et al. [137] lead to a device that can produce time-varying magnetic field and involves generating pulse in a frequency range of 1Hz-100Hz at amplitude of 1-15V. A specific coil of 329 turns of 22 gauge wire with a voltage of 12.5V at 15 Hz has been used to treat soft tissue damage. This set up can be altered by various combinations of wire size, turns and voltage to produce magnetic flux of 0-6mT at coil means. A battery-driven portable and power-efficient non-invasive apparatus for therapeutic stimulation of both tissue and bone was invented by Griffith [138]. The treatment signal generated by the apparatus was a sinusoidal from 5-25 Hz, having a burst width of about 1-10 milliseconds. Source of battery power used was from 10-40 volts and comprised of a volume of 2-6 cubic centimeters. A low frequency portable PEMF system has been described by Stiller et al. [139] to enhance healing of recalcitrant venous ulcers. The transducer (output coil of the system) utilizes an air coil system. This particular system was designed by Geomed Inc. and delivered bidirectional, quasi-symmetrical magnetic stimulus, in contrast to more frequently used unidirectional signals. This is one of the designs that give notable importance to the safety issue in using the device.

Inventions of a magnetotherapy apparatus where magnetic fields of opposite polarity are generated and cumulatively interact for deeper magnetic field penetration have been claimed by Ostrwo et al. [140]. No mention is given about the input parameters necessary to build the air core coil system. More on the development of PEMF device using coil system performing bi-phasic operation can be found in [141]. However, the drawbacks of these designs are its lack of the software support in setting up an efficient combination of parameters for achieving the desired outcomes. Nothing about coil position has been mentioned and therefore their effect on the production of targeted magnetic field remains unknown.



Efforts have been made by researchers in presenting fundamental and practical aspects of therapeutic use of PEMF devices [132, 142]. Since they serve different objectives, comparison between available devices and their applications become difficult, and a need for universal standardization of their optimal performance becomes indispensable. Detailed discussions regarding system architecture of these devices still need to be profoundly looked upon. PEMF devices discussed above and in general are not easy to repeat or reproduce in different laboratory settings and therefore, a chance for parametric generalization becomes unattainable. The results obtained from within these experiments [137,140] have mostly been used by the concerned researchers in an order to solve particular issues pertaining to specific needs.

Improvement to existing PEMF designs also becomes eminent due to the plethora of electrical connections that go inside these devices. Simplification of PEMF circuits are inevitable since fewer electrical connections will make them more reliable and allows less time for trouble shooting and thereby depletes the necessity of professionals to handle the device. Great number of PEMF devices that use Microcontroller/Microprocessor and/or signal generators to produce PEMF signal resembles complex architecture and a network of electrical connections that ultimately lead to more power consumptions.

During the last decades, therapeutic benefits of PEMF have led to extensive research in cell and animal models that have helped to reveal some important insight into the biological effects of PEMF in the form of anti-inflammatory and chondroprotective mechanism, an example of which is an increase in growth factor synthesis [39]. Therapeutic efficacy of PEMF therapy depends on a number of factors, such as age, general health and gender as well as on the stage of disease [143]. With positive reports in the literature documenting PEMF as an effective therapy, its wider adoption as an adjunct therapy seems inevitable.

Bioelectromagnetics is the study of the interaction between non-ionizing electromagnetic fields and biological systems. PEMF have been used as a therapeutic agent over the last 40 years [11, 139]. Difficulties in bioelectromagnetic research include the inability to reproduce and replicate work conducted in other laboratories. Lack of concrete mechanisms of actions has also impeded therapeutic related research [20]. Through continued, research and more concrete mechanism of action, therapeutic value of ELF magnetic fields is set to become a mainstream intervention [11].

## 2.9 PEMF Device

Table 2.1 provides a list of existing ELF PEMF systems and their operational parameters (frequency,  $Hz$ , and magnetic induction,  $T$ ). Advantages of the available systems along with examples of their therapeutic applications have also been included.

Table 2.1: Advantage of existing ELF PEMF system.

PEMF System	Frequency Range (Hz)	Magnetic Field (T)	Advantages
MRS 2000 + Designo (Magnetic Resonance Stimulator)	0.5-25	5-70 $\mu$	Available for home use/Supporting therapy for pain relief and wound healing
Bemer	33	3.5-100 $\mu$	Convenient for Home users/ Sports people and coaches/ Animal owners/ Veterinary Surgeons
QRS (Quantron Resonance System)	0.3-1000	4-40 $\mu$	Appropriate for general health maintenance / Specific health conditions
Magnopro	2-1,000	1 -136 $\mu$	Benefits athletes and patients with less complicated health problems
Ondamed	0.1-32,000	500 $\mu$ -50,000 $\mu$	Convenient for health care provider
PMT- 100 Office Model	1-50	192mT/pulse	Appropriate for use with practitioners
PMT- 100AT	1-50	192mT/pulse	Extremely suitable for Equine use
PMT- 100P	1-50	192mT/pulse	Convenient for athletes and trainers

Large variety of commercially available PEMF devices and the plethora of different techniques [144-146] employed by researchers, make it difficult to compare their physical and engineering characteristics and thus present a major obstacle when attempting to analyze the putative biological and clinical effects obtained when different devices are used [85]. Therefore, standard trend in literatures while describing a PEMF device is actually through its exposure system commonly referred to as PEMF exposure system.

**PEMF Device:** A device with coils as output transducers, receiving pulsed current as input to produce pulsed electromagnetic field (PEMF) as an output. A PEMF exposure system consists of three modules (PEMF waveform generator, Coil driver circuit and Treatment coil system) [131] as can be seen in Figure 2.3. Of note, the treatment coil system module is typically referred in literatures as the PEMF exposure chamber.

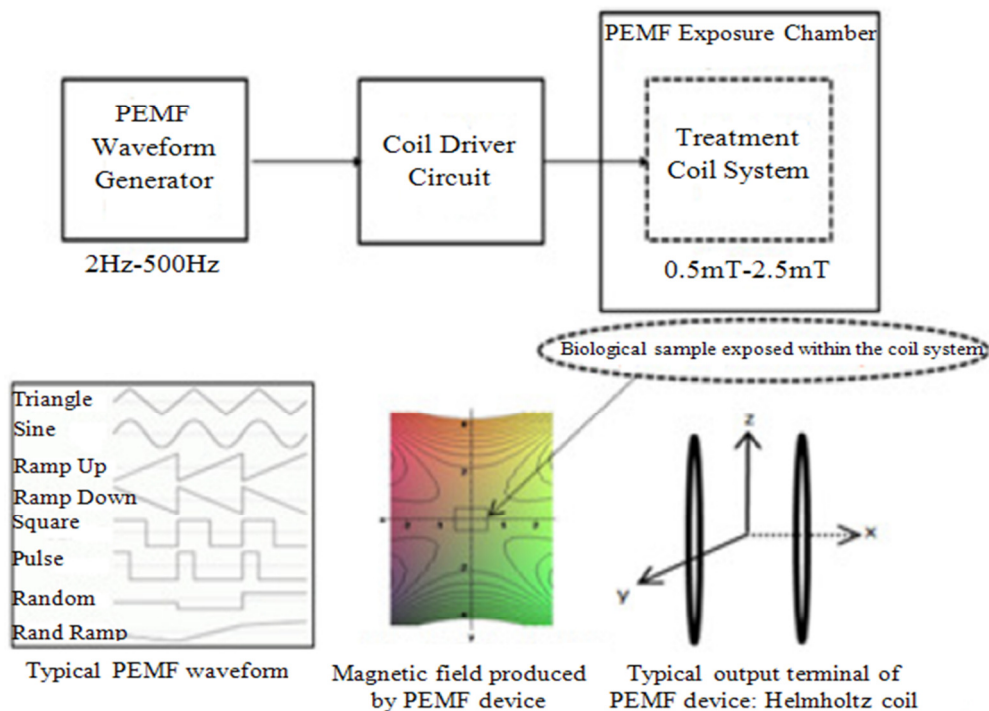


Figure 2.3: Block diagram of a typical PEMF exposure system: Three main modules of PEMF system, typical PEMF waveform, output terminal of the PEMF device and simulation of the corresponding magnetic field profile produced by the output coils [147].

***PEMF waveform generator:*** The first module is the PEMF waveform generator. Most of human studies that have been conducted and investigated upon are that of ELF PEMF exposures at 50/60 Hz. Microcontrollers are mainly used for portable PEMF devices [148]. However, for lab oriented research, standard electrical and electronic components are preferred so that the same procedure can be conducted in other laboratories and standardization be maintained. In most cases a commercial programmable function generator can readily be used for creating the desired PEMF signal [149].

***Coil driver circuit:*** Assigned signal from the waveform generator proceeds to the second module, which is a coil driver circuit. This circuit typically has a voltage to current converter coupled with a current amplifier between the waveform generator and the coil in order to amplify the production of pulsating current required by the network of current carrying treatment coils systems (output module). Preferred embodiment of the coil driver circuit may comprise a solid state switching circuit [150]. In that case each coil pair or axis is usually independently controlled through a dedicated power supply. The solid state switching circuit may comprise any solid state switching elements, e.g., transistors. Transistors may be of any type including bipolar transistors, and/or field- effect transistors. The resultant switching circuit would then switch electrical power from a power supply to provide a periodic electric current to a PEMF coil. It is important to note that, the frequency of the produced periodic electric current in these cases depends on the pre-set value of the waveform generator (module 1). In this study, two field-effect transistors in the form of N-Channel Power metal-oxide-semiconductor field-effect transistor (MOSFET) IRF 520, one between each pair of coils and the power supply were used. As a result of this setup, the magnetic vector generated by each coil pair could be regulated to complement other coil pairs in providing a designed uniformity over the specified sample volume.

**Treatment coil system/exposure chamber:** After the pulsating current reaches the treatment coil system, it produces PEMF of a defined magnetic flux density corresponding to a particular frequency. Applied PEMF at frequency range 2-500Hz and magnetic flux density range 0.5-2.5mT were studied in this project. Generated ELF PEMFs were used to expose biological model examples [122, 123, 147, 151].

Typical output module consists of two pairs of Helmholtz coil (Figure 2.3). A conventional understanding of the Helmholtz coil setup for a single axis system is shown in Figure 2.4, which consist of two identically layer coils, wired in series, with a specific geometry where the mean radius is equal to mean coil spacing. The pair of coils are centred along the axial axis,  $x$  and on either side of the origin at point  $O$ . When wither AC or DC power is applied to the coil geometry, a magnetic field volume is produced in which uniform conditions exists.

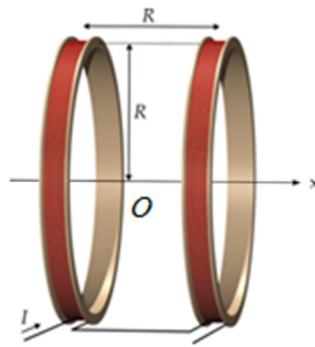


Figure 2.4: A typical output module of a PEMF device in form of a pair of Helmholtz coil [152].

The governing equation of the produced PEMF from the coil configuration shown in Figure 2.4 is expressed in terms of Biot-Savart Law (2.1) (Appendix A):

$$B = \frac{2\mu_0 N I R^2}{2(x^2 + R^2)^{3/2}} \quad (2.1)$$

where,  $B$  = Magnetic flux density (T),  $I$  = coil current (A),  $R$ =coil radius (m),  $x$  = coil distance on axis, to point, in meters,  $N$  = number of wire loops and  $\mu_0$ , permeability constant,

$$\mu_0 = 1.257 \times 10^{-6} \text{ T.m / A.}$$

Coil configurations of greater complexities are sometimes necessary to suffice for specific applications. Systems that consist of two (biaxial) [153] or three [145,154] (triaxial) coils pairs are often required. Equation for magnetic field for coils more than two centred along a common axial axis can be obtained by using superposition principle.

## 2.10 Characteristics of PEMF Device

There are a number of experiments that have been conducted using the devices based on the concept of electromagnetic field exposure. In [155] and [156] experiments were conducted to observe the effect of therapeutic EMF on mice with mammary carcinoma. These experiments showed the positive influence of magnetic field, which significantly reduces the growth of tumor [157] and increases the length of survival. In addition to these experiments, it is possible to use PEMF stimulation along with drug therapy. In [158] the effectiveness of this approach was established for experimentation with rats. Despite these encouraging results from the PEMF exposures, there are conflicting results which can significantly relate to different characteristics of the PEMF exposures. The significance of describing all the elements of the inductively coupled PEMF and biological system while rounding up experimental studies is yet again emphasized by the contradictory results seen between skin wound healing models from Ottani et al. [159] and McGrath et al [160] who have appropriately failed to depict the orientation of the PEMF coil. Coil orientation has been theoretically proven to induce different stimuli for cell cultures [161]. Important elements that can influence the responses to field exposure are discussed below:

### 2.10.1 Frequency

ELF displays frequencies at the lower end of the electromagnetic spectrum from 6Hz up to 500Hz [11]. According to another literature, electromagnetic fields, waves and impulses which occupy the frequency band between 3Hz to 3 KHz, have been termed as extremely low frequency (ELF) [131]. Most of the human studies deal with increasing exposure of man-made ELF fields generated from appliance with a frequency of 50/60Hz [69, 105]. Experiments concerning bacteria adaptability corresponding to PEMF have also mostly been carried out at 50Hz [106, 107, 111, 162].

### 2.10.2 Waveform

Typical PEMF waveforms have been shown as a part of Figure 2.3. PEMF waveforms are produced as an output to the coil driver circuit module of the PEMF device and the response to this signal by the treatment coil (3<sup>rd</sup> module of the PEMF device) results in a time varying magnetic field which is then used to expose biological sample of interest which are usually placed at the center of the coil system. A variety of waveforms has been used in the research of the possible biological effects of ELF and very low frequency (VLF) magnetic fields. Because of the nonsystematic use of the field parameters and experimental organisms by different authors, it is not known whether the effects reported are specific to the frequencies and waveforms used. Therefore, there is a need to experiment with standard PEMF waveform (Figure 2.5), so that any they can be easily replicated at other laboratory settings and a means of standardization could then be achieved. In that vein, an experiment by [163] compared sinusoidal, square, unipolar square and pulsed waveform to distinguish the biological effectiveness on chick embryo at 10Hz and 100Hz. The waveforms used are shown in Figure 2.5. Of note, a square wave is one example of a pulse wave with 50% duty cycle. A pulse wave on the other hand might have varying duty cycle.

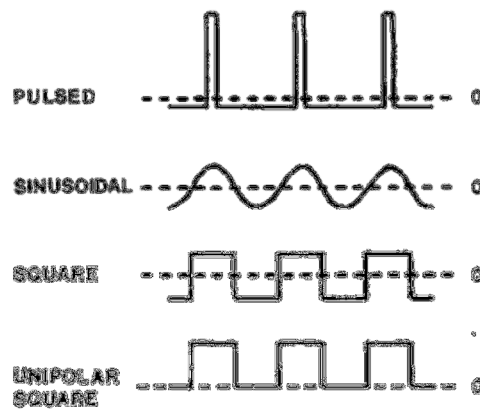


Figure 2.5: Different waveforms used on a trial basis [163].

Results from the above mentioned experimental study showed that only the unipolar square wave could demonstrate an effective change in the development stage of the embryo whereas fields produced as a response to the other waves were apparently ineffective. A 20 Hz square wave was used by [23] in order to demonstrate that PEMF accelerates wound healing in the skin of diabetic rats. Unipolar waveform was used by [164] to show their effectiveness for long period experiments [165-166]. Similar waveform was also found to be effective for the treatment of hyperlipemia [167]. In this research, the above mentioned reasons contribute towards the usage of a unipolar square wave in the form of a signal produced by the PEMF waveform generator.

### 2.10.3 Coils and Coil System

Investigations of bioeffects induced by low frequency magnetic fields resulted in construction of various types of exposure devices with different geometry of coils configuration [144-146]. The integral component of these types of devices is a treatment coil system selected in order to maximize the uniformity of the magnetic field density in the central region between the coils. Therefore, this work extensively stressed on the coil setup of the PEMF exposure system. However, these coils might create some new problems when introduced in the experimental environment. These problems can be in the form of electrical (ohmic) heating effect with the coil and presence of enamels and other insulating materials with unknown



biological effects [57].

Almost all laboratory-based experiments utilized electric coils to generate electromagnetic radiation to expose biological samples. Arranging two planar circular coils in a coaxial and parallel manner to one another and connecting them electrically, can result in a magnetic field being adaptive in the region between the coils. In cases, where the separation between the coils is equal to the coil radius, the magnitude of the magnetic field is independent of a position along their common axis (except at points near the coils) [59]. Most widely used exposure system is the Helmholtz system of two rectangular or circular coils that provides a fairly good uniformity and is frequently used for exposing biological systems such as cells [168-170] but only over a restricted central region between the coils [59]. Therefore, the absolute necessity for a larger volume of uniformity, with respect to the overall size of the system, has given rise to more alternative coil systems [171-173]. Extension of the region of uniformity around the center of symmetry correlates to the vanishing of spatial derivative of the magnetic fields along the coil axis around the center of symmetry. This then results in the desired uniform field. Generally, Helmholtz designed coils are separated at a distance such that the first and second spatial derivatives of the applied fields are zero at the center of the coil system [57]. A much larger volume of uniform ELF EM field inside the setup results from the assembly of increased numbers of well-placed coils [174]. Subsequent work demonstrated that several higher order derivatives can be zeroed using assemblies of three, four, or five coils [57]. Some basic coil reference system commonly used in PEMF therapy is shown below in Figure 2.6 [131]:

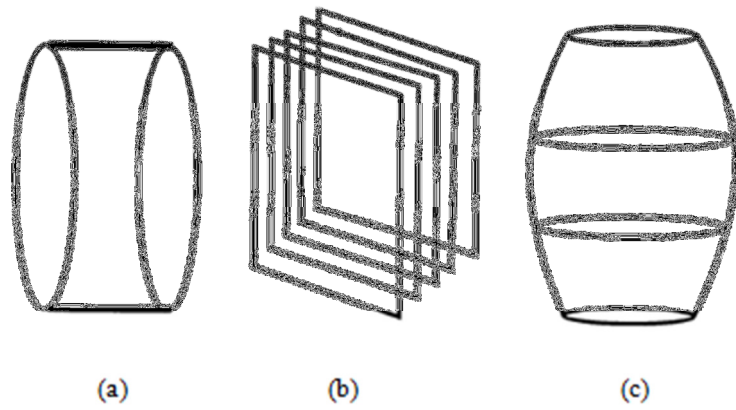


Figure 2.6: Commonly used coil references for ELF PEMF device (a) Helmholtz coils (b) Ruben's coil and (c) Fransleau-Braunbeck coil [131].

Design based on acrylic polymer coil support structures and twisted pair bifilary coil windings have been employed to fabricate several different systems for the exposure of cell cultures to magnetic fields [146]. Usage of bi-phasic coil PEMF transducer for generating PEMF stimulation signals can also be found in [175]. The strength of the magnetic field depends on the magnitude of this pulsating current. For a coil with ferromagnetic core, the inductance will not remain constant but will change with the current getting through the coils and result in distortion of the pulsating current from the power supply via production of higher frequency component. To prevent this, air core coils may be used.

Stimulation effect of induced electric field in the coil depends on coil size, waveform and duration [176]. Coil shape and size are essential for effective stimulation and therefore are mainly designed for stimulation purpose as well as for generating uniform magnetic field. To deliver focal magnetic field, numerous authors have utilized several techniques on coil designs [177]. A system consisting of appropriately spaced four square windings as described by Merritt et al. [172], offers an excellent uniform field to coil volume ratio [146, 178]. Few systems and studies focused on the capability of producing highly uniform magnetic field have been proposed. However, most of them are based on Helmholtz two-coil system [5, 179]. Cakirgil et al. [180] makes a comparison of two-coiled and four-coiled systems and concludes that a four-coil system [172] is much effective than a two-coil system in terms of

PEMF treatments. When four or more coils are used, they can be combined in pairs and arranged such that the induced fields add constructively inside the regions between the pairs of coil. Gottardi et al. [153] introduced a four coil exposure system (Tetracoil) for *in vivo* and *in vitro* experiments to produce a highly uniform magnetic field. These four coils comprises of two couples of circular coils satisfying a spherical constrain. The design also sufficed for accessibility for biological experiments. However, the region of field uniformity with respect to the overall size of the system was not satisfactory.

Key factors determining the geometrical shape of the coils are:

- Absence of sharp corners allowing circular coil to produce a highly uniform magnetic field [153], and
- Fundamental theorem that states that a uniform spherical current shell will produce a complete uniform magnetic field, throughout the enclosed volume [181].

Toroid coils are inefficient and have relatively weak field strength. Another source [205] claims that the square-shaped coils in Merritt's system possess several advantages over the circular coil of classical Helmholtz coil pair. Among the mentioned advantages were: (i) square coil creates a uniform field of approximately square boundaries, which are better suited for practical objects such as cages with animals and (ii) fabrication ease of the rectangular coils and their support structures. A pilot study by Hodgkinson [183], evaluated different methods for inducing a PEMF stimuli within bone cultures. The study conducted have indeed concluded that air coil systems [5, 139, 184, 185] were superior to other methods of PEMF stimulation when considering many factors such as coli size, and the consistency of the produced magnetic field. Thus, air-core coil arrangements have been traditionally opted to

guarantee a certain spatial distribution of electromagnetic fields, when fed by an electric current [70].

Analytical analysis and computational modeling of the ELF uniform magnetic field exposures, prior to the actual hardware design and development of the exposure system is extremely important in terms of design flexibility and efficacy. Chapter 3 compares the lab-built 2-Axis HCS with a conventional 1-Axis HCS. Results discussed in Section 3.2.3 helps to validate the reasoning behind the particular choice of coil orientation for this project.

#### 2.10.4 Magnetic Field Uniformity

The homogeneity of the magnetic field,  $H$ , is a measure of the variability of the magnetic field within a defined region of space. Different approaches have been taken to quantify  $H$ . One of the most common ways is to define the non-homogeneity of the field in terms of the variation in magnetic flux density at a given point in space within the volume of interest, regarding the value of magnetic induction in the central point of the coil system [186]. Hence, that definition for the magnetic field homogeneity considers that it is a point-dependent index, incapable of providing global information about the homogeneity within the volume of interest, and therefore, the above mentioned definition is not useful to describe the whole volume of interest.

In magnetic-field exposure system, acceptable tolerance of magnetic field for most *in-vivo* and *in-vitro* exposure systems have been considered to be less than  $\pm 10\%$  and  $\pm 5\%$ , respectively. Electric-field non uniformity of  $\pm 10\%$  has been considered acceptable for biological studies [172,187-188]. The actual magnetic field homogeneity should be preferably measured in order to rule out any nearby ferrous or conducting structures that can destroy homogeneity calculated in isolation [172]. A study carried by [82] showed that field generated by Electromagnetic Therapeutic Apparatus Kenkobio®, was neither uniform nor

homogeneous and that it varied with position. Also, most of the studies report the value of magnetic flux density in the center point [23] of the exposure system, where the biological sample is to be placed. However, biological samples are not at all times confined to the center. They might extend horizontally or vertically. Therefore, uniform and homogeneous exposure of the biological media to the magnetic flux density must be for the entire body but not only confined to the center. To have a detailed understanding of the field uniformity and the cutting of the magnetic flux lines, field visualization prior to experimentation is extremely important for experimental standardization and replication. Shown in this research through analytical results (Section 3.2.3), is the uniformity of the magnetic field within 10%, 1% and 0.1% of the center field for not only at the center but also at various vertical heights of a centrifuge tube which was used in containing bacterial cultures exposed to ELF PEMF. Theoretical and experimental results were also compared and presented in Section 3.6.

#### **2.10.5 Field Polarity and Intensity**

In general, if a periodic current flows through the coil in one direction, then it would create a pulsed magnetic field emanating from the coil. However, if the current alternates back and forth it would create an AC magnetic field. These concepts are illustrated below:

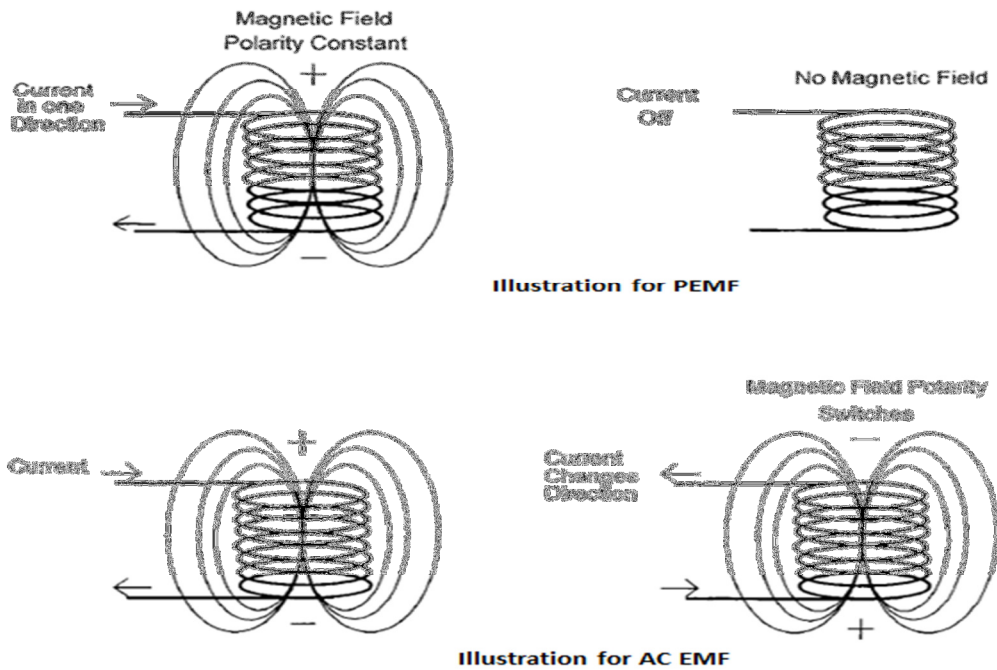


Figure 2.7: Field polarity illustration for AC EMF and PEMF [189].

The plus and minus signs over the coils represent magnetic polarity, not electrical. The plus sign customarily signifies south polarity and the minus north polarity. However, it should be noted that an electric field is also present which pulses and alternates at the same frequency as the current, hence the term electromagnetic field (EMF). Application of circularly and linearly polarized magnetic-field exposure can have significantly different properties which have not been compared thoroughly in literatures [188]. Circularly polarized magnetic field has been used for studies of human, *in-vivo*, and *in-vitro*. This magnetic field can be obtained by placing two coil systems' axis in perpendicular position. If the angle between those two coils is not exact  $90^\circ$  [172], a mixture of linear and circular polarization which is called elliptic polarization will be generated. Then by having phase-shifted current sources, circularly magnetic field can be generated.

The strength of the magnetic field generated is directly proportional to the number of conductor turns in the coils, the applied current, the physical size and the inter-coil spacing. Different researchers have reported the use of various value of magnetic flux induction with

different combinations of ELF and have obtained varying results. Phenomenon of these varying results has been further explained in Section 2.11. It is important to note that, magnetic fields that have been used for exposure systems [190] have shown that magnetic flux densities of 0.5mT, 1.0mT, 1.5mT, and 2.0mT were all effective at ELF for stimulating anabolic activities in cartilages explants.

### **2.10.6 Temperature Concerns**

A byproduct of ELF PEMF production through current carrying coils is the resistive heating of the coils. Resistive heating can elevate the temperature inside the exposure chamber and eventually proceed to transfer this heat to the biological sample itself. Efficient design to combat this is to develop a coil system that will correspond to the usage of low current to create higher magnetic flux densities. In this project, the temperature was efficiently controlled (Section 3.7) to ascertain that the heat generated by the current carrying coils did not affect the experimental data upon ELF PEMF exposure to biological sample in the liquid media.

### **2.10.7 Sham Exposure**

Background and stray magnetic fields are typically  $0.2\mu T$  or less. By using quadruple coil system, this sham exposure can be reduced. Gotardi et al [153] used double wrapped coils, in order to obtain wound (active) or counter-wound (sham) configuration. However, the magnetic field does not disappear entirely using this method. On the other hand, another way to control the sham condition for a developed ELF PEMF was used by McKay et al [191], and created by turning on all equipment but without any presence of current through the single wound coils.

### **2.10.8 Construction Material**

Conducting materials, voltage carrying wires and metal equipment like metallic springs near our system can reduce the strength of electric field to up to 20%. Additional consideration for

the design of EMF exposure system is the pre- sense of ferromagnetic particles in the experiment. Ferromagnetic particles may cause interaction between electromagnetic field with living organisms [192]. Therefore, any contamination by ferromagnetic particles should be cleared [172]. On that vein, in this research, the design and constructed ELF PEMF exposure chamber along with the cuvette holder for containing biological sample and other concerned structure used as accessories in measuring the magnetic flux density were all made of acrylic.

### **2.10.9 Time Schedule**

Time of experiment as well as its duration is very important especially for human being. It is important to record the time of the day that experiments took place. For most experiments with biological samples, a) the time between the disturbance of the cells and exposure, b) the time interval between the exposures, and also c) the time between exposure and assessment of the outcome are crucial [172].

### **2.10.10 Power Constrain**

When designing magnetic coils, one important consideration is how to keep them cool while all the electric power is dissipated in the wire by means of the Joule heating. Details on Joule heating along with concerned equation are explained in Section 3.7. In some instances, no cooling is needed and in others, the coils systems shall be air cooled or water cooled. It really depends on the coil holder structure and air flow available [193]. General consideration to using a water cooling system is for 50W per load [185]. Additionally, current and power constraints must be considered when designing magnetic coil systems, since there are limitations of the power supply that will be used to feed the coil system. Nevertheless, an additional alternative to reduce the power consumption of the coil system is to keep on increasing the number of turns of each coil winding while the current intensity is reduced proportionally in the same amount. This process is tedious and makes the design inflexible. However, magnetic flux produced by individual coils adds up by means of superposition and



therefore, less amount of current per coil is then required to get a desired field. This greatly reduces resistive heating in the coil and has influenced the design of the 2-Axis HCS used in this research.

## 2.11 Window Effect

The physical window mainly constitutes the field parameters: frequency, intensity, duration, waveform, and geometry of exposure. Biological window comprises of experimental model or cell type used, stimulus, age and period of study. Different results will be obtained through different combinations of given physical and, or biological variables [194].

ELF-EMF is a form of non-ionizing low-energy EMF radiation known to affect biological systems. Reports of its effects on the biological functions of living organisms have increased over the last two decades [195, 196]. The therapeutic potentials of ELF can be seen in the proven efficacy of low energy PEMF in non-union bone-fracture healing [197], confirming that, under certain conditions, this energy can influence physiological processes in organisms. Specific changes in the field configuration and exposure pattern mostly likely govern the different effects in the different application. Some authors have additionally observed a sensitivity of the biological response to dosimetry indicating distinct exposure windows [198]. While some researchers [199] emphasize on the important role of frequency to highlight the ‘frequency windows’, some others justify the effects through the intensity as ‘amplitude windows’ [200]. However, due to the specificity of biological processes, it is most likely that a specific set of frequency and intensity would cause a favorable biological response.

Experimental findings from [65] indicate that PEMF does have an effect on collagen synthesis in rat skin. Yet, out of the different frequencies used in the experiments, the 25 Hz frequency at field intensities of 2mT and 4 mT was the most effective. This is to say, the process

demonstrated some kind of ‘window effect’ with regard to the frequency selection employed. The phenomenon of frequency ‘window’ of the EMF biological effects was also reported upon experimentation with bacteria *S. aureus* [201].

Results obtained during this research project and as presented in Chapter 4 and 5 demonstrate this “window effect” upon ELF PEMF exposure to Collagenase enzyme [122] and bacterial culture of *S. aureus* [147].

## 2.12 Commercial PEMF Device: *In vivo* Application

**Portable PEMF device:** The size and cost of a treatment unit and the requirement that it be used in an office setting have rendered it a difficult and expensive form of care. Current PEMF transducers utilize a lot of energy. Devices containing such transducers are often required to carry a rechargeable battery pack. These battery packs are expensive, heavy in weight and thus, less portable. Any means to reduce the battery size and weight will assist to reduce the cost and enhance portability and thus, make them more flexible and convenient to use, especially in home settings and outpatient departments. Typical portable PEMF device are shown in Figure 2.8. [202, 203]. Output modules of the device in the form of current carrying coils are clearly visible.



Figure 2.8: Potable PEMF device: (a) PE200 Coils [202] and (b) Somapulse [203].

**PEMF device for clinical applications:** In clinical practice, ELF PEMF applications offer the possibility of more economical and effective diagnostics and non-invasive therapies for medical problems, including those considered refractory to conventional treatments. PEMF have been used as an adjunctive treatment options to stimulate normal fracture healing, delayed unions, and non-unions. Treatment of post-operative pain and chronic pains are also applications of PEMF devices. Application of PEMF to traumatic injuries allows the tissue to repair more rapidly. Accelerating the rate of healing would reduce both the likelihood and effect of secondary complications. Plethora of commercially available PEMF devices have made it harder to draw a comparison between them and thus made harder to categorize their outcome in both custom and laboratory setting. Few of the diverse application of PEMF devices are shown in Figure 2.9.

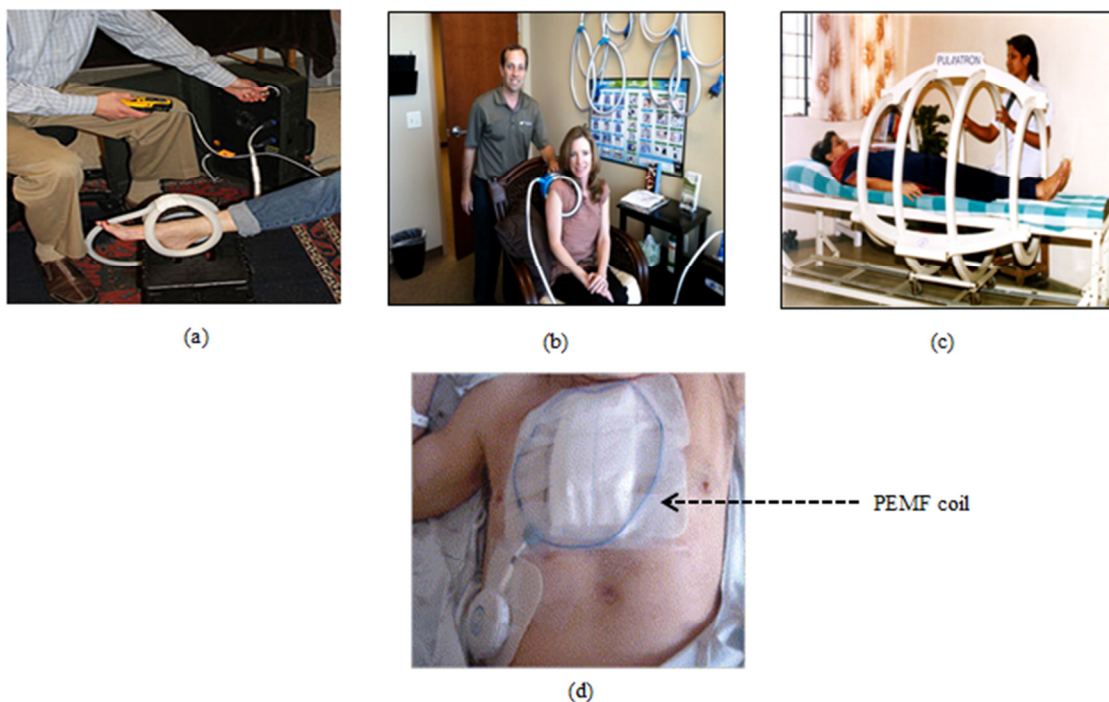


Figure 2.9: *In vivo* PEMF systems: (a) PEMF therapy for the foot [204]; (b) PEMF therapy for the shoulder [205]; (c) PEMF therapy for the whole body [206]; and (d) A modern portable, disposable pulsed electromagnetic field device is incorporated into a dressing for the postoperative treatment of an incisional wound [149].

## 2.13 *In vitro* PEMF System

*In vivo* applications of ELF PEMF are targeted towards the entire wound/area of concern. Studies of isolated cells and tissues (*in vitro* studies) are rather scarce when it comes to ELF fields and their possible role in diseases other than cancer [207, 208]. The data available suggest that exposure to EMF activates the expression of certain proteins, but the biological significance of this study is still unclear. There is a tremendous need for *in vitro* studies to examine the agents of wound healing. This research project applies the ELF PEMF on specific agents that influences the process of damaged and infected tissue repair and thus promotes wound healing.

Selected *in vitro* PEMF systems are shown below in Figure 2.10 [153, 209, 210].

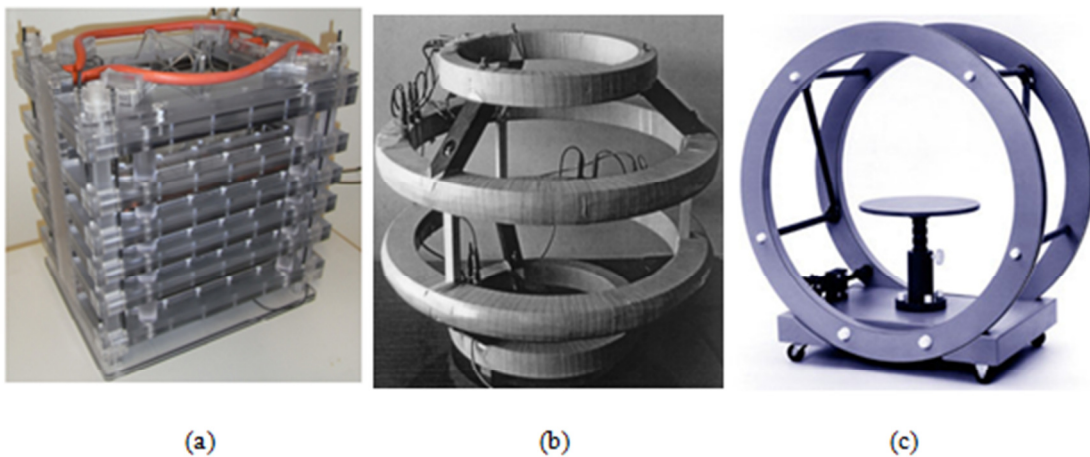


Figure 2.10: *In vitro* PEMF systems (a) PEMF system for exposure of large number of cell culture plates [209] (b) Tetracoil prototype for producing highly uniform magnetic field [153] and (c) One-axis Helmholtz coil system with a sample holder at the center [210].

*In vitro* experiments for studying the effect of the magnetic treatment on biological systems require devices that can generate electromagnetic fields, to apply a controlled and repeatable exposure dose to the samples involved in these experiments, and in addition allow the experimenter to observe, manipulate and easily locate the sample. Therefore, the working volume should be conveniently accessible and the electrical design and construction should be as simple as possible. It is evident that *in vitro* PEMF systems are designed to suffice the need

for particular experiments and are thus strictly built to accommodate experimental needs. An example of ELF PEMF system designed for specific need is shown in Figure 2.10 (a), where the PEMF exposure chamber is built to accommodate 14 cell culture plates at the same time. However, general features of current *in vitro* PEMF devices possess some inherent deficiencies in the following form:

- Most of these devices are bulky in nature and their rigid structural design (Figure 2.10: (a) - (c)) highly impedes coil optimization (shape and positioning). This then greatly compromises the usage of PEMF exposure chamber by restricting its use and thereby compromises with the efficacy of the entire PEMF system.
- Not scalable- Instances where small volume of sample is required, it will not be feasible in terms of power consumption to use these relatively large scale PEMF device for exposure.
- Cuvette holder is an essential part to expose biological sample in liquid media like enzyme solution and bacterial cultures. The holder containing the biological media needs to be placed exactly at the centre of the PEMF chamber where it can then be exposed to a uniform magnetic field created by the PEMF coils. However, most of the current *in vitro* PEMF system do not come with the a priori platform to contain and then position the cuvette holder and therefore do not suffice for the above mentioned types of experiments. However, the ones which do like the one in Figure 2.10 (c), do not accompany a cuvette holder. In that case conventional cuvette holders can be used. However, conventional cuvette holders have two major deficiencies while conducting experiments with biological samples in a liquid media. These are:

- They are only suitable for experimentation with light radiation
- The structure interacts with magnetic field.

Additional details in forms of visual representation of cuvette design deficiencies are appropriately provided in Section 3.3.1.1.

This research deals with exposure of ELF PEMF to biological sample in liquid media. Taking the current deficiencies of *in vitro* PEMF systems for conducting such experiments, this research proposed a novel design of the ELF PEMF exposure chamber (Section 3.3) and successfully demonstrated three applications (Chapter 4 and 5) of this device pertaining to crucial agents that can influence wound healing promotion.

## 2.14 Safety

Studies on human subjects have shown consistently that there is no evidence that prolonged exposure to weak electric fields results in adverse health effects [121, 211]. According to published studies utilizing pulsed therapeutics electromagnetic fields there is no adverse health risk associated with its use. A task group commissioned by FDA together with the World Health Organization (WHO) examined the biological effect of extremely low frequency magnetic field in 1996. They reported that there was no evidence of any adverse effect on human health due to short term exposure to magnetic field of up-to 4mT. Most MRI machines generate magnetic fields up to 2T. However, the question of whether chronic exposure to weak magnetic fields is equally harmless remains debatable. Laboratory studies on animals and cell cultures have shown that weak magnetic fields may have effects on several biological processes. For example, they may alter hormone and enzyme levels and the rate of movement of some chemicals through living tissue [121]. Although these changes do not appear to constitute a health hazard, they need further investigation particularly

for the long term affects.

## 2.15 Wound Healing

Important aspects of ELF PEMF device/system and the role they play in wound healing promotion have been discussed in the previous subsections. However, the biological aspect of wound healing needs to be understood in greater details in order to perceive the role which integral agents play in influencing the process of wound healing in damaged and infected tissues.

The topic of wound healing is systematically discussed through the following subsections:

### 2.15.1 Types of Wound

The term wound has been defined as a disruption of normal anatomical structure and functions due to injury. There are two types of wounds: acute wound and chronic wound.

*Acute wound:* Acute wounds are those that are new and in the first phase of healing. They are characterized by tissue damaged by trauma. This may be deliberate, as in surgical wounds of procedures, or be due to accidents caused by blunt forces or frictions. An acute wound is by definition expected to progress through the phases of normal healing, resulting in the closure of the wound. Acute wound occurs suddenly and has short duration [212].

*Chronic Wound:* Acute wound may progress to a chronic wound if it does not heal within the expected time as a result of poor blood supply, oxygen, nutrients or hygiene. Acute wounds should be properly treated to avoid infection, inflammation or constant pressure. Chronic wound have necrotic burden consisting of both necrotic tissue and exudate. Production of excessive exudate can interfere with healing or with the effectiveness of therapeutic products,

such as growth factors and bioengineered skin [213].

Wound can conveniently be categorized under the following headings:

- Abrasion: caused by friction with other surfaces or objects that scrape off the top layers of skin.
- Laceration -caused by a smooth or jagged cut and the resulting wound is deeper than abrasion.
- Avulsion: caused by trauma or surgery which reached all layers of skin and leaves it completely torn off or hanging.
- Incision: clean cuts caused by surgical incision which can either be superficial or deep depending on the circumstances.
- Puncture: wounds that result from penetrating objects such as needles or nails. The resultant wound is typically the same size and shape as the causative object.
- Burn wounds: can be divided into three categories: (i) 1<sup>st</sup> degree burn: burns limited to the superficial layers of skin; (ii) 2<sup>nd</sup> degree burn: burns that might penetrate to deeper layer of skin but not profound enough to reach the connective tissues and (iii) 3<sup>rd</sup> degree burn: involves all skin layer and might as well reach out to the connective tissues and organs [214].
- Amputation: is the removal of a body extremity by trauma, prolonged constriction, or surgery and is mainly caused by accidents [215].

### 2.15.2 Response to Tissue Injury

There are four basic of response to wound healing (Figure 2.11).



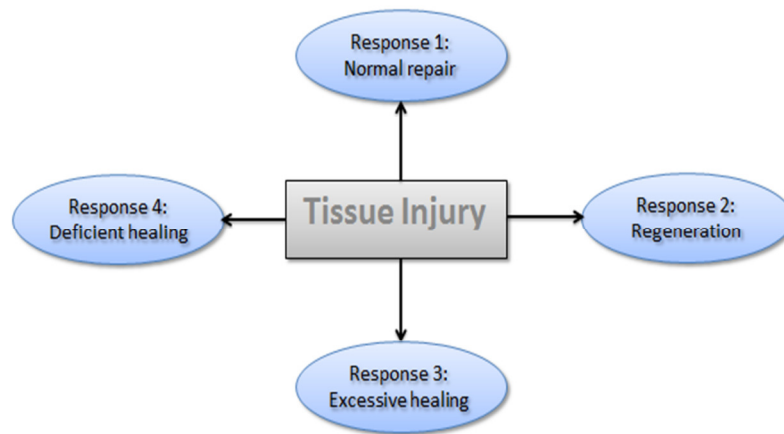


Figure 2.11: Response to tissue injury [216].

**Response 1-** Normal repair: It is the response where there is re-establishment equilibrium between scar formation and scar remodeling.

**Response 2-** Regeneration: Process where there is a loss of structure and function but the organism is capable to replace that structure by replacing exactly what was there before the injury.

**Response 3-** Excessive healing: Result of too much deposition of connective tissues that result in altered structure and thus loss of function.

**Response 4-** Deficient healing: Occurs when there is insufficient deposition of connective tissue matrix and the tissue is weakened to a point where it can fall apart.

## 2.16 Process of Wound Healing

Recent advances in molecular and cellular biology have greatly expanded general understanding on the biological process involved in wound healing and tissue regeneration. The interactive process of wound healing comprise of soluble mediators, blood cells, extracellular matrix and parenchymal cells [217]. Three distinct phases of wound healing are discussed below in greater details.

**(i) Inflammatory phase (Hemostasis, Inflammation)**

**Hemostasis:** The first reaction to a wound is the sealing of the damaged or torn blood vessel.

This is done by platelet cells forms a stable clot to seal the damaged vessels (Figure 2.12).

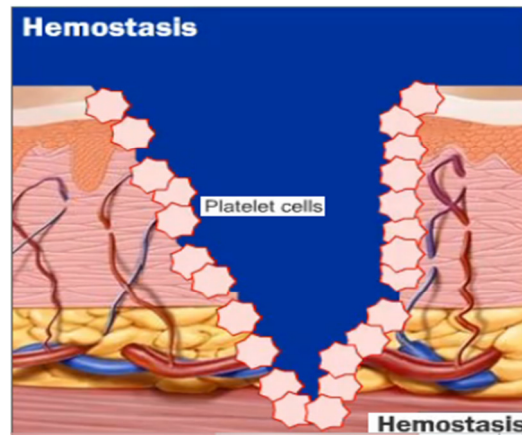


Figure 2.12: Hemostasis phase- First stage of wound healing [218].

As platelet aggregation proceeds, clotting factors required to control the bleeding and loss of fluid are released resulting in the deposition of a fibrin clot at the injury site [216]. The fibrin clot serves as a provisional matrix and sets the stage for the subsequent events of healing [249]. Platelets not only release the clotting factors but also provide a cascade of chemical signals, known as cytokines or growth factors that initiate the healing response. The two most important signals are platelet-derived growth factor (PDGF) and transforming growth factor-beta (TGF- $\beta$ ). The absence of any underlying clotting disorder will allow hemostasis to occur within minutes of the initial injury.

**Inflammation:** The function of this inflammatory stage of the healing process is to remove dead cells and micro-organisms and to stimulate healing. An acute inflammatory reaction can be expected up to approximately three days post-surgery [219]. An inflammatory response will cause the blood vessels to become leaky resulting in releasing plasma and polymorphonuclear neutrophils (PMNs) into the surrounding tissue. The neutrophils phagocytize debris and microorganisms provide the first line of defence against infection. They are aided by local mast cells. As fibrin is broken down as part of this clean-up the

degradation products attract the next cell involved. Macrophages are able to phagocytize bacteria and provide a second line of defence (Figure 2.13). They also secrete a variety of chemotactic and growth factors such as fibroblast growth factor (FGF) and epidermal growth factor (EGF) which appears to direct the next stage.

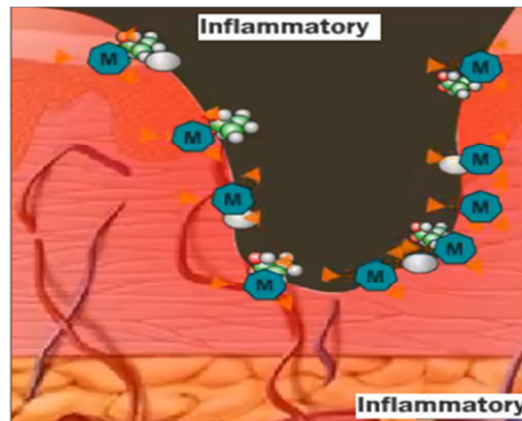


Figure 2.13: Inflammatory phase- First stage of wound healing [218].

**(ii) Proliferative Phase (Granulation, Contraction and Epithelization):**

All three sub phases of the Proliferative phase can be seen in Figure 2.14.

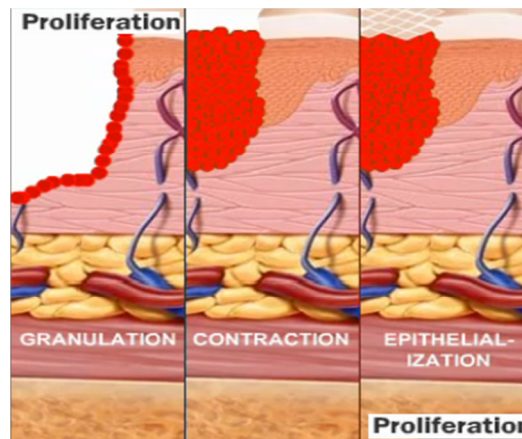


Figure 2.14: Proliferation- Second stage of wound healing [218].

**Granulation:** Granulation tissue comprises of new connective tissue and tiny blood vessels which forms on the surfaces of a wound during its healing process [220]. Granulation tissue typically grows from the base of a wound and is able to fill wounds of almost any size. Granulation tissue is created and modified by fibroblast. Initially, it consists of a network

of type III collagen which is a weaker form of the structural protein that can be produced rapidly. This is later replaced by the stronger, type I collagen. The granulation stage starts approximately four days after wounding and usually lasts until 21 days in acute wounds depending on the size of the wound.

***Contraction:*** Once the wound site has been cleared of debris, fibroblasts secrete collagen framework on which further dermal regeneration occurs [221]. Specialized fibroblasts are responsible for wound contraction. Specific collagenase enzymes in fibroblasts, neutrophils and macrophages clip the molecule at a specific site through all three chains, and break it down to characteristic three-quarter and one-quarter pieces. These collagen fragments undergo further denaturation and digestion by other proteases.

***Epithelization:*** As a part of the healing process, several other important biological responses are activated. The process of epithelization is stimulated by the presence of EGF and TGF that are produced by activated wound macrophages, platelets and keratinocytes [222]. In the final stage of epithelization, contracture occurs as the keratinocytes differentiate to form the protective outer layer or stratum corneum.

### **(iii) Remodeling Phase:**

Wound repair in the healing process involves remodeling the dermal tissues to produce greater tensile strength whereby new collagen matrix then becomes cross-linked and organized for the final remodeling phase. The remodeling phase is characterized by continued synthesis and degradation of the extracellular matrix components trying to establish a new equilibrium [221]. The principle cell involved in this process is the fibroblast.

## 2.17 Collagen in Wound Healing

Most abundant protein found in mammalian tissue is type I collagen [223]. In tissues, type I collagen typically adopts a fibrillar structure. Collagen fibrils are highly organized biopolymers, consisting of a large number of individual collagen molecules linked together in a periodic manner. Collagen is a family of protein rich in glycine and proline (Figure 2.15). They are formed in a tight  $\alpha$ -helical structure [224]. The high degree of tensile strength required to fulfil these structural roles requires elongated proteins characterized by repetitive amino acid sequences and a regular secondary structure. Mature collagen fibril can be found in tendons, bones and connective tissues, providing a combination of strength and flexibility to these biological materials [223]. When tissues are disrupted following injury, collagen is needed to repair the defect and restore atomic structure and function. If excess collagen deposits in the wound side, normal anatomical structure are lost, function is compromised and fibrosis occurs. Conversely, when an insufficient amount of collagen is deposited, the wound is weak and may dehisce [222]. The fibroblast is the connective tissue cell which through growth factors such as PDGF, TGF- $\beta$  and EGF [222] is responsible for collagen deposition that is needed to repair the tissue injury [222].

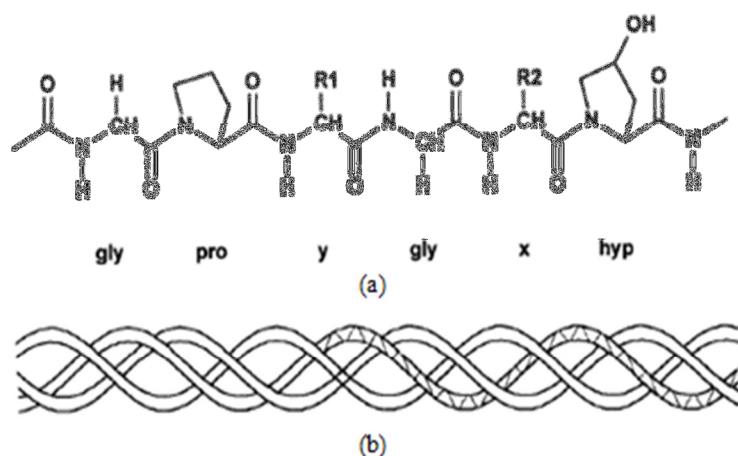


Figure 2.15: (a) Primary and (b) tertiary structure of collagen [225].

## 2.18 Collagenase in Wound Healing

Collagenase is an established enzyme that has been widely used in biomedical research to dissociate tissues and isolated cells since 1970s and has been used as a therapeutic drug for the removal of necrotic wound tissue [226]. The commercially available preparation of Collagenase is derived from bacteria *Clostridium histolyticum*. *Clostridium* collagenase is one of the several bacterial collagenases that have been widely studied for their biochemical and enzymatic properties [227-228]. By nature, collagenase is a water soluble proteinase that specially attacks and breaks down collagen into simple peptides [229] and is most effective in a pH range of 6 to 8.

Collagenase can hydrolyze native collagen and thereby facilitate rapid debridement and is thus involved at several stages of wound healing [230]. They play a major role during the healing of wounded skin, where extensive degradation, resynthesis and remodeling of collagen occur [227]. During early wound healing, collagenase assist with clot debridement and later it assists with wound remodeling by degrading old collagen and allowing the deposition of new collagen [231]. However, until collagenase cleaves collagen, no other enzyme is capable of breaking it down [227].

An investigation of type I collagen reaction to collagenase solution using real-time atomic force microscope revealed that the collagenase degrades the entire fibrillar structure down to shorter and thinner fragments [223]. Collagenase cleaves glycine in helical regions of native collagen containing the sequence x-proline-glycine-proline-z [231]. *In vitro* study investigating the digestive ability of *Clostridium* collagenase on human collagen types I, III, IV, V and VI showed that these enzymes displayed proteolytic power to digest all these types of human collagen present in necrotic tissue, except type IV. Perhaps the best graphical representation (Figure 2.16 (a)) and proposed mechanism (Figure 2.16 (b)) of how

collagenase might have a multiple beneficial effects on wound healing was given by [213]. Collagenase activity in wounds is not only useful for the purpose of debridement but also for more fundamental aspects of cell migration.

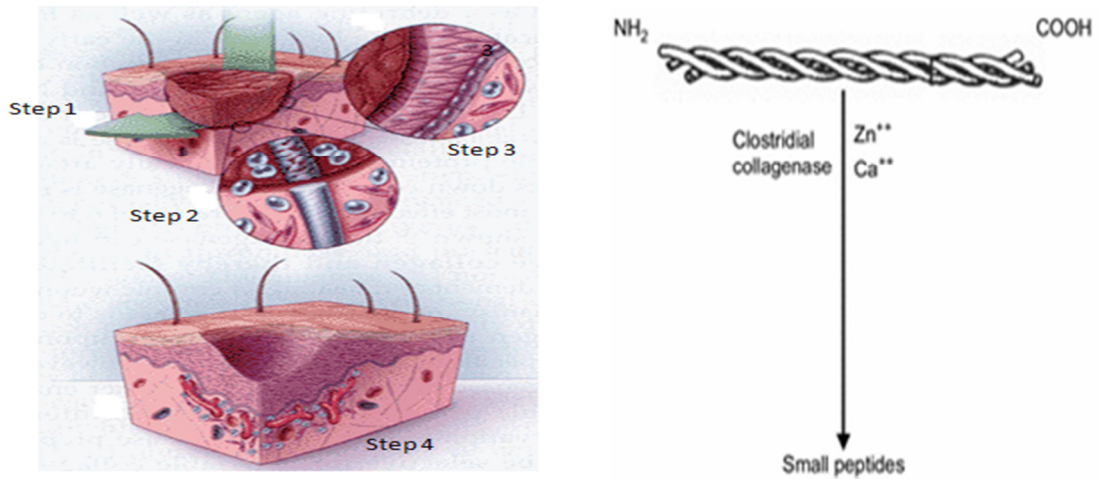


Figure 2.16: (a) A proposed view on how Collagenase might have multiple beneficial effects on wound healing and on wound bed preparation [213] (b) Collagen degradation into smaller fragments upon reaction with Collagenase [227].

In Figure 2.16 (a), Step 1 depicts the enzymatic action in order to free up the necrotic tissue from the wound by acting upon the necrotic plug. Step 2 shows the collagen bundles are being cut at the necrotic-viable tissue interphase. Step 3 illustrates rapid epithelization that might occur by two means: indirectly: as necrotic tissue is removed or directly: through the effect of collagenase which causes the migration and activity of important cells such as wound macrophages, fibroblasts and keratinocyte. Step 4 shows the resulting wound free of necrotic tissue and thereby possessing good granulation tissue and is mostly epithelialized.

There is considerable rationale for using Collagenase in wounds for the purpose of enhancing or accelerating reepithelization [232]. Clinical trials of collagenase reported rapid cleansing and enhanced removal of necrotic debris [231]. A conducted study [233] suggested that Collagenase ointment is more effective than placebo (inactivated ointment or petrolatum ointment) for debridement of necrotic tissue. *In vivo* and *in vitro* studies have shown that collagenase promotes the cellular responses to injury and wound healing [228].

## 2.19 Conventional Debridement Methods and Limitations

Wound debridement is widely used for the removal of devascularised or infected tissue or foreign material from, or adjacent to, a wound with the aim of exposing healthy tissue [234]. Debridement is a process necessary to aid the healing process of chronic wounds. In acute wound debridement is a good way to remove necrotic tissue and decrease the bacteria burden. Clinical experience and existing research strongly supports debridement as a necessary component of wound bed preparation. Multiple techniques are available but the indications for each technique and their efficacy is not clearly established. There is little evidence to guide the clinician in the selection of a safe, effective debridement method for the patient with a chronic wound [233]. There are two types of debridement: Selective (removes mainly necrotic tissues) and nonselective (removes both necrotic and viable tissues). The most common forms of wound debridement are: autolytic, chemical, mechanical, and surgical (sharp), and biological. Advantages and limitations of the above mentioned methods of wound debridement are outlined below:

***Autolytic debridement:*** In this selective process the wound bed clears itself of debris by using phagocytic cells and proteolytic enzymes [235]. Of note, proteolytic enzymes are responsible for breaking down the long chainlike molecules of proteins into shorter fragments (peptides), and eventually into their components, amino acids. In the early stage of wound healing, autolysis debridement occurs through the action of enzymes like elastase and collagenase which helps to minimize potential damage to viable skin at the wound edge. Autolytic debridement process can be facilitated by using air and water tight dressing.

***Advantages:*** It has been termed as the most easiest and natural form of debridement. The process is painless and is useful in wounds with minimal debris.

***Limitations:*** The major limitation of this process is that the healing process is extremely slow and it is not suitable for infected wounds.



***Mechanical debridement:*** This nonselective process physically removes debris from the wound and is mainly used for wound with large amount of necrotic tissue. Mechanical debridement includes wet-to-dry dressing, hydrotherapy, irrigation, and dextranomers [236].

***Advantages:*** Unlike autolytic and chemical debridement this process acts faster in removing debris from the wound bed. It is useful in wounds with necrotic materials and moderate to large amount of exudate.

***Limitations:*** The major limitation of this process due to its nonselective nature is that it might remove viable tissue and also damage surrounding tissues.

***Surgical (sharp) debridement:*** The main goal of this form of selective treatment is to control the deep infection by drainage of any pus, removal of all necrotic or infected tissues, and creating a healthy wound bed. Necrotic tissues are removed with the aid of surgical instruments [237]. This method is typically used in cases where the wound possess substantial amount of necrotic debris or infected tissues.

***Advantages:*** This is the fastest form of debridement which yields immediate results.

***Limitations:*** The duration of surgery is one factor that influences the wound infection rate. Procedure that takes longer than two hours are associated with higher infection rates. The level of bacterial burden is the most significant risk factor [39]. Surgical site infection are still a real risk of surgery and represents a substantial burden of disease for both patients and health care services in terms of morbidity, mortality and economic cost. There is increasing awareness that the type of surgical intervention required also removes some of the senescent cells that are phenotypically altered. This process absolutely needs to be carried out by skilled clinicians and is prone to bleeding and pain.

***Biological (maggot/larval therapy) debridement:*** This highly selective method using certain species of maggots only removes necrotic tissue.

*Advantages:* Clinical study shows that application of this process yields rapid results and enhances oxygenation following therapy [238].

*Limitations:* The major limitation of this process due to its nonselective nature is that it might remove viable tissue and also damage surrounding tissues.

***Chemical debridement:*** This selective process hinges on the application to the wound of proteolytic enzymes that are able to chemically digest and remove cellular debris. Clinically available enzymatic debridement agents [239] are an effective alternative for removing necrotic material from pressure ulcers, leg ulcers, and partial-thickness wounds. Enzymatic agent maybe used as a primary technique for debridement in certain cases, especially when alternative methods such as surgical sharp wound debridement are not feasible owing to blood disorder or other considerations.

*Advantages:* Similar to autolysis debridement, this process is also easy to perform and incurs no pain to the patient. Clinical experience strongly suggest that combined therapy, such as initial surgical debridement followed by serial debridement using enzymatic agent or enzymatic debridement along with serial surgical sharp wound debridement, is effective for many patients with chronic indolent, or nonhealing wounds [233].

*Limitations:* Apart from the slow healing process, the major limitation of this process concerns irritation of surrounding tissues and its ineffectiveness against infected wounds. Possible side effect of chemical debridement includes damage to viable tissue within or around the wound. Concerned enzymes used in this application might actually be inactivated by the wounds pH or other typical agents being used [231].

## **2.20 Bacterial Infection of Wounds**

Bacteria are unicellular microorganisms (microbes) about 1µm in size and are found almost everywhere: skin, water, air, soil, food, inside the body and on most biological object.

Bacteria are classified into three groups according to shape: Cocci (Sphere-shaped), Bacilli (Rod-shaped), Spirillum (Spiral-shaped). They cause wound infection in human body. A bacterium's structure (Figure 2.17) is very simple, consisting of a rigid cell wall that supports and contains the cytoplasm, fragments of RNA, and a single strand of DNA within a non-encapsulated nucleus. According to their cytoplasmic structure, bacteria can be classified as Gram positive (e.g. *S. aureus*) and Gram-negative (e.g. *E. coli*).

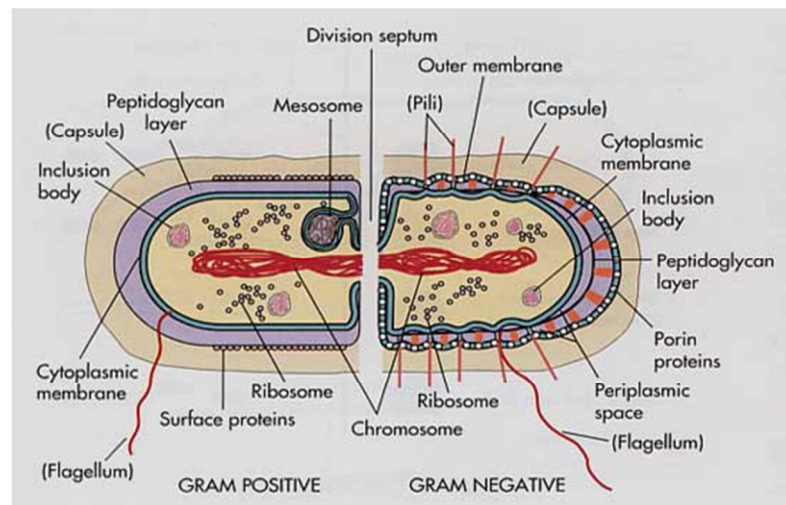


Figure 2.17: Gram positive and Gram negative bacteria [240].

Pictorial representation along with some additional information on the cell wall structure of gram positive and gram negative bacteria can conveniently be found in Section 5.2.

Though bacteria are capable of independent existence, most require a symbiotic relationship with a host organism. Wound infection is the consequence of the interaction between the host immune system, the wound conditions and increased microbial numbers and virulence and can be classified as mild, moderate, or severe. Figure 2.18 shows the probable relationship between bacteria and wounds.

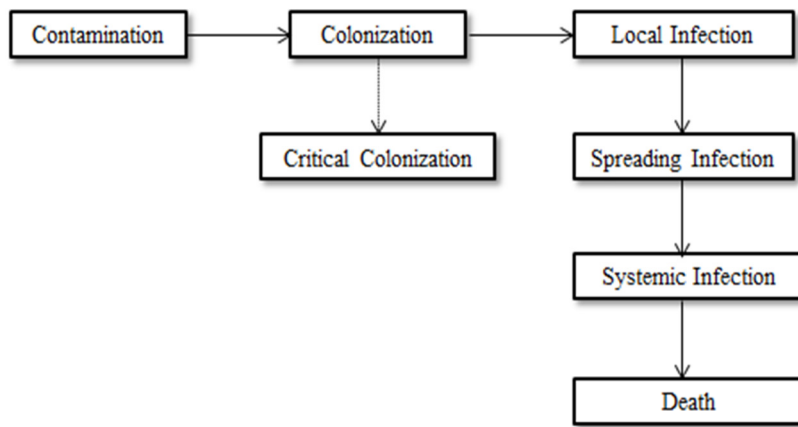


Figure 2.18: Block diagram depicting the relationships between bacteria and wound.

Wound represented by patients might vary from acute surgical wounds, traumatic wounds, burn wounds or chronic wounds. All wounds are contaminated by microorganisms that are part of the skin microflora [241]. Type and quantity of these microorganisms varies from on a wound basis [40]. These contaminating microorganisms can quickly become established within a wound, reaching a state of colonization. In [242], colonization is described as the presence of multiple bacteria with no overt host immunologic reaction. Of note, diabetes foot ulcers are commonly colonized with multiple organisms. Multiplication of bacteria within the wound can reach critical colonization, in which host defenses are unable to maintain a balance, thus resulting in delayed healing [243]. Infection to wound occurs when the invading organisms overwhelm the host defenses, either by sheer number or by impairing the host's immunity. There have been reports on delayed healing in a variety of wounds due to excessive bacterial burden. An increase in the bacterial burden also indicates a rise in infection for injured wounds. Infection confined to a particular wound can be termed as local infection. However, a local infection if remains untreated for a prolonged time will eventually spread in the surrounding and deeper tissues. An infection that affects the blood stream of a patient, with the result that the symptoms spread to the whole of the body is termed as systemic infection. In worst case scenario, severity of the systemic infection can eventually lead to damaged organs and in turn result in death. Most common factors increasing chance of

wound infection: Diabetes, Alcoholism, Post surgery.

The principle barrier against microbial infection is the skin. It constantly interacts with the external environment and is colonized with a diverse population of microbes [35]. The presence of these microbes in the wounded tissue results in spreading cellular injury due to competitive metabolism, toxins, intracellular replication, or antigen-antibody response [241].

## 2.21 Mechanism of Bacterial Infection

Skin is the largest organ in the body- when broken by a wound gives access to bacteria. Although microorganisms are responsible for infection, the exact mechanism as to how they affect non-healing chronic wound is still not clear [241]. Nevertheless, the most acceptable mechanism of skin and soft tissue infection can best be described by the following three stages:

(i) Phagocytosis: It is defined as the process of taking in particles such as bacteria, parasites and cellular and foreign debris by a cell as is seen in Figure 2.19. This process occur after the foreign body, a bacterial cell, for example, has bound to molecules called "receptors" that are on the surface of the phagocyte, for example, macrophages.

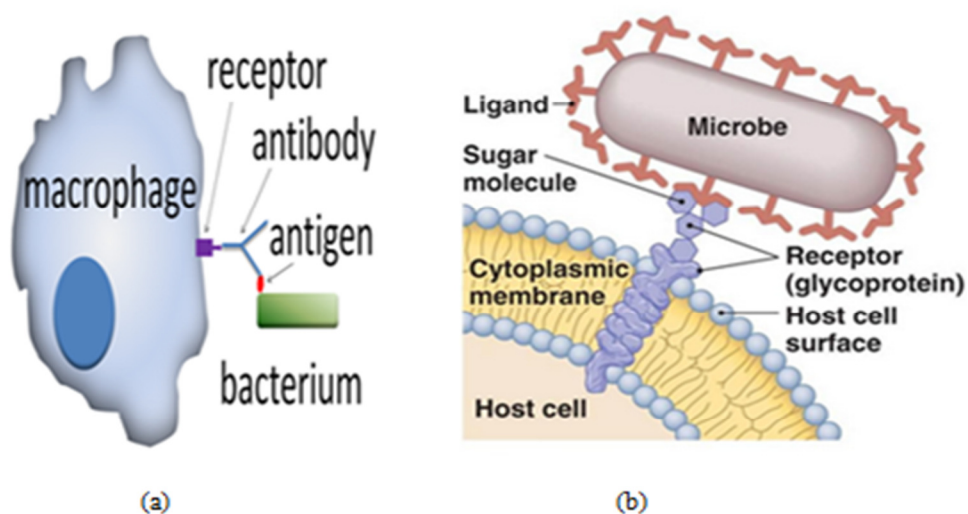


Figure 2.19: (a) Process of Phagocytosis [244] (b) Bacteria binding to receptors [245].

**(ii) Invasion of tissue with evasion of host defence:** Bacteria have developed ways to survive inside phagocytes, where they continue to evade the immune system [246]. After entrance, bacteria hide their antigens to avoid an immune response. To get safely inside the phagocyte they express proteins called "invasins". When inside the cell they remain in the cytoplasm and avoid toxic chemicals.

**(iii) Killing:** There are several ways by which bacteria kills the cells that fight infection (Macrophages). These include cytolysins which form pores in the phagocyte's cell membranes, streptolysins and leukocidins which cause neutrophils' granules to rupture and release substances [247], and exotoxins which reduce the supply of a phagocyte's ATP, needed for phagocytosis. After a bacterium is ingested, it may kill the phagocyte by releasing toxins to target other parts of the cell.

## **2.22 Conventional Treatment Method and Limitations for Bacteria Infected Wound**

Open injuries have a potential for serious bacterial wound infections, including gas gangrene and tetanus, and these in turn may lead to long term disabilities, chronic wound or bone infection, and death. Wound infection is particularly of concern when injured patients present late for definitive care or in disasters where large numbers of injured survivors exceed available trauma care capacity. Appropriate management of injuries is important to reduce the likelihood of wound infections. The following methods explained below provide guidance for appropriate prevention and management of infected wounds.

**Antibiotics:** Antibiotics are drugs of natural or synthetic origin that have the capacity to kill or to inhibit the growth of microorganisms [248]. Antibiotics either kill bacteria or keep them from reproducing. The concept of antibiotics was established in the 1960s when experimental

data established that antibiotics had to be in the circulatory system at a high enough doses at the time of incision to be effective. The antibiotic is chosen based on the bacteria present. Oral antibiotics are taken by mouth, while IV antibiotics are administered through a needle directly into the bloodstream. Antibiotics work by hindering with the ability of the bacterial cells to buildup and repair its cell wall. Some commonly used antibiotics are Cephalexin, Amoxicillin, Augmentin and Methicillin. Amoxicillin Augmentin and Methicillin belongs to the penicillin family of antibiotics. However, one of the drawbacks of using antibiotic is the patients allergic to antibiotics. Problem also lies in regarding the use of prophylactic antibiotics in clean procedures in which prosthetic devices are inserted into a patient's body. Such insertion can potential be dangerous to patient since it gives passage for bacteria like *S. aureus* living in the skin flora, to gain access to the wounded region and eventually created the possibility for bacterial wound infection. The major drawbacks of antibiotics for treating of infected wound are the fact that bacteria are becoming increasingly resistant to antibiotics [103]. This very reason has propelled researchers for development of new treatment modalities in order to better understand and manage wound infection.

***Drainage of pus collection:*** Local collection of necrotic tissue, bacteria and white cells are widely termed as pus. These collections of pus are retained within a wall formed by phagocytes and strands of fibrin [219]. In some instances this membrane may not be able to contain the pus and the build-up of pressure within the membrane may induce bacterial spread along tissue planes or via the vascular or lymphatic systems. There are two ways of drainage of pus collection: active drainage system and passive drainage system [249]. Active drainage system use negative pressure to remove accumulated fluid from a wound. Passive drains depend on the higher pressure inside the wound in conjunction with capillary and gravity to draw fluid out of a wound. However, drainage of pus is not recommended at all times after clean surgical procedure [249]. Although one purpose of surgical drains is to evacuate

excessive fluid accumulation to prevent bacterial proliferation, drains can increase the risk of infection via bacterial migration. Drainage of pus also incurs pain and is a problem for patients with blood disorders like leukaemia and lymphoma.

***Surgical removal of dead tissue:*** This mode of treatment and its limitation have been discussed earlier in Section 2.19.

## 2.23 *Staphylococcus aureus* in Wound Infection

Because of high incidence, morbidity, and antimicrobial resistance, *Staphylococcus aureus* infections are a growing concern for family physicians [250]. The magnitude of hostile methicillin-resistant *S. aureus* (MRSA) infections (Figure 2.21) has already been well documented [251].



Figure 2.21: Methicillin-Resistant *Staphylococcus aureus* (MRSA) soft tissue infections [252].

The skin is colonised by various type of bacteria but up to 50% of these are *S. aureus* [39]. *S. aureus* is a versatile and virulent gram-positive pathogen present in humans, skin microflora [253]. The rates of infections caused by *S. aureus* are increasing steadily. Treatment of these infections is becoming more difficult because of the increasing prevalence of multidrug-resistant strains. *S. aureus* is a leading cause of bacteremia [254] and endocarditis. Bacteremia caused by *S. aureus* is a serious infection associated with high morbidity and mortality. The infectious nature of *S. aureus* demands rigorous management of both suspected and confirmed cases of *S. aureus* infected wounds. Additional information on *S. aureus* as an



agent of wound infection was earlier provided earlier in the introduction section of Section 1.1.

## 2.24 *Escherichia coli* in Wound Infection

When strains of *E. coli* are outside their normal habitat (intestines), they can cause serious wound infections, several of which can be fatal. Potentially dangerous *E. coli* can exist temporarily and harmlessly on the skin, predominately between the waist and knees (mainly around the groin and genitalia), but also on other parts of the body, i.e. a person's hands after using the toilet. Lack of hygiene can easily transport *E. coli* from the hand to an open wound. These infections can be particularly damaging as the patients may well have a weaker immune system, given that they are already receiving treatment for another medical condition (example- diabetes). Figure 2.22 shows a typical wound infection caused by *E. coli*.



Figure 2.22: A typical tissue infection (diabetic foot ulcer) caused by *E. coli* [255].

*E. coli* is a frequent cause of life-threatening bloodstream infections [256] and other common infections, such as urinary tract infections. Over the last 40 years, *E. coli* strains have become increasingly resistant to many antibiotics especially with regard to fluoroquinolones and third- and fourth-generation cephalosporins [256]. Drug-resistant *E. coli* are readily acquired via food and water.

When aerobic culture methods are used, *E. coli* is the dominant species found in feces.

Because of its central position in the microbial research community, the gram-negative bacterium *E. coli* play a leading role in investigations of the fundamental molecular biology of bacteria [257]. Urinary tract infection, sepsis, and neonatal meningitis are the most-studied extraintestinal infection syndromes caused by *Escherichia coli* [258]. It also suggests the possibility of broadly active preventive measures which are urgently required because of the tremendous morbidity, mortality, and increased costs associated with extraintestinal *E. coli* infections [258]. Additional information on *E. coli* as an agent of wound infection was earlier provided earlier in the introduction section of Section 1.1.

## 2.25 Summary

This literature review has established three particular agents responsible for influencing the process of wound healing: Collagenase enzyme and bacteria *S. aureus* and *E. coli*. This review in considerable length have discussed the pivotal role that Collagenase enzyme play in influencing the process of wound healing and have established the importance of studying of wound infected by bacteria, in specific, *S. aureus* and *E. coli*. The merit of studying isolated enzyme solution and bacterial culture as an experimental sample is that, it helps to eliminate many of the complexities that are usually associated with whole-body exposure. This review also discussed the current application and deficiencies of conventional methods for treating damaged and infected wound and thereby suggested a need for non- invasive therapeutic application. Presented overview of the impact and application of ELF PEMF on wound healing shows why it can be a suitable candidate for these kinds of treatment/studies.

This review has also in considerable details discussed the coil designing aspect of PEMF devices. Through the majority of PEMF device characteristics it is evident that the efficacy of PEMF devices for *in vitro* applications is dependent on the optimization of its 3<sup>rd</sup> module (treatment coil system/exposure chamber). Therefore, the focus on this research was made to

be the optimization of the exposure chamber of the ELF PEMF system. Power efficiency can also be enhanced depending on the coil optimization since this will then suffice for generating higher magnetic flux while using limited amount of current. However, limitations that are incorporated with current *in vitro* PEMF devices suggests an inevitable need of modification, especially for experiments with small volume of liquid based biological samples like enzyme solutions and bacterial cultures. Fundamental flaw of the local approach is that the synthesis condition is restricted to the central point. The magnetic fields start to deviate from the required value in an uncontrolled way as the distance from the reference point increases. In practice, the requirements should be met for all the points within the working volume. The unavailability of ready-to-use computer programs to determine the optimal coils configuration (size, positions) with regards to field uniformity within the entire volume of biological sample is another limitation associated with current *in vitro* PEMF systems. Available software capable of performing such task is generally expensive and their modeling complexity is mostly confined to the expertise of engineers and thereby limits its usage in the wider area of Biomedical engineering. Addressing these above limitations via a lab built ELF PEMF exposure chamber along with ready-to-use software for coil optimization was made to be of the major focus of this research.

## **CHAPTER 3**

# **ANALYTICAL APPROACH, DESIGN, MODELLING, AND INSTRUMENTATION OF ELF PEMF DEVICE**

## 3.1 Overview

This Chapter discusses the design and modelling/analytical aspect of a novel ELF PEMF exposure system for *in vitro* experiments. The exposure chamber is built on the basis of a 2-Axis air core Helmholtz coil configuration that produce a uniform time varying magnetic field (magnetic flux density,  $B$ , 0.5–2.5mT for the frequency range,  $f$ , 2-500Hz). Analytical approach for generating a uniform magnetic field using the selected coil configuration is presented in Section 3.2. The reason for using a 2-Axis HCS as opposed to the conventional 1-Axis HCS is discussed in 3.2 subsections. Flow chart of the custom software program built to systematically evaluate the induced magnetic field distribution and its region of uniformity prior to commencing experimentation is provided along with simulation result which clearly illuminates region of field uniformity within 10%, 1% and 0.1% of the center field. Instrumentation and experimental setup required for generating and measuring magnetic flux density within the ELF PEMF system have also been presented in considerable details.

## 3.2 Analytical Approach for Generating Uniform Magnetic Field Using a Two-Axis (Four Coils) Helmholtz Coil System

An apparent advantage of the simulation software is the ease at which different coil shapes can be drawn. However, basic shapes that represent a coil system are either square or circular and since both these shapes have closed form solution pertaining to their production of magnetic field, their simulation output can easily be perceived through analytical results obtained from mathematical and analytic software, Maple™ used in this study.

One of the objectives of this study was to build a ready-to-use software on a common platform without the requirement of having expertise in performing complicated modelling tasks using a commercial simulation software. This would aid professionals from other fields as they could then easily adopt and utilize the ready-to-use program in their field. The

program developed in this project gives a user the benefit of changing coils orientation and observing the corresponding magnetic field patterns and, most importantly magnetic flux lines, throughout the region of a sample containment. For example, in the program written in Maple 14, a simple change in a coil radius at the input for coil pairs will automatically place the coils at their respective vertical or horizontal positions in accordance to the user defined Helmholtz coil axial axis orientation. This provides a great advantage, while trying to observe and compare the magnetic fields produced by different combinations of coil size and positions.

In summary, simulation software is essential for observing the magnetic field pattern within the ferromagnetic material structure. But in case, where the entire structure is made of acrylics (non-conducting material), it is convenient as well as efficient to study the magnetic field patterns through a software that can widely be used by academics and students and not being restricted to specific expertise, cost or licensing issues of the software.

In section 2.10.3 typical coils and coil systems were discussed. The main motivation in selecting a treatment coil in Helmholtz configuration is due to its availability of closed form solution pertaining to the magnetic field they produce in the centre of the coil configuration presented below:

$$B = \left(\frac{4}{5}\right)^{3/2} \frac{\mu_0 NI}{R} \quad (3.1)$$

where,  $B$  = Magnetic flux density (T),  $I$  = coil current (A),  $R$ =coil radius (m),  $N$  = number of wire loops and  $\mu_0$  = permeability constant.

In opting for a larger loop radius, and thus for a larger distance between loops, it is to be noted that, according to the above B-field equation in (3.1), having a larger radius value will yield a smaller value of magnetic field. So the loop radius is another limiting factor of the magnetic

field. The least space occupied by the coil setup in producing the required magnetic flux density (in for this study, 0.5-2.5mT) is important for future applications, where device miniaturization is a key requirement.

The coordinate system of the 2-Axis (four coils) HCS used in the experiments is shown in Figure 3.1. However, the presence of 2-Axis coil system and its related calculation of magnetic flux density necessitates the introduction of a new co-ordinate system as shown in Figure 3.1 (d). The Helmholtz coil pairs axially oriented in the  $z$  axis (Figure 3.1(b)) and  $x$  axis (Figure 3.1(c)) is termed as Pair 1: Top and bottom coils and Pair 2: side coils, respectively.

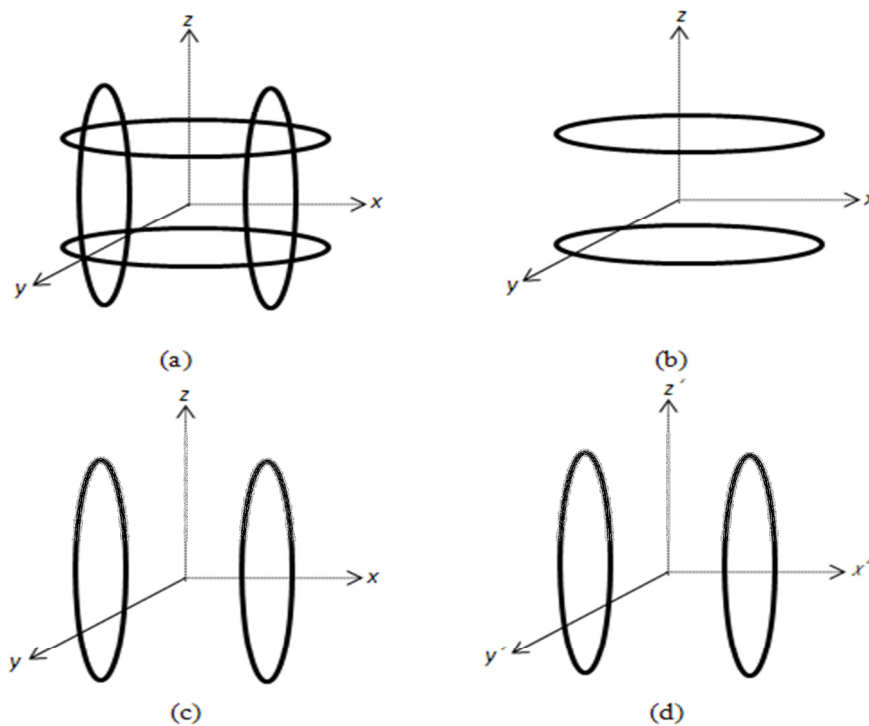


Figure 3.1: Coordinate systems for (a) 2-Axis (four coils) Helmholtz coil system, (b) Pair 1 (top and bottom coil) (c) Pair 2 (side coils) and (d) New coordinate system for Pair 2 after transformation of coordinate.

To calculate the total B-field at any point A ( $x_A, y_A, z_A$ ) within the inner space of the two orthogonal coil pairs, following steps are taken to satisfy superposition theorem.

- Step 1: Calculation of B-field components ( $B_{xAp1}$ ,  $B_{yAp1}$ ,  $B_{zAp1}$ ) generated by coil Pair 1 at A ( $x_A$ ,  $y_A$ ,  $z_A$ ).
- Step 2: Calculation of B-field components ( $B_{xAp2}$ ,  $B_{yAp2}$ ,  $B_{zAp2}$ ) generated by coil Pair 2 at A ( $x_A$ ,  $y_A$ ,  $z_A$ ).
- Step 3: Addition of the field components from Pair 1 and Pair 2 obtained from Steps 1 and 2 respectively in order to calculate the total B-field components ( $B_{xA}$ ,  $B_{yA}$ ,  $B_{zA}$ ) generated by the four coil system at A ( $x_A$ ,  $y_A$ ,  $z_A$ ).

Step 1 and 2: The method is based on the fact that it is possible to estimate, with sufficient accuracy the magnetic flux density generated by a coil system formed by  $N$  independent coils,  $\vec{B}$ , by superimposing the magnetic flux density generated by each coil,  $\vec{B}_i$ , as shown in (3.2).

$$\vec{B} = \sum_{i=1}^N \vec{B}_i \quad (3.2)$$

The selection of  $z$  as the axial axis for the four coils system ascertains that both Pair 1 and the four coil system share the same common orientation of the geometrical coordinate system. Therefore, B-field component from each coil in Pair 1 can be expressed in terms of  $B_{xAp1}$ ,  $B_{yAp1}$ ,  $B_{zAp1}$  for the point in space A ( $x_A$ ,  $y_A$ ,  $z_A$ ) and conveniently be analytically calculated for each  $\vec{B}_i$  using the specific form of Biot-Savart Law (Appendix A) given below:

$$d\vec{B}_i = \frac{\mu_0 I}{4\pi} \frac{d\vec{l} \times \hat{r}}{r^2} \quad (3.3)$$

In (3.3)  $d\vec{B}$  is contribution to the total B-field caused by  $d\vec{l}$ , an arbitrarily small element along the current carrying wire. Also,  $r$  is the distance from  $d\vec{l}$  to the point of interest on the axis of a circular current loop and  $\hat{r}$  is the unit vector from element  $d\vec{l}$ . Equation (3.3) is for a single loop coil with current,  $I$  and permeability constant  $\mu_0$ .



However, the application of superposition theorem entails that all coils must axially share the same axis (we assume  $z$  to be the common axial axis for the four coil system). Since, for the conducted experiments, Pair 1 is axially oriented in the  $z$  direction and Pair 2 in the  $x$  direction; extra steps were needed to be incorporated to suffice for the condition of adding B-field components from both coil pairs.

Since  $x$  (not  $z$ ) is the axial axis for Pair 2, we need to additionally conduct the following steps in order to express and calculate its B-field component:

To express the axial axis  $x$  of Pair 2 in terms of an axial axis  $z$  of both Pair 1 and the four coil system (Figure 3.1 (a)), a transformation of coordinate was required. This resulted in a new Cartesian coordinate system for Pair 2 as seen in Figure 3.1 (d). This coordinate system was obtained by  $90^\circ$  anti-clockwise rotation of the  $y$  axis with respect to the old coordinates (Figure 3.1 (c)). In doing so, point A ( $x_A, y_A, z_A$ ) in the old coordinate is shifted to point A' ( $x_{A'}, y_{A'}, z_{A'}$ ) in the new ones. The following relations are found:

$$x_{A'} = z_A, \quad y_{A'} = y_A, \quad z_{A'} = -x_A. \quad (3.4)$$

B-field components at A' ( $x_{A'}, y_{A'}, z_{A'}$ ) (new coordinate) can be expressed as  $B_{x_{A'}}$ ,  $B_{y_{A'}}$ , and  $B_{z_{A'}}$ . Using relations found in (3.4) the connection between the expressions for Pair 2 B-field components in the new coordinate (Figure 3.1 (d)) with that of the old one (Figure 3.1 (c)) can be established as follows:

$$B_{x_{Ap2}} = -B_{z_{A'}}, \quad B_{y_{Ap2}} = B_{y_{A'}}, \quad B_{z_{Ap2}} = B_{x_{A'}} \quad (3.5)$$

Expressions in (3.5) clearly shows that the axial axis  $x$  of Pair 2 is now represented in terms of  $z$ , thus satisfying the previously mentioned condition of superposition theorem. Finally, the total B-field components at point A ( $x_A, y_A, z_A$ ) can now be expressed as follows:

$$B_{xA} = B_{xAp1} + B_{xAp2} = B_{xAp1} - B_{zA}'. \quad (3.6a)$$

$$B_{yA} = B_{yAp1} + B_{yAp2} = B_{yAp1} + B_{yA}'. \quad (3.6b)$$

$$B_{zA} = B_{zAp1} + B_{zAp2} = B_{zAp1} + B_{xA}'. \quad (3.6c)$$

### 3.2.1 Custom Software Program

A flow chart of a custom made software program built in Maple 14 platform is shown in Figure 3.2. Each block in the flow chart is sufficiently detailed for understanding of the programs architecture. The objective of this program was to envision the pattern of magnetic field created by a 2-Axis HCS. An adaptable square (1cm × 1cm) mimics the base of a sample holder and facilitates the visualization of magnetic flux lines within the enclosure of the experimental sample.

The program sets up one pair of coils along the user defined axial axis and allows for the second pair to be anti-clockwise rotated on any three axes with respect to the first pair. It then carries out the required transformation of coordinate and systematically imposes superposition principle to express the various B field components. The user is then allowed to substitute any values for  $x$ ,  $y$  or  $z$  in the expression of B-field and accordingly express, calculate and then plot the total B-field for cross-section area in the  $yz/xz/xy$  plane. The user is then given an option to continue further and obtain plots for region of field uniformity within 10%, 1% and 0.1% of the centre field. At this stage, the initial input of the square base length (cm) is used to plot a square with the assigned length centred at the origin.

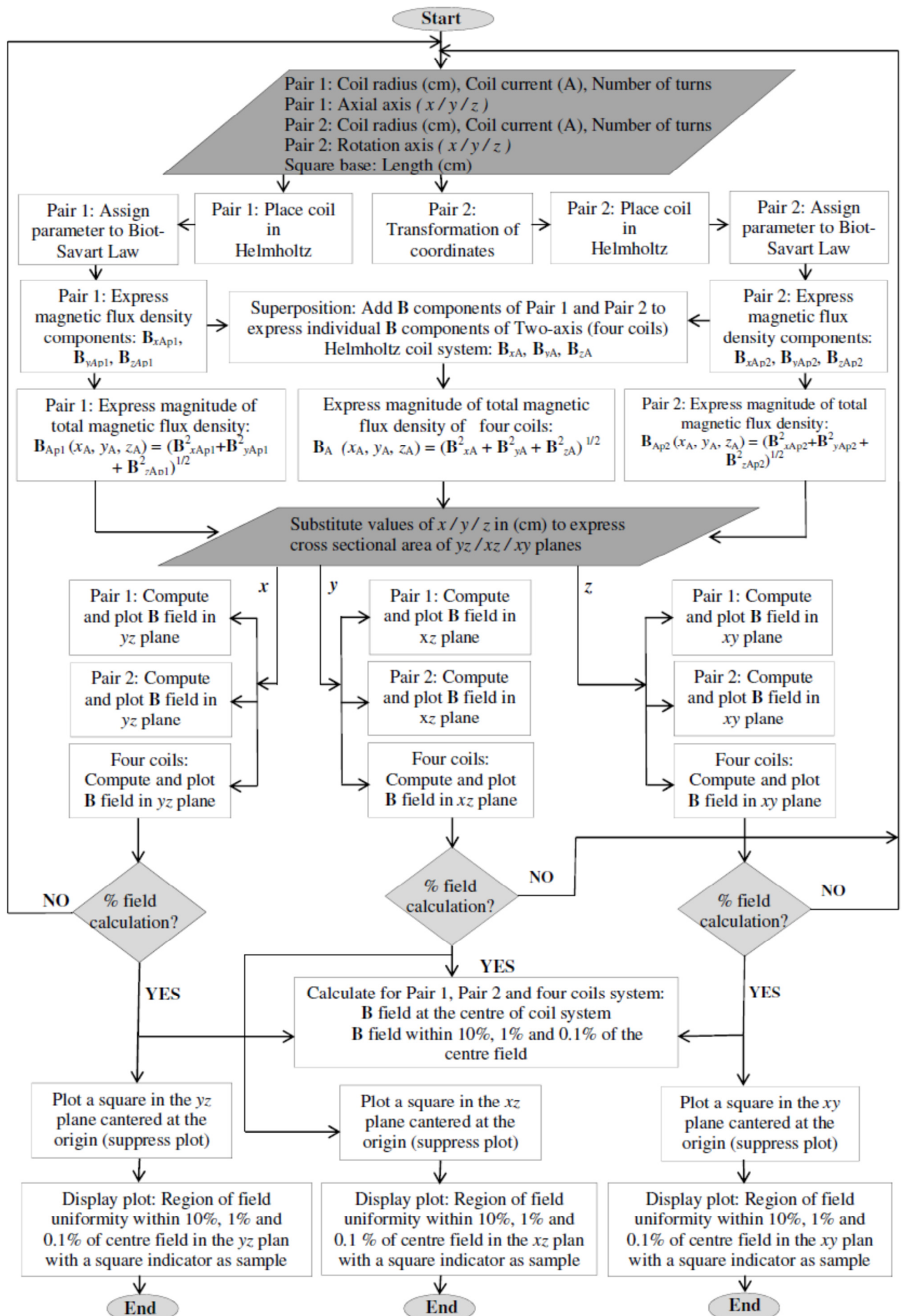


Figure 3.2: Flow chart of the custom built program for the Two-Axis Helmholtz coil system.

### 3.2.2 Geometric Orientation of Biological Sample in the ELF PEMF Exposure Chamber

For experimental evaluation during this study, biological samples in liquid media were exposed to ELF PEMF (magnetic flux density,  $B$ , 0.5–2.5mT over the frequency range,  $f$ , 2–500Hz) at the center of the coil setup (location of exposed samples). The selected biological samples used in this study research were Collagenase enzyme (assay is presented in Section 4.3) and bacterial *S. aureus* and *E. coli* (in Chapter 5). During exposures to ELF PEMF, enzyme solution was kept in a cuvette as shown in Figure 3.3(a) and bacterial cultures were contained in a 2.5ml centrifuge tube and occupied a height of 1cm as indicated in Figure 3.3(b). Figure 3.3 shows the orientation of these biological samples with respect to the local coordinate system used from this point forward and referred to for all analytical, simulation and experimental purposes.

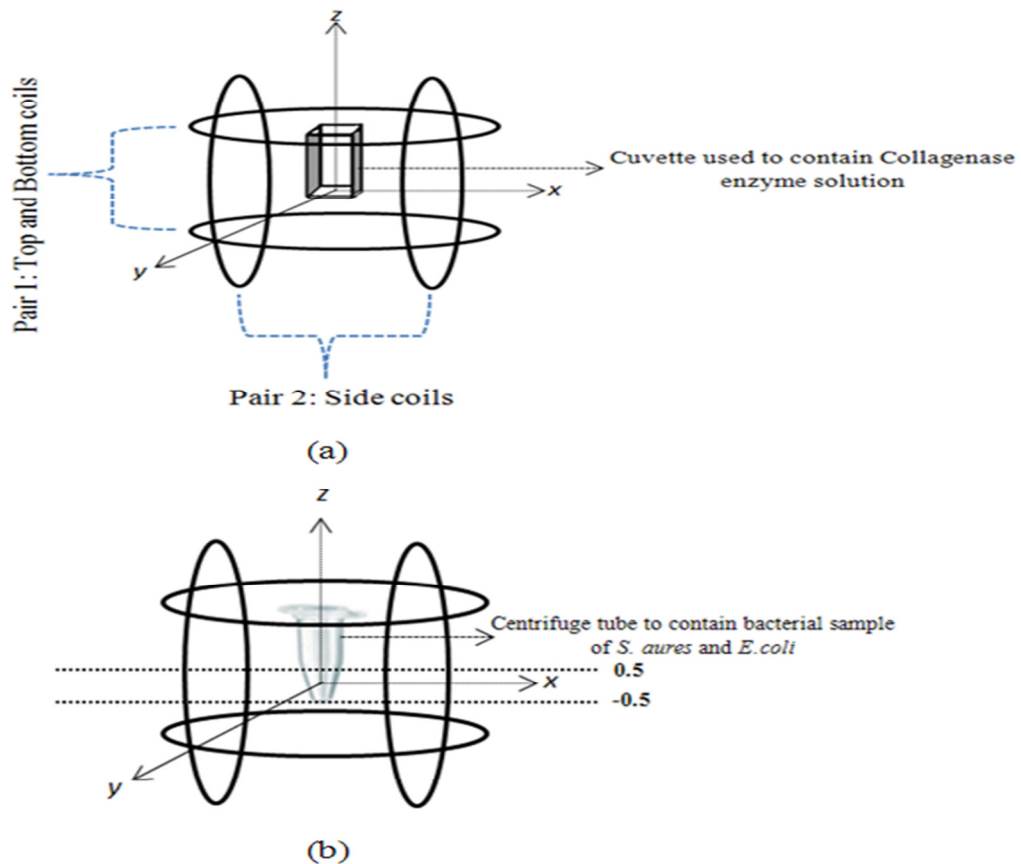


Figure 3.3: Geometrical orientation of biological sample containment (not to scale): (a) Standard cuvette used for experiments with collagenase enzyme solution and (b) 2.5ml centrifuge tube used for experiments with bacterial culture of *S. aureus* and *E. coli*.

### 3.2.3 Analytical Results

One of the most common practices in quantifying magnetic field homogeneity is to determine variation in magnetic flux density at a given point in space within the volume of interest, with respect to the value of magnetic induction in the central point of the coil system [259]. In this research project, the space of interest is the square base of (1cm × 1cm) centred at the origin. Figure 3.4 illustrates B-field distribution corresponding to 10%, 1% and 0.1% of the centre field in the  $xy$  plane for various  $z$  values of -0.5cm, 0cm and 0.5cm. Of note, the base of the cuvette is (1cm × 1cm) and the inner radius of the 2.5mL centrifuge tube is also 1cm. Therefore, the exposed sample for all the experiments can be visioned as being contained inside a cube having a square base of area 1cm<sup>2</sup>. A square base of 1cm have thus been plotted (marked by dots) at the origin of the  $xy$  plane (Figure 3.4, 3.6 and 3.7) and the  $z$  values taken at the origin ( $z = 0$ cm), and the lowest and highest levels occupied by the sample at  $z = -0.5$ cm and 0.5cm, respectively, for drawing comparison of field uniformity.

From the plots in Figure 3.4 it is evident that the B-field distribution in the  $xy$  plane corresponding to 10%, 1% and 0.1% of the centre field for  $z = -0.5$ cm, 0cm and 0.5cm mostly remains unchanged. Most importantly, there are no magnetic flux lines cutting through the dotted square base (sample location), therefore, we summarize that the B-field remains constant. This is a proof of uniformity of the generated magnetic field.

Results shown in Figure 3.4 were obtained via simulation from the developed software built in Maple 14 platform. The flow chart for this program was presented in Section 3.2.1, with the following input parameters:

Pair 1: Coil radius = 5cm, Coil Current  $I=0.3A$ , Number of turns # 200.

Pair 1: Axial axis =  $z$ ,

Pair 2: Coil radius = 6.5cm, Coil Current  $I=0.3A$ , Number of turns # 100.

Pair 2: Rotation axis =  $y$ .

Square base: Length = 1.0cm.

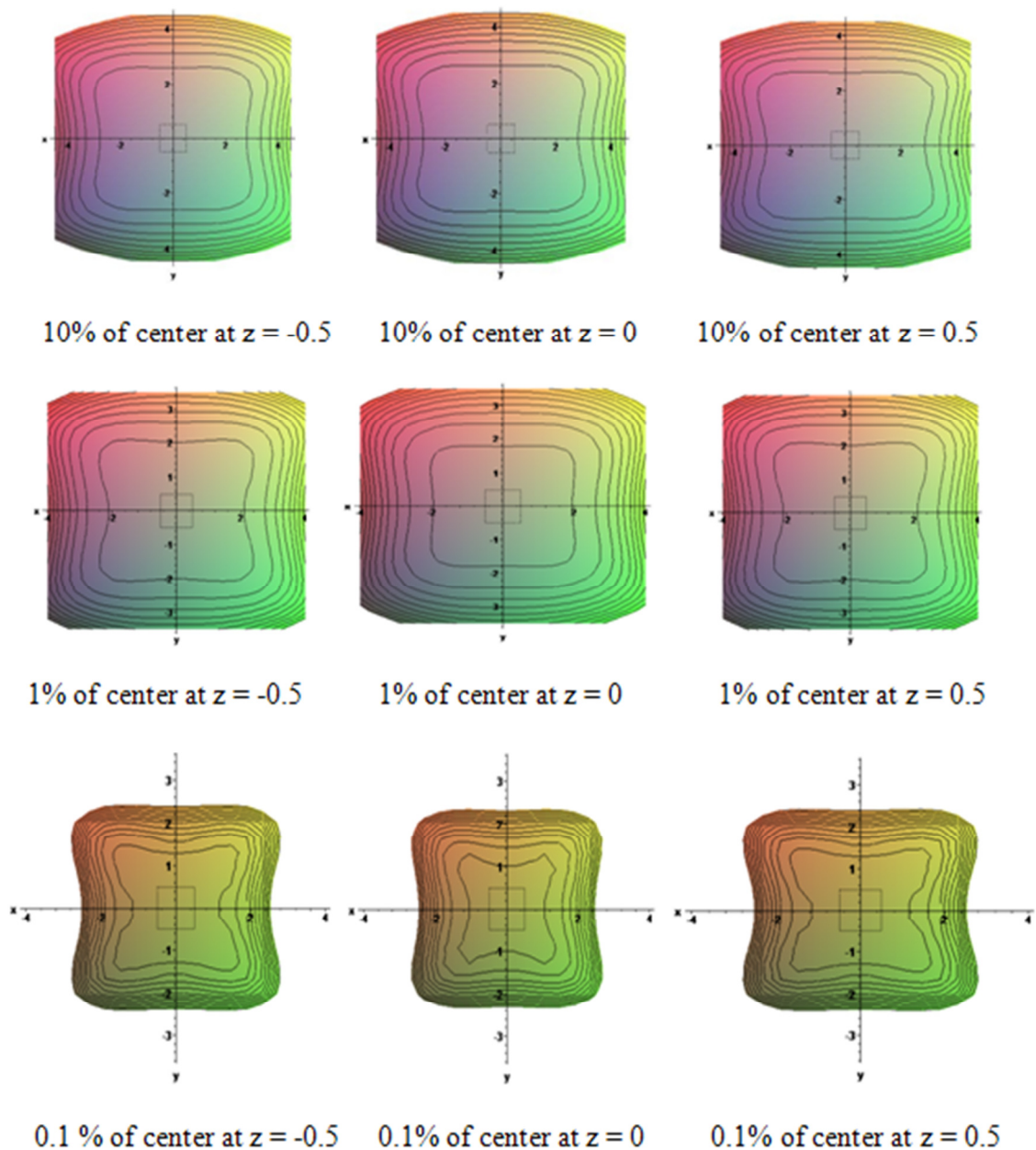


Figure 3.4: Simulation results of B-field distribution corresponding to 10%, 1% and 0.1% of the centre field in the  $xy$  plane for various  $z$  values of -0.5cm, 0cm and 0.5cm, respectively.

The coil parameters used in obtaining the plots shown by Figure 3.4 were used in construction of the exposure chamber for experiment with Collagenase enzyme and bacterial cultures. Simulation results obtained clearly shows that the B-field corresponding to 10% of the centre value of the magnetic flux density is analogous to grater area of uniform magnetic field in comparison to B-field corresponding to 1% and 0.1% of the centre field distribution. Most importantly, the B-field is still uniform corresponding to 0.1% value of the centre field. It is important to mention that simulations of coils using different radiuses and axial orientations were extensively explored and this particular combination of pairs of coils (Pair 1: radius = 5cm, number of turns #200, axial axis =  $z$  and Pair 2: radius =6.5cm, number of turns # 100, axial axis =  $x$ ) yielded the optimal coil configuration in terms of magnetic field strength; power dissipated by individual coil and overall setup space of the coil network.

Figure 3.5 illustrates the concept of superposition of magnetic fields in case of a 2-Axis HCS. Of note, Pair 1 coil is always less in diameter and has more number of coil turns when compared to Pair 2 coils. This particular setting allows the side coils (Pair 2) to envelope the top and bottom (Pair 1) coils from both sides without contact. For this reason the same amount of current fed to all four coils will yield result such that magnetic field produced by Pair 1 coil will always be greater than that of the Pair 2 coils as shown in Figure 3.5 (a) and (b).

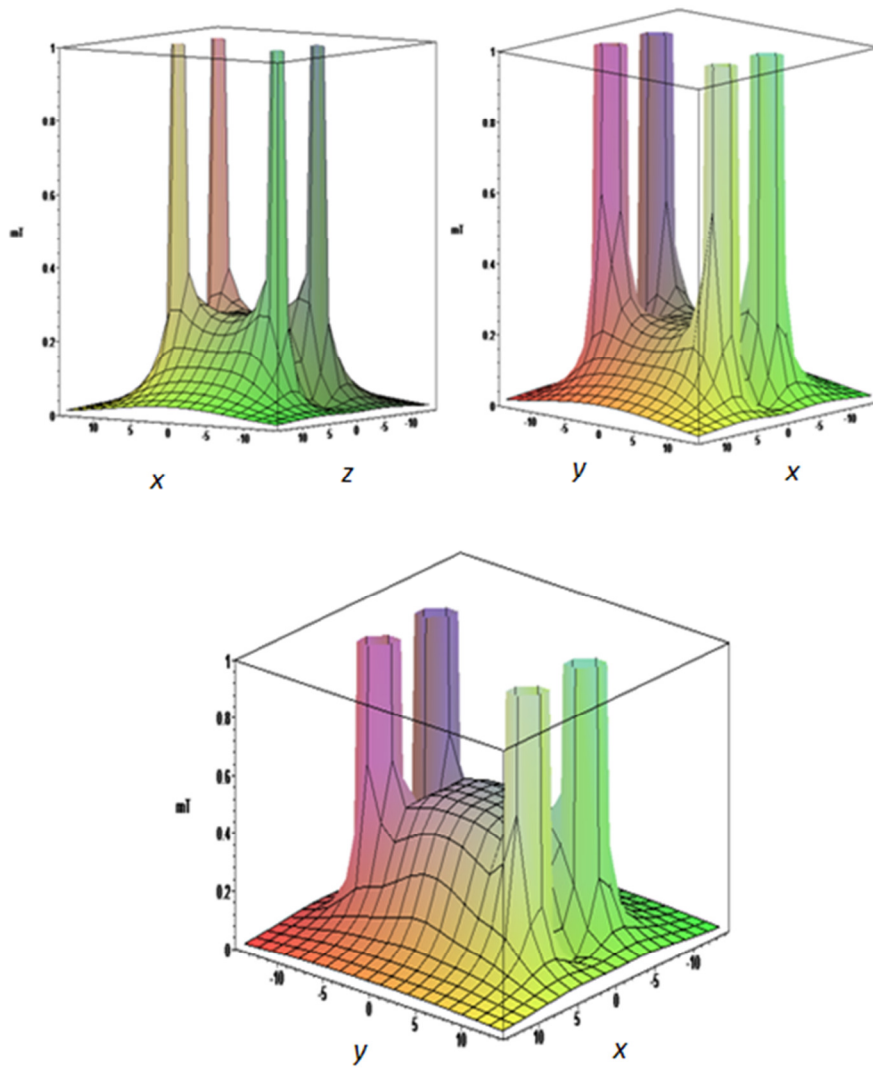


Figure 3.5: (a) B-field produced by Pair 1 coils (b) B-field produced by Pair 2 coils and (c) Superimposed B-field resulting from Pair 1 and Pair 2 coils.

Figure 3.5 (a) shows the uniform magnetic field created by a typical Pair 1 coil with magnetic induction of around 0.3mT. Figure 3.5 (b) shows the uniform magnetic field generated by a typical Pair 2 coils with magnetic induction of around 0.2mT. The magnetic fields generated from Pair 1 and Pair 2 coils results in a superimposed field of a greater magnitude (Figure 3.5 (c)). The value of this superimposed field is around 0.5mT. The reason of using a 2-Axis HCS for this research project is clearly evident through the presented results. With this particular setup, a minimal current will result in a substantially greater magnetic field as opposed to the same current being supplied to a pair of coils of a 1-Axis HCS. In order to attain the same magnitude of magnetic field produced by a 2-Axis



HCS, a 1-Axis HCS would require higher current to pass through individual coils. Since power dissipated in conductor equals  $I^2R$ , therefore, individual coils of a 1-Axis HCS would account for more power loss as opposed to individual coils of the 2-Axis HCS.

For comparison, the same custom written software was used to analyse the magnetic field distribution within the conventional 1-Axis HCS. Results obtained and presented in Figures 3.6 and 3.7 are that of Pair 1 and Pair 2, respectively. The results shown in Figure 3.6 is the B-field corresponding to 1% of the centre field in the  $xy$  plane for  $z = -0.5, 0.0\text{cm}$  and  $0.5\text{cm}$ . It is evident from all plots in Figure 3.6 that the magnetic flux line partially cuts across the vicinity of the experimental sample (shown by the dotted square) for all  $z$  values. Even though there is a uniform portion in between these magnetic flux lines, it does not cover the entire volume of the experimental sample contained in either the cuvette or the 2.5mL centrifuge tube that were used throughout the conducted experiments.

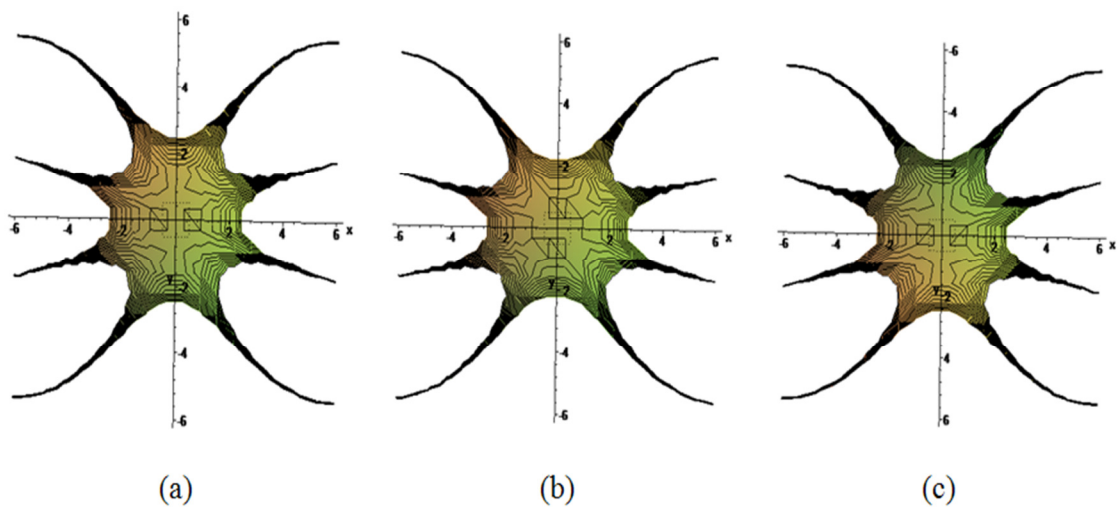


Figure 3.6: Simulation results of B-field distribution corresponding to 1% of the centre field in the  $xy$  plane for various  $z$  values of (a)  $-0.5\text{cm}$ , (b)  $0.0\text{cm}$  and (c)  $0.5\text{cm}$  for One-Axis Helmholtz coil system.

Figure 3.7 further illustrates the characterization of B-fields corresponding to  $z = 0.7\text{cm}$ . For the 2-Axis HCS, we observe that the magnetic flux lines starts to cave in from all the corners and approach towards the experimental sample location. For the 1-Axis HCS, we see that the

magnetic flux line extends towards the  $x$  axis but now cuts across the entire upper and lower portion of the dotted square.

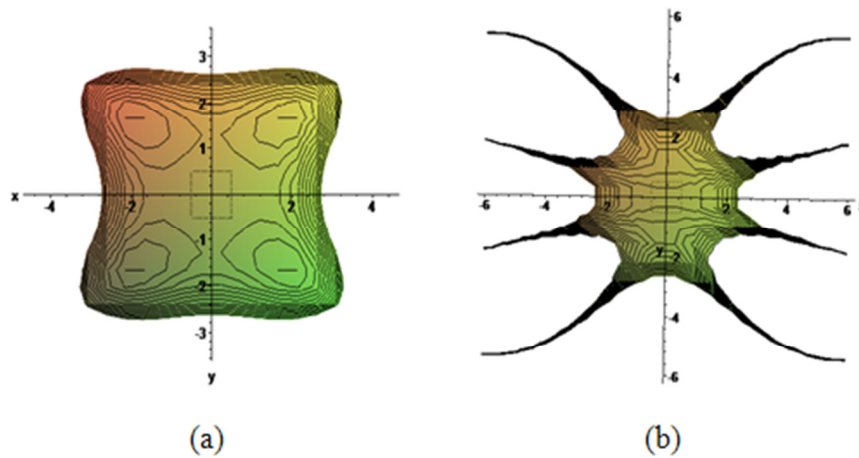


Figure 3.7: Simulation results of B-field distribution corresponding to 0.1% of the centre field in the  $xy$  plane for  $z = 0.7\text{cm}$  in case of (a) Two-Axis Helmholtz coil system and (b) One-axis Helmholtz coil system.

Figure 3.8 shows an illustration of the design scalability of the 2-Axis HCS when the larger coils for both Pair 1 and Pair 2 are used. The versatility of the software program just requires the user to change the coil parameters in order to analyse the magnetic field pattern for a system of larger coils.

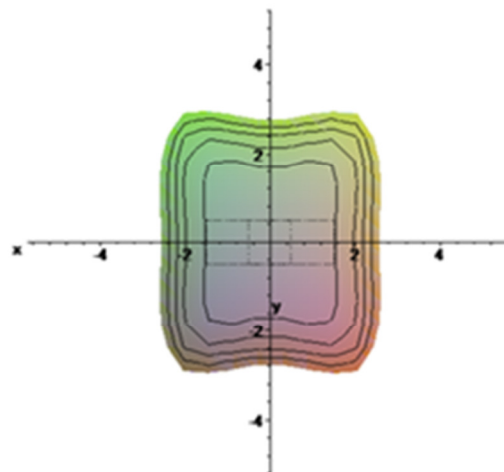


Figure 3.8: Simulation results of B-field distribution corresponding to 0.1% of the centre field in the  $xy$  plane for  $z = 0.0\text{cm}$  in case of a Two-Axis Helmholtz coil system (Pair 1: radius=7cm, Pair 2: radius=9cm).

The particular example (Figure 3.8) illustrates that a greater area of B-field distribution corresponding to 0.1% of the centre field is also attainable using coils of larger diameters and

therefore, increases the possibility of putting in more samples (each sample location denoted by a single square) for exposure. Magnetic field uniformity is evident in both  $x$  and  $y$  axis for the 2-Axis HSC. However, the apparent drawback for the large scale system is the overall setup space required by the coil network which will impeded in applications pertaining to device miniaturization.

### 3.3 Design and Construction of ELF PEMF Exposure Chamber

The initial structure of the ELF PEMF chamber (Figure 3.9 (a)) was designed using Computer Simulation Technology (CST), EM Studio<sup>®</sup> software package. After the structure has been modelled, a fully automatic meshing procedure is applied before the simulation engine is started. A feature of the simulator is the Perfect Boundary Approximation (PBA) technique which enhances the accuracy of simulation. Hexahedral and auto mesh generation option was chosen in order to generate fine mesh. The advantage of using such modelling software lies in the graphical representation of the entire structure of interest. The particular design shown in Figure 3.9 (a) took into consideration that all coils were made of copper with a conductivity of  $\sigma = 5.998 * 10^7 S/m$  and wound in a vacuum environment. The current specified for both models was in phase for both pairs of coils. Variables for the boundary and sub-domain boundary were selected as default in the software. However, the only boundary condition that needed to be specified was for the exterior boundary corresponding to zero magnetic flux ( $n \times A = 0$ ). Properties of the acrylic material used in the system were assigned to the structural materials including the cuvette holder. Properties of plastic material were selected for the cuvette. Water was chosen to represent the biological sample inside the cuvette. The cuvette has a dimension of 1×1×4.5cm. The base of the cuvette holder is placed at (0, 0, 0) on the Cartesian coordinate system (x, y, z) axis. A typical magnetic field generated in the xy plane corresponding to the central location within the coil system is shown in Figure 3.9 (b).

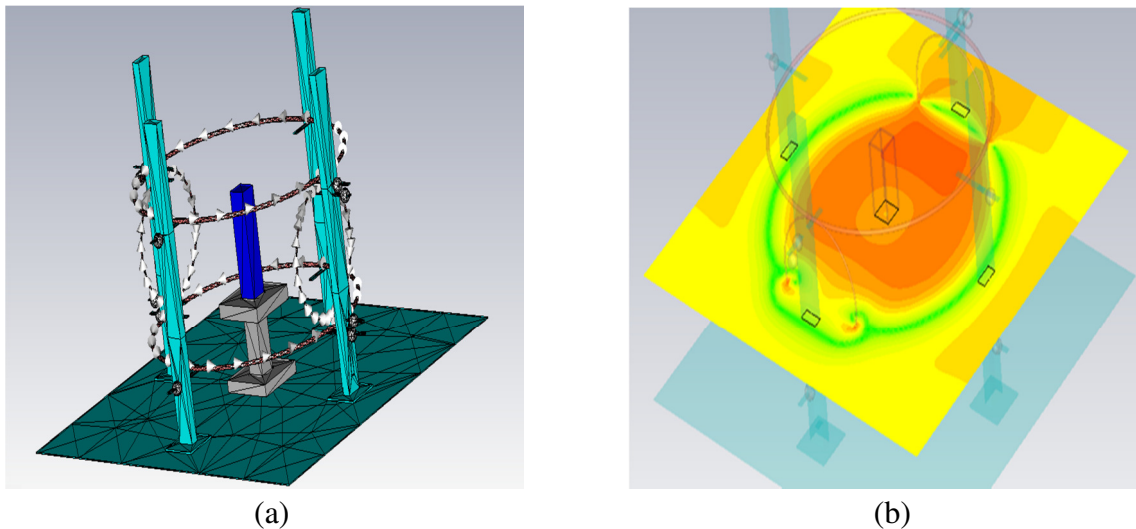


Figure 3.9: CST EM STUDIO used in (a) modelling the initial structure of ELF PEMF chamber and [260] (b) Simulation results showing 2D representation of the magnetic field within and around the ELF PEMF chamber [260].

The aim of this simulation was to show and ascertain that the generated uniform magnetic field is in the vicinity of the cuvette and do not interact with the assigned materials of the cuvette, cuvette holder, supporting structures of the ELF PEMF chamber and the biological sample. Once this was confirmed, then this design was used as a reference and later systematically modified and manufactured in the Technical Workshop at RMIT University.

The ELF PEMF exposure chamber consists of the coils system and four adjustable stands to support coils of different size and their respective positions required for producing a uniform magnetic field at the centre of the coil system. This particular design was introduced to overcome problems encountered with the designs described in Section 2.13. Figures 3.10 and 3.11 shows the gradual evolution of the ELF PEMF exposure chamber.

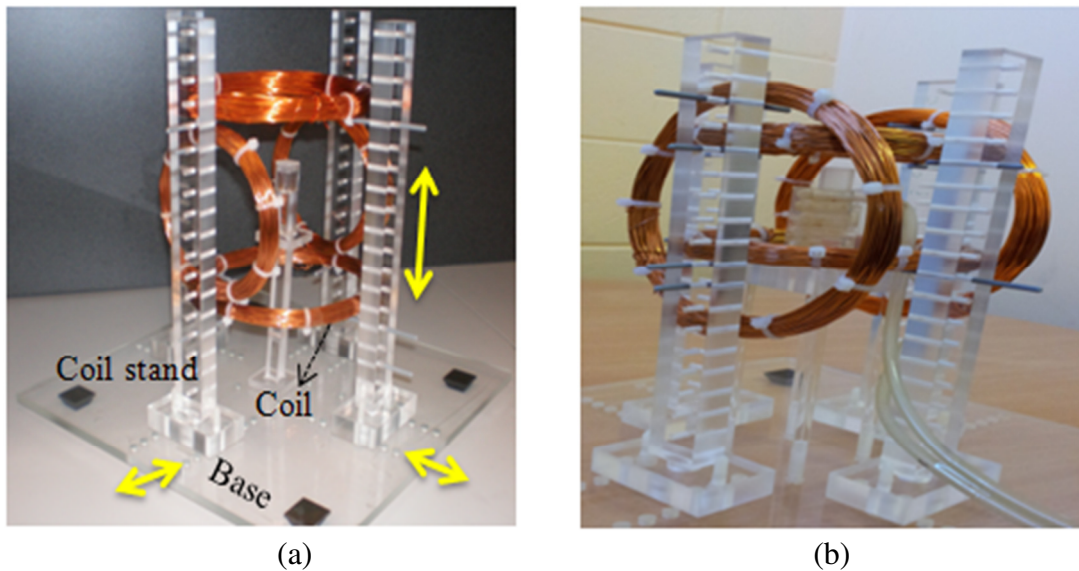


Figure 3.10: Evolution of ELF PEMF chamber (a) Initial design [260] and (b) Exposure chamber with novel cuvette holder design in place [123].

The entire frame work starting from the base to the stands and the cuvette holder is all made out of acrylic in order to avoid interaction with the magnetic field produced by the set of two pairs of air core Helmholtz coil. The base (26cm × 26cm) of the chamber has equidistant holes drilled on four sides. These holes were then aligned with the holes of the coil stands and connected via plastic screws. This particular setup sufficed for the extra holding strength required to hoist up the coils. To accommodate coils with various diameters, the coil stands, (height 24cm) were re- aligned and re- attached to the appropriate hole of the base as indicated by arrows in Figure 3.10 (a). In order to illustrate this point, different coil set up being supported by coil stands are shown in Figure 3.10 (a) and 3.10 (b). Holes in the coil stands were drilled 1cm apart in order to facilitate the required separation of the coils pair. Conscious effort was made to distant the coils from conductive material. Neatly cut Polyvinyl chloride (PVC) rods were then fitted through the coils stands for holding the exact position required to create a homogeneous magnetic field.

Coils used for all experiments were made of 0.65mm copper wire, 22 American Wire Gauge (AWG) / Brown or Sharpe (B&S), wound around a circular bobbin with circular cut plywood

frame attached between two acrylic glasses via two metal screws. After the winding was complete, screws were then slightly loosened and cable ties were slipped through the opening in order to wrap around the coils and maintain coil shape. Complete removal of the screws resulted in separation between the bobbin and the cable tied coils.

The latest version of the ELF PEMF chamber includes extra holes drilled in the base in a diagonal fashion (Figure 3.11 (a)), for the B-field probe to scan through the  $x$  and  $y$  axis for data collection of the magnetic flux densities.

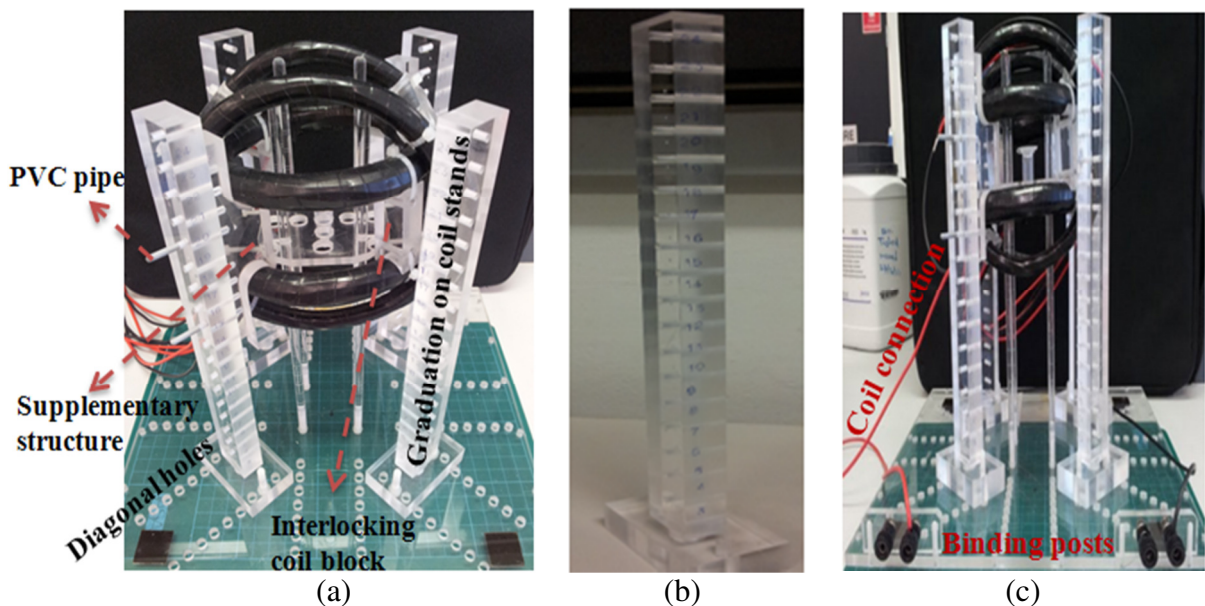


Figure 3.11: (a) Modified ELF PEMF chamber and (b) Close up view- coil stand (c) Viewing for coil connection to binding posts.

Sample holder stands were also elongated to match the height of the coil stands. The sample holder shown in Figure 3.11 (a) was used for experiments with bacterial culture. Graduation on the outer surface of the coil stands were put for convenient viewing from outside the ELF PEMF chamber. A closer view of a graduated coil stand is given in Figure 3.11 (b). Graduation mark on the sample holder stand as well as the coil stands were always aligned together to ascertain the  $z$  coordinate accuracy of Pair 1 coil placement in accordance to

Helmholtz coil criteria. The removable grid mat (each square, 1cm×1cm) sufficed for the  $x$  and  $y$  coordinates within the ELF PEMF chamber and is further explained in Section 3.5.1.

Coil optimization was one of the major concerns in the design of 2-Axis HCS. For the final design, the coils specifications were as follows: Pair 1: Both top and bottom coils have a diameter of 10 cm, each with 200 coil turns. Pair 2: Both side coils have a diameter of 13cm, each with 100 coil turns. After fixing the coil dimensions, few extra steps were taken to customize the coil network. Black electrical taping around the coil added extra support in maintaining the shape of the coils by securing them in their respective tight circular loop.

Four interlocking coil blocks (two for each pair) with “U” shaped groove on both ends were fitted between the coil pairs and connected via cable ties (Figure 3.11 (a)). Two supplementary structures positioned against their respective coils stand further ensured the stability of the coil network (Figure 3.11 (a)). Of note, these blocks will only suffice for the above mentioned coil diameters. However, similar concept can be adopted and materialized to accommodate combination of different coil radiuses. Three pair of holes were drilled in the base on each side to accommodate binding post for inter coil connections and other necessary connections to the coils from external equipment. Ends of the coils were also tinned, so that they could be securely connected to the binding posts (Figure 3.11 (c)).

***Sham exposure chamber:*** Figure 3.12 (a) shows the sham exposure chamber which includes a square base with four sample holder stands.



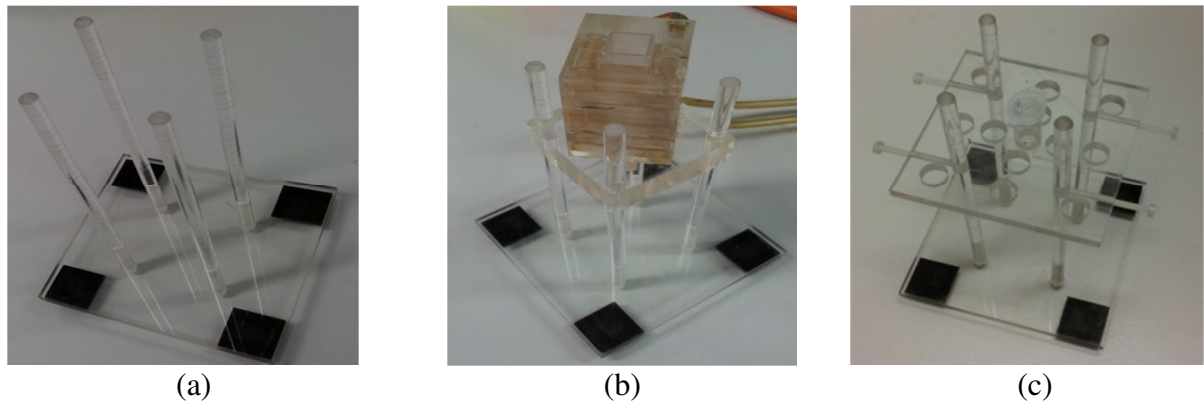


Figure 3.12: Sham exposure chamber structure (a) without sample holder (b) with cuvette holder and (c) with 2.5mL centrifuge tube holder.

Figure 3.12 (b) shows the setup with cuvette holder used for containing the control sample of Collagenase enzyme solution. Figure 3.12 (c) shows the same setup but with a 2.5mL centrifuge tube holder used for keeping the control sample of bacterial cultures. The tube holder is essentially a square piece of acrylic with holes of equal diameters drilled across it. Extra holes can be used for experiments with multiple controls. All structures shown in Figure 3.12 are made of acrylic apart from the plastic screws in Figure 3.12 (b) and (c) which were used to secure the control sample holder structure with the stands.

### 3.3.1 Designing of Cuvette Holder for ELF PEMF Experiments

One of the integral entities of the ELF PEMF exposure chamber is a cuvette holder for containment of a biological sample and its supporting stands which allows the cuvette to shift vertically. Section 3.3.1.1 discusses limitations of commercially available cuvette holders pertaining to EMF ELF experiments. The design and construction of a novel cuvette is presented in Section 3.3.1.2 and cooling system design shown in section 3.3.1.3.

#### 3.3.1.1 Current Limitations of Cuvette Holders

Chapter 2 commented on the areas of improvements necessary for *in vitro* PEMF systems in order to carry out experiments involving biological samples in liquid media. The structural design of commercially available cuvette holders has three following basic limitations to experiments involving EMF radiation in the ELF range:

- They are specifically designed for experimental studies that require external EMF exposure above the ELF range, most common of which are experiments using Infrared radiation [118]. In such systems, the entire radiation can be channelled through a small opening which gives clear passage to the experimental solution contained in the cuvette (Figure 3.13).
- Metal structure around the cuvette holder (Figure 3.13) interferes with the magnetic field used in exposure of biological sample contained in the cuvette. This interaction creates a non-uniform field throughout the sample and results in an unpredictable value of magnetic flux density in the vicinity of the experimental sample. This eventually nullifies the validity of experiments that are based on generating a uniform magnetic field.
- The cuvette holder itself is mainly designed for a standard type cuvette since most experiments would require the cuvette to be put into Spectrophotometer during the post exposure period for measurement of absorption coefficients. However, experimental biological sample requires being vortexed during the post exposure period and especially during the dilution process, thus centrifuge tube is being used. This implies that for experiments with biological media, a standard cuvette cannot be used and therefore the use of conventional cuvette holder is not applicable for irradiation experiments.

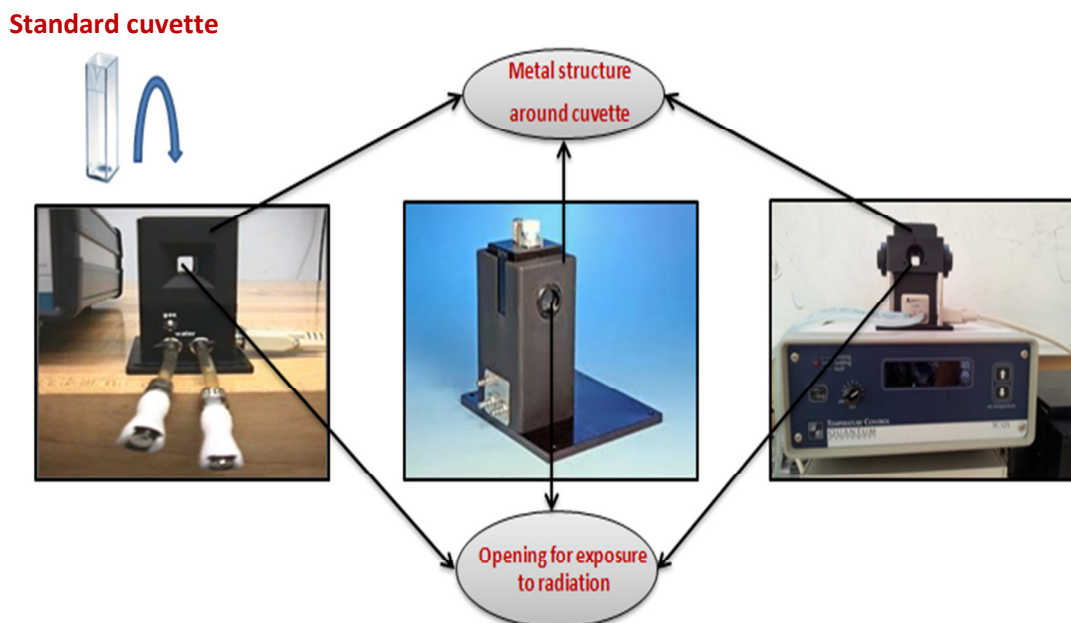


Figure 3.13: Conventional cuvette holders [261].

### 3.3.1.2 Custom Made Cuvette Holders

As discussed above it is evident that utilization of commercially available cuvette holders for experiments involving ELF PEMF exposures is not practical. Therefore, in this study a novel cuvette holder was designed and constructed for use, which can also be utilized in other arrays of experiments with similar constrains.

**Choice of material:** Acrylic was chosen as the material for construction of the cuvette holder as well as the entire structure of the ELF PEMF chamber. Acrylics have a relative magnetic permeability of less or equal to 1. Such materials do not absorb an external magnetic field and do not form any magnetic field within them. Therefore, the emitted magnetic field remains unchanged.

**Design 1:** The first cuvette holder structure (Figure 3.14) includes the base, holder stand and top slab.

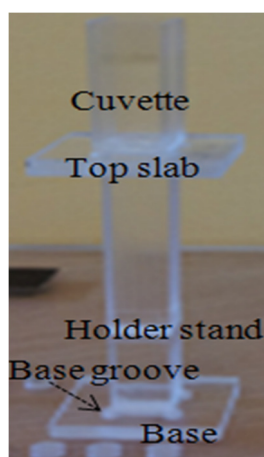


Figure 3.14: Design 1 of the cuvette holder [123].

A 1cm×1cm square base of 0.2cm thickness was grooved in the centre of the top face of the base using a micro milling machine and is shown in Figure 3.14. Groove of similar dimension was also made on both faces of the top slab. These grooves ascertained the stability of the cuvette holder stand as it would fit tightly between the base and the top slab. Groove made on the top surface of the top slab was required to ascertain a fixed position for the cuvette for all experiments. However, this design faced two limitations:

- (i) The design only sufficed for biological experiments conducted at room temperature but not for cases where specific temperature was required. For example, experiments with enzyme solutions would require the biological sample to be kept at temperature of 37°C.
- (ii) The fixed height of the cuvette holder enforces restriction to coils diameters. The location of uniform magnetic field shifts with coil positioning, which in turn is dependent on the coil diameter. The above fact necessitates the use of a cuvette holder with adjustable height.

**Design 2:** Both limitations of Design 1 as explained above were addressed with the construction of a novel cuvette holder (Figure 3.15).

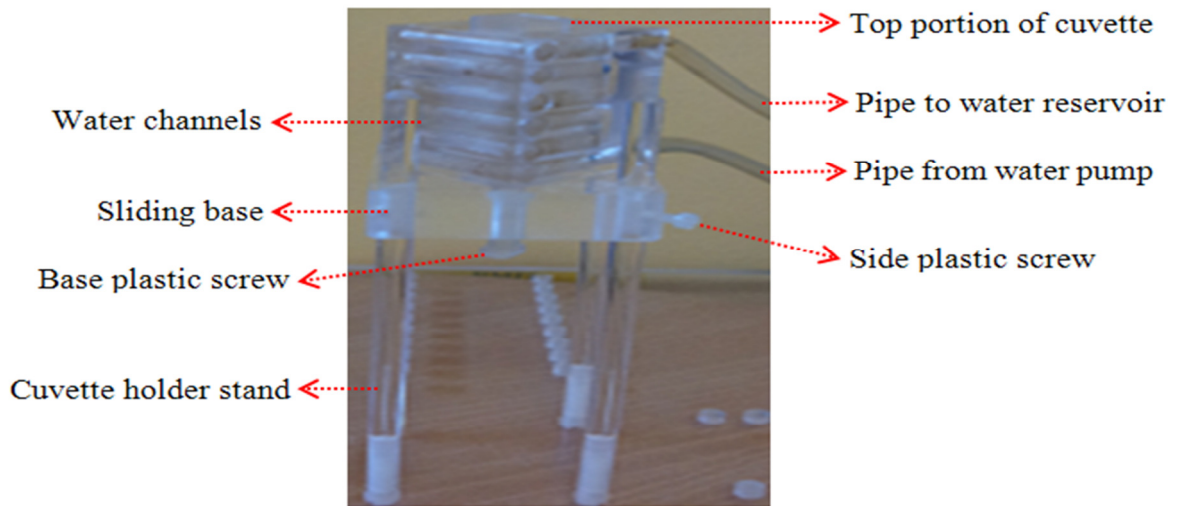


Figure 3.15: Design 2: Novel cuvette holder [123].

As shown in Figure 3.15 the cuvette holder consists of three different blocks of acrylic with professional cut water channels embedded within the blocks. The sliding base of the holder is fitted through the stands and made stable by the slide plastic screw. This screw can easily be manoeuvred to select the desired position of the cuvette holder during experimentation. The cuvette holder stands were also calibrated in circular fashion to ascertain the exact position of the cuvettes vertical orientation. The base plastic screw at the bottom of the cuvette holder helps to eject the cuvette after each experiment is conducted. The holder has in-built cooling system. Two plastic pipes are fitted to the cuvette holder (one at the top and the other above the sliding base). The pipe above the sliding base is connected to the water pump and forces controlled water inside the cuvette holder through the water channels. The pipe at the top part of the cuvette holder channels the water back to the water reservoir for continuous circulation.

### 3.3.1.3 Integrated Custom Made Water Regulatory System

A major challenge was to control a specific temperature in the vicinity of the cuvette placed in the cuvette holder structure. For this, a regulated water circulatory system needs to be integrated in the cuvette holder. Readily available temperature control devices cannot be used since they are connected to the holder via connectors with metallic pins. The design of the custom built water regulatory system is presented in Figure 3.16.

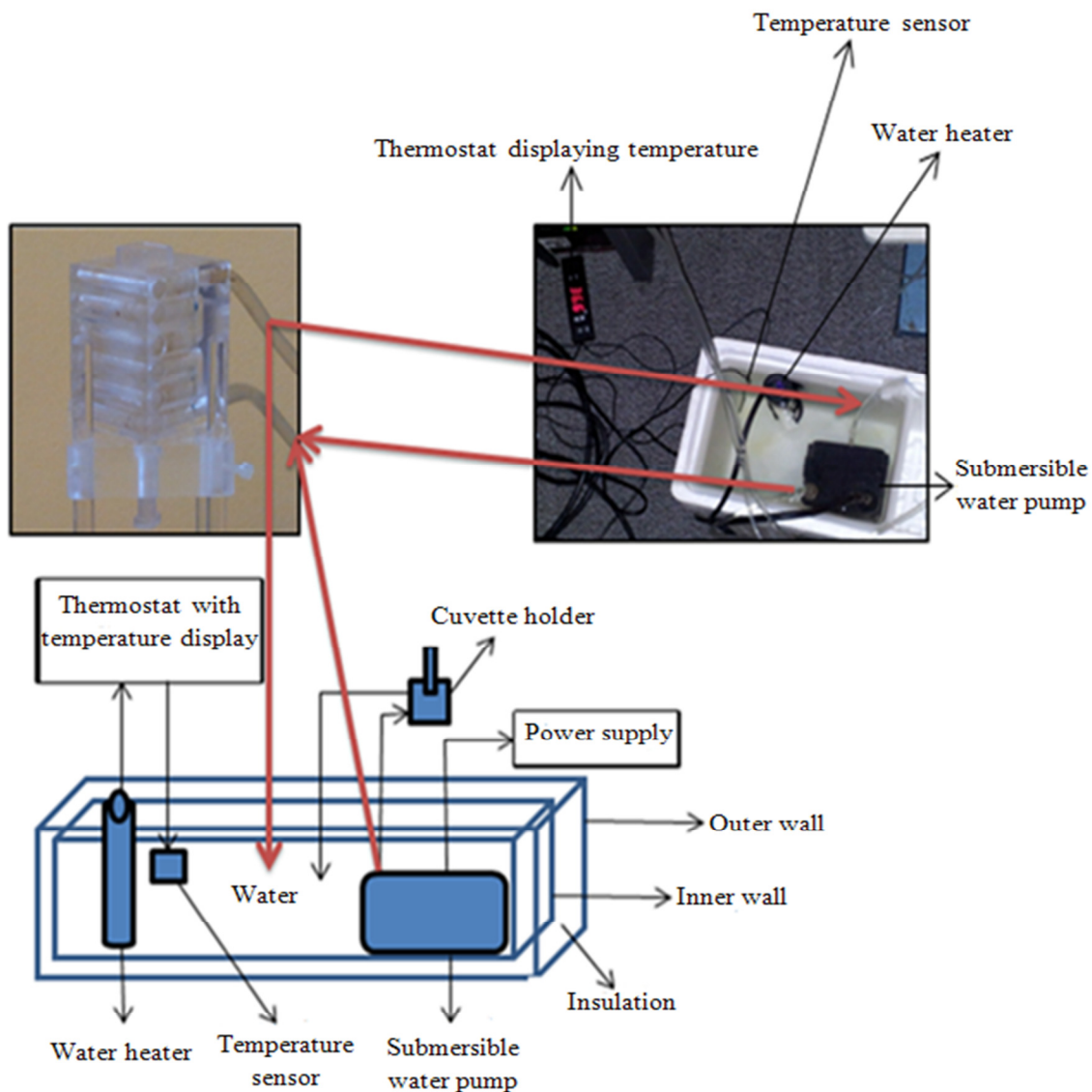


Figure 3.16: Schematic of the custom built water regulatory system used as part of the ELF PEMF system (bottom) [123]. Practical setup (top right), with the upper lid taken off for aiding visualization. Arrows showing the water pipe connection between the cuvette (top left) [123] and the schematic and practical water regulatory system setup.

Foam board have been used as insulation material and was placed between the outer and inner walls of the water reservoir. The connection of the water pump to the cuvette holder has been described in the previous section. The water reservoir contains a water heater connected to a thermostat with a digital display of water temperatures. The temperature sensor from the thermostat is also submerged in the water reservoir. The thermostat maintains the water temperature and accordingly turns on and off the water heater. The entire process ensures that the water temperature (in this study, 37° C for experiments with Collagenase enzyme solution) inside the reservoir is well controlled.

However, the sample temperature (with no magnetic field) is also required to be checked. It is achieved by continuous monitoring of a digital thermometer submerged into a biological sample solution. The time for the heat to be transferred from the water in the reservoir to inner surface of the holder and onto the cuvette and then finally to a sample solution was continuously monitored. For accuracy, we repeated the process three times.

The main objective was to keep a sample solution at the temperature of 37° C. It was observed that for the designed structure it takes approximately 1hr for the temperature to settle at 37° C. Once the temperature reaches 37° C (the same as that of the water reservoir), the temperature remains maintained for the duration (10min) of the experiment with the selected protein solution. Therefore, before running the series of experiment and more specifically before the sample exposures to ELF PEMF, it was ascertained that the cuvette holder is sufficiently warmed up for the heat transfer to the solution. This is ensured by allowing the custom made water regulatory system to commence operating approximately an hour before the actual experiment is conducted.

The demonstration of water circulation through the embedded water channels of the cuvette holder structure (Design 2) is shown in Figure 3.17 and indicated by stages S1 through S5. For visual clarity and understanding of the exact path of water flow and thereby the water channels structure, red dye was mixed with water and placed inside the water reservoir. Of note, clear water was used in all the experiments.

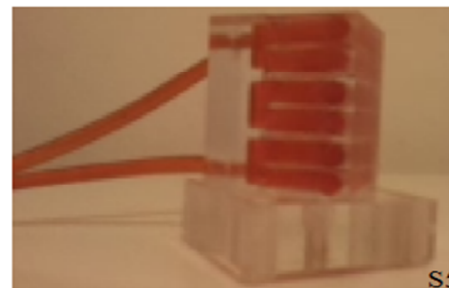
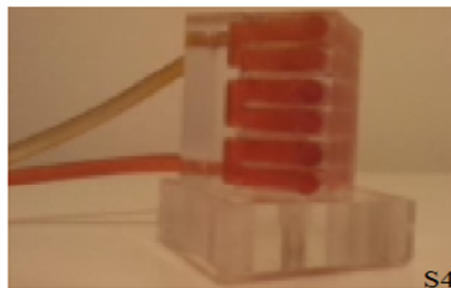
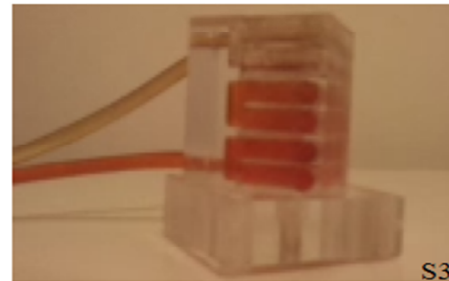
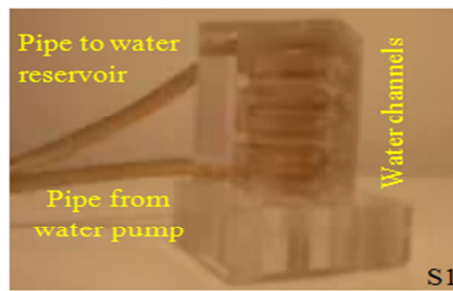


Figure 3.17: Water circulating through the cuvette holder demonstrated in five stages from S1 through S5.

In Figure 3.17, S1 represents the status of the cuvette holder before the submersible water pump is switched on. Therefore there is no water circulating through the cuvette holder. In S2, water starts flowing through the pipe connected to the water pump (bottom pipe) and from the base starts to circulate the cuvette holder via the water channels. In S3, the progress of this circulation is shown and the water channels become more vivid. In S4 the circulation is complete as the water channels are all filled. In S5, water leaves the cuvette holder through the pipe that leads to the water reservoir and is indicated by the presence of red dyed water inside the top pipe.



### 3.4 Equipment and Experiment Setup

Equipment used during experiments can be divided into two categories. (i) General and (ii) Specific. General equipment used is discussed in this chapter. Specific details of equipment required for experimentation with enzyme solution and bacterial culture are provided in Chapter 4 and 5, respectively.

The design and development of the ELF PEMF chamber along with the sample holder design required for all conducted experiments have already been detailed in Section 3.3.

An arbitrary function generator (*Thurlby Thandar Instrumnets, TTi, Model TG4001*) was used to generate unipolar square pulse from 2Hz-500Hz. All concerned parameters like frequency, duty cycle, wave shape, peak-peak voltage, etc. can be entered directly from the numeric keypad. Alternatively most parameters can be maneuverer using the rotary encoder for quasi-analogue control.

A DC power supply (*G<sup>w</sup>INSTEK, DC Power Supply, Model GPC 3030DQ*) was connected to the PEMF coils and adjusted to supply current for generation of ELF PEMF. DC power supply used for all experiments served as a current generator.

A 2-channel oscilloscope (*Agilent Oscilloscope 2-channel 100MHz, Model 54622A*) was used to observe the waveform produced by the function generator and the waveform across the 1 $\Omega$  resistors connected between the multimeter and the power supply as can be seen in Figure 3.20.

The resistance and inductance of the PEMF coils were verified with RLC meter (*Fluke Programmable Automatic RLC meter, Model PM6306*).

Current from power supply goes via the multimeter (*WAVECOM INSTRUMENTS, FLUKE 19*) and reaches the PEMF coil for generating magnetic fields. The current reading from this multimeter was continuously monitored, since it served to show the presence of any

fluctuation in the current being sourced to the coil from the power supply. This was important since a current fluctuation would mean the distortion of the produced magnetic flux density and eventually a misinterpretation of results. Multimeters used for all experiments served as an Ammeter.

**Switching circuit:** Two similar switching circuits were used in this study for each conducted experiments. One of these switching circuits is shown separately in Figure 3.18. Main component of this circuit is a transistor, for this research, an N- channel Power MOSFET (IRF 520) (Appendix B) mounted on a heat sink. Additionally, several binding posts along with a diode installed on a printed circuit board (PCB) complete the switching circuit. Binding posts connect the MOSFET terminals to the other parts of the circuit setup as well as the common ground and is shown Figure 3.18.

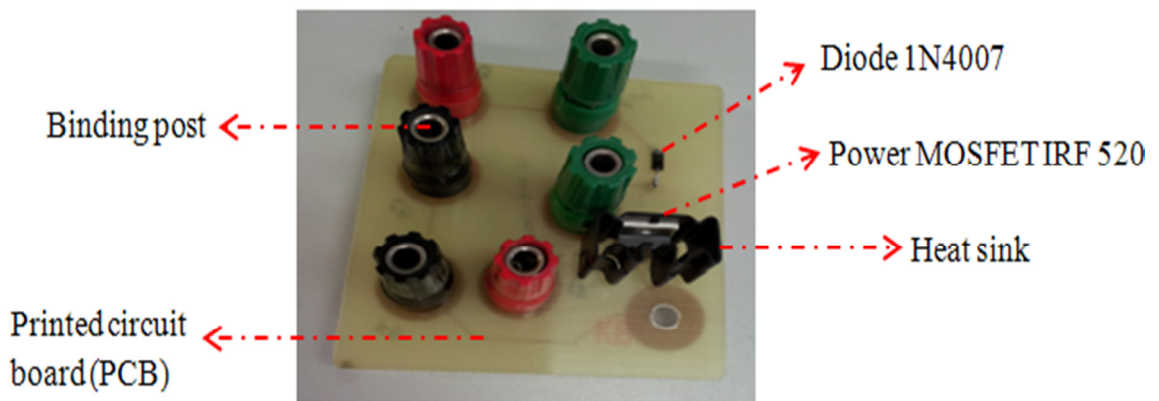


Figure 3.18: Switching circuit used in the ELF PEMF experiments.

Power MOSFETs are well known for their superior switching speed since they require very little gate drive power because of their insulated gate. This makes them a suitable as an “ideal switch”. In N – channel MOSFETs, only electron flow during forward conduction- there are no minority carriers. Switching speed is only limited by the rate charge supplied to or removed from capacitances in the MOSFET. Therefore, switching can be very fast, resulting in low switching losses and thus making the Power MOSFET efficient corresponding to switching frequency.

Necessary tests were carried out before the experimentation to confirm whether or not the DC power supply acting as a current generator was functioning up to its respective standard. For this, a simple test was carried out by using the multimeter, to check whether the current supplied to the multimeter is the same as displayed on the panel of the DC Power supply. This setup was then connected to the coils to test for any losses, as shown in the block diagram below (Figure 3.19(a)). There were no losses in the current being sourced to the coils. This was confirmed by the multimeter which displayed the same current value as supplied by the DC power supply. The multimeter was then connected after the coils to check for any current losses in the coils (Figure 3.19(b)). There were no losses in the coils, due to the setup being in line with their specifications.

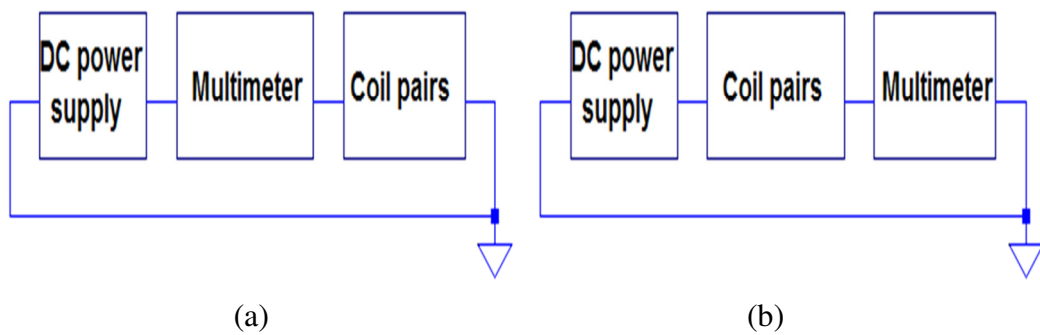


Figure 3.19: (a) Block diagram for pre-testing setup for (b) Set-up to check for any current loss in the coil.

Figure 3.20 shows the circuit set up for the ELF PEMF experiments. Integral measuring instruments used were briefly discussed above and can be visualized in the figure.

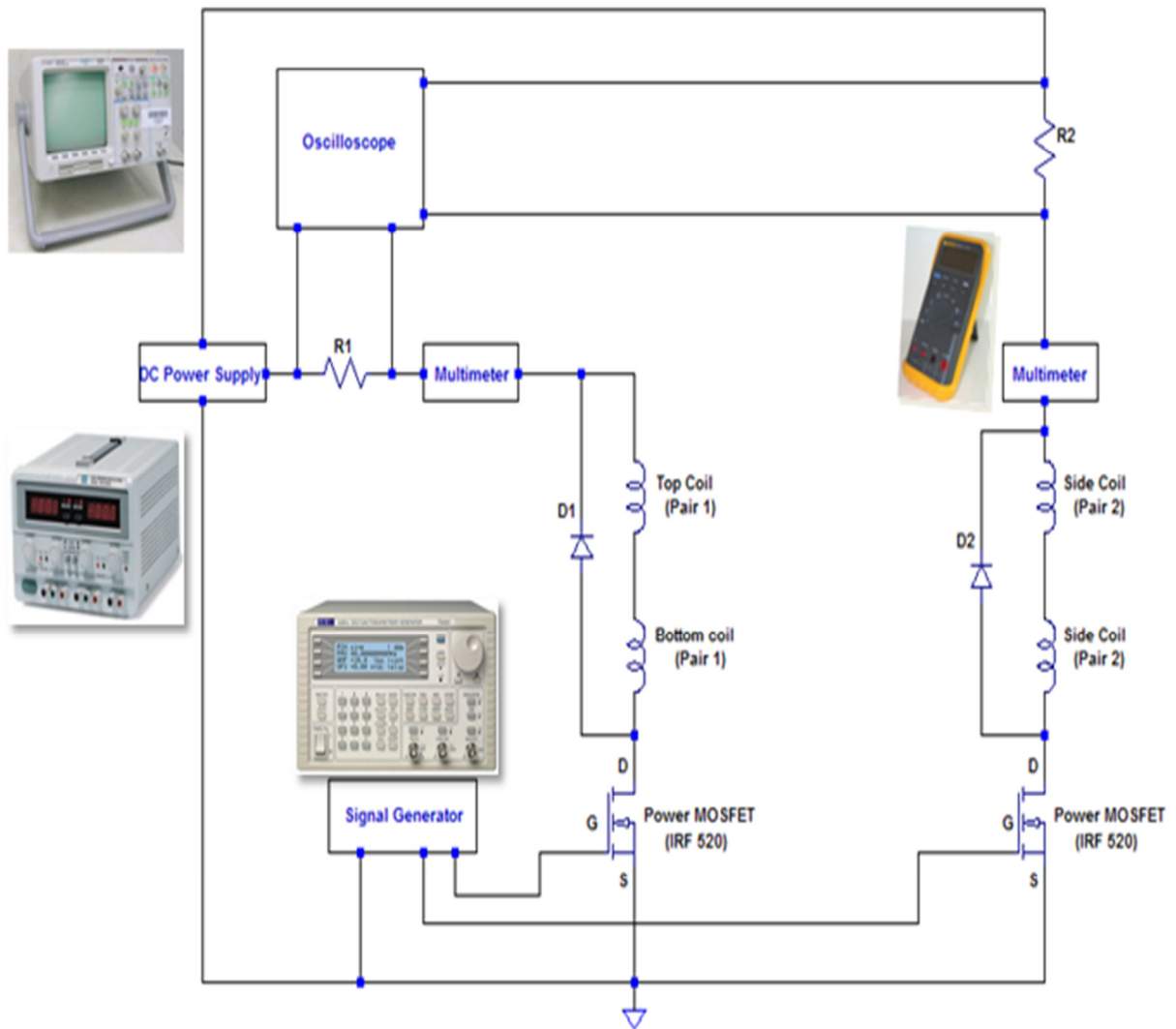


Figure 3.20: Circuit setup for ELF PEMF experiments.

At the beginning of every experiment a unipolar pulse signal (50% duty cycle square wave) corresponding to a single selected frequency between 3Hz-500Hz is set up directly by the numerical keypad of the signal generator. Using a “T” connector, this signal is then fed to the gate terminal of the both the transistors (Power MOSFET IRF520). However, the output from the signal generator was not efficient enough to pass a sufficient current to generate the desired magnetic field. Therefore, a DC power supply was used and connected to the coils via a 1Ω resistor and a multimeter as can be seen in Figure 3.20. The particular setup works on the principle that when the gate terminal receives a high signal, i.e., the high state of square wave signal (Figure 3.21), then the transistor is switched on and the current from the DC power supply is allowed to go through the coils into the drain terminal and flow out of the

source terminal. Similarly, when the gate terminal received a low signal, i.e., low state of the square wave signal (Figure 3.21), then the transistor was switched off and no current flow between the coils. This turning on and off of the current flow results in the pulsating current that the coil is subjected to in order to generate uniform time varying magnetic fields within the ELF PEMF chamber in the frequency range of 2-500Hz, with magnetic induction (magnetic flux density) of 0.5-2.5mT. The process described holds for both the Pair 1 and Pair 2 coil setup.

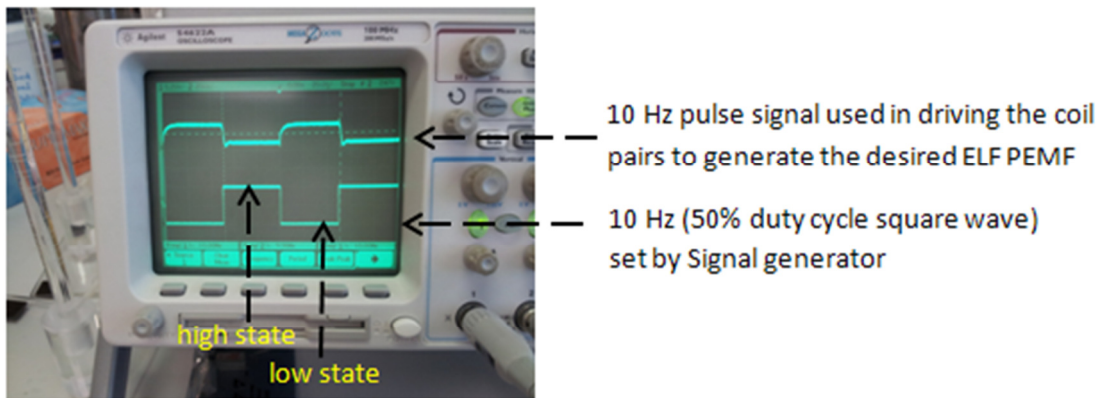


Figure 3.21: Oscilloscope trace of a 10Hz pulse signal set by the signal generator and a 10Hz pulse signal used to drive the coil pairs.

The limitations of the majority of coils are associated with the magnetic field frequency. Within the experimental measurements it was noted that due to increase and decrease of applied frequencies from the signal generator, the current fed through the coils by the power supply also varied. Considering that several frequencies were used in this study, each time the frequency was changed via the signal generator, the power supply was also accordingly adjusted. The frequency of the pulsating current was observed via the Oscilloscope in terms of the frequency of the voltage waveform over a  $1\ \Omega$  resistor connected between the DC power supply and the multimeter (Figure 3.20). This frequency was always found to be similar to the displayed frequency of the signal generator. The frequency of this pulsating current is dependent on the values set at the signal generator connected to the gate of the transistor. The strength of the magnetic flux density is directly related to the amount of current flowing

through individual coils, i.e., the magnitude of the pulsating current and is regulated by the DC power supply connected to the drain of the transistor via the coil pairs.

The flow of pulsating current into the coils ultimately results in the production of a uniform time varying magnetic field within the coil network and inside the ELF PEMF chamber as stated before. However, magnetic field will collapse suddenly when the current is switched off. This collapse will in turn produce brief high voltage across the coils, and is likely to destroy the transistors in that particular circuit setup. To prevent this, a protection diode is intentionally placed in parallel to the coils. This diode prevents the induced voltage to become high enough to cause damage to the transistor.

In this research project air core Helmholtz coils were used for its many documented advantages [183]. Air coil system is superior in comparison with other methods of PEMF stimulation when considering many factors such as usability, size, consistency, etc. Helmholtz coils also have a closed form solution pertaining to the magnetic field they produce in the centre of the coil configuration. Usage of ferromagnetic materials in coil core leads to nonlinear operation when the current through them is large enough to drive their core materials into saturation. This non-linearity can cause the generation of higher frequency components. To prevent this we have used air core coils. Therefore, the only consideration needed to make while winding the coil was for root mean square (rms) value of the current and not for peak harmonic current (sum of individual harmonic currents), as would have been the case if using a coil with ferromagnetic core.

The flexibility of the particular setup discussed above can easily be adopted for generating a rotating uniform magnetic field by just adding a 90° phase shifter to one of the output of the signal generator as was demonstrated in [260]. This would then mean that the pulsating current reaching the coil pairs would be phase shifted by 90°. However, these types of rotating field are mostly used for experiments pertaining to characterization of magnetic fluids

[262]. Of note, for the conducted experiments, there were no phase shift, i.e., a phase shift of  $0^\circ$  between the pulsating current supplied to Pair 1 and Pair 2 coils.

## **3.5 Measurement of ELF PEMF**

In order to maximize the accuracy and efficiency of the magnetic field measurements, it was essential to construct an additional apparatus described in Sections 3.5.1. The design of the new measurement apparatus has prompted to exclude once again the use of any conductive materials that could possibly alter the magnetic field distribution within the coils. It was also taken into account that the coils were placed as far as possible from any neighbouring power supplies, function generators or any conductive materials.

### **3.5.1 Experimental Setup for Magnetic Flux Density Measurement within the ELF PEMF Chamber**

To measure the magnetic flux density along  $z$  axis (axial axis of Pair 1 coils) and  $x$  axis (axial axis of Pair 2 coils), the local coordinates of the ELF PEMF chamber has to be determined. Figure 3.22 (a) shows the origin of the local coordinate system of the ELF PEMF chamber marked by “ $O$ ” which denoted the point  $(0, 0, 0)$ . This local coordinate system was earlier demonstrated in Figure 3.3 with respect to the biological sample containers used in this study.

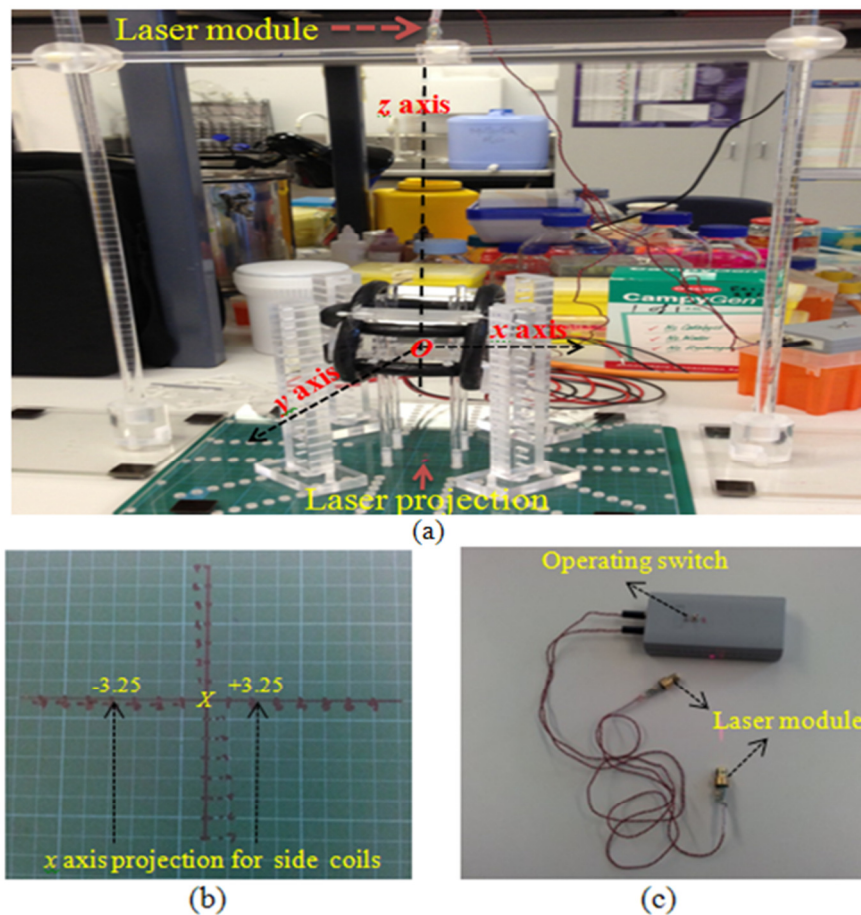


Figure 3.22: (a) Determining the local (coil network) coordinate system inside the ELF PEMF chamber (b) Grid mat used in the ELF PEMF chamber for determining  $x$  and  $y$  axis and the placement of Pair 2 coils (c) Assembly of the Laser module.

To ascertain the precise alignment of a biological sample centred at  $(0, 0, 0)$ , a laser module (purchasing information, Appendix C) was conveniently wired and assembled in the lab (Figure 3.22 (c)). Once mounted, the laser module was then turned on by the operating switch shown in Figure 3.22 (c). This resulted in a projected laser beam (red dot at the centre of the grid map, Figure 3.22 (a) at the marked origin,  $X$ , of the grid mat. A close look of the grid map is given in Figure 3.22(b), where the marked origin  $X$  is clearly shown. The path which this laser beam follows from the laser module through the local origin  $(0,0,0)$  and then into the marked origin,  $X$ , of the grid mat, is denoted by a dotted line and referred to as the  $z$  axis. An empty cuvette/2.5mL centrifuge tube was then aligned with this laser projection and positioned at the local origin  $(0,0,0)$ , and then fitted on to the appropriate sample holder to pinpoint the exact location of the biological sample during exposure to ELF PEMF.



Similar set up was used with two laser modules placed apart at the distance of 6.5cm (radius of the Pair 2 coils) from the origin and two laser beams being projected on the +3.25cm and -3.25cm mark (Figure 3.22(b)) on the  $x$  axis. Side coils (Pair 2) were then aligned with these projected beams in order to ascertain their horizontal separation according to Helmholtz coil configuration. Of note, the particular square from 3cm to 4cm and from -3cm to -4cm was further subdivided into four equal parts with neatly drawn markings. Placement of Pair 1 coils according to Helmholtz coil configuration was earlier discussed in Section 3.3.

The setup of Figure 3.23 (a) clearly demonstrates the method of obtaining magnetic flux density along the  $z$  axis.

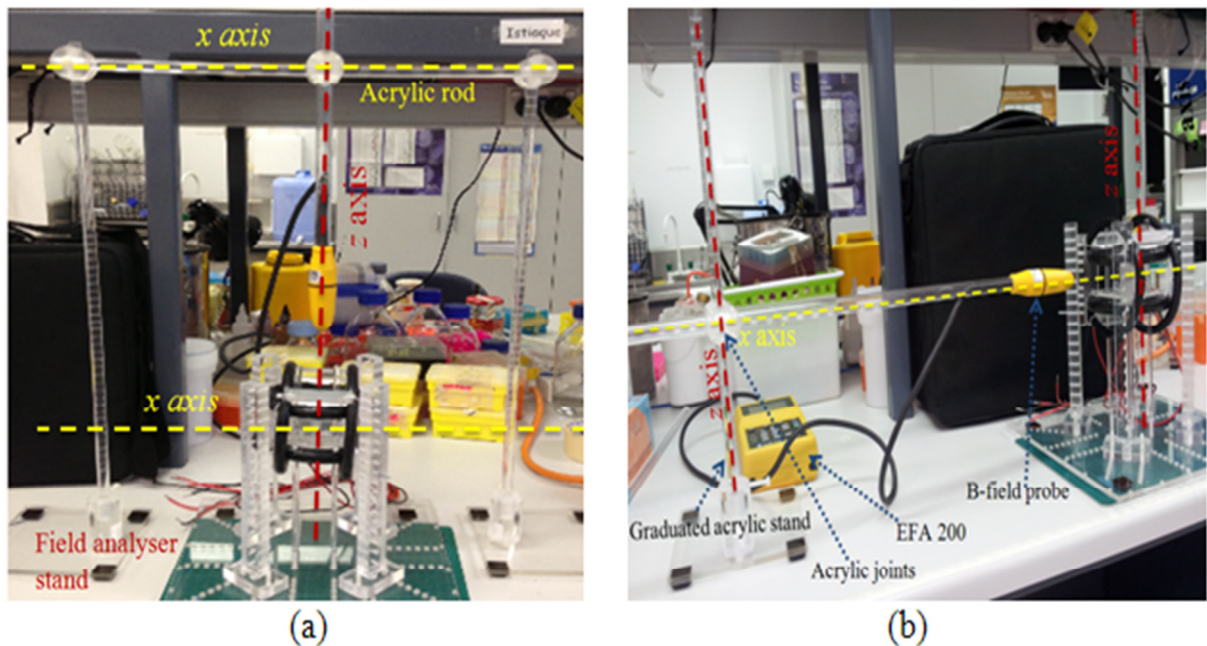


Figure 3.23 : Demonstration of magnetic flux density measurement with EFA 200 Analyser along (a)  $z$  axis (axial axis of Pair 1 coils) and (b)  $x$  axis (axial axis of Pair 2 coils).

A B-field probe was firmly held in place via a vertically placed plastic pipe whose one end was specially design to accommodate the specific geometry of the probe and hence, it's mounting. Two yellow dotted lines ( $x$  axis) have been marked out in Figure 3.23(a). Position of the bottom yellow line represents the  $x$  axis of the 2-Axis HCS. Position of the top yellow line represents the  $x$  axis alignment of the horizontal acrylic rod whose two ends are connected to each of the field analyser stands by means of acrylic joints. Circular graduated

marking on these stands are exactly aligned with the coils and the holder stands of the ELF PEMF chamber. For the B-probe to vertically shift down and scan through the  $z$  axis, the acrylic joints connected to the field analyser stand were loosened resulting in the  $x$  axis oriented acrylic rod to shift down by a vertical distance that can easily be seen from the field analyser stand graduation markings. For magnetic flux density measured along the  $z$  axis corresponding to different  $x$  values, the acrylic joint in line with the  $z$  axis is simply needed to be adjusted and moved along either side of the dotted  $x$  axis Figure 3.23(a) placed along the graduated acrylic rod.

Similar setup (Figure 3.23 (b)) to that explained above was used to measure the magnetic flux density along the  $x$  axis of the 2-Axis HCS. Yellow dotted line denotes the  $x$  axis going through the local origin of the ELF PEMF chamber, and two red dotted lines denote the  $z$  axis. Line denoting the  $z$  axis and placed on the right hand side of Figure 3.33(b) served as the  $z$  coordinate of the ELF PEMF system and passed through the local origin of the system. For the B probe to scan through the  $x$  axis, the single acrylic field analyser stand has to be brought closer to the PEMF chamber.

Experimental setup for magnetic flux density measurement along  $y$  axis going through the local origin of the ELF PEMF system and corresponding to different  $z$  values was the exact same to that mentioned above for the  $x$  axis magnetic flux density measurement. The only difference was that the placement of the field analyser stands was made such that the B-field probe now faced towards the  $y$  axis instead of the  $x$  axis.

### **3.5.2 Actual Measurement of Magnetic Flux Density**

The magnetic flux density was verified by direct measurement using EFA-200 EMF Analyser (Wandel and Goltermann) and an external B-field probe attached to the Analyser. This particular EMF Analyser allows measuring of the source frequency and its corresponding

magnetic flux density (B-field). The analyser uses an innovative technique of “Shaped Time Domain” (STD) to display frequency of magnetic flux density by directly converting the time-domain limits into frequency domain limits [263]. The peak value of the magnetic flux density  $\hat{B}$  is calculated by the EFA Analyser from the variation in time of  $B_x(t)$  through  $B_z(t)$  of the magnetic flux densities in the three measurement axes using the following formula [264]:

$$\hat{B} = \text{Max} \left\{ \sqrt{B_x^2(t) + B_y^2(t) + B_z^2(t)} \right\} \quad (3.7)$$

The frequency and corresponding magnetic flux density reported in this work are measured at the local origin (0,0,0) (Figure 3.22 (a)) of the ELF PEMF chamber where the actual biological sample was later placed and exposed to ELF PEMF. Thus, the reported magnetic flux density corresponding to a given frequency is exclusively measured for the main field source (2-Axis HCS). Figure 3.24 illustrates a typical result as observed at the local origin of the ELF PEMF chamber. A magnetic flux density of 1.0mT corresponding to the source frequency of 250Hz during one of the experimental measurements can clearly be seen [147].

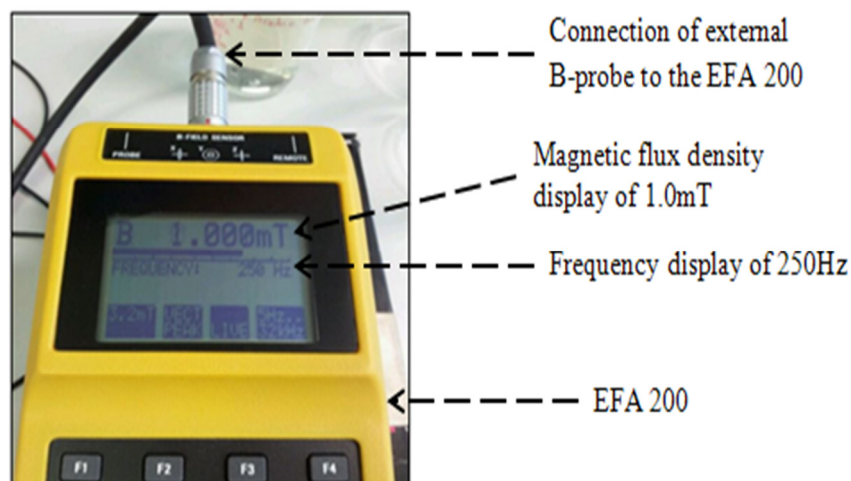


Figure 3.24: EFA 200 Analyser displaying a magnetic flux density value of 1.0mT at 250Hz [147].

Magnetic flux density values measured by the EFA 200 Analyser are changing with respect to the frequency of the particular pulse signal that is fed to the current carrying coils. Source frequency (obtained by the EFA 200, Figure 3.24) for all experiments were always compared with the frequency of the pulse signal (obtained from Oscilloscope, Figure 3.21) fed to the coils and with the frequency (displayed on the signal generator and verified from Oscilloscope, Figure 3.21) of the pulse signal (50% duty cycle square wave) set by the signal generator. These three, above mentioned frequency readings, were always found to be similar and served as a critical checkpoint baseline in order to commence and continue experiments using ELF PEMF.

### 3.6 Comparison of Theoretical and Experimental Results

Inaccuracies in coil positioning are the most important parameters that deteriorate the coil systems performance [172]. The comparison of magnetic flux density between analytic results obtained from Maple 14, and simulation results obtained using CST EM Studio along with experimental results obtained via the EFA- 200 are shown in Figure 3.25.

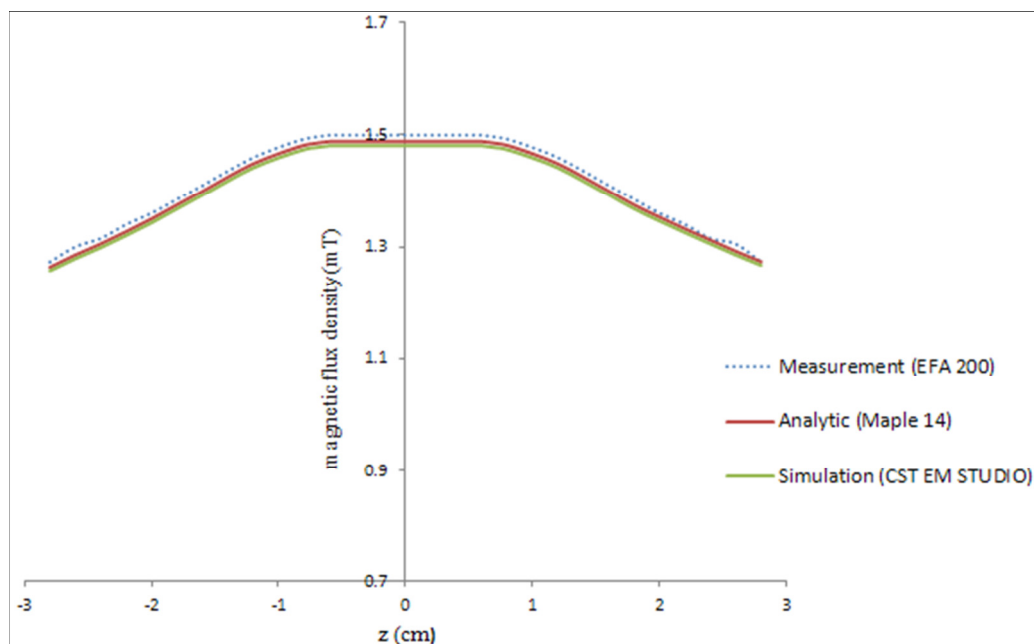


Figure 3.25: Comparison of theoretical and experimental results.

All values of magnetic flux density are measured along the  $z$  axis for the current value of  $I=0.35\text{A}$  in each coil of the 2-Axis HCS. Measured magnetic flux density along  $z$ -axis from  $0.5\text{cm}$  to  $-0.5\text{cm}$  reaches constant at  $1.5\text{mT}$ . Relative differences between experimental and theoretical values of magnetic flux density are  $1.75\%$  (for analytical results using Maple 14) and  $2.25\%$  (for simulation results using CST EM Studio). Thus, the calculated results were confirmed by the measurements. In the central region of the system (approximately  $0.5\text{cm}$  each side of the origin), both the experimental and the calculated results show that the magnetic field is uniform and hence imply that the coil positioning is accurate.

### 3.7 Temperature Control and Power Constrains

One of the major considerations in designing of the ELF PEMF chamber was based on how best to control the temperature inside the chamber, so that a standard room temperature ( $23^\circ\text{C}$ ) was maintained during the exposures. Through resistive heating the coil gives rise to heat. Resistive heating occurs as a result of the coil's resistance to current flowing through it. There is a risk that some of the heat generated will be transferred to a biological sample. To prevent heating of a sample, the heat must be removed from the coil. A cooling mechanism (temperature control) was therefore incorporated from transferring resistive heat to the sample. In some instances, when the input power is low (under a few watts) no cooling is needed, tens of watts may be air cooled or water cooled. Generally a larger power load of more than  $50\text{W}$  is water cooled [193].

Following measures were taken to account for temperature control during conducted experiments.

***Selection of air core coils:*** Coils with nonmagnetic cores are commonly referred to as air core coils. Power is lost in an inductor (e.g. current carrying coil) by means of several different mechanisms. Two such losses are eddy current loss and hysteresis loss. Both loss types result

in sound degradation and not applicable to air core coils. Also, if the coils have anything other than an air as a core, then the concentration and shape of the resulting field can differ with temperature.

**2-Axis Helmholtz coil system:** In this design, the magnetic field produced by individual pair of coils adds up by means of superposition and therefore greatly reduces the amount of current needed to be fed to individual coils in order to attain a higher magnetic flux density. Lower amount of current through the wires greatly reduced resistive heating.

**Air cooling system:** Type of cooling selected for experiments depend upon the coil holder structure and airflow available. Dust and air index variation was also not a problem for the conducted experiments. These compelled for the adoption of an air cooling system for the experiments. The design therefore has been made to accommodate availability of free circulation air circulation, so that enforced air from outside can easily enter the chamber and dissipated the heat and maintain a defined temperature inside.

**Wire temperature concerns:** The resistance and impedance of the coils give rise to heat build-up. Wire temperature analysis was done in order to project whether the build-up temperature could conceivably be great enough to melt the insulation of the wire. According to the analysis, per minute gain of the temperature for copper wire for a maximum current of 0.79A (rms) was found to be insignificant. The equations used in the analysis are presented below:

All calculations are done based on the usage of 22AWG copper wire.

**Diameter** of wire,  $d$  :

$$d = e^{-1.12436 - (.11594 * n)} \quad (3.8)$$

where,  $n$  = rating of the AWG

**Length** of a coil,  $l$ :

$$l = N\pi D_c = N\pi 2r \quad (3.9)$$

where,  $N$  = number of turns  
 $D_c$  = diameter of coil  
 $r$  = radius of coil

**Resistance** of wire,  $R$  :

$$R = \frac{4\rho l}{\pi d^2} \quad (3.10)$$

where,  $\rho$  = resistivity of a material, copper =  $1.68 \times 10^{-8} \Omega m$  (Appendix D1)  
 $l$  = length of a coil  
 $d$  = diameter of the copper wire (Appendix D2)

**Power** calculation,  $P$  :

$$P = I^2 R \quad (3.11)$$

where,  $I$  = current passing through the wire (A)  
 $R$  = resistance ( $\Omega$ )

**Thermal energy** absorbed every minute,  $Q$  :

$$Q = P * t * N \quad (3.12)$$

where,  $P$  = Power (J/s)  
 $t$  = time (s)  
 $N$  = number of turns

**Volume** of copper segment,  $V$ :

$$V = \pi r^2 h \quad (3.13)$$

where, for a coil segment,  $h = l$  = length of the coil  
 $\pi r^2$  = cross-sectional-area (Appendix D2)

**Mass** of copper segment,  $m$  :

$$m = \text{Volume} * \text{Density}$$

$$m = V * D \quad (3.14)$$

where,  $V$ =volume of copper segment

$$D = \text{density of copper} = 8.9 \frac{\text{g}}{\text{cm}^3} \quad (\text{Standard value}) \quad (\text{Appendix D3})$$

Calculation of **gain of temperature**,  $\Delta T$  , each minute is given by:

$$\Delta T = \frac{Q}{mc} \quad (3.15)$$

$Q$  = Thermal energy (J)

$c$  = Specific heat of copper =  $0.385 \frac{\text{J}}{\text{g} \cdot \text{C}}$  , (Standard value) (Appendix D4)

$m$  = Mass of copper (g)

**Joule heating:** It was calculate as the maximum power dissipated by a single coil. The following equation was used:

$$P = I^2 R = I^2 \rho_{\text{copper}} \frac{l}{A} \approx NI \rho_{\text{copper}} \frac{4l_{\text{turns}}}{\pi d^2} \quad (3.16)$$

where,  $R$  is the DC resistance.  $R$  is calculated using the formula  $R = \rho_{\text{copper}} \frac{l}{A}$  ,  $\rho_{\text{copper}}$  is the resistivity of copper,  $l$ , is the length of the wire and  $A$  , is the cross-sectional area of the wire,  $l_{\text{turn}}$  is length of a single turn,  $N$  is the total number of turns in the coil and  $d$  is the diameter of 22 AWG. Maximum power obtained from computing (3.16) was 0.84W for a coil with radius 6.5cm (radius of Pair 2 coils), current of 0.79A (rms) and 100 coil turns. Of note, 0.79A was the maximum current noted to pass through the coils for the entire range of conducted experiment pertaining to this research project.



The resistance of a current carrying wire is inversely proportional to its cross sectional area. Therefore, selecting a thicker copper wire and thereby increasing the cross sectional area can reduce resistance and allow for more current to pass. This influenced the choice of selecting 22AWG for the air core coils.

***Air cooling system:*** Joule/Resistive heating of the current carrying coils can potentially lead to a higher temperature within a sample. The setup shown in Figure 3.26 (a) was used to tackle this problem. The maximum temperature rise during experimental procedure at the centre of the exposure system (location of the biological sample) corresponding to maximum power dissipation by each coil, was measured in the lab via digital thermometer and noted at 4° C (maximum) above 23° C ( lab temperature). Following steps were taken to eliminate this heat factor: 1) A two-socket digital temperature controller thermostat (Figure 3.26 (b)) was set at 23°C. 2) A cooling fan was connected to one of the thermostat socket and 3) The temperature sensor of the thermostat was put through one of the holes of the coil stands, just below the side coil so that it did not perturb the space inside the coil network. This sensor immediately picks up any rise in temperature of the surrounding air due to coil heating and matches it with the pre-set thermostat temperature. A temperature reading higher than 23° C turns on the airflow from the cooling fan and a lower reading turns it off. Meanwhile, a digital thermometer was used to continuously observe and record the temperature at the centre of the exposure chamber (location of exposed samples). A maximum temperature increase of 0.2° C above the lab temperature was recorded at the centre of the ELF PEMF chamber corresponding to the maximum current supplied to the coils (.79A). This is a minimal rise and that considered insignificant in terms of alternation of biological activity of the experimental sample. The fact that results were repeated in triplicates (Chapter 4 and 5) gave clear indications that the temperature on each and every conducted experiment was well maintained.

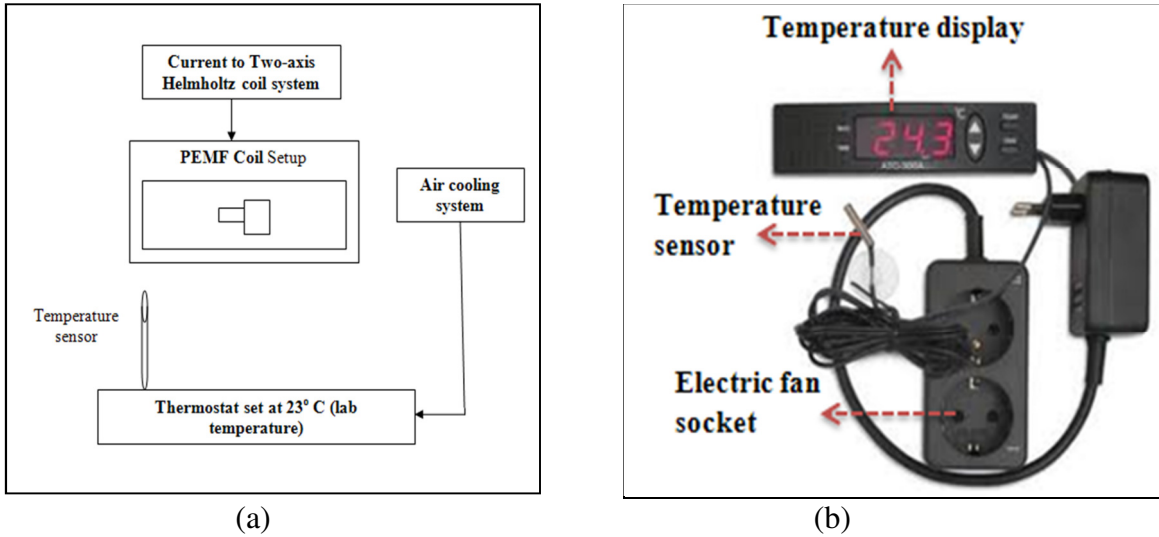


Figure 3.26: (a) Experimental setup for temperature control within the ELF PEMF coil network caused due to Joule heating (b) A two-socket digital temperature controller thermostat (purchasing information, Appendix C).

### 3.8 Data Acquisition

Magnetic flux density measurements at the selected frequency for all conducted experiments were systematically saved in the EFA-200 Field Analyser. Upon completion, the data was imported via a serial port to Data Logger software (EFA-200/300 SW-Tools, Version 1.03, Safety Test Solution from Wandel & Goltermann WG) as a text file. The data was then imported to Excel spread sheet and tabulated for graphical representations.

### 3.9 Inductance and Stability of Magnetic Flux Density

Magnetic field intensity loss is one of the main limitations where for the applied frequency, the rise time of the magnetic field in the coil is influenced by its inductance  $L$  and mutual inductance  $M$ . The inductance is determined by the coil diameter  $D_c$ , number of coil turns  $N$ , wire diameter  $d$ , and permeability constant  $\mu_0$  and is given by [265].

$$L = \mu_0 D_c N^2 [\ln(8D_c / d) - 7/4] \quad (3.17)$$

In the Helmholtz configuration, the mutual inductance  $M$  between the coils is also taken into

account. Therefore, the maximum magnetic field frequency is given as [265].

$$f_{\max} = \frac{32\rho^2 D_c}{4.4\mu_0 R d^4 [\ln(8D_c / d) - 1.36]} \quad (3.18)$$

where,  $\rho$  is the resistivity of the material (copper) and  $R$  is the resistance of the coil. A magnetic field intensity loss occurs if the applied frequency is increased more than the maximum limited frequency,  $f_{\max}$ . The mutual inductance  $M$ , of Helmholtz coil pairs is a maximum when the angle between its magnetic axes is zero as shown in Figure 3.27 (a). However, mutual inductance,  $M$ , of Helmholtz pair would be zero when the when the angle between the coil pairs is  $90^\circ$  (orthogonal axes) [266]. This is shown in Figure 3.27 (b).

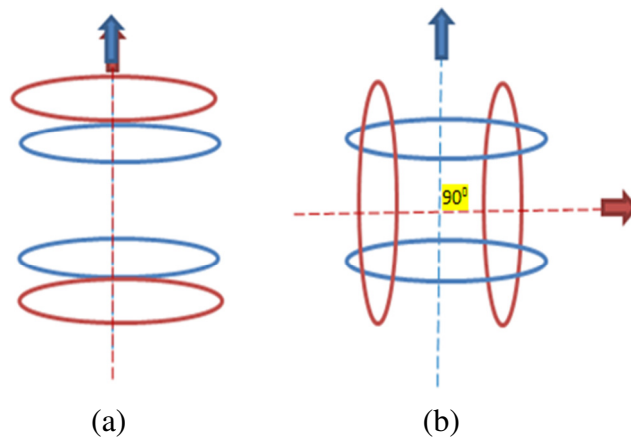


Figure 3.27: Angle between two Helmholtz pair: a)  $0^\circ$  and b)  $90^\circ$ .

From Figure 3.27 it is evident that the particular 2-Axis HCS installed for all experiments conducted during this study causes the mutual inductance between the coils pairs to be zero and therefore yields no contribution towards magnetic field intensity loss.

Excellent magnetic flux density stability was obtained during ELF PEMF experiments by using the 2-Axis HCS. One such example is shown in Figure 3.28. Data acquiring process was earlier explained in Section 3.8.

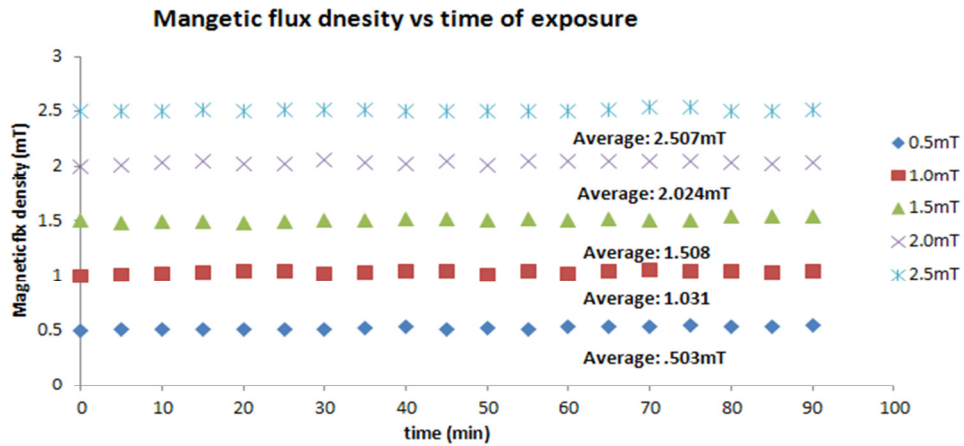


Figure 3.28: Measurement conducted at 250Hz for 0.5-2.5mT over the period of 90 minutes (duration of exposure with experiments relating to bacterial culture), shows excellent field stability during the entire duration of experiment.

The strength of the magnetic flux density is directly related to the amount of current flowing through individual coils. During the experimentation, magnetic flux density steadily remained at a particular B-field value of 0.5mt, 1.0mt, 1.5mt, 2.0mT or 2.5mT, required for experimental exposures.

### 3.10 Summary

A novel design of ELF PEMF exposure chamber was presented. The cuvette holder design and construction has been discussed in details. The custom made software is presented and discussed in details. Results obtained via the custom written software demonstrated the benefits of using the 2-Axis HCS over a 1-Axis HCS. The current coil design scalability for generating magnetic field sufficient for exposure of greater number of samples was also demonstrated via simulation results.

The novelty of the lab-built device correlates to the developed analytical approach and its resulting simulation results along with the systematic design and construction of the ELF PEMF system. Major advantages that the proposed lab-built 2-Axis HCS demonstrates over the existing 1-Axis HCS are listed down in the following fashion:

- The overall magnetic field uniformity of a 2-Axis HCS was shown to be greater than the classical single 1-Axis HCS.
- Superposition of the fields from two coil pairs in the 2-Axis HCS resulted in higher magnetic flux density in the vicinity of the exposed sample while still maintaining the field uniformity.
- With the same amount of current fed into the coils, a higher magnetic flux density was achieved in comparison to the 1-Axis Helmholtz coil system. This greatly enhanced the power efficiency by means of reducing resistive heating for individual coils.
- Conventional device with Helmholtz coils system configuration has no supporting software to map out the uniformity of magnetic field at the centre of the coil configuration (i.e., location of biological sample). The lab built device presented is supported with custom made software to view magnetic field distribution prior to commencing experimentation.
- Existing HCS are rigid in construction and therefore only suffices for coils with fixed radius. The proposed lab-built device can easily be manoeuvred (shifted horizontally and vertically) to accommodate coil optimization (size and position).
- Most existing HCS lacks a cuvette holder. The ones which does is either suitable for experiments conducted under room temperature or are sensitive to magnetic field due to their metal construction. The lab built device incorporates a novel non-metallic cuvette holder and is designed to perform experiments where the biological sample can easily be placed within the vicinity of a user defined temperature. This particularly allows experimentation with enzymes.

Comparison between theoretical and experimental results showed a good agreement.

## **CHAPTER 4:**

# **RESULTS: EFFECT OF ELF PEMF ON COLLAGENASE ENZYME KINETICS**

## 4.1 Overview

The design and development of the ELF PEMF exposure device was detailed in Section 3.4. This chapter presents and discusses the application of the developed exposure system to study the effects of varying parametric changes of ELF PEMF exposures on Collagenase enzyme that plays a key role in wound healing. The experimental procedure and the equipment required for conducting the experiments are also presented. Results from comparative analysis of changes in the enzymatic activity of the exposed vs. non-exposed Collagenase enzyme samples are presented for the selected frequencies of 2-500 Hz and magnetic flux densities of 0.5-2.5mT.

## 4.2 Collagenase Enzyme

Enzyme is a protein that speeds up a chemical reaction in a living organism [267]. It is possible to control the intensity of the enzyme's activity (by activators or inhibitors) without changing the amount of enzyme. This is crucial for any organism. The regulation of the cell metabolism is one of the most important processes regulated by enzymes. The choice of an enzyme is very important for the experimental design.

The most suitable enzyme for this study was Collagenase. In Section 2.18 the role of this enzyme in wound healing process was discussed in great details and in particular its interaction with Collagen. The kinetics of Collagenase enzyme and conformation of its active site are very well known and have been stated in Section 2.18.

## 4.3 Collagenase Enzyme Assay

The assay was chosen to satisfy the following criteria:

1. Time needed for catalyzing of 90% of the substrate should not be longer than 10 min.

2. Buffer does not include any substance that does not absorb in 570nm.

In accordance to the above mentioned prerequisites, the SIGMA assay (SIGMA No. 3.4.24.3) was chosen.

**CONDITIONS:** T = 37° C, pH= 7.4,  $A_{570\text{nm}}$ , Light path=1cm

**METHOD:**

**Continuous Spectrophotometric Rate Determination:** This method is widely used for qualitative analysis in the fields such as chemistry, biochemistry and biology. In this method the course of a reaction is followed by measuring how much light the assay solution absorbs by measuring the intensity of light as a beam of light passes through sample solution. This method is established on the fundamental principle that a compound either absorbs or transmits light over a certain range of wavelength. The device used in conducting this method is a Spectrometer (Section 4.4.1).

**REAGENTS:**

A. 50 mM TES Buffer with 0.36 mM Calcium Chloride, pH 7.4 at 37° C (Prepare 1000 ml in deionized water using TES Free Acid, Sigma Prod. No. T-1375, and Calcium Chloride, Dihydrate, Sigma Prod. No. C-3881. Adjust the pH to 7.4 at 37° C with 1 M NaOH).

B. Collagen Type I

Use Collagen, Type I, Sigma Prod. No. C-9879. Different lots of collagen will produce varying amounts of enzyme activity when used as a substrate for collagenase.



### C. Collagenase Enzyme Solution

Immediately before use, prepare a solution containing 0.05 - 0.1 mg/ml Collagenase in Buffer A.

#### ***PROCEDURE:***

2.5mL cuvettes are filled with the following components (purchasing information, Appendix C):

1. 25mg of Collagen Type I (SIGMA) added to 5ml of Buffer A (50mM TES Buffer with 0.36mM Calcium Chloride in 1000ml deionized water, pH 7.4) and filtered through a 0.8 $\mu$ m syringe filter.
2. 0.10ml of Collagenase enzyme solution (0.075 mg/ml Collagenase in Buffer A).

## **4.4 Experimental Equipment**

General equipment used for investigating the effect of ELF PEMF on Collagenase enzyme kinetic is given below:

1. The designed and constructed ELF PEMF device (Section 3.4) was used to produce a uniform time varying magnetic field [123, 260].
2. EFA-200 EMF Analyser (Section 3.7) fitted with an external B-probe (Wandel and Golterman) was used to measure the magnetic flux density corresponding to selective frequencies produced by the ELF PEMF device. Of note, the detection of magnetic field under the frequency of 5Hz upon switching on the ELF PEMF device was confirmed by the deflection of magnetic compass placed at the centre of the ELF PEMF chamber.

Specific equipment used for investigating the effect of ELF PEMF on Collagenase enzyme kinetic is given below:

To estimate the activity of the particular enzyme accurately, the rate of a change in the optical density of the solution was monitored for the period of time of 600 seconds. In this experiment, the spectrometer USB2000 has been used. Spectrometer USB2000 has following characteristic: CCD detector with 2048 pixels; USB-2 connection with Pentium IV (Windows XP); controlled with OOIBase32 software. The software was set to automatically monitor and save the absorption coefficient at 570nm every 15sec. This spectrometer was connected with the light source USB-ISS-UV/VIS (Ocean Optics, Inc.) of range 190nm-870nm (Figure 4.1).



Figure 4.1: Typical setup of a Spectrometer with the light source and USB connections. A demonstration of a cuvette with experimental solution showing the absorption site and the location of cuvette placement for measuring absorption coefficients is also shown.

Major components of the Spectrometer are shown in Figure 4.2 and its functional parameters are explained in Table 4.1.

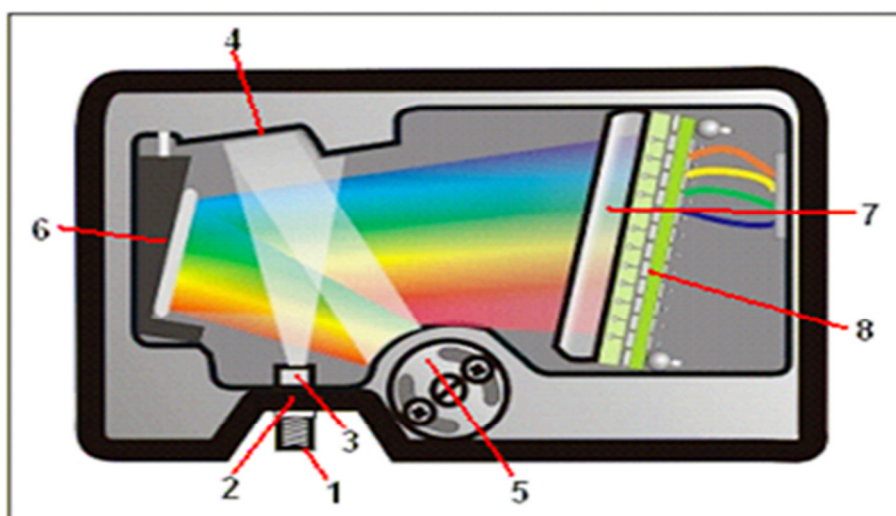


Figure 4.2: Spectrometer USB2000 along with component markings used for measuring optical density (Ocean Optics manual, <http://www.oceanoptics.com/homepage.asp>).

Table 4.1: Components of the spectrometer USB 2000 (Ocean Optics Manual).

1	SMA Connector	The SMA Connector secures the input fiber to the spectrometer. Light from the input fiber enters the optical bench through this connector.
2	Slit	The Slit is a dark piece of material containing a rectangular aperture, and is mounted directly behind the SMA Connector. Aperture size dictates the amount of light that enters the optical bench and controls spectral resolution.
3	Filter	The Filter limits optical radiation to pre-determined wavelength regions. Light passes through the Filter before entering the optical bench.
4	Collimating Mirror	The Collimating Mirror focuses light entering the optical bench towards the Grating of the spectrometer. Light enters the spectrometer, passes through the SMA Connector, Slit, and Filter, and then reflects off the Collimating Mirror onto the Grating.
5	Grating	The Grating diffracts light from the Collimating Mirror and directs the diffracted light onto the Focusing Mirror. Gratings are available in different groove densities to allow specification of wavelength coverage and resolution in the spectrometer.
6	Focusing Mirror	The Focusing Mirror receives light reflected from the Grating and focuses the light onto the CCD Detector or L2 Detector Collection Lens (depending on the spectrometer configuration).
7	L2 Detector Collection Lens (optional)	The L2 Detector Collection Lens attaches to the CCD Detector. It focuses light from a tall slit onto the shorter CCD Detector elements.
8	CCD Detector (UV or VIS)	The CCD Detector collects the light received from the Focusing Mirror or L2 Detector Collection Lens and transforms the optical signal to a digital signal. Each pixel on the CCD Detector responds to the wavelength of light that strikes it, creating a digital response. The spectrometer then transmits the digital signal to the OOIBase32 application.

Microsoft Excel was used to perform spectral analysis. The following steps were followed according to Ocean Optic manual:

1. Spectrum saved in OOIBase32 by selecting File → Save → Processed. Spectrum named according to convenience.
2. Open Excel.
3. In Excel, File → Open. In the top portion of the window proper directory was selected to save the file. In the bottom portion of the window following change was made: “Files of Type” to “All Files”. Selected spectrum file was then opened.
4. From the resulting text import box the following action was conducted: Delimited was selected at the top where it has a filled circle and then the Next button was clicked.
5. Tab was selected as the delimiter (where the check is in the box) and then the Finish button was clicked.

Completion of the above steps opened the spectrum in a form of X, Y data points where the first column was the wavelength and the second was the absorbance.

## **4.5 Measurement of Collagenase Enzyme Activity**

The activity of the Collagenase enzyme is measured by determining the rate of substrate utilization during the enzyme-catalysed reaction. The temperature was controlled during Collagenase irradiation as well as during the activity measurement procedure. Experiments were performed at the temperature of 37° C.

### ***Exposed sample***

The cuvettes were filled with 0.10ml of Collagenase enzyme solutions (Point 2 under “Procedure” in Section 4.3). 0.10ml Collagenase enzyme solutions were exposed to ELF

PEMF of the following characteristics: frequency range,  $f$ , of 2-500Hz and magnetic flux density,  $B$ , of 0.5-2.5mT. Each test consisted of exposing the Collagenase enzyme solution for 10min at the selected values of frequency and magnetic flux density. After exposure the Collagenase enzyme solution was added to the already prepared solution of TES buffer and Collagen Type 1 (Point 1 under “Procedure” in Section 4.3). Standard protocol (Sigma assay) was then used to measure the optical density of the experimental solution at 570nm.

#### ***Non-exposed sample***

0.10ml of Collagenase enzyme solutions were kept (Figure 3.12(b)) under the same experimental conditions apart from the sole exposure to ELF FPEMF for 10 min and then added to the solution of TES buffer and Collagen Type 1. Standard protocol was maintained to obtain results for the optical density of the non-exposed sample.

### **4.5.1 Experimental Procedure**

1. The experimental solutions were prepared according to the assay description provided by Sigma-Aldrich and presented earlier in Section 4.3.
2. A steady temperature of 37° C throughout all the conducted experiments were controlled by custom made integrated water regulatory system (detailed in Section 3.3.1.3 ) fitted with a novel cuvette holder (detailed in Section 3.3.1.2).
3. The enzyme solution (exposed/ non-exposed) was contained in a cuvette and exposed within a lab built ELF PEMF device (Section 3.3). The particular geometrical orientation of the cuvette containing the enzyme inside the ELF PEMF chamber was earlier shown in Figure 3.3 (a) under Section 3.2.2. Graphical demonstration of B-field produced in the vicinity of the enzyme carrying cuvette was earlier shown in Section 3.2.3.
4. After exposure, the continuous measurement of the absorption coefficients of the studied sample (exposed/non-exposed) was conducted using an Ocean Optics USB2000 spectrometer (Section 4.4.1). Sampling rate for absorption coefficients at 570nm was set at 15sec.

5. The frequency of the applied ELF PEMF was in the range from 2Hz-500Hz with 21 unique values.
6. For each frequency of radiation the effect was measured for the following magnetic flux densities: 0.5mT, 1.0mT, 1.5mT, 2.0mT and 2.5mT.
7. For every exposed enzyme sample the absorption spectra for 10 min was measured by recording the solution's absorption values every 15 sec as follows:

$$A_{\lambda} = -\log_{10} \left( \frac{S_{\lambda} - D_{\lambda}}{R_{\lambda} - D_{\lambda}} \right) \quad (4.1)$$

where,  $S_{\lambda}$  is the sample intensity at wavelength,  $\lambda$  defined as the intensity of incident light that passes through the cuvette with the sample,  $D_{\lambda}$  is the dark intensity at wavelength,  $\lambda$  or intensity measured on the surface of the CCD detector (spectrometer) when the light source is switched off.  $R$  is the reference intensity at the wavelength,  $\lambda$ . The activity rate is determined by calculating the gradient of  $A_{\lambda}(t)$ .

8. With the aim of eliminating all possible artefacts (pH, temperature, concentrations), the measurements were repeated at least three times for each unique combination of frequency and magnetic flux density to evaluate changes in collagenase absorbance (change in activity of collagenase solution) before and after the ELF PEMF exposures.

## 4.6 Results and Discussion

In this experimental evaluation the effects of generated ELF PEMF's was examined on Collagenase enzymatic activity, which is defined and calculated as the rate of change of optical density in time. These effects were measured at 21 selected frequencies and five magnetic flux densities (their different combination) as shown in Table 4.2.

Table 4.2: Experimental parameters of ELF PEMF exposure to Collagenase enzyme solution.

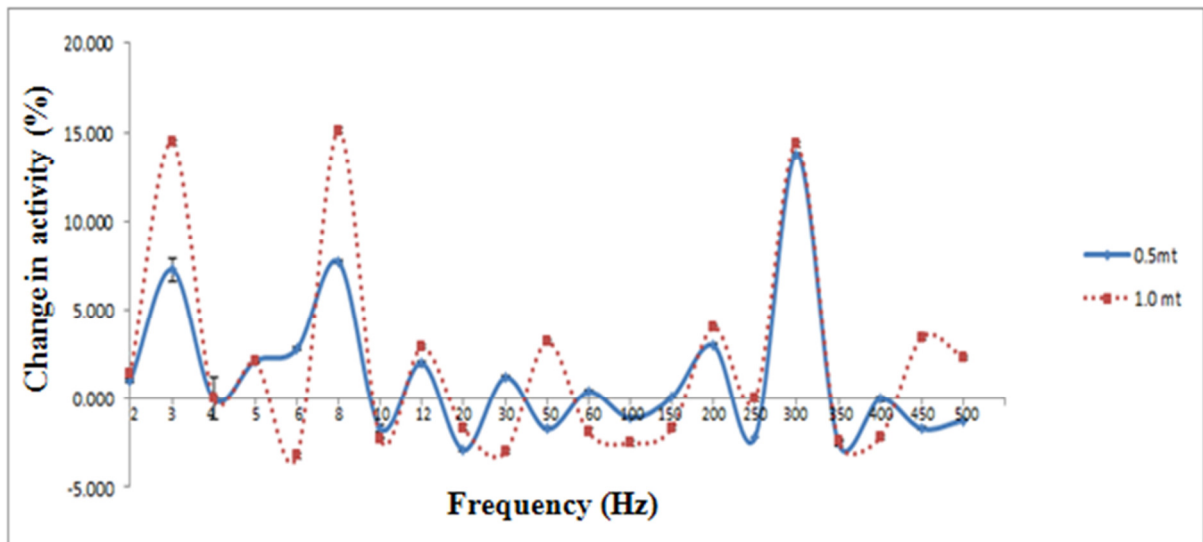
<b>Parameter</b>	<b>Number of variables</b>
Frequency	<b>21</b> (2Hz, 3Hz, 4Hz, 5Hz, 6Hz, 8Hz, 10Hz, 12Hz, 20Hz, 30Hz, 50Hz, 60Hz, 100Hz, 150Hz, 200Hz, 250Hz, 300Hz, 350Hz, 400Hz, 450Hz, 500Hz)
Magnetic flux density	<b>5</b> (0.5mT, 1.0mT, 1.5mT, 2.0mT, 2.5mT)
Duration of experiment	<b>1</b> (10min)
Experiment repetition	<b>3</b>
Number of application	<b>1</b> (Collagenase enzyme solution)

Collagenase enzyme solutions were exposed at the selected frequencies in the range of 2-500Hz and five magnetic flux densities (0.5mT, 1.0mT, 1.5mT, 2.0mT and 2.5mT). The measurements were repeated three times for each experimental setting. The results of the independent two-sided t-test showed that the difference between exposed and control samples were always significant ( $P < 0.001$ ).

For each measurement, the relative difference in activity of Collagenase enzyme solutions for exposed vs. non-exposed samples was assessed and calculated (%) and shown in Figures 4.3(a)-4.3(c). Figures 4.5(a), 4.5(b) and 4.5(c) show the difference in significance between the mean values of the activities of exposed and non-exposed samples and thereby provide a visual representation of the changes in Collagenase activity after exposure with different combinations of the selected frequencies and magnetic flux densities. The bars in the Figures

4.3(a)-4.3(c) represent standard deviation of the data set for the relative difference in activity between exposed and non- exposed samples.

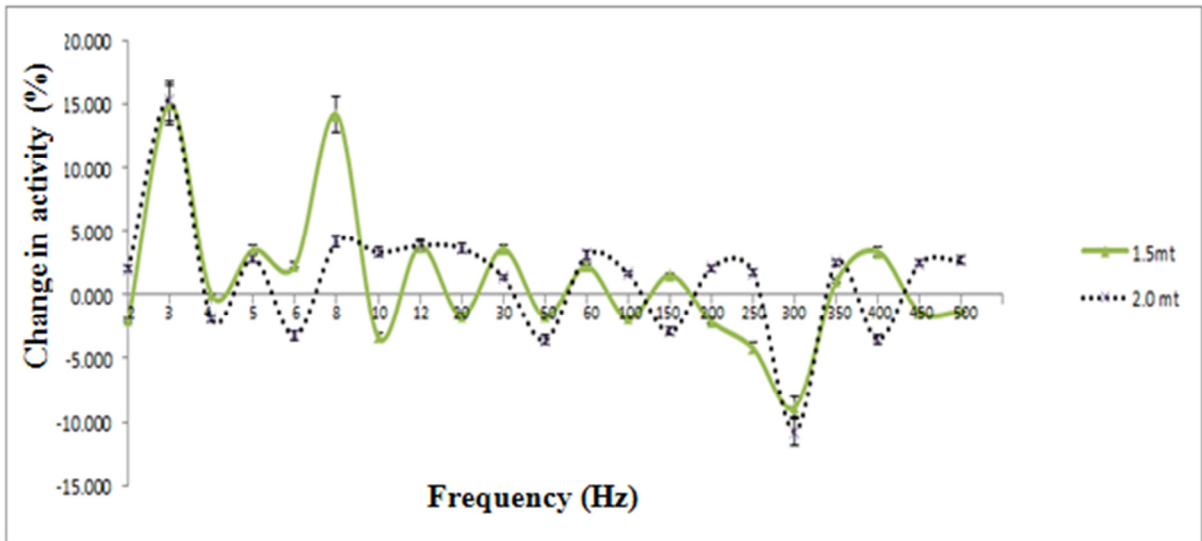
The rate of change of optical density per second for non-exposed sample remains constant throughout the whole range of studied frequencies and magnetic flux densities, and hence no separate plots/tables are presented for these samples. However, the consistent average rate of change in optical density for non-exposed sample is shown as a horizontal bold line in Figures 4.5(a)-4.5(c). Additionally, the data for non-exposed sample are incorporated within the relative change data for generating relevant plots.



(a)

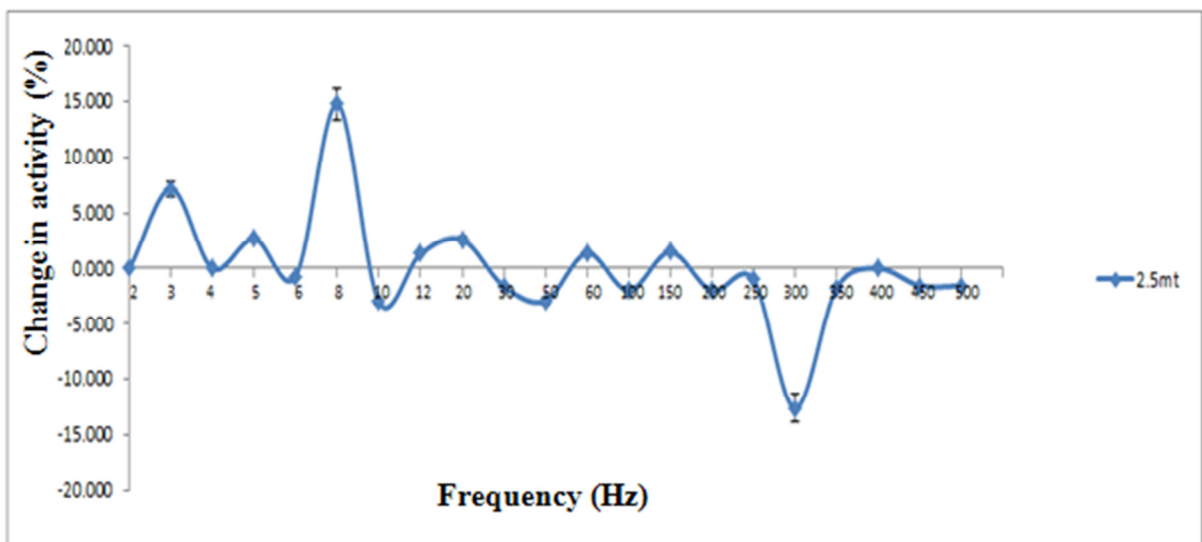
Figure 4.3(a): Relative changes in the collagenase enzyme activity (%) induced by the ELF PEMF at the frequency range of 2-500Hz magnetic flux densities 0.5mT and 1.0mT [122].





(b)

Figure 4.3(b): Relative changes in the collagenase enzyme activity (%) induced by the ELF PEMF at the frequency range of 2-500Hz and magnetic flux densities 1.5mT and 2.0mT [122].



(c)

Figure 4.3(c): Relative changes in the collagenase enzyme activity (%) induced by the ELF PEMF at the frequency range of 2-500Hz and magnetic flux density 2.5mT [122].

Findings from the results obtained and presented in Table 4.1 and Figure 4.4(a)-4.4(c) reveal that the biological activity of Collagenase enzyme is increased by 7-15% and 4-15% after respective irradiation at 3Hz and 8Hz for the magnetic flux densities of 0.5-2.5mT.

It can be also seen that the biological activity of Collagenase can be modulated as follows:

- Increased upon exposures at the frequency of 3Hz and magnetic flux densities of 0.5-2.5mT (Figures 4.3(a)- 4.3(c) and Figure 4.4(a)).
- Increased upon radiation at the frequency of 8Hz and magnetic flux densities of 0.5-2.5mT (Figures 4.3(a)-4.3(c) and Figure 4.4(b)).
- Increased upon radiation at the frequency of 300Hz and magnetic flux densities 0.5mT and 1.0mT (Figure 4.3(a) and Figure 4.4(c)).
- Decreased upon radiation at the frequency of 300Hz and magnetic flux densities 1.5mT, 2mT and 2.5mT (Figures 4.3(b), 4.3(c) and Figure 4.4(c)).

Through the obtained results in Figure 4.3(a)-4.3(c) and from the modulated biological activity of Collagenase presented above, it is evident that specific set of frequency and intensity (magnetic flux density) leads to a favorable/distinct biological response. From the explanation earlier presented in Section 2.11, it is evident that the effect of ELF PEMF on Collagenase enzyme clearly demonstrates the presence of “window” effect.

An important finding from the conducted experiments also reveals an increase in Collagenase enzyme activity upon exposure to ELF PEMF at almost all studied frequencies in the lower end of the ELF spectrum (2-12Hz). Significant changes in its activity were obtained at the frequencies 3Hz and 8Hz for all five studied magnetic flux densities (0.5mT, 1.0mT, 1.5mT, 2.0mT and 2.5mT). The non- exposed Collagenase solution has an average rate of change 0.009167 with the standard deviation  $\pm 0.000138$ . The obtained results show the increase of Collagenase enzyme activity in order of 15.33% ( $p < 0.001$ ) at 3Hz and 15.091% ( $p < 0.001$ ) at 8Hz, respectively.

Table 4.3 Activity of the enzyme and standard deviation upon exposure to ELF PEMF [122].

Frequency (Hz)	0.5mT activity	STD( $\pm$ )	1.0 mT activity	STD( $\pm$ )	1.5mT activity	STD( $\pm$ )	2.0 mT activity	STD( $\pm$ )	2.5mT activity	STD( $\pm$ )
2	1.000	0.739	1.379	0.739	-2.000	0.167	2.015	2.429	-0.003	1.528
3	7.261	0.651	14.429	1.337	15.000	0.835	15.333	3.108	7.143	1.528
4	0.000	1.165	0.000	0.996	0.000	1.679	-1.887	0.754	0.000	1.311
5	2.130	1.165	2.071	0.996	3.500	1.679	2.889	0.754	2.698	1.311
6	2.800	0.853	-3.197	1.443	2.286	1.528	-3.234	0.793	-0.685	2.887
8	7.692	0.965	15.091	1.443	14.222	1.371	4.167	1.115	14.769	1.832
10	-1.667	1.883	-2.231	0.905	-3.351	1.000	3.333	1.954	-3.031	1.055
12	2.000	1.422	2.875	0.835	3.803	1.165	3.875	1.497	1.333	1.044
20	-2.867	1.446	-1.667	1.567	-1.636	0.953	3.665	0.953	2.615	1.240
30	1.189	0.835	-2.996	1.138	3.581	0.900	1.400	1.138	-1.590	0.522
50	-1.705	0.900	3.182	0.853	-1.680	1.658	-3.570	1.084	-2.920	0.492
60	0.380	0.900	-1.900	1.784	2.205	0.965	3.091	0.793	1.385	0.996
100	-1.091	0.900	-2.500	1.231	-1.875	1.073	1.667	0.953	-2.000	0.754
150	0.080	0.718	-1.667	0.953	1.538	1.443	-2.941	1.881	1.500	1.348
200	2.989	0.965	3.999	0.718	-2.099	0.953	2.111	0.853	-2.000	1.913
250	-2.154	1.240	0.000	1.485	-4.215	0.778	1.733	0.778	-1.000	1.206
300	13.786	0.866	14.330	1.422	-8.840	0.937	-10.768	1.279	-12.667	0.888
350	-2.500	1.371	-2.389	0.953	1.066	0.996	2.500	1.348	-1.790	1.782
400	0.000	1.403	-2.195	1.165	3.364	0.669	-3.500	1.485	0.000	1.165
450	-1.688	1.030	3.412	0.622	-1.333	1.485	2.457	0.866	-1.538	0.669
500	-1.230	0.937	2.348	0.965	-1.322	1.621	2.667	0.853	-1.578	0.900

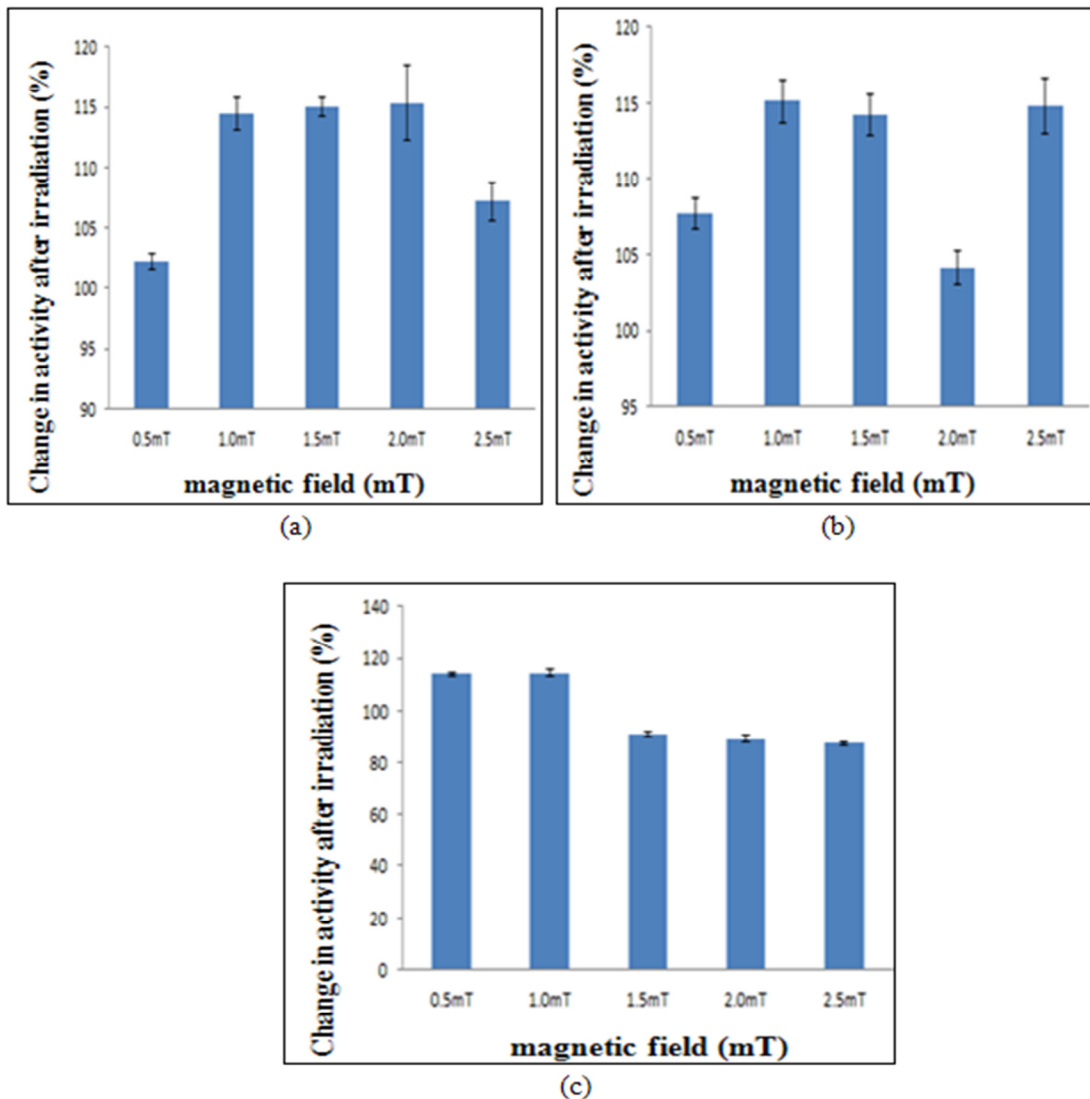
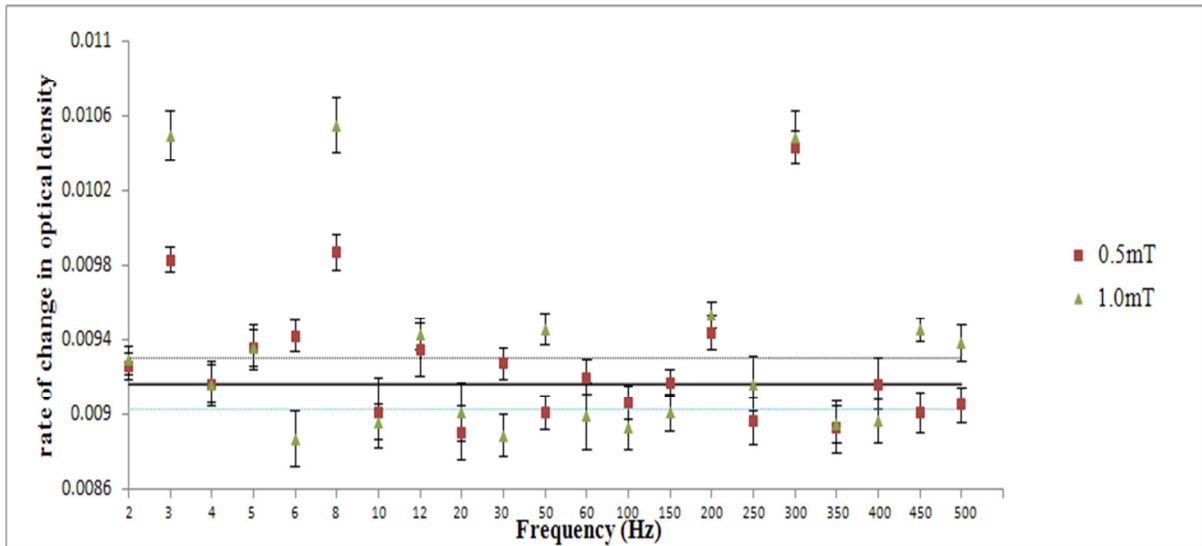


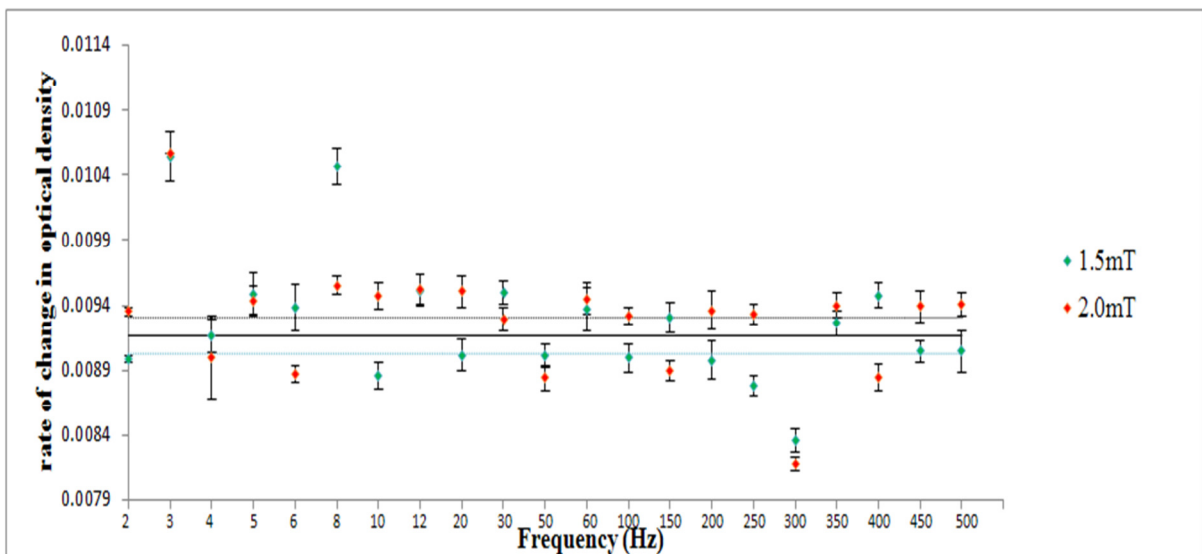
Figure 4.4(a), 4.4(b) and 4.4(c): Bar charts with the standard errors (standard deviation) of the relative change in the Collagenase enzyme activity (%) versus frequencies: 3Hz (Figure 4.4(a)), 8Hz (Figure 4.4(b)), 300Hz (Figure 4.4(c)) and magnetic flux densities 0.5- 2.5mT. The percentage represents relative change to the non-exposed samples [122].

In addition to the modulated Collagenase activities presented before, results in Figure 4.5(a) also shows a significant increase in Collagenase activity at the frequencies 5Hz, 6Hz and 12Hz and the decrease in its activity at 20Hz for the magnetic flux density 0.5mT. Moreover, a significant increase in Collagenase activity can be also observed at 12Hz, 50Hz and 450Hz with a decrease in activity at 30Hz and 400Hz for the magnetic flux density 1mT. Furthermore, Figure 4.5(b) demonstrates an increased enzymatic activity for 1.5mT and 30Hz and 400Hz, and decreased activity at 10Hz and 300Hz. The increase in activity for 2.0mT and 10Hz, 12Hz and 20Hz, and the decrease at 6Hz are shown in Figure 4.5(b). A noticeable

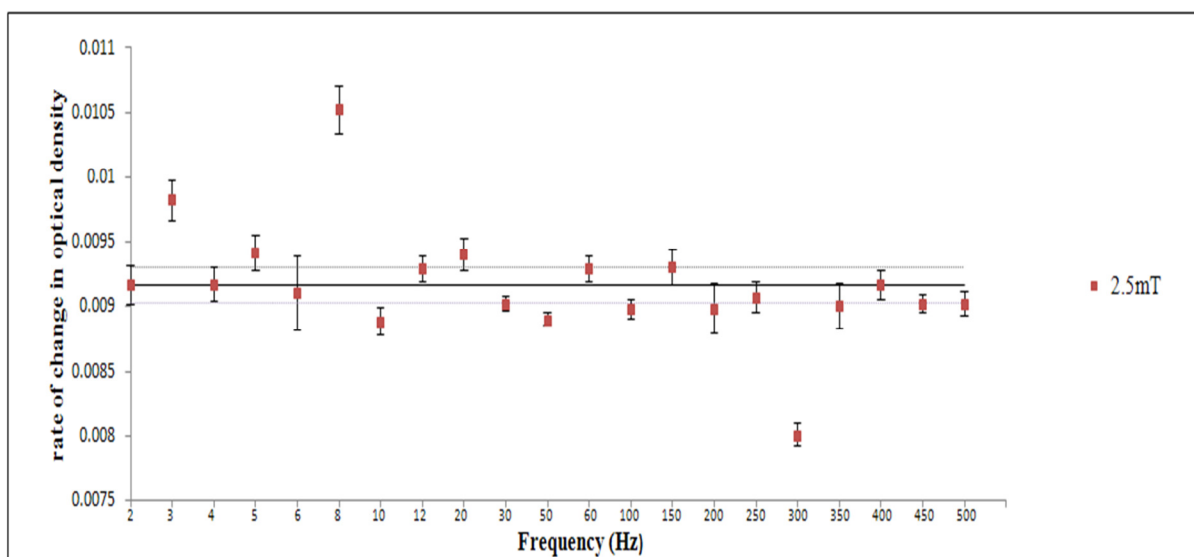
increase in activity is observed at 5Hz and 20Hz and a decrease in activity is seen at 10Hz for a magnetic field intensity of 2.5mT (Figure 4.5 (c)).



(a)



(b)



(c)

Figure 4.5(a), 4.5(b) and 4.5(c): The activity of the Collagenase enzyme was measured after PEMF exposures at frequencies of 2-500Hz and magnetic flux densities of 0.5-1.0mt (Figure 4.5(a)), 1.5-2.0mT (Figure 4.5(b)) and 2.5mT (Figure 4.5(c)). The ordinate represents the rate of change of the buffered solution of Collagen Type 1. The rate of change represents the rate of change of the buffered solution of Collagen Type I concentration per unit of time, or activity of Collagenase enzyme. Horizontal bold line represents an average ( $\bar{x}$ ) for the non-exposed samples. Horizontal dash lines are values distant for one standard deviation(s) up and below for average value [122].

## 4.7 Summary

The findings of this study show that generated fields of magnetic flux densities in the range of 0.5-2.5mT and frequencies 2-500Hz can induce changes in Collagenase enzymatic activity, and thus can affect the specific biological process involving the Collagenase enzyme. The findings may explain some non-thermal effect of ELF PEMF on biomolecules and lead to a whole range of possibilities of controlled modulation of protein activity, which could benefit the development of non-invasive treatments and advanced technologies. This could have major implication in drug design, medicine, pharmacology and biotechnology. These outcomes have direct implication in determining the optimal characteristics of the applied ELF PEMF for possible treatment and promotion of wound healing.

## **CHAPTER 5:**

### **RESULTS: EFFECT OF ELF PEMF ON SURVIVAL OF BACTERIA *Staphylococcus aureus* AND *Escherichia coli***

## 5.1 Overview

Two applications of the constructed ELF PEMF exposure device (Chapter 3) are presented in this chapter. These applications include: irradiation of gram-positive bacterial culture *S. aureus* and gram-negative bacterial culture *E. coli*. The changes in bacterial growth and proliferation are evaluated experimentally. Characteristic of bacterial growth curve is shown along with the selected growth curve obtained experimentally that demonstrate bacterial phase of the exposed and non-exposed samples. Also, provided in considerable details are the experimental procedure and the equipment required for conducting this experimental investigation. Result obtained show the pattern of bacterial survival upon ELF PEMF exposures at the selected frequencies of 2-500Hz and magnetic flux densities of 0.5-2.5mT.

## 5.2 Characterization of Bacteria

Structure and features of gram-positive and gram-negative bacteria were generally explained in Section 2.20 and graphically presented in Figure 2.17. Schematic diagram of the cross sections of gram-positive and gram-negative bacteria are shown in Figure 5.1.

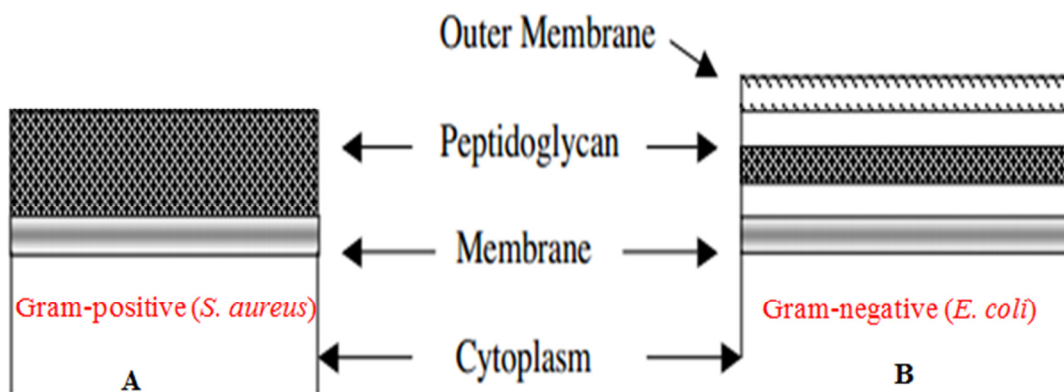


Figure 5.1: Schematic of cross-section of bacterial cell walls: A) Gram-positive bacteria and B) Gram-negative bacteria [268].

Most bacteria are characterized by having not only a cell membrane but also a cell wall which lies outside of the cell membrane [268]. This cell wall is composed mostly of peptidoglycan and helps to give the cell its rigidity and characteristics shape. Some groups of bacteria also



comprise of an outer membrane (Figure 5.1B) attached to the peptidoglycan by small lipoprotein molecules. The difference in outermost cell structure forms the basis of classification of bacteria.

Section 5.2.1 provides a brief explanation of the phases of bacterial growth curve.

### 5.2.1 Characteristics of Bacterial Growth Curve

When bacteria are inoculated into a fresh medium, the resulting culture exhibits a characteristic growth curve of four distinct phases (Figure 5.2).

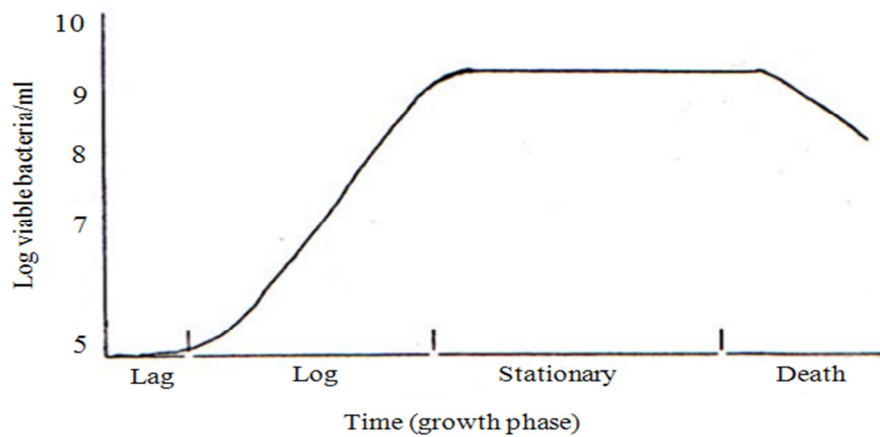


Figure 5.2: Bacterial growth curve [268].

**Lag phase:** During this phase the cells prepare for synthesis of DNA and enzymes needed for cell division. There is no increase in cell number.

**Log/Exponential phase:** During this phase the culture reaches its maximum rate of growth for specific conditions. The time required for the population to double is called the generation time. The generation time varies between organisms and different environmental conditions.

**Stationary phase:** As bacteria multiply, nutrients are exhausted and inhibitory metabolic end products accumulate. These conditions give rise to the stationary phase which represents no net increase in number (growth rate equals death rate).

**Death phase:** This phase represents an eventual decline in cell number.

### 5.3 Experimental Equipment

The equipment used for investigating the efficacy of ELF PEMF exposures in affecting the growth and proliferation of selected bacterial cultures of *S. aureus* and *E. coli* are given below:

1. ELF PEMF exposure system (Section 3.3) is used to generate uniform time varying magnetic fields in the frequency range of 2-500Hz, with magnetic induction (magnetic flux density) of 0.5-2.5mT.
2. EFA-200 EMF Analyser (Section 3.5.2) fitted with an external B-probe (Wandel and Golterman) is used to measure the magnetic flux densities at the selective frequencies produced by the ELF PEMF device.
3. Eppendorf BioPhotometer Spectrophotometer UV/VIS is used to measure the Optical Density (OD) reading of the bacterial culture before and after exposures to ELF PEMF. Figure 5.3 shows the usage of Eppendorf BioPhotometer Spectrophotometer UV/VIS in measuring the OD reading.

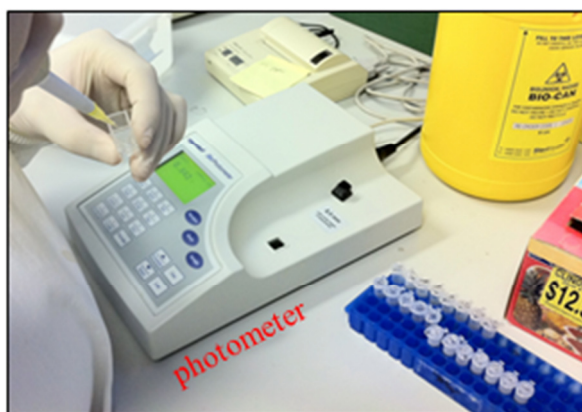


Figure 5.3: Using the Eppendorf BioPhotometer Spectrophotometer UV/VIS for OD measurements.

The following considerations are required to be taken into account:

1. The intensity of light scattering and thus the OD of a culture are dependent on the wavelength. Any wavelength of measurement can be chosen but needs to be maintained throughout all measurements of conducted experiments. Typically while dealing with bacterial culture, the wavelength of 600nm is selected.
2. Measured OD of a photometer is dependent on the geometry of the light beam, the position of the cuvette, and on the photometer model and manufacturer. This entails the usage of the same model of photometer for all concerned experiments. Even two photometers of the same model might give a slight different result and can therefore lead to misinterpretation of data.
3. The main purpose is to measure only the OD caused by the cells; therefore, any light absorption caused by the medium has to be subtracted. This is accomplished by initially filling up the cuvette with sterile (clear) growth medium placed in the photometer and adjusting the OD value to 0.00 (Figure 5.4 A). Hence, every subsequently measured value above this (Figure 5.4 B) will always be caused by the presence of bacterial cells (visually recognized by the turbidity of the growth medium).

Figure 5.4 shows the operation of a photometer in measuring the OD of a culture.

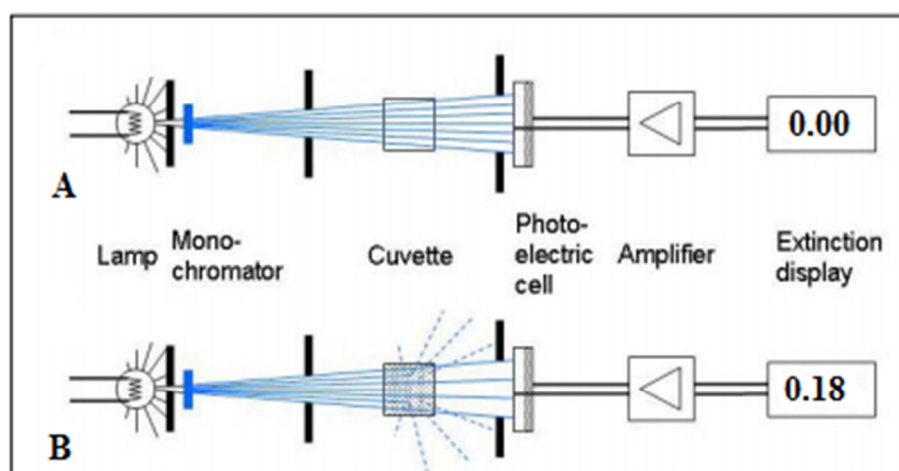


Figure 5.4: Working methodology of a Photometer for measurement of the OD of a culture [269]. A) For a clear sterile medium contained in the cuvette, the intensity of the light that reaches the photoelectric cell is taken as the reference intensity and adjusted to zero OD. B) With bacterial cells in the cuvette, a significant portion of light is scattered and no longer reaches the photoelectric cell. The weaker electric signal is converted to an OD value.

## 5.4 Experimental Materials

**Bacterial Strains:** The bacterial strains selected for experimental evaluation of ELF PEMF effects are *Staphylococcus aureus* - American Type Culture Collection (ATCC) 25923 and *Escherichia coli* (ATCC 25922). Of note, Bacterial strains were kindly supplied by the School of Applied Science, RMIT University (Bundoora campus).

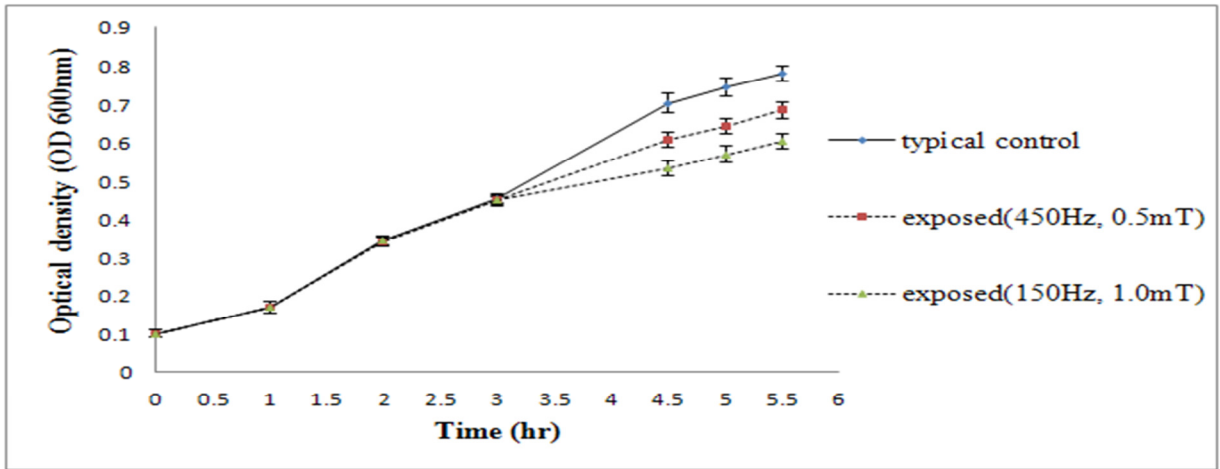
**Growth Medium:** Colombia agar (purchasing information, Appendix C) was used as the growth medium for all bacterial cultures. The composition for Colombia agar is: 10g pancreatic digest of casein, 5g meat peptic digest, 3g heart pancreatic digest, 5g yeast extract, 1g maize extract, 5g sodium chloride and 12g Agar.

**Suspension Medium:** Colombia broth (purchasing information, Appendix C) was used as the bacterial suspension medium for all experiments. The composition for Colombia broth is: 5g enzymatic digest of casein, 5g enzymatic digest of animal tissue, 10g yeast enriched peptone, 3g enzymatic digest of heart muscle, 5g sodium chloride, 25g dextrose, 0.1g L-cysteine, 0.1g magnesium sulfate, 0.02g ferrous sulfate, 0.83g Tris (hydroxymethyl) aminomethane, 2.86g Tris (hydroxymethyl) aminomethane-HCL and 0.6g sodium carbonate).

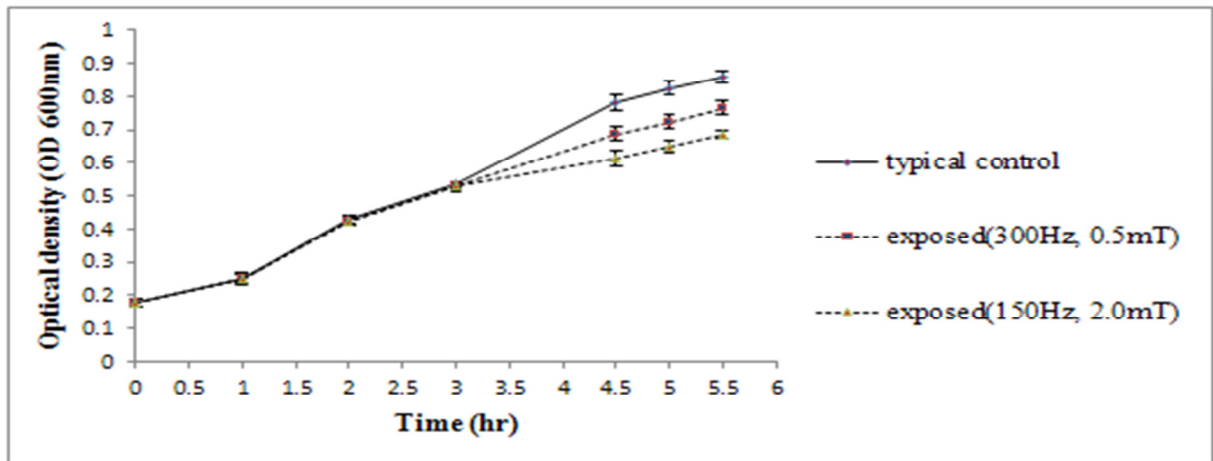
## 5.5 Experimental Procedure

**Determining Phase of Bacterial Growth:** In order to investigate the phase of bacterial growth of *S. aureus* and *E. coli* in suspension, OD reading for both control (non-exposed) and exposed samples at 600nm at every hour within the first 3h (before ELF PEMF exposure) and then again, after the exposures at 4.5h, 5h and 5.5h were measured. The resulting growth curves monitored via OD values for a typical sample and two arbitrarily picked exposed samples at 450Hz and 0.5mT, and at 150Hz and 1.0mT for *S. aureus* are shown in Figure 5.5 (a). Similarly, growth curves monitored via OD values for a typical control sample and two

arbitrarily picked exposed samples at 300Hz and 0.5mT, and at 150Hz and 2.0mT for *E. coli* are shown in Figure 5.5 (b).



(a)



(b)

Figure 5.5: Growth curve: Typical control and ELF PEMF exposed bacterial culture of a) *S. aureus* [147] and b) *E. coli* monitored via OD reading.

Growing cultures overnight can produce very different initial conditions for the experiments. In order to ensure controlled initial conditions, it is required to bring the culture to exponential growth and keep it there for several generations while verifying that the culture is indeed growing exponentially. Individual growth curves showed no decrease in the bacterial concentration within the above mentioned time frame. Therefore, it implies that bacteria are not in the death phase but rather still growing in their exponential phase. In order to ensure controlled initial conditions for individual conducted experiments, it was always ascertained that bacterial cultures were indeed in their exponential phase of growth.

### 5.5.1 Experimental Stages

A block diagram of the experimental procedure is shown in Figure 5.6. This procedure is similar for experiments conducted on both bacterial cultures *S. aureus* and *E. coli*. The only difference is the initial OD reading of bacterial suspension (0.1A for *S. aureus* and 0.18A for *E. coli*).

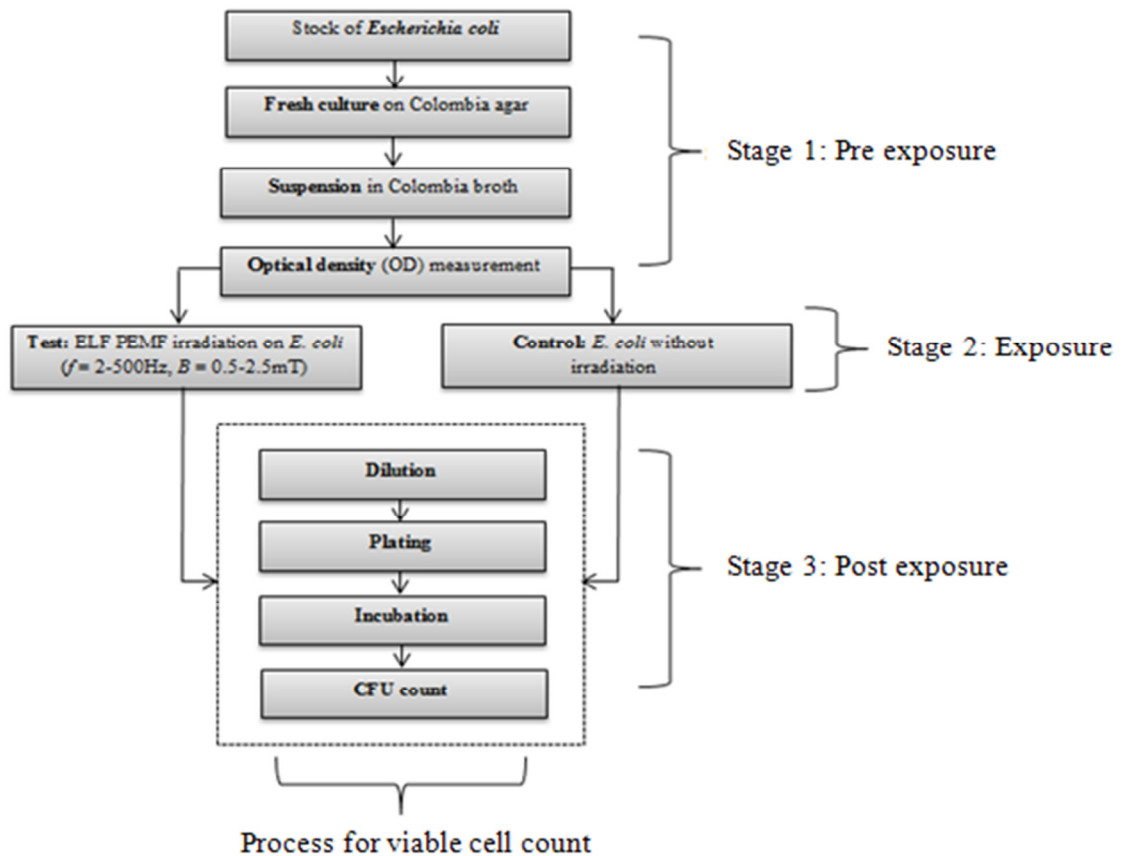


Figure 5.6: Block diagram of the experimental procedure for investigating the effect of ELF PEMF exposures on bacteria *Staphylococcus aureus* and *Escherichia coli*.

The experimental procedure can be divided into the following three stages, where relevant phases of the lab work were conducted under the strict rules and regulations of Aseptic Techniques (Appendix E).

### ***Stage 1: Pre - exposure***

Bacterial cultures were first cultivated in an agar medium (Columbia agar) and incubated aerobically for 24 hours at 37° C (Figure 5.7).

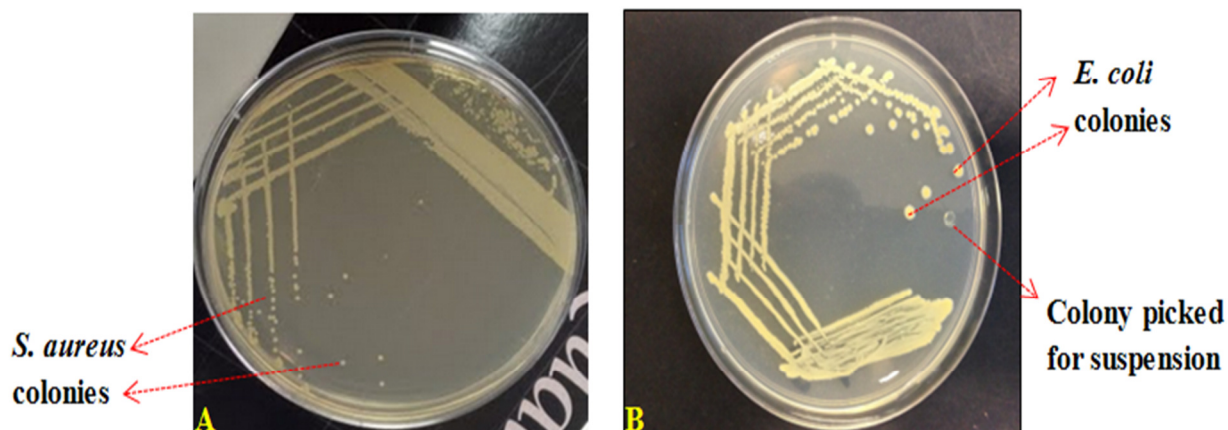


Figure 5.7: Typical fresh bacterial culture in Colombia agar medium: A) *S. aureus* B) *E. coli*.

The colonies formed were then picked (Figure 5.7 B) and suspended (Figure 5.8) in a broth medium (Columbia broth). Optical density for the suspended bacterial culture was measured at 600nm and adjusted to a specific value of  $0.1 \pm .005A$  for *S. aureus* and  $0.18 \pm .005A$  for *E. coli*, prior to commencing experimentation.

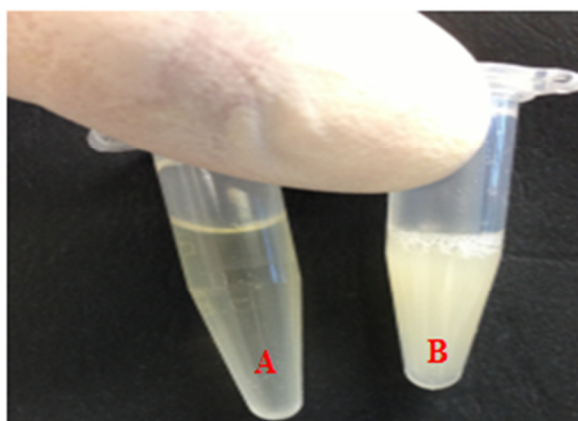


Figure 5.8: A) Colombia broth B) Bacterial colonies suspended in Colombia broth.

This step was necessary for maintaining the standardization for all conducted experiments. Typical control curves shown in Figure 5.5 (a) for *S. aureus* and Figure 5.5 (b) for *E. coli* were obtained in order to ascertain that all bacterial culture were indeed in exponential phase during the pre-exposure period.

### ***Stage 2: Exposure***

A total of 360 experiments were carried out during the evaluation on the growth of *S. aureus* and *E. coli*. Bacterial cultures were placed in 2.5 mL centrifuge tube and exposed to ELF PEMF (3 hour since suspension) of magnetic flux densities,  $B$ , (0.5mT, 1.0mT, 1.5mT, 2.0mT and 2.5mT), frequency,  $f$ , range of 2-500 Hz and exposure duration,  $t$ , 90 min. Demonstration of the top view for a typical experimental setup is shown in Figure 5.9.

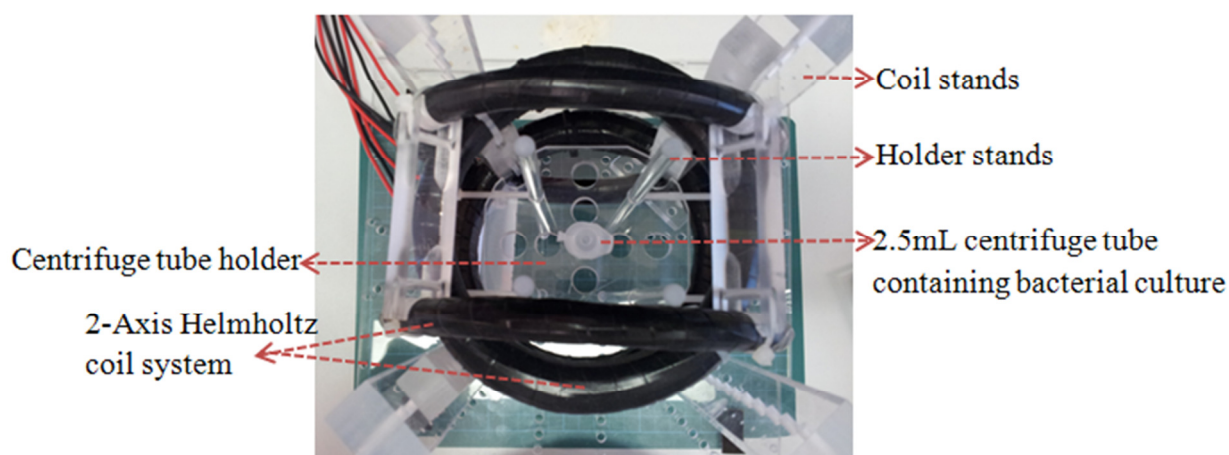


Figure 5.9: Top view of the ELF PEMF chamber used during exposure of the bacterial culture.

Control cultures (sham/non-exposed) for all experiments were kept under the same conditions as the exposed ones apart from their sole exposure to the magnetic fields. The stand for the control sample holder was earlier presented in Figure 3.12 (c).

### ***Stage 3: Post - exposure***

The viability of these bacterial cultures (number of live cells as colony-forming units (CFUs)) was measured for both control samples and for samples exposed to ELF PEMF in order to quantify the effects of applied exposure on survival of the bacteria. To determine the CFU value per mL, a serial dilution using the bacterial culture was performed. The process of serial dilution is graphically illustrated in Appendix F. After five serial dilutions, a volume of 100 $\mu$ l from the last tube was inoculated in the agar plates (dilution factor (DF)  $1 \times 10^6$ ) by spread plating (Figure 5.10 A) (Appendix F). Spread plating is a method that uses a glass/metal rod



to spread a broth culture (Colombia broth) of bacteria over the solid medium (Colombia agar plate). The purpose of this technique is to grow and isolate colonies of bacteria. Finally, after incubation (Figure 5.10 B), the colonies formed on the plates were visually counted (Figure 5.10 C). This is done in order to compare the effectiveness of ELF PEMF exposures on the studied bacterial cultures. Since the number of colonies growing on the solid media (Colombia agar) denotes the number of live bacterial cells, it does not contain organisms that might not have survived during the plating period.



Figure 5.10: A) Spread-plating, B) Colombia agar plates kept inside the incubator C) After incubation- isolated colonies of bacteria are clearly visible and the value of CFU can easily be determined (in this particular case, CFU, n= 24).

## 5.6 Effects of ELF PEMF Interaction with Bacteria

Explanation of the possible ELF PEMF interaction with specific materials, environment, and molecules in broth, media and bacteria in general are presented below:

- ***ELF PEMF interaction with specific material:*** The entire structure of ELF PEMF exposure chamber was constructed using acrylic. Therefore, there is no interaction between the produced ELF PEMF and the concerned material inside the ELF PEMF exposure chamber [147].
- ***ELF PEMF interaction with environment:*** Bacteria are known to produce stress protein when exposed to elevated temperature from the environment [270]. This elevated temperature can commonly occur due to resistive heating of the coils used to produce the ELF PEMF. For all conducted experiments, temperature was efficiently controlled (Section 3.7) to ascertain that the bacterial cultures were not affected by the heat generated by the current carrying coils [147].
- ***ELF PEMF interaction with molecules in broth and different broth composition:*** Columbia broth (ingredients presented in Section 5.4) is a complex media with undetermined chemical compositions. Due to this undetermined chemical composition, its response to ELF PEMF exposures cannot be established. Of note, only one particular broth composition was used for all conducted experiments [147].
- ***ELF PEMF interaction with solid media:*** Solid media (Columbia agar plates) were never exposed to ELF PEMF [147].

## 5.7 Results and Discussion

To establish the time exposure for all future experiments on bacteria irradiation, the preliminary study was conducted. The preliminary results showed that ELF PEMF exposures for less than 1 h produced no effects on bacterial cultures and failed to reduce a number of live cells present. Thus, all further exposures were set for 90 min. The effects of ELF PEMF on the viability of *S. aureus* and *E. coli* were quantified in terms of the Colony-Forming Unit (CFU) - the number of live bacterial cells in 1mL of sample. The CFU values of the exposed and control samples were measured at twelve selected frequencies and five magnetic flux densities (their different combinations) – shown in Table 5.1.

Table 5.1: Experimental parameters of ELF PEMF exposure to bacterial culture of *S. aureus* and *E. coli*.

Parameter	Number of variables
Frequency	<b>12</b> (3Hz,10Hz, 50Hz, 100Hz, 150Hz, 200Hz, 250Hz, 300Hz, 350Hz, 400Hz, 450Hz, 500Hz)
Magnetic flux density	<b>5</b> (0.5mT, 1.0mT, 1.5mT, 2.0mT, 2.5mT)
Duration of experiment	<b>1</b> (90min)
Experiment repetition	<b>3</b>
Number of application	<b>2</b> (bacterial culture of <i>S. aureus</i> and <i>E. coli</i> )

Experimental results revealed an overall decrease of CFU values of bacterial cultures compared to the control samples. Of note, CFU values for the control samples remained almost constant, around 77, throughout the entire range of different ELF PEMF exposures (Figures 5.11-5.15 and 5.21-.25). For each measurement, the relative difference in CFU between the exposed and control samples were calculated. Higher CFU values correspond to less significant effects of ELF PEMF on bacterial cultures and thus, yielded a lower relative change in bacterial growth. Similarly, lower CFU values indicate the most significant effect of ELF PEMF on bacteria which accounted for a higher relative change in bacterial growth. Plots for relative change in bacterial count is shown in Figures 5.16-5.17 for *S. aureus* and

5.27-5.28 for *E. coli*.

**Statistical analysis:** For statistical analysis, each experiment was repeated in triplicate for every unique combination of the selected frequency and magnetic flux density. Total number of combinations used in the experiments accounted to ( $12 \times 5 = 60$ ), where number of selected frequencies equaled 12 and magnetic flux densities equaled 5. Due to the absence of *a priori* knowledge of whether the entire range of ELF PEMF would positively or negatively alter the Collagenase enzyme activity, for the null hypothesis, it was assumed that the mean value of the rate of change of optical density to be equal for both the control (non-exposed) and ELF PEMF exposed sample ( $H_0: \mu_1 = \mu_2$ , where mean of the exposed sample,  $\mu_1$  is equal to the mean of the control sample  $\mu_2$ ). Therefore, for statistical credibility and experimental relevance of the conducted study, the hypothesis was tested with the data analysis tool of Microsoft Excel (2010) and used the independent two-sided t- test with sample size ( $n = 3$ ) and degrees of freedom = 4. For significance testing, an alpha ( $\alpha$ ) value of 0.05 was used in the equation,  $100 \cdot (1 - \alpha) \%$ , to determine a 95 % confidence interval (data not shown). Each test yielded variance value for both control and exposed data set. Square root of variance resulted in the calculation of standard deviation. Standard deviation values ( $\pm$ ) were then used as upper and lower bound of error bars for plotted data. The results of the t-test showed that the difference between exposed and control samples were always significant ( $P < 0.05$ ).

### 5.7.1 Effect of ELF PEMF on Bacterial Culture of *S. aureus*

Experimental data were plotted and presented in Figures 5.11-5.17. Figures 5.11-5.15 shows the significant difference between the CFU values of exposed and control (non-exposed) *S. aureus* cultures.

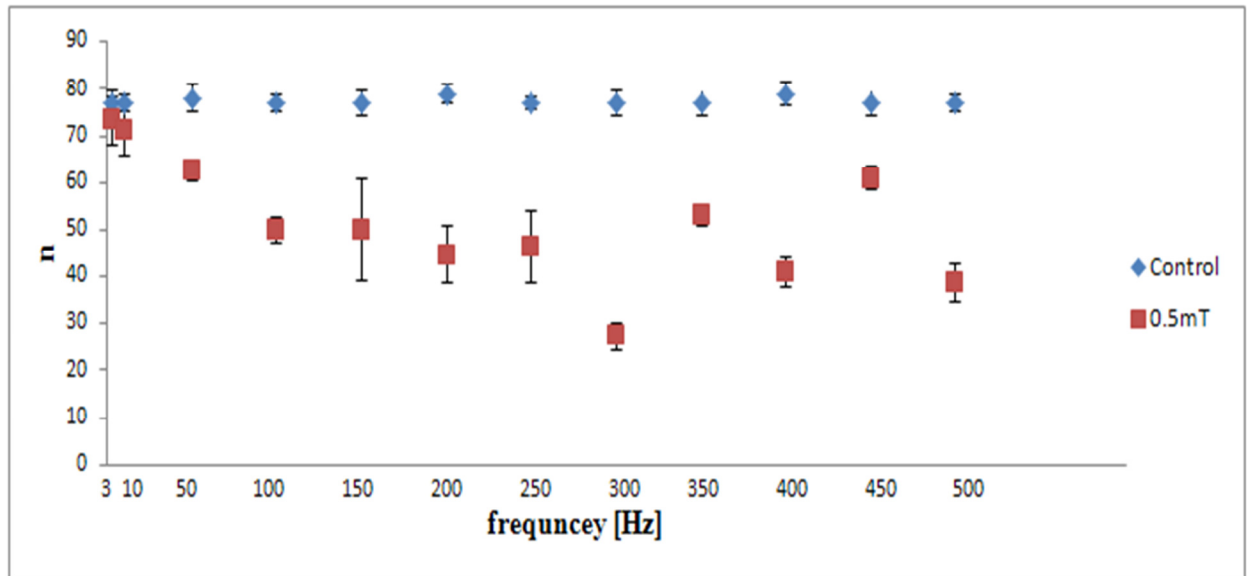


Figure 5.11: Changes in CFU value of *S. aureus* after ELF PEMF exposure: (n- number of bacteria in 100 $\mu$ l of suspension).  $\diamond$ -control sample,  $\square$ -ELF PEMF exposed sample at 0.5mT [147].

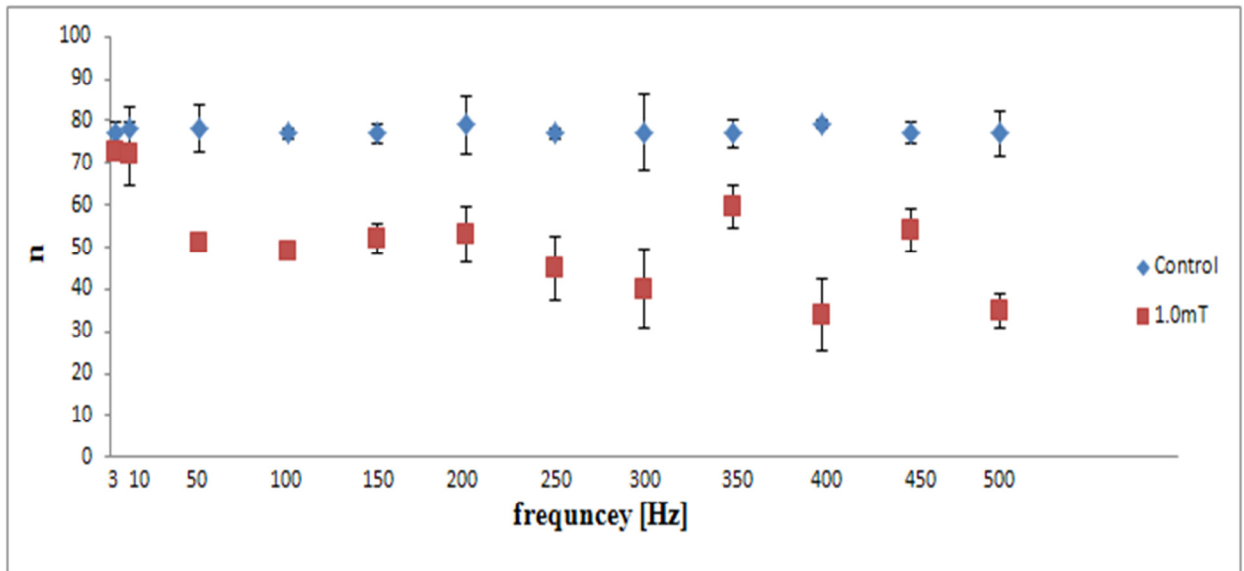


Figure 5.12: Changes in CFU value of *S. aureus* after ELF PEMF exposure: (n- number of bacteria in 100 $\mu$ l of suspension).  $\diamond$ -control sample,  $\square$ -ELF PEMF exposed sample at 1.0mT [147].

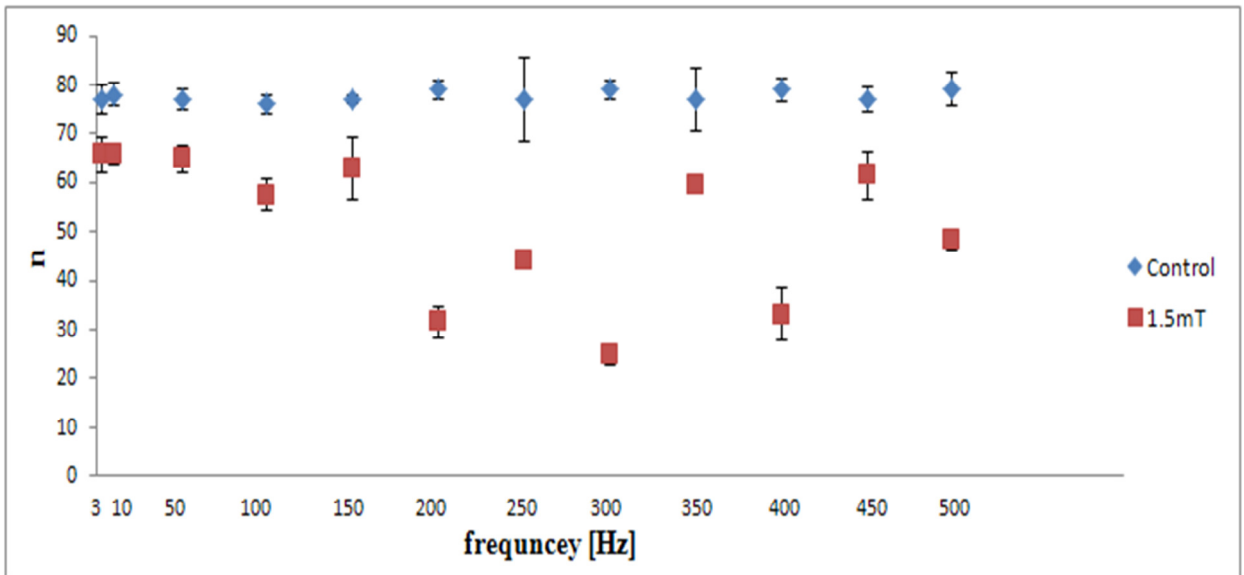


Figure 5.13: Changes in CFU value of *S. aureus* after ELF PEMF exposure: (n- number of bacteria in 100 $\mu$ l of suspension).  $\diamond$ -control sample,  $\square$ -ELF PEMF exposed sample at 1.5mT [147].

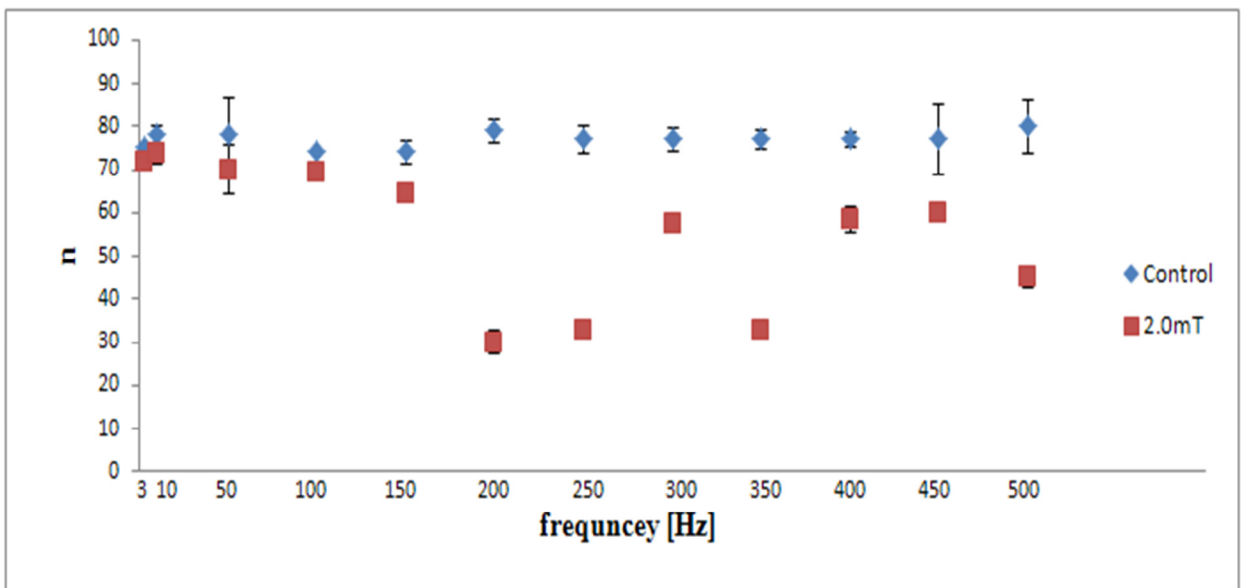


Figure 5.14: Changes in the CFU value of *S. aureus* after ELF PEMF exposure : (n- number of bacteria in 100 $\mu$ l of suspension).  $\diamond$ -control sample,  $\square$ -ELF PEMF exposed sample at 2.0mT [147].

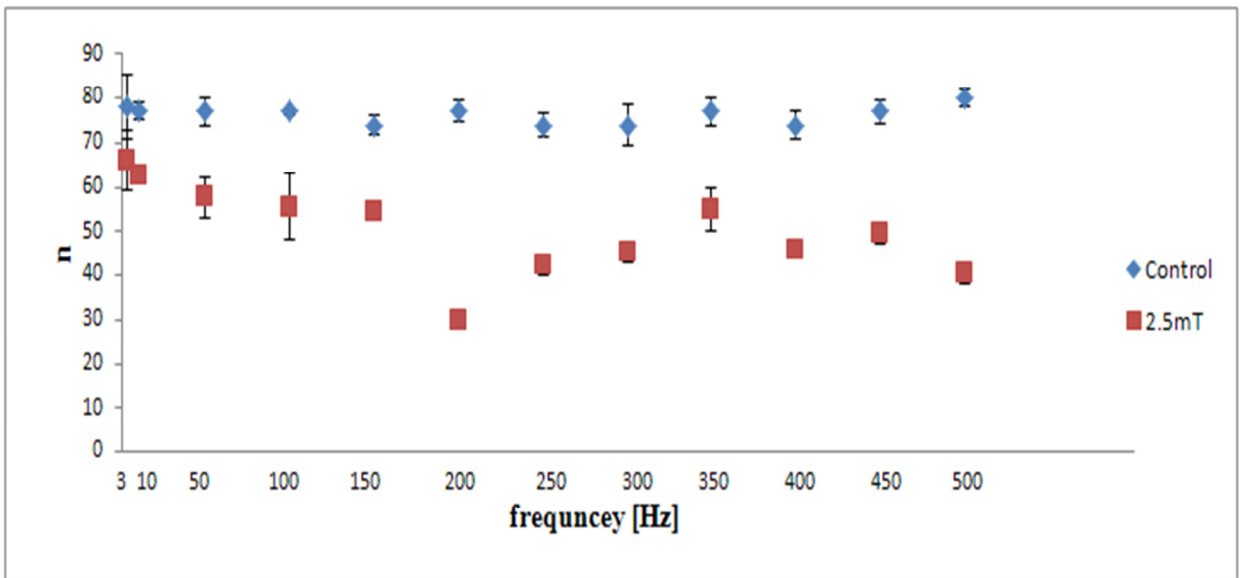


Figure 5.15: Changes in the CFU value of *S. aureus* after ELF PEMF exposure: (n- number of bacteria in 100 $\mu$ l of suspension).  $\diamond$ -control sample,  $\square$ -ELF PEMF exposed sample at 2.5mT [147].

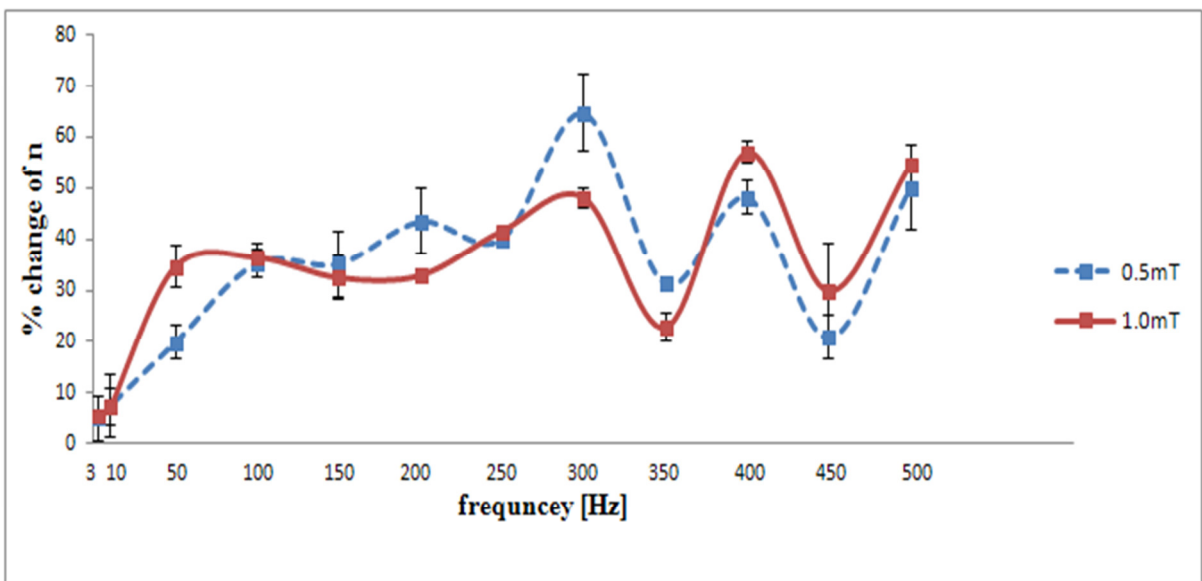


Figure 5.16: Relative change (%) in the number of bacteria count for *S. aureus* after ELF PEMF exposure at 0.5mT and 1.0mT [147].

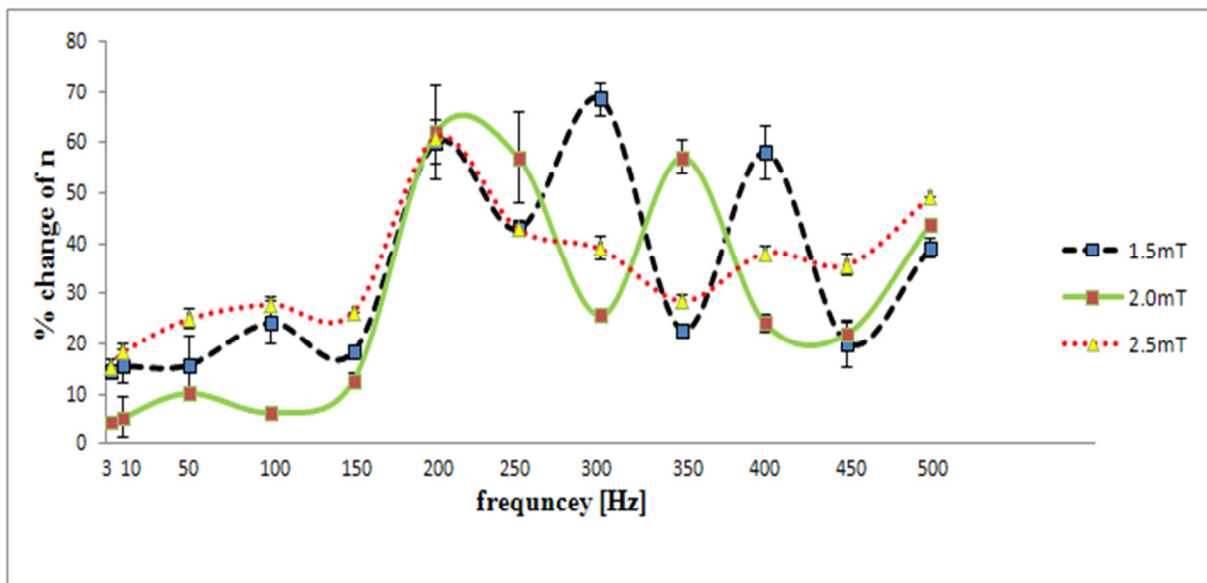


Figure 5.17: Relative change (%) in the number of bacteria count for *S. aureus* after ELF PEMF exposure at 1.5mT, 2.0mT and 2.5mT [147].

The CFU values at the frequencies 3Hz and 10Hz and all five studied magnetic flux densities (0.5mT, 1.0mT, 1.5mT, 2.0mT and 2.5mT) were consistently higher (minimum decrease) as opposed to the effects observed at the higher frequencies of ELF PEMF. As shown in Figures 5.11 and 5.12, CFU values are 73 (cells per mL) and 72 for exposures at 3Hz and 0.5mT and 3Hz and 1.0mT, respectively. This corresponds to a relative percentage decrease of 4.95% at 0.5mT and 5.50% at 1.0mT, respectively (Figure 5.16). Figures 5.11 and 5.12 graphically depict CFU values of 71 and 72 for exposures at 10Hz and 0.5mT, and at 10Hz and 1.0mT respectively. This resulted in a relative decrease of 7.52% and 7.25%, respectively (Figure 5.16). Maximum decreases of CFU values ( $n = 27$  and  $n = 24$ ) were recorded at the frequency 300Hz and flux densities of 0.5mT and 1.5mT (Figures 5.11 and 5.13). This corresponds to relative decreases of 64.63 % and 68.56%, respectively (Figures 5.16 and 5.17). CFU values, along with corresponding relative change value for studied frequencies and magnetic flux densities are shown in Table 5.2.



Table 5.2: Minimum CFU number and Maximum percentage change for ELF PEMF exposure of bacterium *S. aureus* [147].

Frequency (Hz)	CFU value, <i>n</i> (Minimum)	Percentage change (%) (Maximum)	Corresponding value of magnetic flux density (mT)	Corresponding Figure Numbers
3	66	15.38	2.5	5.15 & 5.17
10	63	18.27	2.5	5.15 & 5.17
50	51	34.62	1.0	5.12 & 5.16
100	49	36.36	1.0	5.12 & 5.16
150	50	35.06	0.5	5.11 & 5.16
200	30	62.02	2.0	5.14 & 5.17
250	33	57.04	2.0	5.14 & 5.17
300	25	68.56	1.5	5.13 & 5.17
350	33	57.14	2.0	5.14 & 5.17
400	33	58.15	1.5	5.13 & 5.17
450	49	35.71	2.5	5.15 & 5.17
500	35	54.55	1.0	5.12 & 5.16

Figures 5.16-5.17 reveal non-uniform oscillatory patterns for the relative changes (%) of the number of bacteria upon exposure to ELF PEMF. Interestingly, similar trends were also observed with previous findings on the investigation of the effect of ELF PEMF on Collagenase enzyme kinetics (Section 4.6). As can be seen from the figures the bacterial cultures are extremely responsive to exposures at the different combinations of magnetic flux density and frequency. Figure 5.18 shows the presence of a specific viability pattern “quadrature polynomial” for the ELF PEMF exposures on *S. aureus* cultures at the lower end of the ELF spectrum.

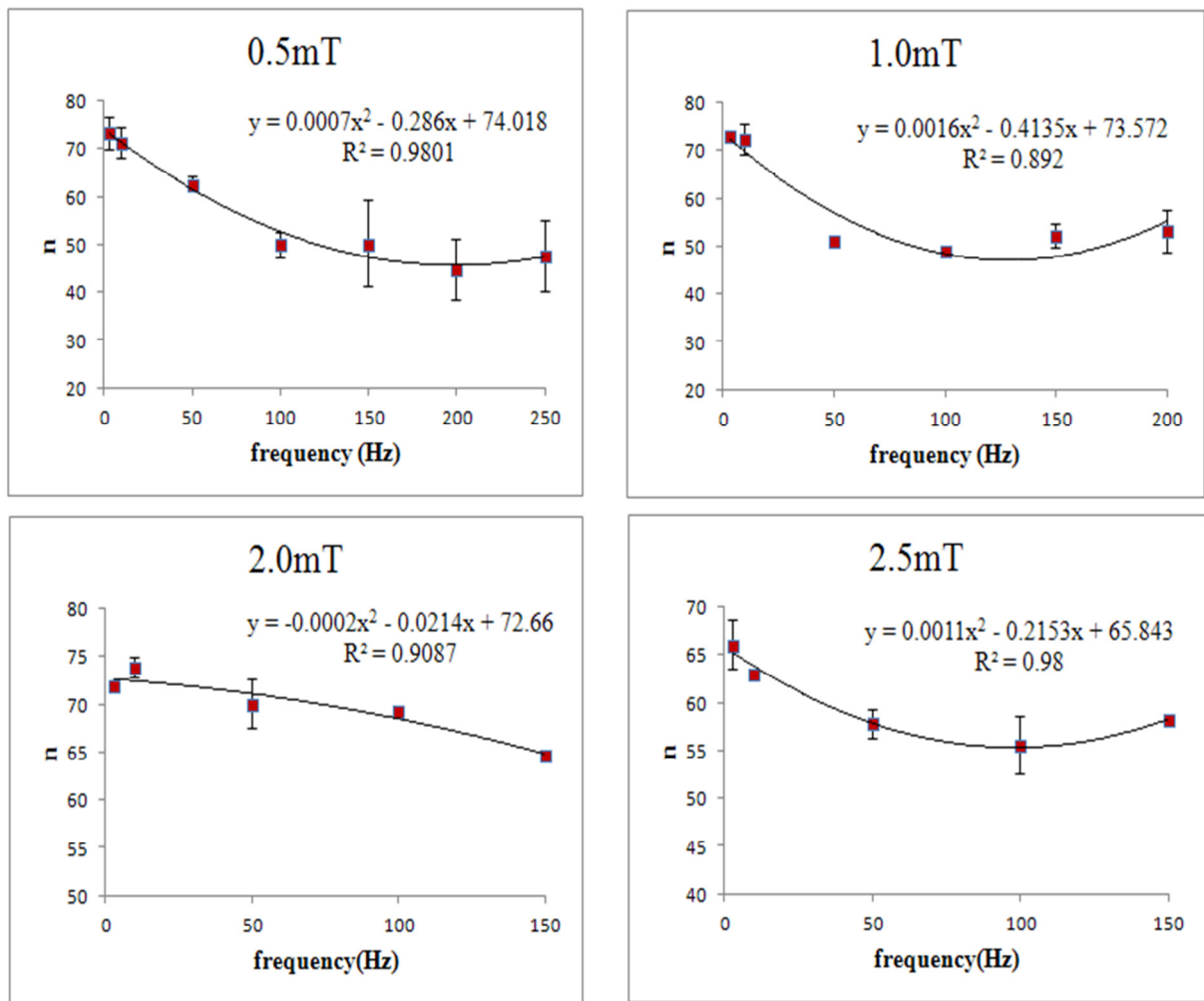


Figure 5.18: Viability pattern “quadrature polynomial” of bacterial culture of *S. aureus* exposed to ELF PEMF [147].

The pattern can potentially be used to predict the changes in CFU at the particular frequencies. Concerned patterns occur at the exposures of the following parameters: 0.5mT for 3-250Hz, 1.0mT for 3-200Hz, and 2.0mT and 2.5mT for 3-150Hz. The coefficients of determination were 0.98, 0.89, 0.91 and 0.98 for 0.5mT, 1.0mT, 2.0mT and 2.5mT, respectively.

Figure 5.19 summarizes the results obtained during experimentation.

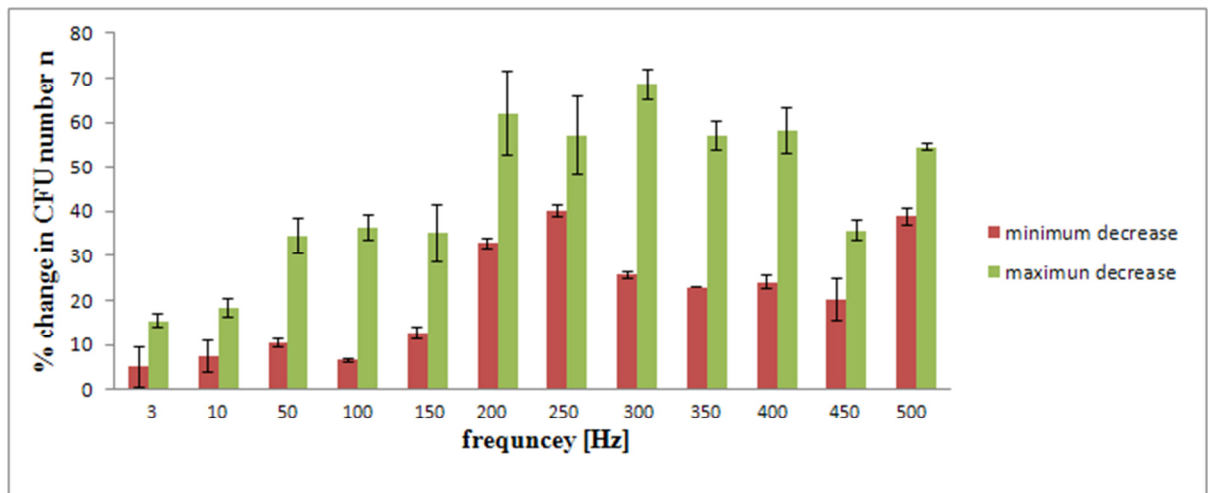


Figure 5.19: Relative minimum and maximum change (%) in CFU value: CFU values corresponds to individual frequencies after *S. aureus* exposure to ELF PEMF from 0.5-2.5mT [147].

Figure 5.19 presents the relative changes (%) in CFU values for the selected frequencies. Higher relative change (%) indicates that more bacterial cells have been affected (eliminated) by ELF PEMF exposures and thus, accounted for a lower CFU value. Minimum relative change (decrease) corresponding to the magnetic flux density range of 0.5-2.5mT were observed within 3Hz to 150Hz and varied from 4.95% to 12.73%. Maximum percentage decrease altered significantly in two phases: (i) a change from 18.27% to 34.61% from 10Hz-50Hz and (ii) a change from 35.06% to 62.05% from 150Hz-200Hz. The only exception was at 450Hz, where the maximum decrease of 35.71% was noted. Generally, the most significant changes (increase or decrease) in CFU values on and above 150Hz are considerably greater as opposed to the changes noticed with the exposures in the lower end of ELF spectrum.

Figure 5.20 is self-explanatory and clearly shows the formation of colony forming units on a Colombia agar petri dish after the post exposure stage of experimentation. Selected plates are only displayed in an order to gain a better understanding from a visual perspective of the varying effect of ELF PEMF exposure to the bacterial culture of *S. aureus*. The average value of CFU, n, for all experiments was noted as 77 and is clearly indicated in the figure below.

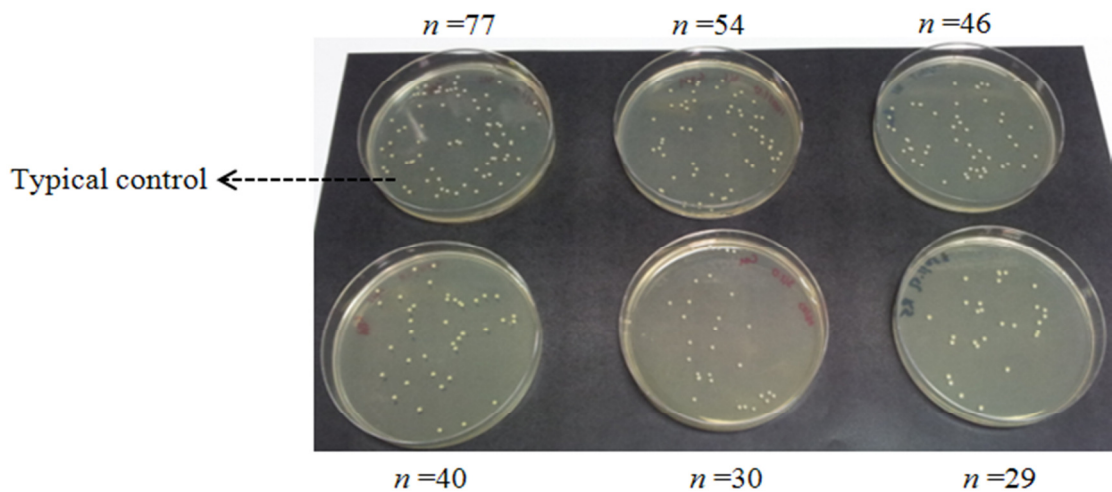


Figure 5.20: Sorted results of Columbia agar plates after incubation showing the formation of *S. aureus* colony-forming units (CFU). CFU values,  $n$ , for each plate are specified.

A decrease in growth rate compared to control samples for all bacterial cultures of *S. aureus* subjected to ELF EMF was reported by [271]. The post exposure effect reported by [271] is comparable with results obtained through this investigation. In [271], morphological alteration of *S. aureus* upon exposure to ELF EMF (50Hz at 0.5mT) for 120 minutes was also presented. An apparent cell wall disruption was not observed but cytoplasmic changes were evident. Studies conducted by [69] have also reported similar morphological changes to *S. aureus* upon exposures to ELF EMF.

ELF magnetic fields are known to affect biological systems. In many cases, biological effects display "windows" in biologically effective parameters of the magnetic fields: interestingly weaker magnetic fields are more effective [272]. Magnetic fields cause an interference of ion quantum states and change the probability of ion-protein dissociation. This ion-interference mechanism predicts specific magnetic-field frequency and amplitude windows within which the biological effects occur. This type of amplitude phenomenon suggests a nonlinear physical mechanism [272]. Other similar results (absence of correlation between experimental and control samples) suggest that degree of non-thermal effects is almost independent of the absorbed frequency and magnetic flux density. This phenomenon of frequency 'window' of

the EMF biological effects was reported for *S. aureus* in [201]. It was suggested that these ‘frequency’ windows are caused when EMF are creating biological effects through interaction with non-linear and cooperative process within cells [272]. With regards to the results from this study, we observed both frequency and magnetic flux density ‘windows’, especially for frequency range greater than 250Hz at 0.5mT, 200Hz at 1.0mT, 150Hz at 2.0mT and 2.5mT. One such example is the effect of ELF PEMF (in terms of CFU number) at 300Hz for 0.5mT was 27 (Figure 5.11) where as for the same frequency at a higher magnetic flux density of 2.5mT the CFU number was 45 (Figure 5.15).

### 5.7.2 Effect of ELF PEMF on Bacterial Culture of *E. coli*

Experimental data were plotted and presented in Figures 5.21-5.28. Figures 5.21-5.25 shows the significant difference between the CFU values of exposed and control (non-exposed) *E. coli* cultures. For each measurement, the relative difference in CFU between the exposed and control samples were calculated. All bacterial cultures of *E. coli* subjected to ELF PEMF exposure showed decrease in growth rate compared to control sample. An exponential relationship in CFU values across the entire ELF range corresponding to every selected value of magnetic flux density was observed. The coefficients of determination for the exponential trends were 0.97, 0.98, 0.96, 0.98 and 0.95 for 0.5mT, 1.0mT, 1.5mT, 2.0mT and 2.5mT, respectively (Figure 5.26). Occurrence of minimal and maximum changes amongst the CFU values for exposed sample were reported at 3Hz and 500Hz corresponding to 0.5mT and 2.5mT, respectively. The highest CFU value (minimum decrease) was recorded as 75 for 3Hz at 0.5mT (Figure 5.21). This corresponded to relative percentage decrease of 1.8% (Figure 5.27). The lowest CFU value (maximum decrease) was recorded as 18 for 500Hz at 2.5mT (Figure 5.30). This corresponded to relative percentage decrease of 77.26%. CFU value for the control samples remained almost constant, around 77, throughout the entire range of different ELF PEMF exposures (Figures 5.21-5.25).

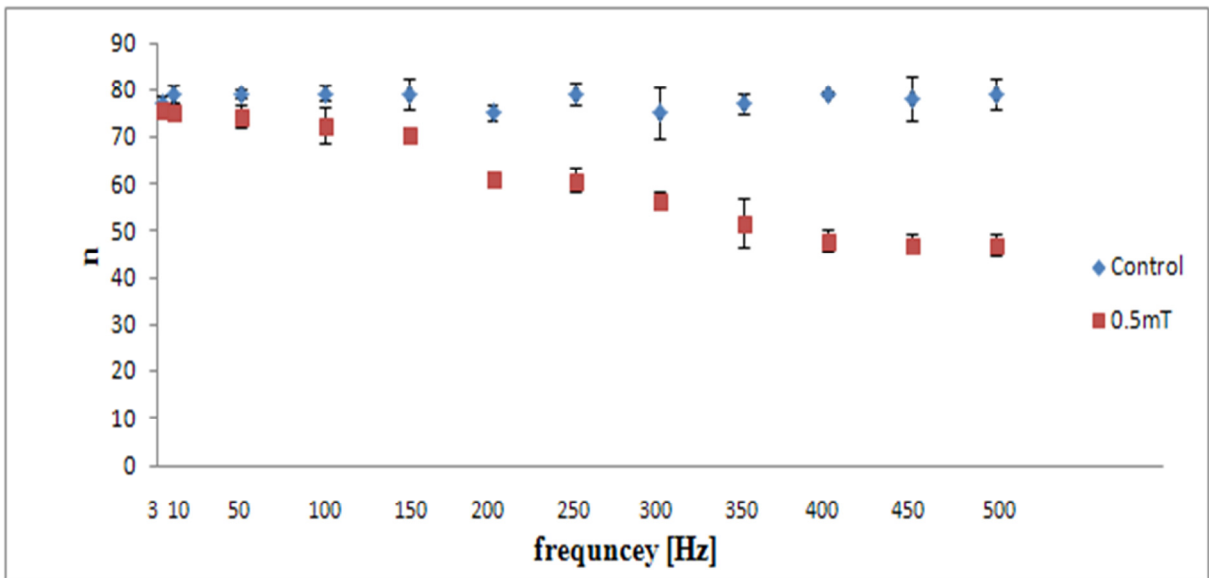


Figure 5.21: Changes in the CFU value of *E. coli* after ELF PEMF exposure: (n- number of bacteria in 100 $\mu$ l of suspension).  $\diamond$ -control sample,  $\square$ -ELF PEMF exposed sample at 0.5mT.

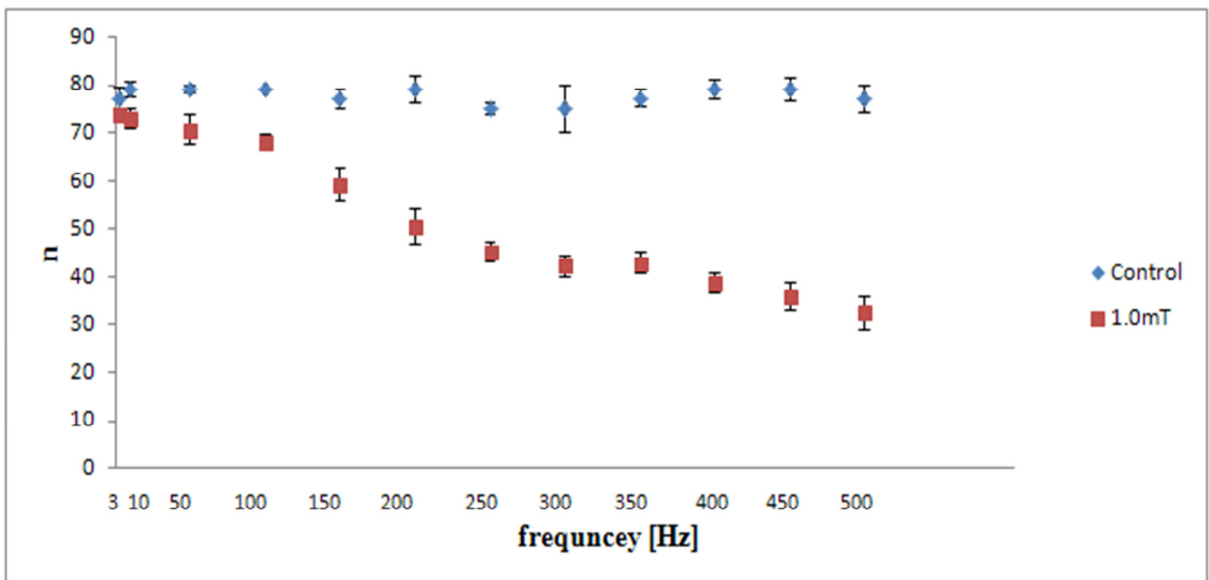


Figure 5.22: Changes in CFU value of *E. coli* after ELF PEMF exposure: (n- number of bacteria in 100 $\mu$ l of suspension).  $\diamond$ -control sample,  $\square$ -ELF PEMF exposed sample at 1.0mT.

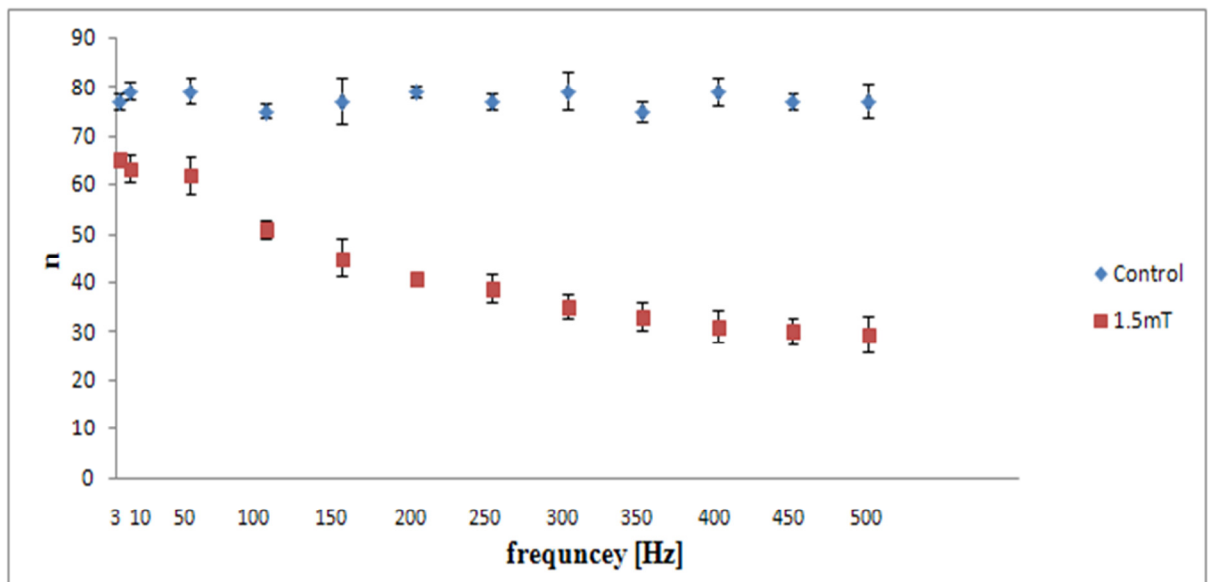


Figure 5.23: Changes in the CFU value of *E. coli* after ELF PEMF exposure: (n- number of bacteria in 100 $\mu$ l of suspension).  $\diamond$ -control sample,  $\square$ -ELF PEMF exposed sample at 1.5mT.

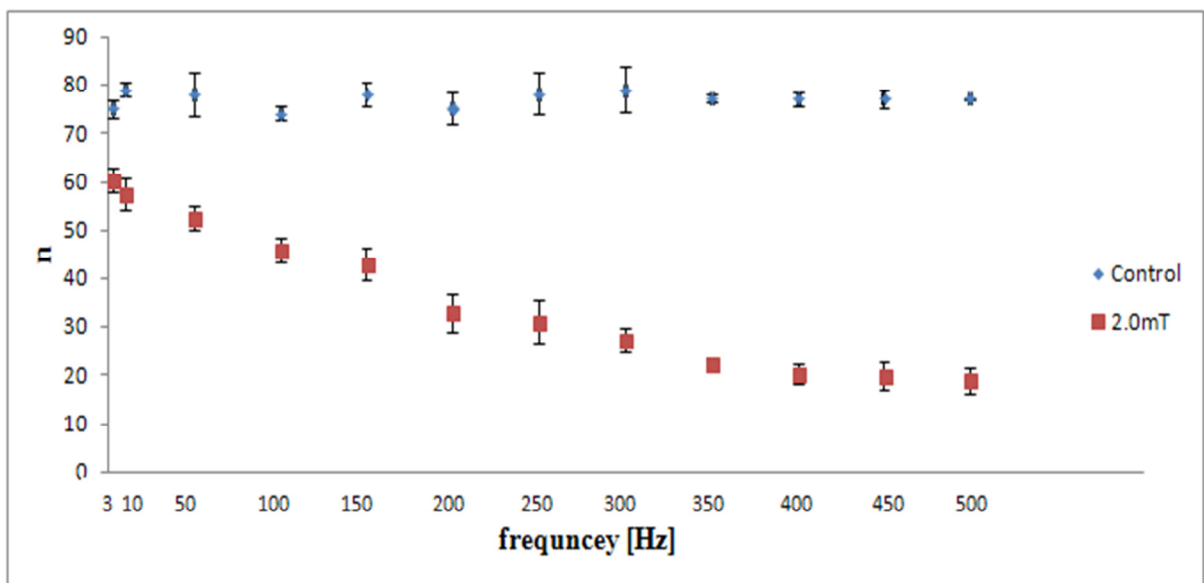


Figure 5.24: Changes in the CFU value of *E. coli* after ELF PEMF exposure: (n- number of bacteria in 100 $\mu$ l of suspension).  $\diamond$ -control sample,  $\square$ -ELF PEMF exposed sample at 2.0mT.



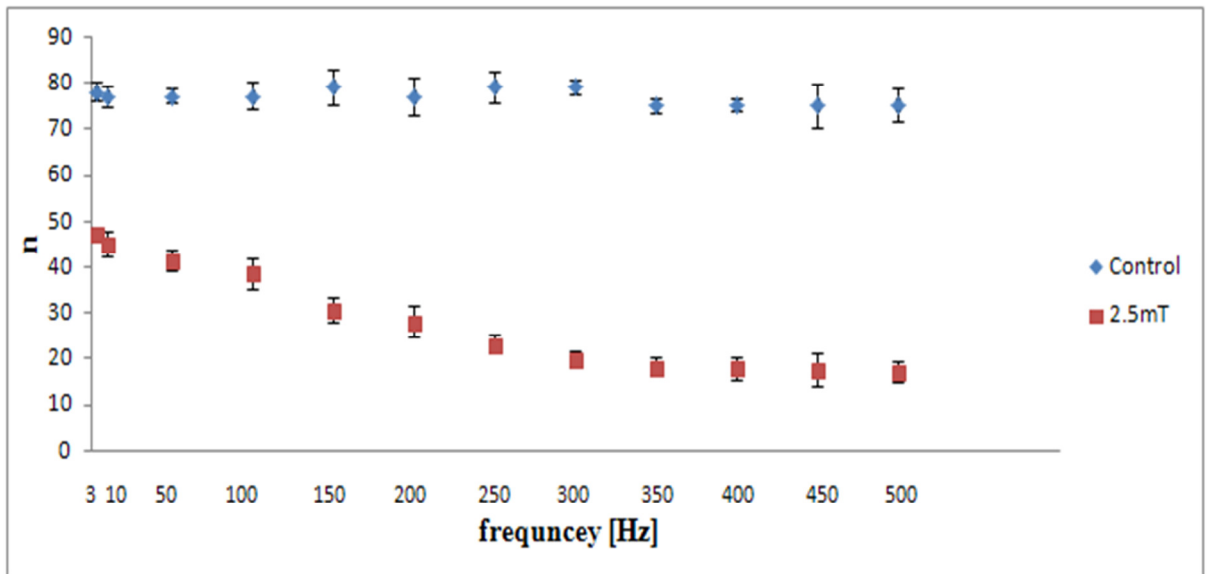


Figure 5.25: Changes in the CFU value of *E. coli* after ELF PEMF exposure: (n- number of bacteria in 100 $\mu$ l of suspension).  $\diamond$ -control sample,  $\square$ -ELF PEMF exposed sample at 2.5mT.

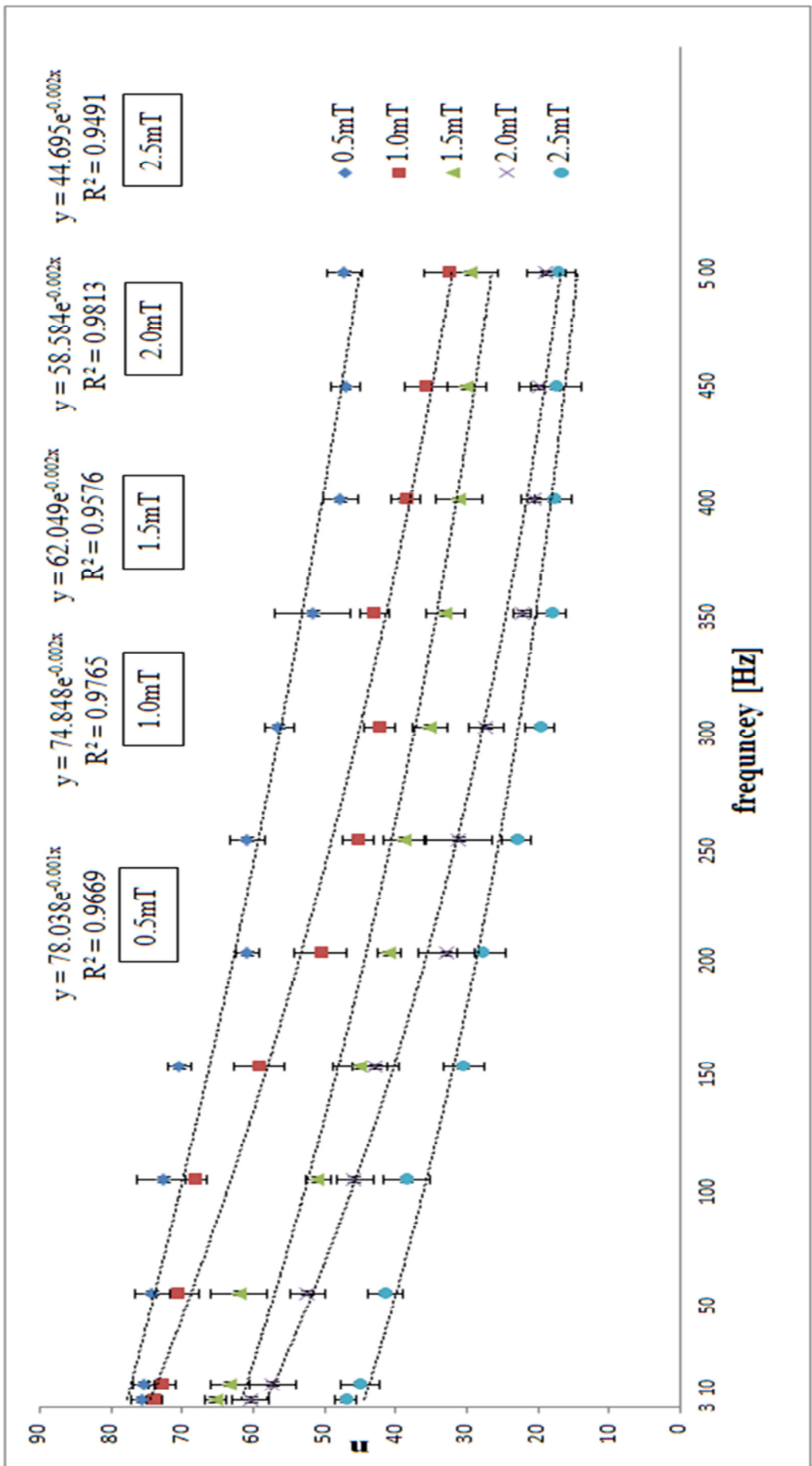


Figure 5.26: Exponential trend of CFU corresponding to exposure of ELF PEMF to *E. coli*.

Table 5.3 shows the combination of frequency and magnetic flux density for which minimum CFU value was obtained. The highest decrease (lowest CFU value) for all studied frequencies was attained at 2.5mT.

Table 5.3 Minimum CFU value and Maximum percentage change for ELF PEMF exposure of bacterium *E. coli*.

Frequency (Hz)	CFU value, <i>n</i> (Minimum)	Percentage change (%) (Maximum)	Corresponding value of magnetic flux density (mT)	Corresponding Figure Numbers
3	47	39.71	2.5	5.25 & 5.28
10	45	41.67	2.5	5.25 & 5.28
50	38	46.15	2.5	5.25 & 5.28
100	30	50.03	2.5	5.25 & 5.28
150	26	61.39	2.5	5.25 & 5.28
200	25	63.70	2.5	5.25 & 5.28
250	22	70.89	2.5	5.25 & 5.28
300	19	75.05	2.5	5.25 & 5.28
350	18	75.84	2.5	5.25 & 5.28
400	18	76.25	2.5	5.25 & 5.28
450	17	76.80	2.5	5.25 & 5.28
500	17	77.26	2.5	5.25 & 5.28

Figure 5.27 and 5.28 shows that bacterial cultures are extremely responsive to irradiation at the different combinations of magnetic flux density and frequency. It is apparent that the relative percentage change in the number of bacteria count is at all times higher for increasing magnetic flux density corresponding to individual frequencies. Therefore, at any experimental frequency, the relative percentage change is the highest at 2.5mT and lowest at 0.5mT.

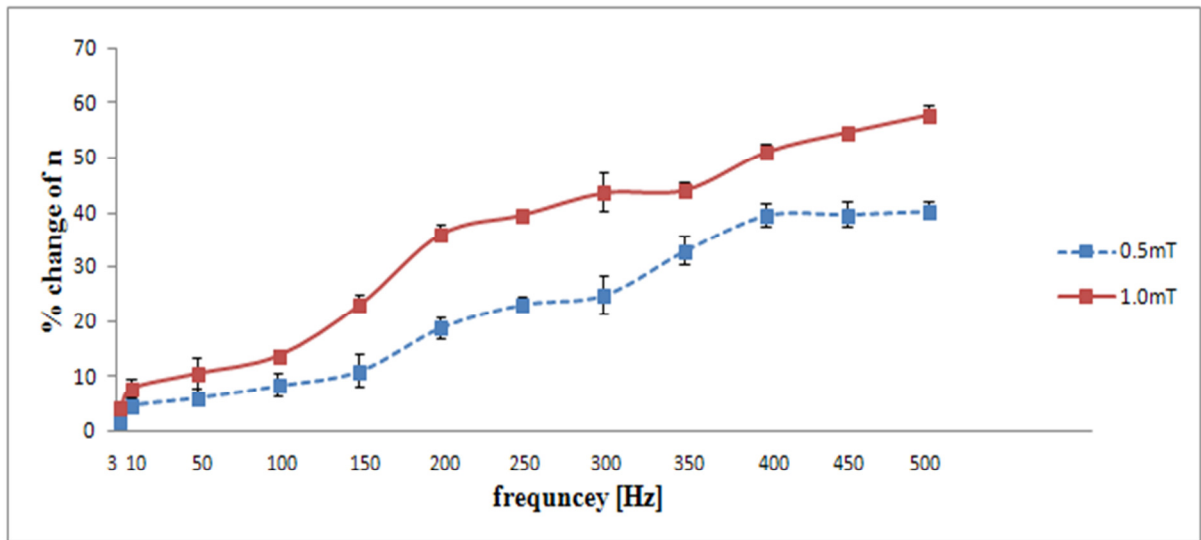


Figure 5.27: Relative change (%) in the number of bacteria count of *E. coli* after ELF PEMF exposure at 0.5mT and 1.0mT.

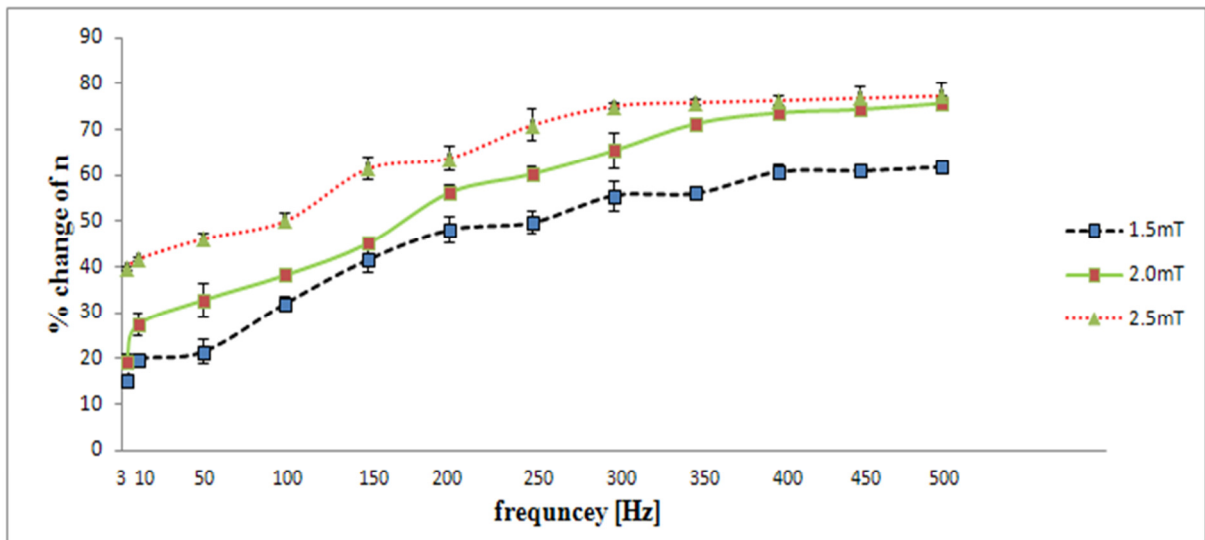


Figure 5.28: Relative change (%) in the number of bacteria count of *E. coli* after ELF PEMF exposure at 1.5mT, 2.0mT and 2.5mT.

Figure 5.29 conveniently summarizes the results obtained during experimentation. This figure presents the relative changes (%) in CFU values for all experimental frequencies. Higher relative change (%) indicates that more bacterial cells have been affected (eliminated) by ELF PEMF exposures and thus, accounted for a lower CFU value.

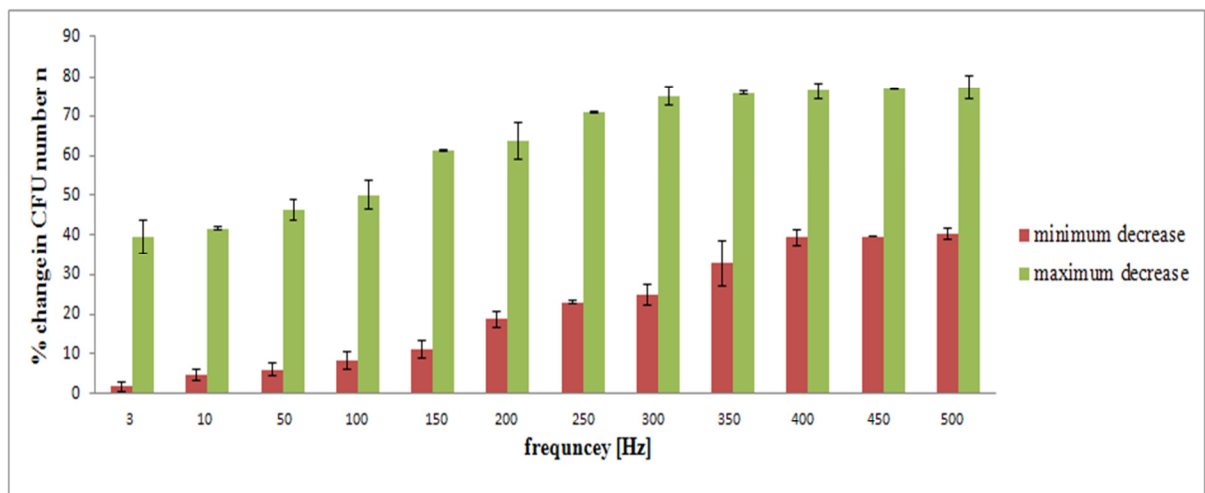


Figure 5.29: Relative minimum and maximum change (%) in CFU value: CFU values corresponds to individual frequencies after *E. coli* exposure to ELF PEMF from 0.5-2.5mT.

Maximum relative change (decrease) corresponding to the magnetic flux density range of 0.5-2.5mT altered significantly in two phases:

- (i) A change from 39.71% to 70.89% at the frequencies of 3Hz-250Hz.
- (ii) A change from 75.05% to 77.26% at the frequencies of 300Hz-500Hz

Minimum relative change (decrease) corresponding to the magnetic flux density range of 0.5-2.5mT altered significantly in two phases:

- (i) A change from 1.78% to 33% at the frequencies of 3Hz-350Hz.
- (ii) A change from 39.5% to 40.3% at the frequencies of 400Hz-500Hz.

Figure 5.30 shows selected results in terms of CFU values for the effect of ELF PEMF exposure to the bacterial culture of *E. coli*. One again, to avoid redundancy, and to show the varying effect of ELF PEMF, selected plates are only displayed. The average value of CFU, n, was noted at 77 for all conducted experiments. Maximum effect (minimum CFU value) was obtained for *E. coli* exposure to ELF PEMF at 500Hz corresponding to the magnetic flux density of 2.5mT and is clearly indicated in the figure below.

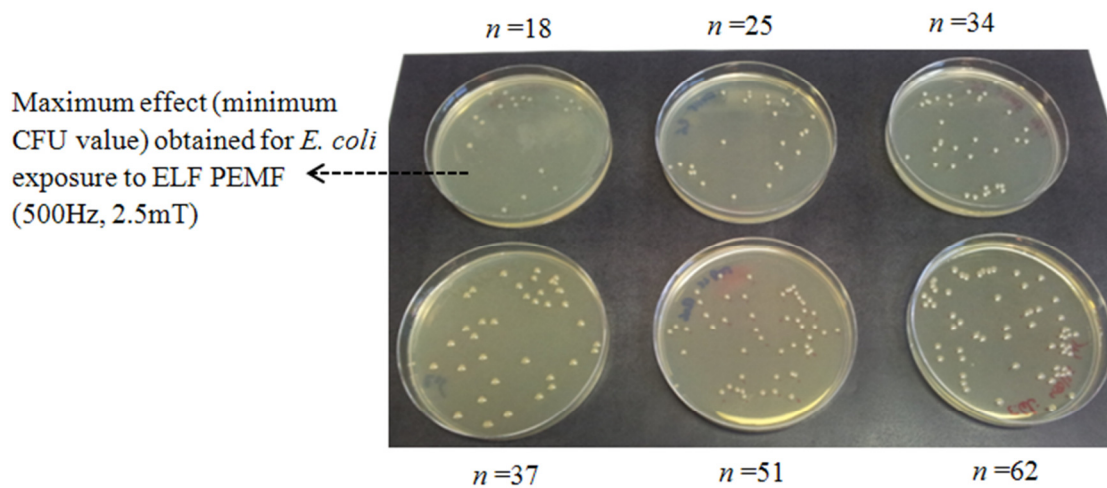


Figure 5.30: Sorted results of Columbia agar plates after incubation showing the formation of *E. coli* colony-forming units (CFU). CFU values, *n*, for each plate are specified.

### 5.7.3 General Discussion

The established method for evaluating the effects of ELF PEMF exposures on viability of bacterial is the method of CFU- colony forming unit [69], where the decrease in CFU number observed after EMF exposures is correlated with bacterial death (CFU number represents bacteria, which remains alive after all treatments) [69, 273, 274]. Similar to the above mentioned studies, this research also employed this method to study the viability of bacterial culture of *S. aureus* and *E. coli* exposed to ELF PEMF [69]. From the growth curve shown in Figure 5.5 and 5.6, it was observed that even after exposures bacteria were not in the death phase but rather still growing in their exponential phase. Similar to [275], it was observed that the ELF PEMFs effects are not bacteriostatic (blocking their growth during exposures), but rather dynamic, i.e. a number of bacteria still increases upon exposures. However, the growth rate of the exposed samples is suppressed in comparison to the controls (Figure 5.5 & 5.6). Therefore, similar to [275] it was concluded that EMFs can partially eliminate the exposed bacteria.

Similar to other studies [69, 274- 275] the question of how magnetic field can kill bacteria has not been solved within the scope of this research. The mechanism of interaction of ELF PEMFs and biological systems in terms of simple quantitative models is given in [64]. Since induces effects can only result from a direct interaction of the EMF with molecular targets, including ions, any adequate description must be of physical chemical nature [276]. Hypothesis of proposed biophysical model theories [64, 276] for ELF PEMFs effects are based on the isolated cell culture and are therefore, differ from natural organism [277]. These theories suggests that external PEMF disrupts the electrochemical balance of the plasma membrane and therefore the entire cell function by causing a forced-vibration to each free ion [278]. So far, no characteristics physical chemical reaction parameters for bacteria have been established such that they can be compared with those extracted from the molecular physical chemical approach [273].

The focus of this study centres on determining the optimal characteristics of applied ELF PEMF that suppress the bacterial growth. The mechanistic aspects of PEMF effects on cells were proposed by different research studies. The interaction of ELF EMF with electrons in DNA of bacterial culture is also suggested by [277]. The biochemical compound in living cells are composed of charges and dipoles that can interact with electric and magnetic field by various mechanisms. For instance, displacement of electrons in DNA could cause local charging that has been shown to lead to disaggregation of biopolymers. Secondly, very weak ELF fields have been shown to affect the rate of electron transfer reaction [279]. Low EMF energy can move electrons and cause small changes in charge structure [280]. ELF EMF has also shown to interact and accelerate electrons moving within DNA [281]. Applied PEMF can affect the permeability of ion channels in a cell membrane that in turn affects ion transport into a cell and ultimately results in alteration of biological function and/or structure of a cell [282]. Formation of free radicals upon irradiation with a magnetic field is another suggested outcome for EMF interaction with biological samples [282].

## 5.8 Summary

The significance of studying wound infected with bacteria and in particular the selection of *S. aureus* and *E. coli* as wound infecting agents were previously discussed in Sections 2.20-2.24. This chapter reports on the results obtained from the experimental study of the entire range of ELF PEMF exposures on bacterial cultures of *S. aureus* and *E. coli* at the frequency range of 2-500Hz and at the magnetic flux density ranging from 0.5mT to 2.5mT. The presence of “window effect” was demonstrated by the results obtained via ELF PEMF irradiation of bacterial culture of *S. aureus*. The exponential relationship in CFU values across the entire ELF range corresponding to the studied magnetic flux densities was observed with *E. coli* bacteria. Determining the optimal parameters of the applied ELF PEMF for bacteria elimination is vital in the development of efficient and non-invasive treatment of infected



tissues and thus, wound healing promotion. The optimal ELF PEMF parameters (frequency and magnetic induction), which induce the most statistically significant effects on bacteria growth, were obtained from the experiments conducted in vitro with bacterial cultures of *S. aureus* and *E. coli* and are given below:

- frequency 300Hz and magnetic induction 1.5mT; and
- frequency 500Hz and magnetic induction 2.5mT, respectively.

Optimal ELF PEMF parameters obtained through these investigations can also be used to explore the possibility of utilizing ELF PEMF as an adjunct treatment on *S. aureus* and *E. coli* infected wound treated with antibiotic.

## **CHAPTER 6:**

## **CONCLUSIONS**

## 6.1 Conclusions

This research has been successfully accomplished with the aims and objectives set forth in Chapter 1 are being completed. The following has been achieved with the PhD research project:

1. ***Design and construction of ELF PEMF system:*** The exposure system for studying the effects of ELF PEMF on molecules and cells was designed and constructed. The exposure chamber is built on the basis of a Two-Axis (four coils) Helmholtz coil system. By means of superimposed field, this four coil system can produce higher magnetic flux densities and greater field uniformity compared to a conventional 1-Axis Helmholtz coil system. Structural design of the lab-built ELF PEMF chamber allows experiments to be conducted at specific regulated temperatures.

2. ***Custom made software:*** A custom software program was written which aids to visualize the uniformity of magnetic field for a user defined size and orientation of coils and therefore, permits a systematic magnetic field analysis. In particular, the program can calculate and generate plots for region of B-field uniformity within 10%, 1% and 0.1% of the centre field.

3. Experimental evaluation of ELF PEMF irradiation on protein (Collagenase enzyme) and bacterial culture (*S. aureus* and *E. coli*);

- Collagenase Enzyme: Optimal ELF PEMF parameters were determined for enzyme that can lead to the increase in its enzymatic activity. The experimental results obtained successfully demonstrated that the biological activity of a selected protein,

Collagenase enzyme, can be modulated by irradiation with ELF PEMF and thus can affect the specific biological process involving this particular enzyme. Results show an increase in the biological activity of Collagenase enzyme upon ELF PEMF irradiation at 3Hz and 8Hz corresponding to each and every magnetic flux density ranging from 0.5-2.5mT. Notable increase in enzyme activity was also recorded at 300Hz corresponding to 0.5 mT and 1.0mT. Results also show a decrease in enzyme activity upon ELF PEMF irradiation at 300Hz corresponding to magnetic flux densities of 1.5mT, 2.0mT and 2.5mT.

- **Bacterial culture of *S. aureus*:** Maximum decreases of CFU values (n = 27 and n = 24) were recorded at the frequency 300Hz and flux densities of 0.5mT and 1.5mT. This corresponds to respective relative decreases of 64.63 % and 68.56%. Decreases of at least 20% in CFU values were obtained at the frequencies above 200Hz and all five studied magnetic flux densities. The presence of “window effect” was also prevalent from experimental results with *S. aureus*. Specific viability pattern “quadrature polynomial” was identified for ELF PEMF irradiation of bacterial culture of *S. aureus*. These patterns were evident at the exposures of the following parameters: 0.5mT for 3-250Hz, 1.0mT for 3-200Hz, and 2.0mT and 2.5mT for 3-150Hz. The respective coefficients of determination were 0.98, 0.89, 0.91 and 0.98 for 0.5mT, 1.0mT, 2.0mT and 2.5mT.
- **Bacterial culture of *E. coli*:** Minimal and maximum changes amongst the CFU values for exposed sample were reported at 3Hz and 500Hz corresponding to 0.5mT and 2.5mT, respectively. The lowest CFU value (maximum decrease) of n=18 was recorded for 500Hz at 2.5mT and corresponded to relative percentage decrease of 77.26%. Exponential relation in CFU values were obtained for the entire ELF range

corresponding to the studied magnetic flux densities while studying the effect of ELF PEMF irradiation of bacterial culture of *E. coli*. The respective coefficients of determination for the exponential trends were 0.97, 0.98, 0.96, 0.98 and 0.95 for 0.5mT, 1.0mT, 1.5mT, 2.0mT and 2.5mT.

Outcomes of this research project supported the fact that optimal ELF PEMF parameters can induce therapeutic effect and thereby can be used for possible treatment and wound healing promotion.

## 6.2 Suggestions for Further Research

Results presented in this research project form the basis for a series of potential further studies as presented below:

- Optimal characteristics of ELF PEMF exposures determined within this project for the selected bacterial cultures can be investigated on tissue cultures. Studies of such nature can provide better understanding of the mechanistic aspects of ELF PEMF interaction with cells and thus, offer a deeper insight into the process of wound repair.
- A large area of uniform magnetic field could be used to expose bacterial strains in a solid medium (Agar Petri dish). Thus, a study on comparison of the survival dynamics under irradiation with ELF PEMF and its probable combination with additional field (e.g. AC EMF, DC electric field (EF)).
- The viability of other bacteria (based on their colonization environment) upon ELF EMF exposures can be also studied. For example, the bacterium *Pseudomonas*

*aeruginosa* can be studied for its frequent colonization in medical instruments that causes cross-infections in clinics and hospitals.

- Investigating the effect of ELF PEMF on bacteria in a semi-solid medium will closely relate to food constituents. Results from such studies will prove beneficial for food sterilization and can play a vital role in the food industry.
- Integral part of wound exposure to magnetic field pivots around the field uniformity across the entire wounded tissue. Because of geometrical complexities of humans and animals, it is often difficult to expose the wounded tissue to uniform magnetic field. On that note, a development of a flexible coil structure that can be molded according to the geometry of a wound and also can easily be strapped to the host body could prove vital for actualizing the effect of ELF PEMF on wound healing.

## 6.3 Publications

During the course of this research project, two (2) journal publications have been published along with three (3) full peer-reviewed conference papers. Additionally, one (1) more journal paper has been submitted and currently awaiting acceptance.

### Journal papers:

- **I. Ahmed**, T. Istivan, I. Cosic and E. Pirogova: Evaluation of the effects of Extremely Low Frequency (ELF) Pulsed Electromagnetic Fields (PEMF) on survival of the bacterium *Staphylococcus aureus*. *EPJ Nonlinear Biomedical Physics*. Heidelberg, Germany, Springer; doi:10.1140/epjnbp12, 2013: 1(5): 1-17.
- **I. Ahmed**, V. Vojisavljevic and E. Pirogova: The effect of Extremely Low Frequency (ELF) Pulsed Electromagnetic Field (PEMF) on Collagenase Enzyme Kinetics, *MD-Medical Data*, Belgrade, Serbia, Mostart d.o.o, Peter Spasis; 2012: 4(4):357-362.
- **I. Ahmed**, T. Istivan and E. Pirogova: Irradiation of *Escherichia coli* by Extremely Low Frequency (ELF) Pulsed Electromagnetic Fields (PEMF): evaluation of bacterium survival. Submitted to *Journal of Electromagnetic Waves and Applications*.

### Full peer-reviewed conference papers:

- **I. Ahmed**, V. Vojisavljevic and E. Pirogova: Design and development of extremely low frequency (ELF) pulsed electromagnetic Field (PEMF) system for wound healing promotion. *IFMBE Proceedings World Congress on Medical Physics and Biomedical*

*Engineering*. Heidelberg, Germany, Springer: Mian Long; 2012 (3): 27-30.

- **I. Ahmed**, V. Vojisavljevic and E. Pirogova: Investigation of the effect of Extremely Low Frequency (ELF) Pulsed Electromagnetic Field (PEMF) on Collagenase Enzyme Kinetics. In *BIODEVICES 2013 the Proceedings of the 6<sup>th</sup> International Joint Conference on Biomedical Engineering Systems and Technologies*. Lisbon, Portugal, INSTICC: Mireya Fernandez; 2013:143-147.
- **I. Ahmed**, T. Istivan and E. Pirogova: The effect of Extremely Low frequency (ELF) Pulsed Electromagnetic Field (PEMF) on Bacteria *Staphylococcus Aureus*, In the *Proceedings of Progress in Electromagnetic Research Symposium (PIERS 2013 in Taipei proceedings)*. Massachusetts, USA, The Electromagnetic Academy; 2013: 388-391.



## **REFERENCES**

- [1] Mercandetti M, Cohen AJ (2008) Wound healing, healing and repair. *eMedicine WebMD* [Online]. Accessed from <http://emedicine.medscape.com/article/1298129-overview>.
- [2] Clark RA (1996) *The molecular and cellular biology wound repair*. 2<sup>nd</sup> Ed. New York: Plenum Press.
- [3] Bouzarjomehri F, Hajizadeh S, Sharafi AA, Firoozabadi SMP (2000) Effects of Low-Frequency Pulsed Electromagnetic Fields on Wound Healing in Rat Skin. *Archives of Iranian Medicine* 3:23-27.
- [4] Jercinovic A, Bobanovic F, Vodonovik L (1993) Endogenous potentials in two different models of human skin injuries. *Bioelectrochem Bioenerng* 30: 221-7.
- [5] Pilla AA (2006) Mechanisms and therapeutic applications of time-varying and static magnetic fields. In: *Handbook of biological effects of electromagnetic fields*, 3<sup>rd</sup> Edition, Barnes F, Greenebaum B, CRS Press.
- [6] Pilla AA (1974) Electrochemical information transfer at living cell membranes. *Ann NY Acad Sci* 238:149-170.
- [7] Zhadin MN (1998) Combined action of static and alternating magnetic fields on ion motion in a macromolecule: Theoretical aspects. *Bioelectromagnetics* 19:279-292.
- [8] Zhadin MN, Barnes F (2005) Frequency and amplitude windows in the combined action of DC and low frequency AC magnetic fields on the ion thermal motion in a macromolecule: Theoretical analysis. *Bioelectromagnetics* 26:3232-330.
- [9] McCreary CR, Thomas AW, Prato FS (2002) Factors confounding cytosolic calcium measurements in Jurkat E6.1 cells during ELF magnetic fields. *Bioelectromagnetics* 23:315-328.
- [10] O'Connor JA, Lanyon JE (1982) The influence of strain rate on adaptive bone modelling. *J Biomech* 15(10):767-781.
- [11] Shupak NM (2003) Therapeutic uses of pulsed magnetic- field exposure: a review. *Radio Science Bulletins* No 307:9-32.
- [12] Milgram J, Shahar R, Levin-Harrus T, Kass P (2004): The effect of short, high intensity magnetic field pulses on the healing of skin wounds in rats. *Bioelectromagnetics* 25(4):271-277.
- [13] Athanasiou A, Karkambounas S, Batistatou A, Lykoudis E, Katsaraki A, Kartsiouni T, Papalois A, Evangelou A (2007). The effect of pulsed electromagnetic fields on secondary wound healing: An experimental study. *Bioelectromagnetics* 28(5): 362-368.

- [14] Baum JW, Keuhner AV, Benz RD, Carsten AL (1991) A system for simultaneous exposure of small animals to 60-Hz electric and magnetic fields. *Bioelectromagnetics* 12:85-89.
- [15] Stuchly MA, Lawyer DW, McLean J (1991) Cancer promotion in a mouse skin model by a 60Hz magnetic field. Experimental design and exposure system. *Bioelectromagnetics* 12:261-271.
- [16] Jones RA, Sheppard AR (1992) An integrated magnetic ELF field generator and incubator for long-term in vitro studies. *Bioelectromagnetics* 13:199-207.
- [17] Mullins RD, Sisken JE, Hejase HN, Sisken B (1993) Design and characterization of a system for exposure of cultured cells to extremely-low frequency electric magnetic fields over a wide range of field strengths. *Bioelectromagnetics* 14:173-183.
- [18] Polk C, Postow E (1986) *Handbook of biological effects of electromagnetic fields*. Boca Raton, FL, CRC Press.
- [19] Juutilainen J, Lang S (1997) Genotoxic, Carcinogenic and Tetragenic effects of electromagnetic fields: Introduction and overview. *Mutation Research* 387:165-171.
- [20] Rubik B (1997) Bioelectromagnetics & the future in medicine. *Administrative Radiology Journal*. 16(8):38-46.
- [21] Sisken BF, Walker J (1995) Therapeutic aspect of electromagnetic fields for soft tissue healing. *Electromagnetic Fields: Biological interactions and Mechanisms, Advance in Chemistry* 250:277-286.
- [22] Baladi E, Lithgow B, Heath B, Cohen M, Cosic I, Grace RJ (1999) A pilot study on the extremely low frequency (ELF) pulsing magnetic field (PMF) effect on soft tissue injuries: A preliminary analysis of the results. *Med Biol Eng Comp* 37 (Suppl1):103-104.
- [23] Goudarzi I, Hajizadeh S, Salmani ME, Abrari K (2010) Pulsed electromagnetic fields accelerate wound healing in the skin of diabetic rats. *Bioelectromagnetics* 31(4):318-323.
- [24] Kumar VS, Kumar DA, Kalaivani K, Gangadharan AC, Raju KVS, Thejomoorthy P, Manohar BM, Puvanakrishnan R (2005). Optimization of pulsed electromagnetic field therapy for management of arthritis in rats. *Bioelectromagnetics* 26:431-439.
- [25] Ganesan K, Gengadharan AC, Balachandran C, Manohar BM, Puvanakrishnan R (2009). Low frequency pulsed electromagnetic field- a viable alternative for arthritis. *Indian Journal of Experimental Biology* 47(12):939-948.
- [26] Chang K, Chang WH (2003) Pulsed electromagnetic fields prevents osteoporosis in an ovariectomized female rat model: a prostaglandin E<sub>2</sub> –associated process *Bioelectromagnetics* 24:189-198.
- [27] Hopper RA, VerHalen JP, Tepper O, Mehrara BJ, Detch R, Chang EI, Baharestani S, Simon BJ, Gurtner GC (2009) Osteoblasts stimulated with pulsed electromagnetic fields HUVEC proliferation via a VEGF- a Independent mechanism. *Bioelectromagnetics* 30:189-197.

- [28] Adey WR (2004) Potential therapeutic application of non thermal electromagnetic fields: Ensemble organization of cells in tissue as a factor in biological tissue sensing. In Rosch PJ and Markov MS (Eds.) *Bioelectromagnetic medicine*, New York, Marcel Dekker (1-15).
- [29] Sun LY, Hsieh DK, Yu TC, Chiu HT, Lu SF, Luo GH, Kuo TK, Lee OK, Chiou TW (2009) Effect of pulsed electromagnetic field on the proliferation and differentiation potential of human bone marrow mesenchymal stem cells. *Bioelectromagnetics*: 30 (4):251-60.
- [30] Anderson I (2006) Debridement methods in wound care. *Nurs Stand*. 22(24):65-72.
- [31] Lei S, Ryan E, Anastacia G, Dale T, Duncan A (2010) Degradation of human collagen isoforms by *Clostridium* collagenase and the effects of degradation products on cell migration. *International Wound Journal* 7(2):87-95.
- [32] Enzyme Nomenclature. Accessed from <http://www.chem.qmul.ac.uk/iuimb/enzyme>.
- [33] Enzyme. Accessed from <http://enzyme.expasy.org/EC/3.4.24.3>.
- [34] Ruiz-Gómez MJ, De la Peña L, Prieto-Barcia MI, Pastor JM, Gil L, Martínez-Morillo M. (2002) Influence of 1 and 25 Hz, 1.5 mT magnetic fields on antitumor drug potency in a human adenocarcinoma cell line. *Bioelectromagnetics* 23(8):578-85.
- [35] Vincent K, Coleman R (2008) Bacterial skin and soft tissue infections in adults: a review of their epidemiology, pathogenesis, diagnosis, treatment and site of care. *Can J Infect Dis Med Microbiology* 19(2):173-184.
- [36] Ahmed M, Alam SN, Khan O, Manzar S (2007) Post-operative wound infection: A surgeon's dilemma. *Pakistan journal of surgery* 23 (1): 41-47.
- [37] Landis SJ (2008) Chronic wound infection and antimicrobial use. *Adv Skin Wound Care* (21):531-540.
- [38] Eliza R, Bianca G (2011) Vascular graft infections management. *Clinical Management, Management in Health* XV/316-19.
- [39] Finn G (2005) An overview of surgical site infections: aetiology, incidence and risk factors. *European Wound Management Association Journal*. 5(2):11-15.
- [40] Lucinda JB, Paolo F, Mara DG, Luigina C (2013) Bacterial isolates from infected wounds and their antibiotic susceptibility pattern: some remarks about wound infection. *International Wound Journal* doi: 10.1111/iwj.12049.
- [41] McCaig LF, McDonald LC, Mandal S, Daniel BJ (2006) *Staphylococcus aureus*-associated Skin and Soft Tissue Infections in Ambulatory Care. *Emerging Infectious Diseases* 12(13): 1715-1723.
- [42] Green M, Bradley A (2004) *Staphylococcus aureus* mastitis in cattles. *Clinical Forum UK VET*, Uk Vet publication, Jessica Daniels, Oxford, Uk (9): 1-9.
- [43] *E. coli* infection (2010) Treatment Overview. *WebMD Medical Reference from Healthwise*. Accessed from <http://www.webmd.com/a-to-z-guides/e-coli-infection-treatment-overview>.

- [44] Wei Y, Xiaolin H, Tao S. (2008) Effects of extremely low-frequency-pulsed electromagnetic field on different- derived osteoblast-like cells. *Electromagn Biol Med* 27(3):298-311.
- [45] Martino CF, Belchenko D, Ferguson V, Nielsen-Preiss S, Qi HJ (2008) The effects of pulsed electromagnetic fields on the cellular activity of SaOS-2 cells. *Bioelectromagnetics* 29(2):125-32.
- [46] Selvamurugan N, Kwok S, Vasilov A, Jefcoat SC, Partridge NC (2007) Effects of BMP-2 and pulsed electromagnetic field (PEMF) on rat primary osteoblastic cell proliferation and gene expression. *J Orthop Res* 25(9):1213-20.
- [47] Mahmoud S, Fang Q, Cosic I, Hussain Z (2005) Effects of extremely low frequency electromagnetic fields on electrocardiogram: analysis with quadratic time-frequency distributions. *Conf Proc IEEE Eng Med Biol Soc* 1:837- 40.
- [48] Thomas AW, Drost DJ, Prato FS (2001) Human subjects exposed to a specific pulsed (200 microT) magnetic field: effects on normal standing balance. *Neurosci Lett* 12;297(2):121-4.
- [49] Grabiner MD, Sakai Y, Patterson TA, Wolfman A, Zborowski M, Midura RJ (2006) Distinct wave for characteristics of pulsed electromagnetic fields underline post-exposure changes in  $\alpha 1(1)$  collagen concentration in conditioned medium of mouse osteoblasts. *J Orthop Res* 24:242-53.
- [50] Pilla, A A, Figueiredo, M, Nasser PR, Kaufman JJ, Siffert, RS (1992) Pulse burst electric fields significantly accelerate bone repair in an animal model. In: *Engineering in Medicine and Biology Society, 14<sup>th</sup> Annual International Conference of the IEEE*.
- [51] Grote V, Lackner H, Kelz C, Trapp M, Aichinger F, Puff H, Moser M (2007) Short-term effects of pulsed electromagnetic fields after physical exercise are dependent on autonomic tone before exposure. *Eur J Appl Physiol* 101(4):495-502.
- [52] Mishima S. (1988) The effect of long-term pulsing electromagnetic field stimulation on experimental osteoporosis of rats. *Journal of UOEH* 10(1):31-45.
- [53] Capone F, Dileone M, Profice P, Pilato F, Musumeci G, Minicuci G, Ranieri F, Cadossi R, Setti S, Tonali PA, Di Lazzaro V (2009) Does exposure to extremely low frequency magnetic fields produce functional changes in human brain? *J Neural Transm.* 16(3):257-65.
- [54] Weintraub MI, Herrmann DN, Smith AG, Backonja MM, Cole SP (2009) Pulsed electromagnetic fields to reduce diabetic neuropathic pain and stimulate neuronal repair: a randomized controlled trial. *Arch Phys Med Rehabil* 90(7):1102-9.
- [55] Liburdy RP, Yost MG (1993) Time - varying and static magnetic fields acts in combination to alter calcium signal transduction in the Lymphocyte. In: Blank, M., ed. *Electricity and Magnetism in Biology and Medicine*. San Fransisco press, pp. 331-334.
- [56] Chang K, Chang WH, Wu M, Shih C (2003) Effects of different intensities of extremely low frequency pulsed electromagnetic fields on formation of osteoclast- like celled. *Bioelectromagnetics* 24:432-439.

- [57] Kirschvink JL (1992) Uniform magnetic fields and double-wrapped coil systems: Improved techniques for the design of bioelectromagnetic experiments. *Bioelectromagnetics* (13) 401-411.
- [58] Kaune WT (1979) Exposure Systems. In: *Biological Effects of High Strength Electric Fields in Small Laboratory Animals*. Report No. DOE/TIC-10084, NTIS, Springfield, VA 22161.
- [59] Bell GB, Marino AA (1989) Exposure system for production of uniform magnetic fields. *Journal of Bioelectricity* 8(2):147-158.
- [60] Müller CH, Schierz C, Krueger H (1999) Short Overview of EMF exposure systems and exposure system used in an ongoing study (Project NEMESIS, Non-ionising. *Electric and Magnetic fields and Electrical hypersensitivity Syndrome* In Switzerland). ETH-Zurich, Institute for Hygiene and Applied Physiology.
- [61] What is EMF? Accessed from <http://www.safespaceprotection.com/overview-electromagnetic-fields.aspx>.
- [62] Peter Stavroulakis (2003) *Biological Effects of Electromagnetic Fields*, 2003 Edition, Springer.
- [63] Durney C.H., Massoudi H. and Iskander M.F. (1986) Radiofrequency radiation dosimetry handbook. Salt Lake City, UT: University of Utah. Accessed from <http://www.brooks.af.mil/AFRL/HED/hedr/reports/handbook/home.html>.
- [64] Foster KR (2003) Mechanisms of interaction of extremely low frequency electric fields and biological systems. *Radiation Projection Dosimetry* 106(4):301-310.
- [65] Shahin A, Saeed RZ, Bahram B (2006) Effects of extremely-low-frequency pulsed electromagnetic fields on collagen synthesis in rat skin. *Biotechnol. Appl. Biochem* 43: 71–75.
- [66] Alvarez DC, Pérez VH, Justo OR, Alegre RM (2006) Effect of the extremely low frequency magnetic field on nisin production by *Lactococcus lactis* subsp. *lactis* using cheese whey permeate. *Process Biochemistry* 41:1967-1973.
- [67] Baureus KCLM, Sommarin M, Persson BRR, Salford LG, Eberhard JL(2003) Interaction between weak low frequency magnetic fields and cell membranes. *Bioelectromagnetics* 24:395–402.
- [68] Saeed N, Asghar T, Davoud K, Seyyed RM, Kaveh EP , Khorshid B (2012) Study the effects of high and low frequencies pulsed square electromagnetic fields on the logarithmic growth of the *e. coli*. *Bull. Environ. Pharmacol. Life Sci* 1(6):26-29.
- [69] Fojt L, Strasak L, Vetterl V, Smarda J (2004) Comparison of the low-frequency magnetic field effects on bacteria *Escherichia coli*, *Leclercia adecarboxylata* and *Staphylococcus aureus*. *Bioelectrochemistry* 63: 337-341.
- [70] Cvetkovic D, Cosic I (2007) Modelling and design of extremely low frequency uniform magnetic field exposure apparatus for in vivo bioelectromagnetic studies. *Proceedings of the 29th Annual International Conference of the IEEE EMBS*. IEEE, M. Akay, G. Delhomme, J. Rousseau, Piscataway, USA. 1675-1678.

- [71] Gholampour F, Javadifar TS, Owji SM, Bahaoddini A (2011) Prolonged Exposure to Extremely Low Frequency Electromagnetic Field Affects Endocrine Secretion and Structure of Pancreas in Rats . *International Journal of Zoological Research* 7(4):338–344.
- [72] Sakurai T, Yoshimoto M, Koyama S, Miyakoshi J (2008) Exposure to extremely low frequency magnetic fields affects insulin-secreting cells. *Bioelectromagnetics* 19(2):118-124.
- [73] Akpolat V, Celik MS, Celik Y, Akdeniz N, Ozerdem MS (2009) Treatment of osteoporosis by long-term magnetic field with extremely low frequency in rats. *Gynecol Endocrinol* 25(8): 524-529.
- [74] Salansky N, Fedotchev A, Bondor A (1998) Response of the nervous system to lw frequency stimulation and EEG rythms. *Clinical implications. Nuerosciences & Behavioral Review* 33(3): 395-409.
- [75] De Loof A (1986) The electrical dimensions of cells: the cell as miniature electrophoresis chamber. *Int Rev Cytol* 104:251-352.
- [76] Antov Y, Barbul A (2004) Electroendocytosis : stimulation of adsorptive and fluid-phase uptake by pulsed low electric fields. *Exp Cell Res* 297(2):348-62.
- [77] Smith DH, Wolf JA (2001) A new strategy to produce sustained growth of central nervous system axons: Continuous mechanical tension. *Tissue Engr* 7(2): 131-139.
- [78] Goodman EM, Henderson AS (1986) Some biological effects of electromagnetic fields. *Bioelectrochem Bioenrg* 15(1) 39-55.
- [79] Volpe P (2003) Interactions of zero-frequency and oscillating magnetic fields with biostructures and biosystems. *Photochem, Photobiol, Si* 2:637-648.
- [80] Kirschvink JL, Kobayashi-Kirschvink A, Diaz JC, Kirschvink JS (1992) Magnetite in Human Tissues: A Mechanism for the Biological Effects of Weak ELF Magnetic Fields. *Bioelectromagnetics Supplement 1* :101-113.
- [81] Sonier H, Marion AA (2001) Sensory transduction as a proposed model for biological detection of electromagnetic fields. *Electrom and Magnetobiology* 20(2):153-175.
- [82] Paulo SOR, Claudia MBP, Viviane DCR, Roberto RBTM, Melina DAM, Luiz CM, Iuri P, Paulo HPA, Stella MBM (2006) Evaluation of treatment with a pulsed electromagnetic field on wound healing and clinical pathologic variables of rats subjected to nicotine treatment. *Journal of Animal and Vitenary Advances* 5(8):615-622.
- [83] Bowler PG, Duerden BI, Armstrong DG (2001) Wound Microbiology and Associated Approaches to Wound Management. *Clin Microbiol Rev* 14(2):244-269.
- [84] Lee RC, Canady DL, Doong H (1993) A review of the biophysical basis for the clinical application of electric fields in soft-tissue repair. *J Burn Care Rehabil* 14:319-335.
- [85] Markov MS (2004a) Magnetic and electromagnetic field therapy: basic principles of application for pain relief. In Rosch PJ, Markov MS, eds. *Bioelectromag. Med.* New York : Marcel Dekker, 251-264.

- [86] Markov MS (2010) Expanding Use of Pulsed Electromagnetic Field Therapies. *Electromagnetic Biology & Medicine* 26(3): 257–274.
- [87] Harden N, Ramble T (2007) Prospective, randomized, single-blind, sham treatment controlled study of the safety and efficacy of an electromagnetic field device for the treatment of chronic low back pain: a pilot study. *Pain Practice* 7(3):248-255.
- [88] Aaron RK, Ciombor DMcK, Simon BJ (2004) Treatment of nonunions with electric and electromagnetic fields. *Clin Orthop* (4)19:21-29.
- [89] Akai M, Hayashi K (2002) Effect of electrical stimulation on musculoskeletal systems: a meta-analysis of controlled clinical trials. *Bioelectromagnetics* 23:132-143.
- [90] Salzberg CA, Cooper SA, Perez P, Viehbeck MG, Byrne DW (1995) The effects of non-thermal pulsed electromagnetic energy on wound healing of pressure ulcers in spinal cord-injured patients: a randomized, double-blind study. *Ostomy Wound Management* 41:42-51.
- [91] Aaron RK, Boyan BD, Ciombor D, Schwartz Z, Simon BJ (2004) Stimulation of growth factor synthesis by electric and electromagnetic fields. *Clin Orthop* 419:30-37.
- [92] Stadelmann WK, Digenis AG, Tobin GR (1998) Impediments to wound healing. *Am J Surg* 176:39S–47S.
- [93] Murray JC, Farndale RW (1985) Modulation of collagen production in cultured fibroblasts by a low frequency pulsed magnetic fields. *Biochim Biophys Acta* 838:95–105.
- [94] Johnson DJ, Hentz VR (1987) Electromagnetic field enhancement of rat wound tensile strength and pedicle skin flap survival. *Trans BRAGS* 7:78–83.
- [95] Katsir G, Baram SC, Parola AH (1998) Effect of sinusoidally varying magnetic fields on cell proliferation and adenosine deaminase specific activity. *Bioelectromagnetics* 19:46–52.
- [96] Sermov D, Karba R, Valencic V (1997) DC electrical stimulation for chronic wound healing enhancement. *Bioelectrochem Bioenerg* 43:271–277.
- [97] Strauch B, Patel MK, Rosen DJ, Mahadevia S, Brindzei N, Pilla AA (2006) Pulsed magnetic field therapy increases tensile strength in a rat Achilles' tendon repair model. *J Hand Surg* 31(7):1131–1135.
- [98] Strauch B, Patel MK, Navarro A, Berdishevsky M, Pilla AA (2007) Pulsed magnetic fields accelerate wound repair in a cutaneous wound model in the rat. *Plast Reconstr Surg* 120:425-430.
- [99] Yen-Patton GPA, Patton WF, Deer DM, Jacobson BS (1988) Endothelial cell response o pulsed electromagnetic fields: stimulation of growth rate and angiogenesis *in vitro*. *J Cell Physiol* 134:37-46.
- [100] Lundeberg TCM, Eriksson CV, Malm M (1992) Electrical nerve stimulation improves healing of diabetic ulcers. *Ann Plast Surg* 29:328–331.



- [101] Tepper OM, Callaghan MJ, Chang EI, Galiano RD, Bhatt KA, Baharestani S, Gan J, Simon B, Hopper RA, Levine JP, Gurtner GC (2004). Electromagnetic fields increase in vitro and in vivo angiogenesis through endothelial release of FGF-2. *Faseb J* 18(11):1231–1233.
- [102] Callaghan MJ, Chang EI, Seiser N, Aarabi S, Ghali S, Kinnucan ER, Simon BJ, Gurtner GC (2008) Pulsed electromagnetic fields accelerate normal and diabetic wound healing by increasing endogenous FGF-2 release. *Plast Reconstr Surg* 121(1):130–141.
- [103] Bush K, Courvalin P, Dantas G (2011). Tackling antibiotic resistance. *Nature Reviews Microbiology* 9 (12): 894-896.
- [104] El-Sayed AG, Magda SH, Eman YT, Mona HI (2006) Stimulation and control of *E. Coli* by using an extremely low frequency magnetic field. *Romanina J Biophysc* 16(4): 283-296.
- [105] Segatore B, Setacci D, Bennato F, Cardigno R, Amicosante G, Iorio R (2012) Evaluations of the effect of extremely low-frequency electromagnetic fields on growth and antibiotic susceptibility of *Escherichia coli* and *Pseudomonas aeruginosa*. *International Journal of Microbiology* Article ID 587293.
- [106] Strašák L, Vetterl V, Fojt L (2005) Effects of 50 Hz magnetic fields on the viability of different bacterial strains. *Electromagnetic Biology and Medicine* 24(3): 293-300.
- [107] Fojt L, Strašák L, Klapetek P, Vetterl V (2009) 50 Hz magnetic field effect on the morphology of bacteria. *Micron* 40(8): 918-922.
- [108] Nascimento F, Botura GJ, Mota RP (2003) Glucose consume and growth of *E.coli* under electromagnetic field. *Rev. Inst. Med. Trop* 45(2): 65-67.
- [109] Babushkina IV, Borodulin NA, Shmetkova NA et al: The influence of alternating magnetic field on *Escherichia coli* bacteria cells. *Pharmaceutical Chemistry Journal* 2005 39(8):398-400.
- [110] Gaafar ESA, Hanafy MS, Tohamy ET, Ibrahim MH (2008). The effect of electromagnetic field on protein molecular structure of *E coli* and its pathogenesis. *Romanian Journal of Biophysics* 18(2):145-169.
- [111] Cellini L, Grande R, Di Campli E (2008). Bacterial response to exposure of 50Hz electromagnetic fields. *Bioelectromagnetics* 29(4): 302-311.
- [112] Ieran M, Zaffuto S (1990) Effect of low frequency electromagnetic fields on skin ulcers of venous origin in humans: a double blind study. *J. Orthop. Res* 8:276-282.
- [113] Seaborne D, Quirion DG, Rousseau CM (1996) The treatment of pressure sores using pulsed electromagnetic energy (PEME). *Physiotherapy Canada* 48:131-137.
- [114] Pilla AA (2006) Mechanisms and therapeutic applications of time-varying and static magnetic fields. In: Barnes, F., Greenebaum, B., edss. *Handbook of Biological Effects of Electromagnetic Fields* 3<sup>rd</sup> ed. Boca Raton, FL: CRC Press.
- [115] Bental RHC (1986) low-level pulsed radiofrequency fields and the treatment of soft tissue injuries. *Bioelectrochem Bioenerg* 16:531-548.

- [116] Stiller MJ, Pak GH, Shupak JL, Thaler S, Kenny C, Jondreau L (2006) A portable pulsed electromagnetic field (PEMF) device to enhance healing of recalcitrant venous ulcers: a double-blind, placebo-controlled clinical trials. *British Journal of Dermatology* 127(2):147-154.
- [117] Vianale G (2008) Extremely low frequency electromagnetic field enhances human keratinocyte cell growth and decreases proinflammatory chemokine production. *British Journal of Dermatology* 158(6):1189-1198.
- [118] Elena Pirogova, Vuk Vojisavljevic and Irena Cosic (2009) Biological Effects of Electromagnetic Radiation, *Biomedical Engineering*, Carlos Alexandre Barros de Mello (Ed.), ISBN: 978-953-307-013-1.
- [119] Vojisavljevic V, Pirogova P, Cosic I (2007) The effect of electromagnetic radiation (550nm-850nm) on 1-Lactate Dehydrogenase Kinetics. *Int Journal of Radiation Biology* 83(4):221-230.
- [120] Breckenamp J, Berg G, Blettner M (2003) Biological effects of human healths due to radiofrequency/microwave exposure : a synopsis of cohort studies. *Radiat Environ Biophys* 42:141-154.
- [121] APRANSA Australia Radiation Protection and Nuclear Safety Agency (2008) Maximum exposure level to radiofrequency fields – 3Khz-300GHz, *Annex 3: Epidemiological studies of exposures to radiofrequencies and human health*.
- [122] Ahmed I, Vojisavljevic V and Pirogova E (2012) The effect of Extremely Low Frequency (ELF) Pulsed Electromagnetic Field (PEMF) on Collagenase Enzyme Kinetics, *MD- Medical Data*, Belgrade, Serbia, Mostart d.o.o, Peter Spasis; 4(4):357-362.
- [123] Ahmed I, Vojisavljevic V and Pirogova E (2013) Investigation of the effect of Extremely Low Frequency (ELF) Pulsed Electromagnetic Field (PEMF) on Collagenase Enzyme Kinetics. In *BIODEVICES 2013 the Proceedings of the 6<sup>th</sup> International Joint Conference on Biomedical Engineering Systems and Technologies*. Lisbon, Portugal, INSTICC: Mireya Fernandez; 143-147.
- [124] Pavicic I, Trosic I (2008) Impact of 864 MHz or 935 MHz radiofrequency microwave radiaton on the basic growth parameters of V79 cell line. *Acta Biol Hung* 59(1): 67-76.
- [125] Pinnequin A, Piriou A, Mathieu J, Dabouis V, Sebbah C, Malabiau R, Debouzy JC (2000) Non-thermal effects of continuous 2.45GHz microwave on Fas-induce apoptosis in human Jurkat T-cell line. *Biochemistry* 51:157-161.
- [126] Bassett CAL (1993) Beneficial effects of electromagnetic fields. *J Cell Biochem* 51:387-393.
- [127] Binder A, Parr G, Hazleman B (1984) Pulsed electromagnetic field therapy on persistent rotator cuff tendinitis. *Lancet* 1:695-698.
- [128] Auer JA, Burch GE, Hall P (1983) Review of pulsing electromagnetic field therapy and its possible application to horses. *Equine Vet J* 15:354-360.

- [129] Scardino MS, Swaim SF, Sartin EA (1998) Evaluation of treatment with a pulsed electromagnetic field on wound healing, clinicopathologic variables, and central nervous system activity in dogs. *AmJ Vet Res* 59:1177-1181.
- [130] Ellis WV (1993) Pain control using high-intensity pulsed magnetic stimulation. *Bioelectromagnetics* 14:553-556.
- [131] Kalaivani G, Akelayil CG, Chidambaram B, Bhakthavatsalam MM, Rengalajulu P (2009) Low frequency pulsed electromagnetic field- a viable alternative therapy for arthritis. *Indian Journal of Experiment Biology* 47:939-948.
- [132] M. S. Markov (2007) Pulsed electromagnetic field therapy history, state of the art and future. *Environmentalist* 27:465-475.
- [133] On PEMF treatment. Accessed from <http://www.pemfinfo.com/index.php/general-links>.
- [134] Markov MS (2000) Magnetic and electromagnetic fields- a new frontier in clinical biology and medicine. *Proceedings of the Millennium International Workshop on Biological Effects in Biology and Medicine* ISBN 960-86733-0-5 363-372.
- [135] Salzberg CA, Cooper-Vastola SA, Perez F, Viehbeck MG, Byrne DW. The effects of nonthermal pulsed electromagnetic energy on wound healing of pressure ulcers in spinal cord-injured patients: a randomized, double-blind study. *Ostomy Wound Manage* 41:42-446.
- [136] Anupam G, Arun BT, Abhishek S, Sendhil K, Murali T (2009) Efficacy of pulsed electromagnetic field therapy in healing of pressure ulcers: a randomized control trial. *Neurology India* 57(5):622-626.
- [137] Haines WJ, Baker LL (1987) Pulse electro-magnetic field therapy device with auto bias circuit. *US Patent*, Patent No. 4674482.
- [138] Griffith N (1991) Portable electro-therapy system. *US Patent* 4998532.
- [139] Stiller MJ, Grace HPAK, Shupack JL, Thaler S, Kenny C, Jondreau L (1994) A portable pulsed electromagnetic field (PEMF) device to enhance healing of recalcitrant venous ulcers: a double-blind study, placebo- controlled clinical trial. *British Journal of Dermatology* 127:147-154.
- [140] Ostrow AS, Grinshpon G (1994) Magnetotherapy apparatus. *US Patent* No. 5344384.
- [141] Tepper JC, Richardson PK, Kuo P, Winstrom W (2001) Flexible coils pulsed electromagnetic field (PEMF) stimulation therapy system. *US Patent* No. 6261221 B1.
- [142] Bassett CA (1989) Fundamental and practical aspects of therapeutic use of pulsed electromagnetic fields (PEMFs). *Critical Reviews in Biomedical Engineering* 17 (5): 451-529.
- [143] Markkov MS, Todorov NG (1984) Electromagnetic field stimulation of some physiological process. *Studia Biophysica* 99:155-156.
- [144] McLeod KJ, Rubin CT (1991) Method and apparatus for inducing a current and voltage in living tissues. *US Patent* No. 4993413.

- [145] Raganella L, Guelfi M, D'Inezo G (1994) Triaxial exposure system providing static and low-frequency magnetic fields for in vivo and in vitro biological studies. *Bioelectrochemistry and Bioenergetics* 35:121-126.
- [146] Wilson BW, Caputa K, Stuchly MA, Saffer JD, Davis KC, Washam CE, Washam LG, Washam GR, Wilson M (1994) Design and fabrication of well confined uniform magnetic field exposure systems. *Bioelectromagnetics* 15:563-577.
- [147] Ahmed I, Istivan T, Cosic I, Pirogova E (2013) Evaluation of the effects of Extremely Low Frequency (ELF) Pulsed Electromagnetic Fields (PEMF) on survival of the bacterium *Staphylococcus aureus*. *EPJ Nonlinear Biomedical Physics*. Heidelberg, Germany, Springer; doi:10.1140/epjnbp12, (1):5.
- [148] Tepper JC, Kup P, Emge TM, Winstrom WL (1998) High efficiency pulsed electromagnetic field (PEMF) stimulation therapy method and system. *US Patent* No. 5743844.
- [149] Strauch B M, Charles H, Richard D, Louis JI, Pilla AA (2009) Evidence-Based Use of Pulsed Electromagnetic Field Therapy in Clinical Plastic Surgery. *Aesthetic Surg J* 29:135-143.
- [150] Blackwell LL (2001) Magnetic coils for pulsed electromagnetic fields. *US Patent* No. 6186941 B1.
- [151] Ahmed I, Istivan T, Pirogova E (2013) The effect of Extremely Low frequency (ELF) Pulsed Electromagnetic Field (PEMF) on Bacteria *Staphylococcus Aureus*, *In the Proceedings of Progress in Electromagnetic Research Symposium (PIERS 2013 in Taipei proceedings)*. Massachusetts, USA, The Electromagnetic Academy 388-391.
- [152] Helmholtz Coil. Accessed from [http://en.wikipedia.org/wiki/Helmholtz\\_coil](http://en.wikipedia.org/wiki/Helmholtz_coil).
- [153] Gottardi G, Mesirca P, Agostini C, Remondini D, Bersani F (2003) A four coil exposure system (Tetracoil) producing a highly uniform magnetic field. *Bioelectromagnetics* 24:125-133.
- [154] Yamazaki K, Fujinami H, Shigemitsu T, Nishimura I (2000) Low stray ELF magnetic fields exposure system for *in vitro* studies. *Bioelectromagnetics* 21:75-83.
- [155] Bellossi A, Desplaces A (1991) Effect of a 9 mT Pulsed Magnetic Field on C3H/Bi Female Mice with Mammary Carcinoma: A comparison between the 12 Hz and the 460 Hz Frequencies, *In Vivo* 5: 39-40.
- [156] Williams CD, Markov MS, Hardman WE, Cameron IL (2001) Therapeutic Electromagnetic Field Effects on Angiogenesis and Tumor Growth. *Anticancer Research* 21, 6A, 3887-3891.
- [157] Seze RD, Tuffet S, Moreau JM, Veyret B (2000) Effects of 100mT Time Varying Magnetic Fields on the Growth of Tumors in Mice. *Bioelectromagnetics* 21: 107-111.
- [158] Omote y, Hosokawa M, Komatsumoto M, Namieno T, Nakajima S, Kubo Y, Kobayashi H (1990) Treatment of Experimental Tumors with a Combination of a Pulsing Magnetic Field and an Antitumor Drug. *Japanese Journal of Cancer Research* 81: 956-961.

- [159] Ottani V, De Pasquale V, Govoni P, Franchi M, Zaniol P, Ruggeri A (1988) Effects of pulsed extremely-low-frequency magnetic fields on skin wounds in the rats. *Bioelectromagnetics* 9(1):53-62.
- [160] McGrath MH, Glassman LS, Bassett CAL (1983) Effect of external pulsing electromagnetic fields on the healing of soft tissues. *Surg Forum* 34:615.
- [161] McLeod BR, Pilla AA, Sampsel MW (1983) Electromagnetic fields induced by Helmholtz aiding coils inside saline-filled boundaries. *Bioelectromagnetics* 4(4):357-370.
- [162] Pawel N, Karol F, Magdalena S, Marian K, Rafal R (2013) Effects of 50Hz rotating magnetic fields on the viability of escherichia coli and staphylococcus aureus. *Electromagnetic Biology and Medicine*. Early Online DOI: 10.3109/15368378.2013.783848.
- [163] Juutilaine J, Harri M, Saali K, Lahtinen T (1986) Effects of 100-Hz magnetic fields with various waveforms on the development of chick embryos. *Radiat Environ Biophys* 25:65-74.
- [164] Jing D, Shen G, Huang J, Xie K, Cai J, Xu Q (2009) Circadian rhythm affects the preventive role of pulsed electromagnetic fields on ovariectomy-induced osteoporosis in rats. *Bone* 46:487-495.
- [165] Yu L, Luo E, Han L (2004) Preventive effect of low intensity pulse electromagnetic fields in osteoporosis of ovariectomized rats. *Chin J Clin Rehabil* 8:3590-3591.
- [166] Li C, Liu Z, Zhang R, Luo E, Shen G, Liu L (2008) Therapeutic effect of pulsed electromagnetic field on postmenopausal osteoporosis. *Chin J Osteoporosis* 14:52-54.
- [167] Luo E, Shen G, Xie K, Wu X, Xu Q, Lu L (2007) Alimentary hyperlipemia of rabbits is affected by exposure to low-intensity pulsed magnetic fields. *Bioelectromagnetics* 28: 608-614.
- [168] Jahns M, Durdle N, Lou E, Rason VJ (2006) A programmable ramp waveform generator for PEMF exposure studies on Chondrocytes. *Proceedings of the 28<sup>th</sup> IEEE EMBS Annual International Conference* FrC08.2:3230-3233.
- [169] Marron TT, Goodman EM, Sharpe PT, Greenbaum B (1988) low frequency electric and magnetic fields have different effects on the cell surface. *Fed. European Biochem. Soc.* 230:13-16.
- [170] Thomson RAE, Michaelson SM, Nguyen QA (1988) influence of 60-Hertz magnetic fields on leukemia. *Bioelectromagnetics* 9:149-158.
- [171] Alldred JC, Scollar I (1967) Square cross section coils for the production of uniform magnetic fields. *J Sci Instrum* 44:755-760.
- [172] Merritt R, Purcell C, Stoink C (1983) Uniform magnetic field produced by three, four, and five square coils. *Rev.Sci. Instrum.* 54:879-882.
- [173] Shigemitsu T, Takeshita K, Shiga Y, Kato M (1993) 50-Hz magnetic field exposure system for small animals. *Bioelectromagnetics* 14:107-116.

- [174] Magdaleno-Adame S, Olivares-Galvan JC, Campero-Littlewood E, Escarela-Perez R, Blanco-Brisset E (2010) Coil system to generate uniform magnetic field volumes. Excerpt from the *proceedings of the COMSOL conference*, COSMOL, Inc, Lindsay Paterson, Massachusetts, USA 13:401-411.
- [175] Tepper JC, Richardson PK, Kuo P, Winstrom W (2000) Pulse electromagnetic field (PEMF) stimulation therapy with bi-phasic coils. *US Patent* No. 6132362.
- [176] Kairu PE, Maria AS (1992) Neural stimulation with magnetic fields: analysis of induced electric fields. *IEEE Trans Biomed Eng* 39:693.
- [177] Cohen CH, Roth BI, Nilson J, Dang N, Panizza M, Bandirelli S, Friauf W (1990) Effects of coil design on delivery of focal magnetic stimulation , Technical consideration. *Electroencephalograph Clin Neurophys* 75:350.
- [178] Lee-Whiting GE (1957) Uniform magnetic fields. Atomic energy of Canada Limited Chalk River Project, *Report CRT-673*, Chalk River, Ontario.
- [179] Sisken BF, Kanje M, Lundborg G, Herbst E, Kurtz W (1989) Stimulation of rat sciatic nerve regeneration with pulsed electromagnetic fields. *Brain Research* 485(2):309-316.
- [180] Cakirgil GS, Saplakoglu A, Yazar T (1989) The compared effect of a four-coiled system in pulsed EMF stimulation. *Orthopedics* 12(11):1481-1484.
- [181] Everett JE, Osemikhian JE (1966) Spherical coils for uniform magnetic fields. *Rev Sci Instrum* 43:470-474.
- [182] Caputta K, Stuchly MA (1998) Computer controlled system for producing uniform magnetic fields and its applications in biomedical research. *IEEE Transaction on instrumentation and Meseasurement* 45(3):701-709.
- [183] Hodgkinson GG (2001) Pulsed electromagnetic field effects on osteoblast-like cell cultures. *School of Mechanical, Manufacturing and school of Engineering*. Brisbane, Queensland University of Technology : 85.
- [184] Cadossi R, Marazzi D (1987) Method and device for treating living tissues and/or cells by means of pulsating electromagnetic fields. *US Patentn* No. 4683873.
- [185] Franzen W (1962) Generation of uniform magnetic fields by means of air-core coil. *Review of Scientific Instruments* 33(9): 933-938.
- [186] Azpurna MA (2012) A semi-analytical method for the design of coil-systems for homogeneous magnetostatic field generation. *Progress in Electromagnetic Research* 37:171-189.
- [187] Peter A. Valberg (1995) Designing EMF Experiments: What is Required to Characterize “Exposure”?. *Gradient Corporation*, Cambridge, Massachusetts, and Department of Environmental Health, Harvard School of Public Health, Boston.
- [188] M. Misakian (1984) *Topic 4: Exposure Systems (Synopsis)*, National Institute of Standards and Technology, Gaithersburg, MD. Accessed from <ftp://ftp.emf-data.org/pub/emf-data/symposium98/topic-04-synopsis.pdf>.

- [189] Nu –Magnetics Inc (2009) Pulsed and AC Electromagnetic Fields Vs. Dynamic DC Magnetic Fields.
- [190] De Mattei M, Caruso A, Pazzetti F, Pellati A, Stabellini G, Sollazzo V, Triana GC (2001) Effects of pulsed electromagnetic fields on human chondrocyte proliferation. *Connect Tissue Res* 42:269.
- [191] McKay JC, Corbacio M, Tyml K, Prato FS, Thomas AW (2010). Extremely low frequency pulsed electromagnetic field designed for Antinociception does not affect microvascular responsiveness to the Vasodilator Acetylcholine. *Bioelectromagnetic* 31:64-76.
- [192] Adair K (1994) Constraints of thermal noise on the effects of weak 60-Hz magnetic fields acting on biological magnetite. *Proc. Natl. Acad. Sci.* 91:2925-2929.
- [193] Meyrath, T (2004) Electromagnet design basics for cold atom experiments," University of Texas, Austin. Accessed from <http://www.george.ph.utexas.edu/meyrath/informal>.
- [194] Cadossi B, Bersani F, Cossarizza A, Zucchini P, Emilia G, Torelli G, Franceschi C (1992) Lymphocytes and low-frequency electromagnetic fields. *The FASEB J* 6:2667.
- [195] Tenforde, T. S. (1995) in Handbook of Biological Effects of Electromagnetic Fields, 2nd edn Polk, C. and Postow, E., eds., CRC Press, Boca Raton, FL, 185-230.
- [196] Manni, V., Lisi, A., Pozzi, D., Rieti, S., Serafino, A., Giuliani, L. and Grimaldi, S. (2002) Effects of extremely low frequency (50 Hz) magnetic field on morphological and biochemical properties of human keratinocytes. *Bioelectromagnetics* 23: 298–305.
- [197] Nelson FRT, Bighton CT, Ryaby J, Simon BJ, Nielson JH, Lorich DJ, Bolander M, Seelig J (2003) Use of physical forces in bone healing. *Journal of the American Academy of Orthopaedic Surgeons* 11:344-354.
- [198] Markov MS (2004c) Myosin phosphorylation – a plausible tool for studying biological windows. Ross Adey memorial lecture. In: Kostarikas, P., ed. *Proceedings of Third International Workshop on Biological Effects of EMF* 4(8):1-9.
- [199] Adey WR (1993) Biological Effects of Electromagnetic Fields. *Journal of Cellular Biochemistry* 51:410-416.
- [200] Markov MS (2005) “Biological Windows: A tribute to W. Ross Adey. *Environmentalist* 25: 67-74.
- [201] Renzo C, Francesco D (2012) Possible non-thermal microwave effects on the growth rate of *pseudomonas aeruginosa* and *staphylococcus aureus*. *International Review of Chemical Engineering (I. RE. CH. E)* 4(4): 392-398.
- [202] PE 200 Coils. Accessed from <http://www.med-phoenix.com/products/pe200-coils>.
- [203] SomaPulse P2- The sports car of PEMF (by ElectroM3ds). Accessed from <http://electromeds.com/2492/somapulse-p2-the-sportscar-of-pemf>.
- [204] Portable PEMF device. Accessed from <http://www.drtraviselliott.com/services-pulsed-magnetic-field-therapy.htm>.

- [205] Pulsed electromagnetic force therapy (PEMF therapy applied to the shoulder). Accessed from <http://www.biltmoreparkchiropractic.com/pulsed-electromagnetic-force-therapy>.
- [206] Pulsatron- Novas Pharma, Chennai, India, Information on PEMF therapy and the benefits. Accessed from <http://pulsatron-novuspharma.blogspot.com.au>.
- [207] Leman ES, Siskin BF, Zimmer S, Anderson KW (2001) Studies of the interactions between melatonin and 2 Hz, 0.3 mT PEMF on the proliferation and invasion of human breast cancer cells. *Bioelectromagnetics* 22(3):178-84.
- [208] Verginadis, A. Velalopoulou, I. Karagounis, Y. Simos, D. Peschos, S. Karkabounas and A. Evangelou (2012) Beneficial Effects of Electromagnetic Radiation in Cancer, Electromagnetic Radiation, Prof. S. O. Bashir (Ed.), ISBN: 978-953-51-0639-5.
- [209] Christina V, Jurg F (2010) Novel in vitro PEMF exposure system for a large number of cell dishes. In: *6th International Workshop on Biological Effects of Electromagnetic Fields* doi: Accessed from <http://dx.doi.org/10.3929/ethz-a-006256557>.
- [210] One-Axis Helmholtz coil. Accessed from <http://www.indiamart.com/ets-lie-pvtltd/products.html>.
- [211] ICNIRP (1998) Guidelines for limiting exposure to time varying electric, magnetic and electromagnetic fields (up to 300 GHz), *Health Physics* 74:494-522.
- [212] McManus J (2007) Principles of skin and wound care: the palliative approach. Clinical Skills, End of Life Care 1:1.
- [213] Falanga V (2002) Wound bed preparation and the role of enzymes: a case for multiple actions of therapeutic agents. *Wounds* 14(2):47-57.
- [214] Wound Care Centres. Accessed from <http://www.woundcarecenters.org/wound-basics/acute-wound-basics.html>.
- [215] Amputation. Accessed from <https://en.wikipedia.org/wiki/Amputation>.
- [216] Diegelmann RF, Evans MC (2004) Wound healing: an overview of acute, fibrotic and delayed healing. *Frontiers in Biosciences* 9:283-289.
- [217] Singer AJ, Richard AF, Clark MD (1999) Cutaneous wound healing. *The New England Journal of Medicine* 341(10):738-746.
- [218] Blakemore C, Jennett S (2001) Wound Healing. *The Oxford Companion to the Body*. Accessed from <http://www.encyclopedia.com/doc/1O128-woundhealing.html>.
- [219] Cutting KF (1994) Criteria for identifying wound infection. *Journal of Wound Care* 3(4):198-201.
- [220] Granulation tissue. Accessed from [http://en.wikipedia.org/wiki/Granulation\\_tissue](http://en.wikipedia.org/wiki/Granulation_tissue).



- [221] Howard GW, John JJ, George PS, William TR, Arthur AE (1980) Characteristics of the action of human skin fibroblast Collagenase on fibrillar Collagen. *The Journal of Biological Chemistry* 255(14):6806-6813.
- [222] Hunt TK, Knighton DR, Thakral KK, Goodson WH, Andrews WS (1984) Studies on inflammation and wound healing: angiogenesis and collagen synthesis stimulated in vivo by resident and activated wound macrophages. *Surgery* 96:48.
- [223] Matthew FP, Alvin CL, Goh MC (2002) real-time enzymatic biodegradation of collagen fibrils monitored by atomic force microscopy. *International Biodeterioration & Biodegradation* 50:1-10.
- [224] David LS (1997) The role of growth factors in wound healing. *Surgical Clinics of North America* 77(3):575-586.
- [225] Wolfgang F (1998) Collagen- biomaterial for drug delivery. *European Journal of Pharmaceutics and Biopharmaceutics* 45:113-136.
- [226] Lei S, Ryan E, Anastacia g, Dale T, Duncan A (2010) Degradation of human collagen isoforms by *Clostridium* collagenase and the effects of degradation products on cell migration. *International Wound Journal* 7(2):87-95.
- [227] Jung W, Winter H (1998) Considerations for the use of Clostridial Collagenase in Clinical Practice. *Clin. Drug Invest* 15(3):245-252.
- [228] Kathleen NR, Ira MH (2005) Collagenase promotes the cellular responses to injury and wound healing In Vivo. *Journal of Burns and Wounds* 4:112-124.
- [229] French MF, Bhowan A, Van WHE (1992) Limited proteolysis of types I, II and III collagens at hyperactive site by *Clostridium histolyticum* collagenase. *Matrix Suppl* 1:134-135.
- [230] Krane SM (1982) Collagenases and collagen degradation. *J Invest Dermatol* 79: 83–86.
- [231] Anna FF (2006) Debridement and wound bed preparation. *Dermatologic Therapy* 19: 317–325.
- [232] Alvarez OM, Fernandez-Obregon A, Rogers RS (2000) Chemical debridement of pressure ulcers: A prospective, randomized, comparative trial of collagenase and papain/urea formulations. *WOUNDS* 12:15–25.
- [233] Janet R, Mikel G (2008) Enzymatic wound debridement. *J Wound Continence Nurs* 35(3):273-280.
- [234] Jan CR (2012) Conservative sharp wound debridement- state of play in Australia. *EWMA Journal* 12(3):33-38.
- [235] Hellgren L, Vincent J (1993) Debridement: an essential step in wound healing. In: Westerhof W, ed. *Leg ulcers: diagnosis and treatment*. Amsterdam: Elsevier Science Publishers, 305–312.

- [236] Donati L, Magliano E, Colonna M (1994) Surgical versus enzymatic debridement. In: Westerhof W, Vanscheidt W, eds. *Proteolytic enzymes and wound healing*. New York: Springer-Verlag, 38–39.
- [237] Berger MM (1993) Enzyme debriding preparations. *Ostomy Wound Manage* 39: 61–62.
- [238] Wollina U, Liebold K, Schmidt WD (2002) Biosurgery supports granulation and debridement in chronic wounds – clinical data and remittance spectroscopy measurement. *Int J Dermatol* 41: 635–639.
- [239] Westerhof W (1994) Future prospects of proteolytic enzymes and wound healing. In: Westerhof W, Vanscheidt W (eds). *Proteolytic Enzymes and Wound Healing*. New York, NY: Springer-Verlag and Co 99–102.
- [240] Medical Microbiology, bacterial morphology, Bacterial structures, Cytoplasmic structures. Accessed from <http://micro.digitalproteus.com/morphology2.php>.
- [241] Williams DT, Hilton JR, Harding KG (2004) Diagnosing foot infection in Diabetese. *Defining and Diagnosing Infection* 39:S83-s86.
- [242] Ayton M (1985) Wounds that won't heal. *Nurs Times* 81:16-19.
- [243] Kingsley AA (2001) A proactive approaches to wound infection. *Nurs Stand* 15:50-58.
- [244] Ernst JD, Stendahl O (2006). Phagocytosis of Bacteria and Bacterial Pathogenicity. New York: Cambridge University Press. ISBN 0-521-84569-6 .
- [245] Microbiology Ch15 Microbial Mechanisms of Pathogenicity. Available at URL <http://www.cram.com/cards/microbiology-ch15-microbial-mechanisms-of-pathogenicity-896684>.
- [246] Sansonetti P (2001) Phagocytosis of bacterial pathogens: implications in the host response. *Semin. Immunol* 13 (6): 381–90.
- [247] Watsuki K, Yamasaki O, Morizane S, Oono T (2006). Staphylococcal cutaneous infections: invasion, evasion and aggression. *J Dermatol Sci* 42(3): 203-212.
- [248] Pilar HS (2004) Responsible use of antibiotics in aquaculture. *FAO Fisheries Technical Paper* 469.
- [249] Rajaraman D, philips CH (2010) Surgical vacuum diseases: types, uses and complications. *AORN Journal* 91(2):266-274.
- [250] David MB, Sarah EB (2005) Management of *Staphylococcus aureus* infections. *Am Fam Physician* 15(72):2474-2481.
- [251] Kallen A, Mu Y, Bulens S, Reingold A, Petit S, Gershman K (2010) Healthcare-Associated Invasive MRSA Infections. *JAMA* 304(6):641-648.
- [252] Dermatologist Mainfestations. HIV Web study, Case based modules. Accessed from <http://depts.washington.edu/hiv aids/derm/case6>.

- [253] Corey GR (2009) Staphylococcus aureus bloodstreams infections: definitions and treatments. *Infectious Diseases Society of America* 48: S254-259.
- [254] Fluit AC, Jones ME, Schmitz FJ, Acar J, Gupta R, Verhoef J (2000) Anti- microbial susceptibility and frequency of occurrence of clinical blood isolates in Europe from the SENTRY Antimicrobial Surveillance Pro- gram, 1997 and 1998. *Clin Infect Dis* 30:454–60.
- [255] Spices for life. Accessed from <http://www.spicesforlifemd.com/diabetes>.
- [256] Collignon P (2009) Resistant *Escherichia coli*— We Are What We Eat. *Clinical Infectious Diseases* 49(2):202-204.
- [257] Hu P, Janga SC, Babu M, Díaz-Mejía JJ, Butland G (2009) Global Functional Atlas of *Escherichia coli* Encompassing Previously Uncharacterized Proteins. *PLoS Biol* 7(4): e1000096. doi:10.1371/journal.pbio.1000096.
- [258] James RJ, Abby G, Alan JL, Thomas AR (2003) Extraintestinal pathogenic *Escherichia coli* as a cause of invasive nonurinary infections. *Clin Microbiol* 41(12):5798-5802.
- [259] Sato S, Sakaguichi K, Futamata K, Katao K (2000) Coil optimization for homogeneous magnetic field with small leakage field. *IEEE Transactions on Magnetics* 36(4):649-653.
- [260] Ahmed I, Vojisavljevic V, Pirogova E (2012) Design and development of extremely low frequency (ELF) pulsed electromagnetic Field (PEMF) system for wound healing promotion. *IFMBE Proceedings World Congress on Medical Physics and Biomedical Engineering*. Heidelberg, Germany, Springer: Mian Long (3): 27-30.
- [261] Quantum Northwest Inc. Temperature contriller cuvette holder. Accessed from, [http://www.qnw.com/products/prod\\_cd\\_250.php](http://www.qnw.com/products/prod_cd_250.php).
- [262] Zakinyan A, Nechaeva O, Dikansky Yu (2012) Motion of a deformabel drop of magnetic fluid on a solid surface in a rotating magnetic field. *Experimental Thermal and Fluid Sciences* 39:265-268.
- [263] Narda Safety Test Solutions GmbH, EFA-200/300 EM Field Analyzer operating manual (2006). Accessed from <http://www.narda-sts.de/about-narda/narda-safety-test-solutions.html>.
- [264] Miodrag M, Nikola D, Dragisa M (2013) Utilization of the EFA-300 for continuous monitoring in semont information network. The 6<sup>th</sup> PSU-UNS International Conference on engineering Technology (ICET) T.12-4.2:1-4.
- [265] Seze RD, Lahitte A, Moreau JM, Veyret B (1994) Generation of extremely-low frequency magnetic fields with standard available commercial equipments implications for experimental bioelectromagnetic work. *Bioelectrochemistry and Bioelectromagnetics* 35:127-131.
- [266] Alberto RM (2011) Measuring the orthogonality in Helmholtz coils. NAS003-i.doc Accessed from <http://www.serviciencia.es/not-apli/NAS03-i.pdf>.
- [267] Bisswanger H (2002) Enzyme Kinetics: Principles and methods, Willey-VCH.

- [268] Bacterial growth, Background, growth measurements. Accessed from <http://www.bowdoin.edu/biology/grants/spec/pdf/bacteria-growth.pdf>.
- [269] Friedrich W (2007) Theory and measurement of bacterial growth. Online Microbiology Notes from University of Bremen, Germany. Accessed from <http://www.mpi-bremen.de/Binaries/Binary13037/Wachstumsversuch.pdf>
- [270] Helena TH, Renata S, Tomas H, Ludmila T, Bozena C, Reja LZ, Hana K (2004) Commensal bacteria (normal microflora), mucosal and chronic inflammatory and autoimmune diseases. *Immunology Letters* 2(3): 97-108.
- [271] Ayse IG, Burak A, Zafer A, Dilek A, Ozaydin AN, Tangu S (2011) Effect of extremely low frequency electromagnetic fields on growth rate and morphology of bacteria. *International Journal of Radiation Biology* 87(12): 1155-1161.
- [272] Binhi VN, Savin AV (2002) Molecular gyroscopes and biological effects of weak extremely-low frequency magnetic fields. *Phys Rev E Stat Nonlinear Soft Matter Phys* 65: (5 Pt 1):051912.
- [273] Fojt L, Strasak L, Vetterl V (2010) Extremely-low frequency magnetic field effects on sulfatereducing bacteria viability. *Electromagnetic Biology and Medicine* 29:177-185.
- [274] Fojt L, Strasak L, Vetterl V (2007) Effect of electromagnetic fields on the denitrification activity of *paracoccus denitrificans*. *Bioelectrochemistry* 70: 91-95.
- [275] Strasak L, Vetterl V, Smarda J (2002) Effects of low-frequency magnetic fields on bacteria escherichia coli. *Bioelectrochemistry* 55: 161-164.
- [276] Fojt L, Vetterl V (2012) Electrochemical evaluation of extremely-low frequency magnetic field effects on sulphate-reducing bacteria. *Short Communication, Folia Biologica (Parha)* 258: 44-48.
- [277] Shobin G, Guowei L, Ying W, Schichang Li, Yunxia Zhao, Kewei L (2012) A study of the interaction between elf-pemf and bacteria. *Advanced in Electric and Electronic, LNEE, W. Hu, Springer-Verlag, Berlin, Heidelberg*, 155: 243-254.
- [278] Dimitris JP Andras K, Lukas HM (2002) Mechanism for action of electromagnetic fields on cells. *Biochemical and Biophysical Research Communications* 298:95-102.
- [279] Blank M, Goodman R (2003) Electromagnetics acceleration of the Belousov Zhabotinski reaction. *Bioelectrochem* 61: 93-97.
- [280] Blank M (2008) Protein and DNA interaction with electromagnetic fields. *Eletromagn. Biol. Med.* 28: 3-23.
- [281] Blank M, Goodman R (2008) A mechanism for stimulation of biosynthesis by electromagnetic fields: charge transfer in DNA and base pair separation. *J. Cell Physiol.* 214: 20-26.
- [282] Ryan WH, Andrey Z, Ashish B, Senthil C, Kesav CD (2009) Electromagnetic biostimulation of living vultures for biotechnology, biofuel and bioenergy applications. *International Journal of Molecular Sciences* 10: 4515-4558.

## Appendix A: Biot-Savart Law to calculate magnetic field

Adapted from: Physics lab online, resource lesson, magnetic field along the axis of a current loop:

[http://dev.physicslab.org/Document.aspx?doctype=3&filename=Magnetism\\_BiotSavartLaw2.xml](http://dev.physicslab.org/Document.aspx?doctype=3&filename=Magnetism_BiotSavartLaw2.xml)

Chapter 9: Sources of Magnetic fields

<http://www.scribd.com/doc/4705015/27/Appendix-2-Helmholtz-Coils>

**Biot-Savart Law:** Currents which arise due to motion of charges are the source of magnetic fields. When charges move in a conducting wire and produce a current  $I$ , the magnetic field at any point  $P$  due to current can be calculated by adding up the magnetic field contributions,  $d\vec{B}$ , from small segments of the wire  $d\vec{l}$ , (Figure A1).

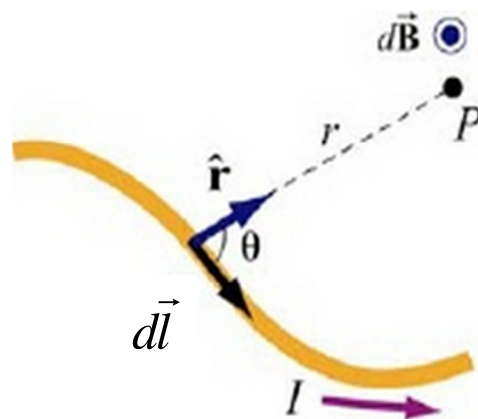


Figure A.1: Magnetic field  $d\vec{B}$ , at point  $P$  due to a current-carrying elements  $I d\vec{l}$ .

These segments can be thought of as a vector quantity having a magnitude of the length of the segment and pointing in the direction of the current flow. The infinitesimal current source can then be written as  $I d\vec{l}$ .

Let  $r$  to be the distance from the current source to the field point  $P$ , and  $\hat{r}$  the corresponding unit vector. The **Biot-Savart Law** gives an expression for the magnetic field contribution,  $d\vec{B}$ , from the current source,  $I d\vec{l}$ ,

$$d\vec{B} = \frac{\mu_0}{4\pi} \frac{I d\vec{l} \times \hat{r}}{r^2} \quad (\text{A.1})$$

**Application of Biot-Savart Law: Circular coil:**

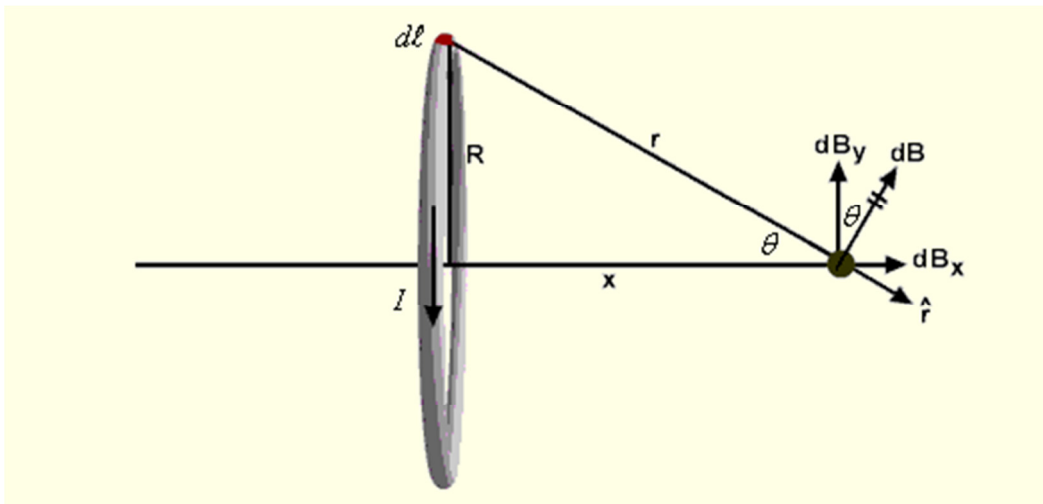


Figure A.2: Circular current carrying loop with  $x$  as the axial axis.

Magnetic field contribution,  $d\mathbf{B}$ , of each current segment,  $I dl$ , is perpendicular to the radius vector  $\hat{r}$ .

Using (A.1) from above, and applying to Figure A.2, the following can be stated:

$$dB = \frac{\mu_0}{4\pi} \frac{I dl \times \hat{r}}{r^2} \quad (\text{A.2})$$

$$dB = \frac{\mu_0}{4\pi} \frac{I dl \times \sin 90^\circ}{r^2} \quad (\text{A.3})$$

$$dB = \frac{\mu_0}{4\pi} \frac{I dl}{r^2} \quad (\text{A.4})$$

The components perpendicular to the loop's axis,  $dB_y$  will cancel as integration is conducted around the loop. The horizontal component  $dB_x$  can be derived as:

$$dB_x = dB \sin \theta \quad (\text{A.5})$$

$$dB_x = \frac{\mu_0 I dl}{4\pi r^2} \sin \theta \quad (\text{A.6})$$

$$dB_x = \frac{\mu_0 I R}{4\pi r^2 r} dl \quad (\text{A.7})$$

$$dB_x = \frac{\mu_0 IR}{4\pi r^3} dl \quad (\text{A.8})$$

$r$  can be expressed in terms of  $x$  and  $R$  using Pythagoras Theorem;

$$r = \sqrt{x^2 + R^2} \quad (\text{A.9})$$

Therefore, the new expression for  $dB_x$  becomes:

$$dB_x = \frac{\mu_0 IR}{4\pi \sqrt{x^2 + R^2}^3} dl \quad (\text{A.10})$$

All contribution of resultant magnetic field can now be expressed as below:

$$B_x = \oint dB_x \quad (\text{A.11})$$

$$B_x = \oint \frac{\mu_0 IR}{4\pi \sqrt{x^2 + R^2}^3} dl \quad (\text{A.12})$$

$$B_x = \frac{\mu_0 IR}{4\pi \sqrt{x^2 + R^2}^3} \oint dl \quad (\text{A.13})$$

$$B_x = \frac{\mu_0 IR}{4\pi\sqrt{x^2 + R^2}^3} 2\pi R \quad (\text{A.14})$$

$$B_x = \frac{\mu_0 IR^2}{2\sqrt{x^2 + R^2}^3} \quad (\text{A.15})$$

For a pair of 1-Axis Helmholtz coil system with two circular coils oriented in the  $x$  axis, the expression of the total magnetic field can be written by simply multiplying 2 with equation A.15. Therefore the magnetic field expression for the 1-Axis Helmholtz coil system becomes:

$$B_x = \frac{\mu_0 IR^2}{2\sqrt{x^2 + R^2}^3} * 2 \quad (\text{A.16})$$

Since, both coils have  $N$  number of turns, the final expression for the total magnetic field becomes:

$$B_x = \frac{\mu_0 IR^2}{2\sqrt{x^2 + R^2}^3} * 2 * N \quad (\text{A.17})$$

$$B_x = \frac{2\mu_0 NIR^2}{2\sqrt{x^2 + R^2}^3} \quad (\text{A.18})$$

$$B_x = \frac{2\mu_0 NIR^2}{2(x^2 + R^2)^{3/2}} \quad (\text{A.19})$$



## **Appendix B: Power MOSFET IRF520N**

Adapted from data sheet of International Rectifier

([http://www.redrok.com/MOSFET\\_IRF520N\\_100V\\_9.7A\\_200mO\\_Vth4.0\\_TO-220.pdf](http://www.redrok.com/MOSFET_IRF520N_100V_9.7A_200mO_Vth4.0_TO-220.pdf))

# IRF520N

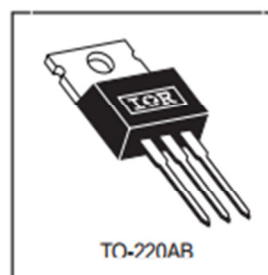
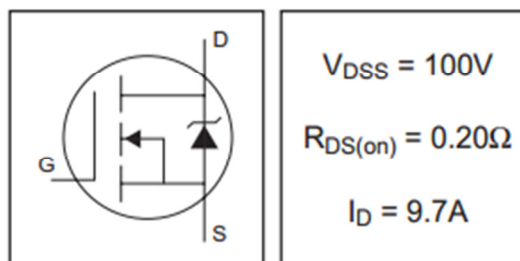
HEXFET® Power MOSFET

- Advanced Process Technology
- Dynamic dv/dt Rating
- 175°C Operating Temperature
- Fast Switching
- Fully Avalanche Rated

### Description

Fifth Generation HEXFETs from International Rectifier utilize advanced processing techniques to achieve extremely low on-resistance per silicon area. This benefit, combined with the fast switching speed and ruggedized device design that HEXFET Power MOSFETs are well known for, provides the designer with an extremely efficient and reliable device for use in a wide variety of applications.

The TO-220 package is universally preferred for all commercial-industrial applications at power dissipation levels to approximately 50 watts. The low thermal resistance and low package cost of the TO-220 contribute to its wide acceptance throughout the industry.



### Absolute Maximum Ratings

	Parameter	Max.	Units
$I_D @ T_C = 25^\circ C$	Continuous Drain Current, $V_{GS} @ 10V$	9.7	A
$I_D @ T_C = 100^\circ C$	Continuous Drain Current, $V_{GS} @ 10V$	6.8	
$I_{DM}$	Pulsed Drain Current $\text{\textcircled{D}}$	38	
$P_D @ T_C = 25^\circ C$	Power Dissipation	48	W
	Linear Derating Factor	0.32	W/°C
$V_{GS}$	Gate-to-Source Voltage	$\pm 20$	V
$E_{AS}$	Single Pulse Avalanche Energy $\text{\textcircled{D}}$	91	mJ
$I_{AR}$	Avalanche Current $\text{\textcircled{D}}$	5.7	A
$E_{AR}$	Repetitive Avalanche Energy $\text{\textcircled{D}}$	4.8	mJ
dv/dt	Peak Diode Recovery dv/dt $\text{\textcircled{D}}$	5.0	V/ns
$T_J$	Operating Junction and	-55 to + 175	°C
$T_{STG}$	Storage Temperature Range		
	Soldering Temperature, for 10 seconds	300 (1.6mm from case )	
	Mounting torque, 6-32 or M3 screw	10 lbf•in (1.1N•m)	


### Thermal Resistance

	Parameter	Typ.	Max.	Units
$R_{\theta JC}$	Junction-to-Case	—	3.1	°C/W
$R_{\theta CS}$	Case-to-Sink, Flat, Greased Surface	0.50	—	
$R_{\theta JA}$	Junction-to-Ambient	—	62	

5/13/98

## Appendix B- Power MOSFET IRF520N cont..

## Electrical Characteristics @ $T_J = 25^\circ\text{C}$ (unless otherwise specified)

	Parameter	Min.	Typ.	Max.	Units	Conditions
$V_{(BR)DSS}$	Drain-to-Source Breakdown Voltage	100	—	—	V	$V_{GS} = 0V, I_D = 250\mu A$
$\Delta V_{(BR)DSS}/\Delta T_J$	Breakdown Voltage Temp. Coefficient	—	0.11	—	V/°C	Reference to $25^\circ\text{C}, I_D = 1mA$
$R_{DS(on)}$	Static Drain-to-Source On-Resistance	—	—	0.20	$\Omega$	$V_{GS} = 10V, I_D = 5.7A$ ④
$V_{GS(th)}$	Gate Threshold Voltage	2.0	—	4.0	V	$V_{DS} = V_{GS}, I_D = 250\mu A$
$g_{fs}$	Forward Transconductance	2.7	—	—	S	$V_{DS} = 50V, I_D = 5.7A$
$I_{DSS}$	Drain-to-Source Leakage Current	—	—	25	$\mu A$	$V_{DS} = 100V, V_{GS} = 0V$
		—	—	250		$V_{DS} = 80V, V_{GS} = 0V, T_J = 150^\circ\text{C}$
$I_{GSS}$	Gate-to-Source Forward Leakage	—	—	100	nA	$V_{DS} = 20V$
	Gate-to-Source Reverse Leakage	—	—	-100		$V_{GS} = -20V$
$Q_g$	Total Gate Charge	—	—	25	nC	$I_D = 5.7A$
$Q_{gs}$	Gate-to-Source Charge	—	—	4.8		$V_{DS} = 80V$
$Q_{gd}$	Gate-to-Drain ("Miller") Charge	—	—	11		$V_{GS} = 10V$ , See Fig. 6 and 13 ④
$t_{d(on)}$	Turn-On Delay Time	—	4.5	—	ns	$V_{DD} = 50V$
$t_r$	Rise Time	—	23	—		$I_D = 5.7A$
$t_{d(off)}$	Turn-Off Delay Time	—	32	—		$R_G = 22\Omega$
$t_f$	Fall Time	—	23	—		$R_D = 8.6\Omega$ , See Fig. 10 ④
$L_D$	Internal Drain Inductance	—	4.5	—	nH	Between lead, 6mm (0.25in.) from package and center of die contact
$L_S$	Internal Source Inductance	—	7.5	—		
$C_{iss}$	Input Capacitance	—	330	—	pF	$V_{GS} = 0V$
$C_{oss}$	Output Capacitance	—	92	—		$V_{DS} = 25V$
$C_{rss}$	Reverse Transfer Capacitance	—	54	—		$f = 1.0MHz$ , See Fig. 5

## Source-Drain Ratings and Characteristics

	Parameter	Min.	Typ.	Max.	Units	Conditions
$I_S$	Continuous Source Current (Body Diode)	—	—	9.7	A	MOSFET symbol showing the integral reverse p-n junction diode.
$I_{SM}$	Pulsed Source Current (Body Diode) ④	—	—	38		
$V_{SD}$	Diode Forward Voltage	—	—	1.3	V	$T_J = 25^\circ\text{C}, I_S = 5.7A, V_{GS} = 0V$ ④
$t_{rr}$	Reverse Recovery Time	—	99	150	ns	$T_J = 25^\circ\text{C}, I_F = 5.7A$
$Q_{rr}$	Reverse Recovery Charge	—	390	580	nC	$di/dt = 100A/\mu s$ ④

### Notes:

① Repetitive rating; pulse width limited by max. junction temperature. ( See fig. 11 )

②  $V_{DD} = 25V$ , starting  $T_J = 25^\circ\text{C}$ ,  $L = 4.7mH$   
 $R_G = 25\Omega, I_{AS} = 5.7A$ . (See Figure 12)

③  $I_{SD} \leq 5.7A, di/dt \leq 240A/\mu s, V_{DD} \leq V_{(BR)DSS}$ ,  
 $T_J \leq 175^\circ\text{C}$

④ Pulse width  $\leq 300\mu s$ ; duty cycle  $\leq 2\%$ .

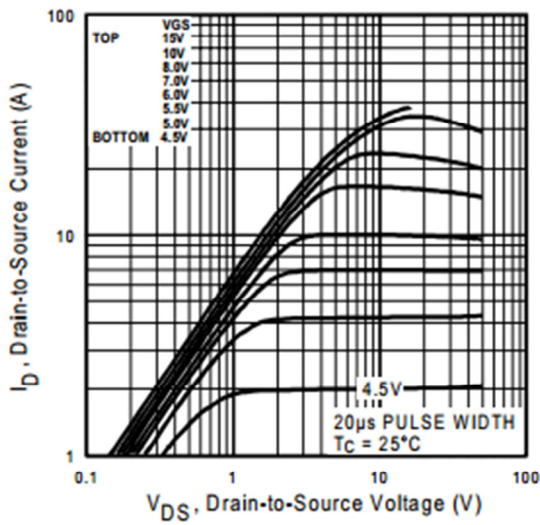


Fig 1. Typical Output Characteristics

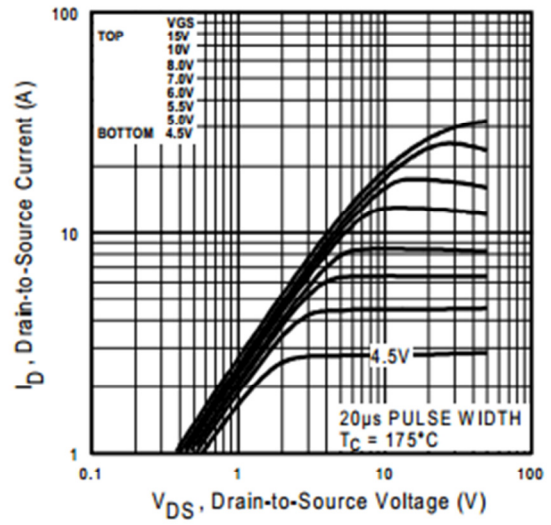


Fig 2. Typical Output Characteristics

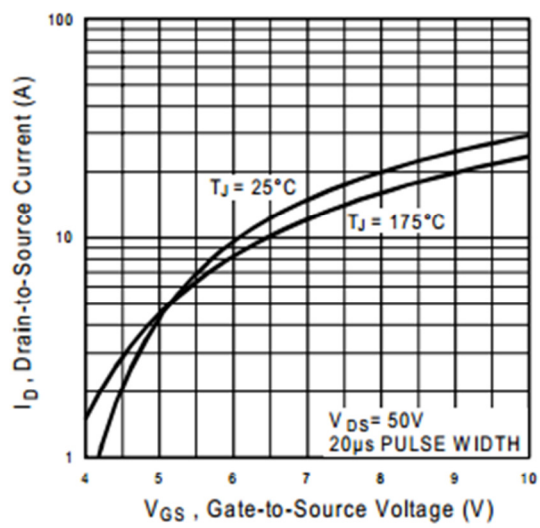


Fig 3. Typical Transfer Characteristics

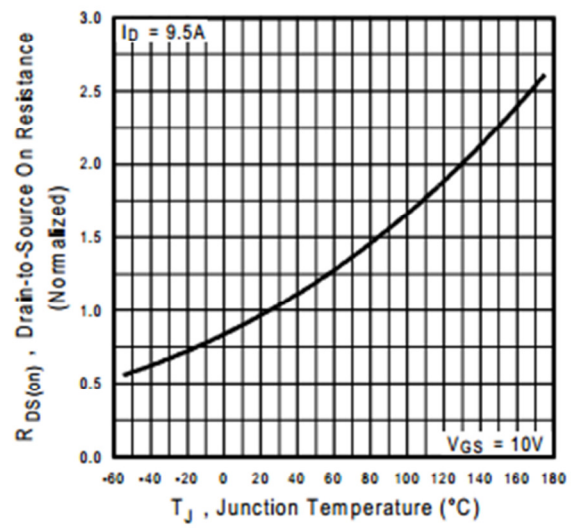


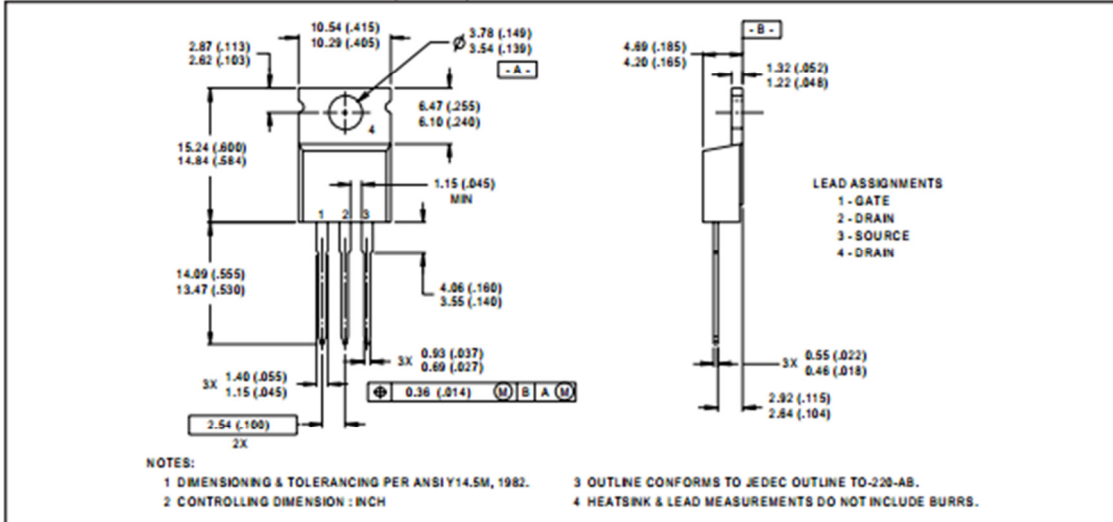
Fig 4. Normalized On-Resistance Vs. Temperature

# IRF520N

## Package Outline

### TO-220AB Outline

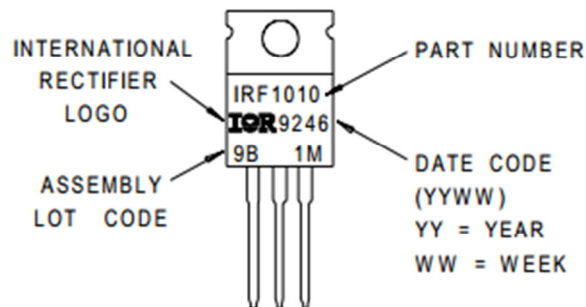
Dimensions are shown in millimeters (inches)



## Part Marking Information

### TO-220AB

EXAMPLE : THIS IS AN IRF1010  
WITH ASSEMBLY  
LOT CODE 9B1M



**WORLD HEADQUARTERS:** 233 Kansas St., El Segundo, California 90245, Tel: (310) 322 3331  
**EUROPEAN HEADQUARTERS:** Hurst Green, Oxted, Surrey RH8 9BB, UK Tel: ++ 44 1883 732020  
**IR CANADA:** 7321 Victoria Park Ave., Suite 201, Markham, Ontario L3R 2Z8, Tel: (905) 475 1897  
**IR GERMANY:** Saalburgstrasse 157, 61350 Bad Homburg Tel: ++ 49 6172 96590  
**IR ITALY:** Via Liguria 49, 10071 Borgaro, Torino Tel: ++ 39 11 451 0111  
**IR FAR EAST:** K&H Bldg., 2F, 30-4 Nishi-Ikebukuro 3-Chome, Toshima-Ku, Tokyo Japan 171 Tel: 81 3 3983 0086  
**IR SOUTHEAST ASIA:** 315 Outram Road, #10-02 Tan Boon Liat Building, Singapore 0316 Tel: 65 221 8371  
<http://www.irf.com/> Data and specifications subject to change without notice. 5/98

**Jaycar Electronics**

45 A'Beckett St, Melbourne, VIC, Australia

Ph: (03) 9663 2030

Web: <http://www.jaycar.com.au>

**Product:** 10mW Laser Module

**My Pet Warehouse - South Melbourne**

65-79 Moray Street, South Melbourne Victoria 3205.

Ph: (03) 8199-9999

**Product:** ECO TECH Advanced Reptile Thermostat with Timer TC 100

**Sigma-Aldrich**

PO Box 970, Castle Hill NSW 1765, AUSTRALIA

Phone: Free call 1800 800 097, Direct: 61 2 9841 0555

Web: <http://www.sigmaaldrich.com/australia/customer-service.html>

**Products:** Collagen Type I, Sigma Prod. No. C-9879

TES Free Acid, Sigma Prod. No. T-1375

Calcium Chloride Dihydrate Prod. No. C-3881

Collagenase from *Clostridium histolyticum* Prod. No. C0130

**Cell Biosciences Pty Ltd**

ABN: 94 991 513 272

(The Trustee for the F & M Family Trust trading as Cell Biosciences Pty Ltd)

PO Box 243, Heidelberg, Vic 3084, Australia

Phone: +61 (0)3 9499 1117

Fax: +61 (0)3 8678 3956

email: [info@cellbiosciences.com.au](mailto:info@cellbiosciences.com.au)

**Products:** Columbia Broth (product code 294420)

Columbia Agar (product code 297596)

**Appendix D1: Resistivity of Copper**

Table: resistivity, conductivity and temperature coefficient of various materials at 20 °C (68° F, 293K). Adapted from: Giancoli, Douglas (2009) [1984]. "25. Electric Currents and

Resistance". In Jocelyn Phillips (ed.). *Physics for Scientists and Engineers with Modern Physics* (4th ed.). Upper Saddle River, New Jersey: Prentice Hall. p.658. ISBN 0-13-149508-9. ([http://en.wikipedia.org/wiki/Electrical\\_resistivity\\_and\\_conductivity#cite\\_note-Giancoli-12](http://en.wikipedia.org/wiki/Electrical_resistivity_and_conductivity#cite_note-Giancoli-12)).

Material	$\rho$ ( $\Omega\cdot\text{m}$ ) at 20 °C	$\sigma$ (S/m) at 20 °C	Temperature coefficient <sup>[note 1]</sup> ( $\text{K}^{-1}$ )	Reference
Carbon (graphene)	$1 \times 10^{-8}$	-	-	[8]
Silver	$1.59 \times 10^{-8}$	$6.30 \times 10^7$	0.0038	[9][10]
Copper	$1.68 \times 10^{-8}$	$5.96 \times 10^7$	0.003 862	[11]
Annealed copper <sup>[note 2]</sup>	$1.72 \times 10^{-8}$	$5.80 \times 10^7$	0.003 93	[12]
Gold <sup>[note 3]</sup>	$2.44 \times 10^{-8}$	$4.10 \times 10^7$	0.0034	[9]
Aluminium <sup>[note 4]</sup>	$2.82 \times 10^{-8}$	$3.5 \times 10^7$	0.0039	[9]
Calcium	$3.36 \times 10^{-8}$	$2.98 \times 10^7$	0.0041	
Tungsten	$5.60 \times 10^{-8}$	$1.79 \times 10^7$	0.0045	[9]
Zinc	$5.90 \times 10^{-8}$	$1.69 \times 10^7$	0.0037	[13]
Nickel	$6.99 \times 10^{-8}$	$1.43 \times 10^7$	0.006	
Lithium	$9.28 \times 10^{-8}$	$1.08 \times 10^7$	0.006	
Iron	$1.0 \times 10^{-7}$	$1.00 \times 10^7$	0.005	[9]
Platinum	$1.06 \times 10^{-7}$	$9.43 \times 10^6$	0.003 92	[9]
Tin	$1.09 \times 10^{-7}$	$9.17 \times 10^6$	0.0045	
Carbon steel (1010)	$1.43 \times 10^{-7}$	$6.99 \times 10^6$		[14]
Lead	$2.2 \times 10^{-7}$	$4.55 \times 10^6$	0.0039	[9]
Titanium	$4.20 \times 10^{-7}$	$2.38 \times 10^6$	X	
Grain oriented electrical steel	$4.60 \times 10^{-7}$	$2.17 \times 10^6$		[15]
Manganin	$4.82 \times 10^{-7}$	$2.07 \times 10^6$	0.000 002	[16]
Constantan	$4.9 \times 10^{-7}$	$2.04 \times 10^6$	0.000 008	[17]
Stainless steel <sup>[note 5]</sup>	$6.9 \times 10^{-7}$	$1.45 \times 10^6$		[18]
Mercury	$9.8 \times 10^{-7}$	$1.02 \times 10^6$	0.0009	[16]
Nichrome <sup>[note 6]</sup>	$1.10 \times 10^{-6}$	$9.09 \times 10^5$	0.0004	[9]
GaAs	$5 \times 10^{-7}$ to $10 \times 10^{-3}$	$5 \times 10^{-8}$ to $10^3$		[19]
Carbon (amorphous)	$5 \times 10^{-4}$ to $8 \times 10^{-4}$	$1.25 \times 10^3$ to $2 \times 10^3$	-0.0005	[9][20]
Carbon (graphite) <sup>[note 7]</sup>	$2.5 \times 10^{-6}$ to $5.0 \times 10^{-6}$ //basal plane $3.0 \times 10^{-3}$ $\perp$ basal plane	$2 \times 10^5$ to $3 \times 10^5$ //basal plane $3.3 \times 10^2$ $\perp$ basal plane		[21]

## Appendix D2: Diameter, Cross-sectional Area and Allowable Current for Copper wire

Table: Various data including –standard nominal diameters and Cross-sectional Areas of solid Copper Wire. Fusing current (melting wire) is estimated based on 25°C ambient

temperature Adopted from (American Wire Gauge: [http://en.wikipedia.org/wiki/American\\_wire\\_gauge](http://en.wikipedia.org/wiki/American_wire_gauge)).

AWG	Diameter		Turns of wire, no insulation		Area		Copper resistance <sup>[6]</sup>		NEC copper wire ampacity with 60/75/90 °C insulation (A) <sup>[7]</sup>	Approx. metric equivalents	Fusing current, copper <sup>[8][9]</sup>		
	(in)	(mm)	(per in)	(per cm)	(kcmil)	(mm <sup>2</sup> )	(Ω/km) (mΩ/m)	(Ω/kft) (mΩ/ft)			Preece, ~10 s	Onderdonk, 1 s	Onderdonk, 32 ms
0000 (4/0)	0.4600*	11.684*	2.17	0.856	212	107	0.1608	0.04901	195 / 230 / 260		3.2 kA	31 kA	173 kA
000 (3/0)	0.4096	10.405	2.44	0.961	168	85.0	0.2028	0.06180	165 / 200 / 225		2.7 kA	24.5 kA	137 kA
00 (2/0)	0.3648	9.266	2.74	1.08	133	67.4	0.2557	0.07793	145 / 175 / 195		2.3 kA	19.5 kA	109 kA
0 (1/0)	0.3249	8.251	3.08	1.21	106	53.5	0.3224	0.09827	125 / 150 / 170		1.9 kA	15.5 kA	87 kA
1	0.2893	7.348	3.46	1.36	83.7	42.4	0.4066	0.1239	110 / 130 / 150		1.6 kA	12 kA	68 kA
2	0.2576	6.544	3.88	1.53	66.4	33.6	0.5127	0.1563	95 / 115 / 130		1.3 kA	9.7 kA	54 kA
3	0.2294	5.827	4.36	1.72	52.6	26.7	0.6465	0.1970	85 / 100 / 110	196/0.4	1.1 kA	7.7 kA	43 kA
4	0.2043	5.189	4.89	1.93	41.7	21.2	0.8152	0.2485	70 / 85 / 95		946 A	6.1 kA	34 kA
5	0.1819	4.621	5.50	2.16	33.1	16.8	1.028	0.3133		126/0.4	795 A	4.8 kA	27 kA
6	0.1620	4.115	6.17	2.43	26.3	13.3	1.296	0.3951	55 / 65 / 75		668 A	3.8 kA	21 kA
7	0.1443	3.665	6.93	2.73	20.8	10.5	1.634	0.4982		80/0.4	561 A	3 kA	17 kA
8	0.1285	3.264	7.78	3.06	16.5	8.37	2.061	0.6282	40 / 50 / 55		472 A	2.4 kA	13.5 kA
9	0.1144	2.906	8.74	3.44	13.1	6.63	2.599	0.7921		84/0.3	396 A	1.9 kA	10.7 kA
10	0.1019	2.588	9.81	3.86	10.4	5.26	3.277	0.9989	30 / 35 / 40		333 A	1.5 kA	8.5 kA
11	0.0907	2.305	11.0	4.34	8.23	4.17	4.132	1.260		56/0.3	280 A	1.2 kA	6.7 kA
12	0.0808	2.053	12.4	4.87	6.53	3.31	5.211	1.588	25 / 25 / 30		235 A	955 A	5.3 kA
13	0.0720	1.828	13.9	5.47	5.18	2.62	6.571	2.003		50/0.25	198 A	758 A	4.2 kA
14	0.0641	1.628	15.6	6.14	4.11	2.08	8.286	2.525	20 / 20 / 25	64/0.2	166 A	601 A	3.3 kA
15	0.0571	1.450	17.5	6.90	3.26	1.65	10.45	3.184		30/0.25	140 A	477 A	2.7 kA
16	0.0508	1.291	19.7	7.75	2.58	1.31	13.17	4.016	— / — / 18		117 A	377 A	2.1 kA
17	0.0453	1.150	22.1	8.70	2.05	1.04	16.61	5.064		32/0.2	99 A	300 A	1.7 kA
18	0.0403	1.024	24.8	9.77	1.62	0.823	20.95	6.385	— / — / 14	24/0.2	83 A	237 A	1.3 kA
19	0.0359	0.912	27.9	11.0	1.29	0.653	26.42	8.051			70 A	189 A	1 kA
20	0.0320	0.812	31.3	12.3	1.02	0.518	33.31	10.15		16/0.2	58.5 A	149 A	834 A
21	0.0285	0.723	35.1	13.8	0.810	0.410	42.00	12.80		13/0.2	49 A	119 A	662 A
22	0.0253	0.644	39.5	15.5	0.642	0.326	52.96	16.14		7/0.25	41 A	94 A	525 A
23	0.0226	0.573	44.3	17.4	0.509	0.258	66.79	20.36			35 A	74 A	416 A
24	0.0201	0.511	49.7	19.6	0.404	0.205	84.22	25.67		1/0.5, 7/0.2, 30/0.1	29 A	59 A	330 A
25	0.0179	0.455	55.9	22.0	0.320	0.162	106.2	32.37			24 A	47 A	262 A
26	0.0159	0.405	62.7	24.7	0.254	0.129	133.9	40.81		1/0.4, 7/0.15	20 A	37 A	208 A

### Appendix D3: Density of Copper

Table: Density (kg / m<sup>3</sup>) of common metals and alloys. Adopted from The Engineering Tool Box ([http://www.engineeringtoolbox.com/metal-alloys-densities-d\\_50.html](http://www.engineeringtoolbox.com/metal-alloys-densities-d_50.html))



<b>Metal or Alloy</b>	<b>Density (kg/m<sup>3</sup>)</b>
Actinium	10070
Admiralty Brass	8525
Aluminum	2712
Aluminum - melted	2560 - 2640
Aluminum - 1100	2720
Aluminum - 6061	2720
Aluminum - 7050	2800
Aluminum - 7178	2830
Aluminum bronze (3-10% Al)	7700 - 8700
Aluminum foil	2700 -2750
Antifriction metal	9130 -10600
Antimony	6690
Babbitt	7272
Barium	3594
Beryllium	1840
Beryllium copper	8100 - 8250
Bismuth	9750
Brass - casting	8400 - 8700
Brass - rolled and drawn	8430 - 8730
Brass 60/40	8520
Bronze - lead	7700 - 8700
Bronze - phosphorous	8780 - 8920
Bronze (8-14% Sn)	7400 - 8900
Brushed metal	7860
Cadmium	8640
Caesium	1873
Calcium	1540
Cast iron	6800 - 7800
Cerium	6770
Chemical Lead	11340
Chromium	7190
Cobalt	8746
Constantan	8920
Columbium	8600
Constantan	8880
Copper	8940
Cupronickel	8908 - 8940



## Appendix D4: Specific heat capacity of Copper

Table: specific heat capacity of various materials at 25 °C (298K). Adapted from [http://en.wikipedia.org/wiki/Heat\\_capacity](http://en.wikipedia.org/wiki/Heat_capacity).

Substance	Phase	(mass) specific heat capacity $c_p$ or $c_m$ $\text{J}\cdot\text{g}^{-1}\cdot\text{K}^{-1}$	Constant pressure molar heat capacity $C_{p,m}$ $\text{J}\cdot\text{mol}^{-1}\cdot\text{K}^{-1}$	Constant volume molar heat capacity $C_{v,m}$ $\text{J}\cdot\text{mol}^{-1}\cdot\text{K}^{-1}$	Volumetric heat capacity $C_v$ $\text{J}\cdot\text{cm}^{-3}\cdot\text{K}^{-1}$	Constant vol. atom-molar heat capacity in units of R $C_{v,m(atom)}$ $\text{atom}\cdot\text{mol}^{-1}$
Air (Sea level, dry, 0 °C (273.15 K))	gas	1.0035	29.07	20.7643	0.001297	~ 1.25 R
Air (typical room conditions <sup>A</sup> )	gas	1.012	29.19	20.85	0.00121	~ 1.25 R
Aluminium	solid	0.897	24.2		2.422	2.91 R
Ammonia	liquid	4.700	80.08		3.263	3.21 R
Animal tissue (incl. human) <sup>[21]</sup>	mixed	3.5			3.7*	
Antimony	solid	0.207	25.2		1.386	3.03 R
Argon	gas	0.5203	20.7862	12.4717		1.50 R
Arsenic	solid	0.328	24.6		1.878	2.96 R
Beryllium	solid	1.82	16.4		3.367	1.97 R
Bismuth <sup>[22]</sup>	solid	0.123	25.7		1.20	3.09 R
Cadmium	solid	0.231	26.02			3.13 R
Carbon dioxide CO <sub>2</sub> <sup>[17]</sup>	gas	0.839*	36.94	28.46		1.14 R
Chromium	solid	0.449	23.35			2.81 R
→ Copper	solid	0.385	24.47		3.45	2.94 R
Diamond	solid	0.5091	6.115		1.782	0.74 R
Ethanol	liquid	2.44	112		1.925	1.50 R
Gasoline (octane)	liquid	2.22	228		1.64	1.05 R
Glass <sup>[22]</sup>	solid	0.84				
Gold	solid	0.129	25.42		2.492	3.05 R
Granite <sup>[22]</sup>	solid	0.790			2.17	
Graphite	solid	0.710	8.53		1.534	1.03 R
Helium	gas	5.1932	20.7862	12.4717		1.50 R
Hydrogen	gas	14.30	28.82			1.23 R
Hydrogen sulfide H <sub>2</sub> S <sup>[17]</sup>	gas	1.015*	34.60			1.05 R

## Appendix E: Aseptic Techniques

Adapted from: Bacterial Growth <http://www.bowdoin.edu/biology/grants/spec/pdf/bacterial-growth.pdf>.

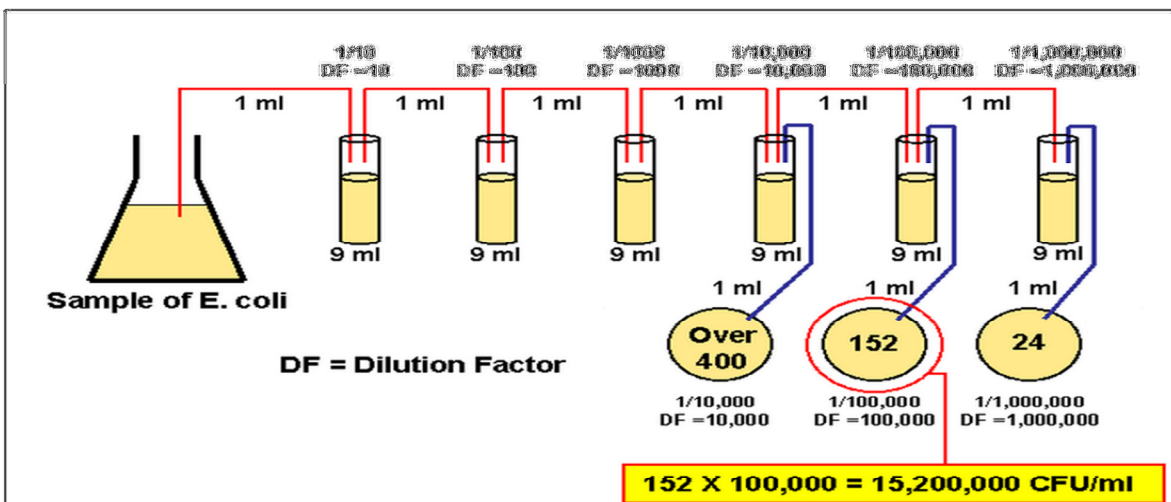
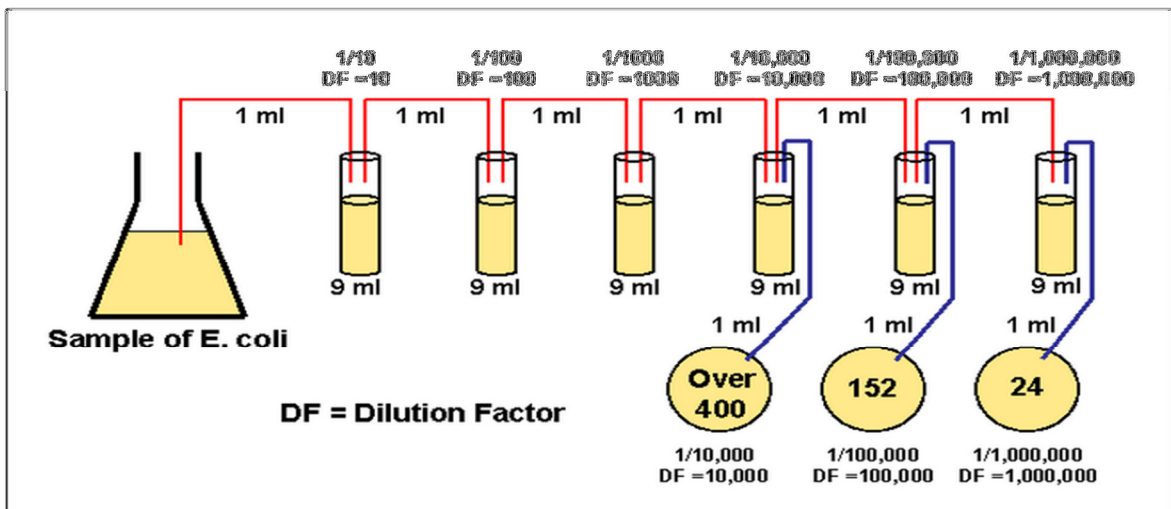
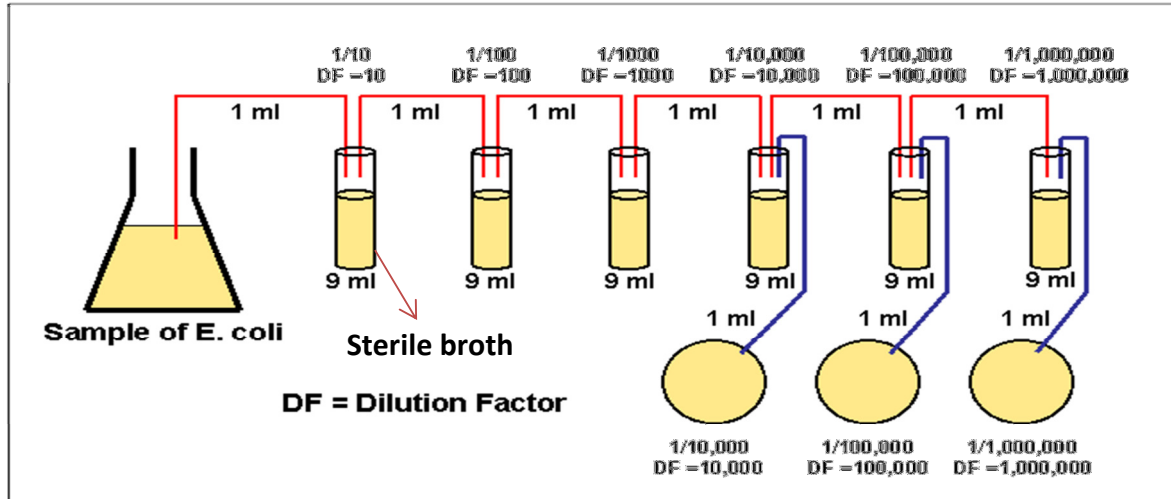
### Aseptic Techniques

1. Before handling of cultures:
  - a. Remove all unnecessary items from workspace.
  - b. Be sure your hair is tied back
2. Before and after handling cultures:
  - a. Wash your hands
  - b. Disinfect your area
  - c. Sterilize instruments
  - d. Dispose of all contaminated materials in appropriate containers
3. While working with cultures:
  - a. Do not talk
  - b. Never lay caps or covers on the bench tops
  - c. Open petri dishes only when adding and/or spreading bacteria. Tilt the petri dish lid to form a barrier between the culture and you
  - d. Work quickly
  - e. Use sterile pipets right out of the package (don't use one that has been on the lab bench)
  - f. Only take the caps off the dilution tubes or bacterial cultures when pipeting material either into or out of containers. Do not leave caps off for any longer than necessary

## Appendix F: Serial Dilution Technique and Viable Cell Count

Adopted from: Lab 6 Bacteria Enumeration.

<http://biologyonline.us/Microbiology/Fall%2008%20White%20Earth/Micro%20Lab%20Manual/Lab%206/12.htm>.



CFUs per ml of sample = The number of colonies  $\times$  The dilution factor of the plate counted